



# *University of* **HUDDERSFIELD**

## **University of Huddersfield Repository**

Diryak, Ramadan

Design of Rheological Measurements for Rapidly Gelling Polysaccharides on Exposure to External Cross-Linkers

### **Original Citation**

Diryak, Ramadan (2018) Design of Rheological Measurements for Rapidly Gelling Polysaccharides on Exposure to External Cross-Linkers. Doctoral thesis, University of Huddersfield.

This version is available at <http://eprints.hud.ac.uk/id/eprint/34574/>

The University Repository is a digital collection of the research output of the University, available on Open Access. Copyright and Moral Rights for the items

on this site are retained by the individual author and/or other copyright owners.

Users may access full items free of charge; copies of full text items generally can be reproduced, displayed or performed and given to third parties in any format or medium for personal research or study, educational or not-for-profit purposes without prior permission or charge, provided:

- The authors, title and full bibliographic details is credited in any copy;
- A hyperlink and/or URL is included for the original metadata page; and
- The content is not changed in any way.

For more information, including our policy and submission procedure, please contact the Repository Team at: [E.mailbox@hud.ac.uk](mailto:E.mailbox@hud.ac.uk).

<http://eprints.hud.ac.uk/>

# DESIGN OF RHEOLOGICAL MEASUREMENTS FOR RAPIDLY GELLING POLYSACCHARIDES ON EXPOSURE TO EXTERNAL CROSS-LINKERS

---

By

**RAMADAN DIRYAK**

A Thesis Submitted to the University of Huddersfield

in Partial Fulfilment of the Requirement

for the Degree of Doctor of Philosophy



**Huddersfield University**

**October 2017**

## **Copyright statement**

- I. The author of this thesis (including any appendices and/or schedules to this thesis) owns any copyright in it (the “Copyright”) and he has given The University of Huddersfield the right to use such copyright for any administrative, promotional, educational and/or teaching purposes.
- II. Copies of this thesis, either in full or in extracts, may be made only in accordance with the regulations of the University Library. Details of these regulations may be obtained from the Librarian. This page must form part of any such copies made.
- III. The ownership of any patents, designs, trademarks and any and all other intellectual property rights except for the Copyright (the “Intellectual Property Rights”) and any reproductions of copyright works, for example graphs and tables (“Reproductions”), which may be described in this thesis, may not be owned by the author and may be owned by third parties. Such Intellectual Property Rights and Reproductions cannot and must not be made available for use without the prior written permission of the owner(s) of the relevant Intellectual Property Rights and/or Reproductions.

## ABSTRACT

This research project focused on a range of gel forming polysaccharides, including sodium alginate pectin and gellan gum. All of these materials have ability to form a gel responding to different stimuli, such as pH and crosslinking ions. Their capability to undergo sol-gel transition in presence of mono or divalent cations can often occur in seconds making it particularly difficult to measure the gelation in real time. Therefore, the aim of the work presented in this thesis was to design a new technique that allows commercially available rheological equipment to monitor the gelation progress of these materials.

The first part of study involved the design a new method to measure the gelation of alginate and pectin *in situ* on exposure to an external source of calcium ions. Direct mixing of alginate or low methoxy pectin with divalent cations such as  $\text{Ca}^{2+}$  generally produces heterogeneous gels that form almost instantaneously. Therefore, it is particularly difficult to measure the rheological properties of this gelation event due to the rapid gelation kinetics. In this study the gelation progress was measured on exposure to three different concentrations of  $\text{CaCl}_2$  and gel dissolution time was measured by removing the crosslinking  $\text{Ca}^{2+}$  from freshly formed alginate and pectin gels by exposure to calcium chelators. The modification of the rheometer to facilitate these measurements used a petri dish attached to the lower plate of the rheometer, into which a piece of filter paper submerged with calcium chloride solutions (50, 100 and 200 mM) was placed. On top of the filter paper dialysis membrane (MWCO 14000) was placed as a barrier to prevent the filter paper imbibing polysaccharide samples. Samples of alginate and pectin 4% w/w were loaded on to the membrane and small deformation oscillatory measurements of elastic modulus ( $G'$ ) and viscous modulus ( $G''$ ) were taken in the linear viscoelastic region, to monitor the gelation as a function of time. Once the gelation was complete the filter paper was

removed and replaced with filter paper immersed with calcium chelating agents (500 mM of EDTA and sodium citrate (Na citrate)) to degrade the gel *in situ*. The results demonstrated that this technique was suitable for analysing the external gelation of alginate and pectin with a sharp increase in  $G'$  in the first three minutes which then plateaued over the remainder of the test. It was also shown that gel stiffness reduced to a greater extent on exposure to EDTA compared with Na citrate. This method is not only suitable for measuring rapid gelation kinetics on exposure to cross-linkers, but has potential applications in modelling the *in situ* gelation behaviour in simulated physiological environments.

The second part of the study investigated using the method developed for the alginate and pectin gelation for the *in situ* gelation of gellan gum under simulated physiological conditions using different types of simulated body fluids, simulated wound fluid (SWF), artificial saliva (AS), artificial lacrimal fluid (LF) and artificial gastric fluid (GF), measuring the gelation of gellan gum solutions (0.25, 0.5, 0.75 and 1% w/w) in response to ionic crosslinking and acidic pH.

The results showed that gellan made the stiffest gels with GF, followed by LF and SWF (which were of similar stiffness to each other) and the weakest gel was formed with AS. The results indicate that this method is not only of use to measure rapid gelation kinetics on external exposure to cross-linkers but could find application in designing bioresponsive delivery systems in the food, pharmaceutical and biomedical industries.

The final section of this thesis focused on the design and proof of concept of a new device that was 3D printed using Acrylonitrile Butadiene Styrene polymers (ABS), termed a rheo-dissolution cell. This was investigated to overcome the limitations of the petri dish method used in the initial studies. The cell was designed to contain a reservoir capable of holding crosslinking solutions and dissolution media allow with sampling ports to be able evaluate rheology measurements of *in situ* gel forming systems while simultaneously measuring release

of molecules loaded into the gel. On the top of the reservoir a retractable stainless steel mesh was used as the lower plate of the rheometer which allowed the polysaccharide samples to be in contact with the fluid in the reservoir during the gelation and gel dissolution. Proof of concept was determined using 1% w/w alginate solution loaded with 50 mg of methylene blue. Rheological measurements were performed with  $\text{CaCl}_2$  in the rheo-dissolution reservoir to initiate gelation. Once the gels were formed gel dissolution was initiated by replacing the  $\text{CaCl}_2$  with calcium chelating agents EDTA and Na citrate. During both of these processes samples from the reservoir were removed and analysed for methylene blue release. The results showed the device was capable of allowing the formation strong gels on exposure to  $\text{CaCl}_2$  and gel dissolution when the formed gels were exposed to the calcium chelators. It was also found that mesh opening size was an important factor in the final gel strength and subsequent gel dissolution time. The strongest gels were formed when the mesh had a large opening area and the chelating of calcium was faster with EDTA than Na citrate. Methylene blue was detected in the reservoir during both gelation and gel dissolution with gel strength appearing to be an important factor on the quantity released gels increased. This study indicated that the rheo-dissolution cell has the potential to be used as a model system for measuring rheological changes and release rate of loaded drugs in gel forming formulations simultaneously by a simple modification of a commercially available rheometer.

*Dedicated to my lovely family, wife and son who  
supported me all the way towards this achievement*

*My beloved son (Mohamad)*

# Acknowledgments

Praise is to almighty Allah who has provided me with blessings in my life.

Firstly, I would like to express my sincere gratitude to my supervisory team Dr Alan Smith and Dr Gordon Morris for their invaluable help and support throughout my journey to produce my PhD thesis. It would have not been possible for me to produce this thesis without their support, motivation and enthusiastic research plan.

Secondly, I would like to thank Dr Muhammad Ghorri for his contribution to the final thesis work. I am very lucky to work with such a wonderful professional environment with this research group. I would like to extend my thanks to all technicians at University of Huddersfield for their assistance during my laboratory work particularly Hayley Markham and Ibrahim George. I would like to thank my special friend Mohamad Abdallah, who has been a friend and brother for me, we helped each other during difficult circumstance, and we enjoyed all the good times together.

Thirdly, I would like to express my deep sense of gratitude and thanks to my parents, family and friends who have helped me a lot during my difficult situation and they provided me with support to finish my PhD. It has been very difficult years for me and for them studying abroad so I would like to thank you all without your presence life has no taste.

Finally, I would like to extend my thanks to Libyan government, culture attaché for giving me the opportunity and fund me to do my PhD.



## Table of Contents

ABSTRACT .....	I
Acknowledgments.....	V
Table of Contents .....	VI
List of Figures .....	XII
List of Tables .....	XX
List of Abbreviations .....	XXI
<b>Chapter 1 General Introduction .....</b>	<b>1</b>
1.1 Gelling materials .....	2
1.1.1 <i>In situ</i> gelling agents .....	3
1.1.2 Current techniques for measuring rapid gelation <i>in situ</i> .....	4
1.2 Aims and objectives .....	6
1.3 Thesis structure .....	8
1.4 Publications and presentations .....	10
<b>Chapter 2 Rheology .....</b>	<b>11</b>
2.1 Introduction to rheology.....	12
2.2 Stress and strain .....	13
2.2.1 Longitudinal (Young's) modulus.....	14
2.2.2 Shear modulus.....	15
2.2.3 Bulk modulus .....	16
2.3 Rheological measurements of biopolymer gels .....	16
2.3.1 Common oscillatory tests.....	21
2.3.2 Determining the linear viscoelastic region.....	21
2.3.3 Mechanical spectra (Frequency sweeps).....	23
2.3.4 Determination of the gelation/melting point .....	25
2.4 Adaptations and limitations.....	26
2.4.1 Specialised modifications to commercial rheometers .....	27

2.4.1.1 Molecular characterisation rheometer (add-ons).....	27
2.4.1.2 Application specific rheometer accessories .....	28
2.4.1.2.1 Light curing lower plate .....	28
2.4.1.2.2 Electro-rheology accessory .....	28
2.4.1.2.3 Relative humidity accessory .....	28
2.4.1.2.4 Immobilization cell .....	28
2.4.2 Limitations .....	29
<b>Chapter 3 Polysaccharide Gels.....</b>	<b>30</b>
3.1 Introduction to polysaccharides .....	31
3.2 Polysaccharide structure.....	32
3.3 Polysaccharide gelation.....	34
3.4 <i>In situ</i> sol-gel transitions .....	38
3.5 Alginate.....	39
3.5.1 Alginate gelation .....	40
3.5.1.1 Mechanism of internal and external gelation .....	42
3.5.1.2 Acid gelation .....	44
3.6 Pectin.....	45
3.6.1 Gelation of pectin.....	47
3.7 Gellan gum.....	49
3.7.1 Gelling characteristics of gellan gum.....	50
3.7.2 Acid gelation of gellan.....	52
3.8 Mechanism of <i>in situ</i> gelling in drug delivery system .....	53
3.9 Application of <i>in situ</i> gelling techniques .....	53
3.9.1 <i>In situ</i> Gelation based on ionic crosslinking .....	54
3.9.2 <i>In situ</i> Gelation based on pH triggered systems .....	54
3.9.3 Thermally triggered systems .....	55
3.10 Applicability of <i>in situ</i> polymeric drug delivery systems .....	55
3.10.1 Oral delivery .....	56

3.10.2 Nasal delivery .....	58
3.10.3 Ocular delivery.....	59
3.10.4 Wound healing hydrogels .....	61
<b>Chapter 4 <i>In situ</i> rheological measurements of the external gelation of alginate and pectin.....</b>	<b>63</b>
4.1 Introduction.....	64
4.2 Material and methods.....	67
4.2.1 Materials.....	67
4.2.2 Solutions preparation .....	67
4.2.2.1 Preparation of alginate solutions.....	67
4.2.2.2 Preparation of pectin solutions.....	68
4.2.2.3 Preparation of calcium chloride solution .....	68
4.2.2.4 Preparation of ethylene diamine tetraacetic acid (EDTA) solution .....	68
4.2.2.5 Preparation of sodium citrate (Na citrate) solution .....	68
4.2.3 Rheological methods.....	68
4.2.3.1 <i>In situ</i> gelation.....	69
4.2.3.2 <i>In situ</i> gel dissolution (degradation).....	70
4.3 Results.....	70
4.3.1 Alginate <i>in situ</i> gelation results.....	70
4.3.2 Alginate gel <i>in situ</i> dissolution results .....	72
4.3.3 Pectin <i>in situ</i> gelation results.....	73
4.3.4 Pectin <i>in situ</i> gel dissolution results.....	75
4.3.5 Comparing the <i>in situ</i> gelation (G') values and dissolution time between alginate and pectin. .....	76
4.3.6 Mechanical spectra.....	78
4.3.7 Discussion .....	81
4.4 Conclusion .....	83
4.5 Limitations and future perspectives .....	84

## Chapter 5 Experimental simulation of the gelation behaviour of *in situ* cross-linked gels on contact with physiological fluids ..... 85

5.1 Introduction.....	86
5.1.1 Physiological fluids.....	87
5.1.1.1 Wound fluid (Exudate).....	87
5.1.1.2 Saliva.....	87
5.1.1.3 Lacrimal fluid.....	88
5.1.1.4 Gastric fluid .....	90
5.1.1.5 Gelation in physiological fluids .....	91
5.2 Materials and methods .....	92
5.2.1 Materials.....	92
5.2.2 Methods.....	92
5.2.2.1 Preparation of gellan solution .....	92
5.2.2.2 Preparation of physiological fluids .....	92
5.2.2.2.1 Preparation of stimulated gastric fluid .....	92
5.2.2.2.2 Preparation of stimulated saliva fluid .....	93
5.2.2.2.3 Preparation of stimulated lacrimal fluid.....	93
5.2.2.2.4 Preparation of stimulated wound fluid.....	94
5.2.2.3 Experimental of <i>in situ</i> gelation .....	94
5.2.2.4 Kinetic modelling.....	95
5.2.2.5 Microstructure analysis .....	96
5.2.2.5.1 Freeze drying protocol .....	96
5.2.2.5.2 Polymer network and surface texture analysis.....	96
5.2.2.5.3 Micro computer tomography (Micro CT) .....	97
5.3 Results.....	98
5.3.1 <i>In situ</i> gelation of gellan gum using artificial saliva (AS) .....	98
5.3.2 <i>In situ</i> gelation of gellan gum with simulated wound fluid (SWF).....	99
5.3.3 <i>In situ</i> gelation test of gellan with simulated lacrimal fluid (LF).....	100

5.3.4 <i>In situ</i> gelation of gellan gum using gastric fluid (GF) .....	101
5.3.5 Frequency dependence.....	102
5.3.6 Comparison of <i>in situ</i> gelation of gellan gum (0.25, 0.5, 0.75 and 1%) with four different types of physiological fluids .....	106
5.3.7 Gelation kinetics .....	108
5.3.7.1 Microstructure growth.....	109
5.3.8 Polymer network and surface texture analysis results .....	111
5.3.9 Micro ct imaging.....	115
5.4 Discussion .....	117
5.5 Conclusion .....	122
<b>Chapter 6 Novel model for simultaneous measurement of rheology and drug release .</b>	<b>123</b>
6.1 Introduction.....	124
6.2 Rheo-dissolution cell device .....	126
6.3 Material and methods.....	127
6.3.1 Material .....	127
6.3.2 Samples and reagents preparation.....	128
6.3.2.1 Preparation of 1% alginate labelled solution for rheology measurements.....	128
6.3.2.2 Preparation calcium chloride solution (200 mM) .....	128
6.3.2.3 Preparation of EDTA solution and sodium dihydrogen citrate.....	128
6.3.3 Rheological measurements .....	128
6.3.4 Release study.....	130
6.4 Results.....	131
6.4.1 Rheology results.....	131
6.4.1.1 <i>In situ</i> gelation results for alginate 1% using three different types of mesh .....	131
6.4.1.2 <i>In situ</i> gel dissolution results for alginate 1% using mesh size 10 (opening area 61%) .	133
6.4.1.3 <i>In situ</i> gel dissolution results for alginate 1% using mesh size 40 (opening area 42%) .	135
6.4.1.4 <i>In situ</i> gel dissolution results for alginate 1% using mesh size 60 (opening area 39%) .	137
6.4.1.5 <i>In situ</i> gel dissolution results for alginate 1% using three different types of mesh.....	139

6.4.2 Release time results.....	140
6.4.2.1 Calibration curve of methylene blue .....	140
6.4.2.2 Release time .....	141
6.4.2.3 Simultaneous measurements of gelation, gel dissolution using EDTA and release of methylene blue .....	143
6.4.2.4 Simultaneous measurements of gelation, gel dissolution using Na citrate and release of methylene blue .....	145
6.4.2.5 Comparison of dissolution time and % release of methylene blue from 1% alginate using three different mesh sizes .....	147
6.5 Discussion .....	148
6.6 Conclusion .....	152
<b>Chapter 7 General Conclusions and Future Recommendations.....</b>	<b>153</b>
7.1 Evaluation of external gelation of alginate and pectin by rheological measurements .....	155
7.2 Effect of physiological body fluids on the rheological behaviour of gellan gum .....	156
7.3 Novel model for simultaneous measurement of rheology and drug release (the Rheo-dissolution cell).....	157
<b>Chapter 8 References .....</b>	<b>160</b>

## List of Figures

Figure 1-1: Schematic diagram of highlighting the concept of <i>in situ</i> gelling formulations in comparison with non-gelling systems. ....	3
Figure 1-2: Diagram highlighting the concept of a simple rheological test whereby the sample is placed between a stationary lower plate and a rotating upper plate. ....	4
Figure 2-1: A schematic diagram demonstrating various types of deformation when force is applied in a longitudinal, lateral and isotropic direction (adapted from Mahdi, 2016).See the text for more details .....	14
Figure 2-2: A schematic diagram of basic geometries used for measuring biopolymer gels (A) cone and plate and (B) parallel plate. ....	17
Figure 2-3: Differences in stress response for elastic, viscous and viscoelastic materials, adapted from (Moxon, 2017).....	19
Figure 2-4: The relationships between stress in strain both within and beyond the LVR of viscoelastic materials. ....	21
Figure 2-5: Experimental determination of the LVR to enable the selection of an appropriate stress or strain for use in further small deformation oscillatory testing. ....	22
Figure 2-6: Characteristic mechanical spectra of dilute biopolymer solutions, concentrated entangled biopolymer solutions, structured liquids (weak gels) and strong gels , adapted from (Moxon, 2017).....	23
Figure 2-7: Characteristic temperature sweep showing changes in $G'$ and $G''$ as a function of temperature on cooling and heating highlighting the gel point and melting point for a thermoreversible gel. ....	26
Figure 3-1: Example of the condensation reaction that occurs during the formation of a glycosidic bond between monosaccharides. ....	32

Figure 3-2: Structural differences between a neutral sugar and an uronic acid showing the presence of a negative charge using glucose and glucuronic acid as an example.....	34
Figure 3-3: Representation of A) an entangled polymer solution and B) an ordered crosslinked gel. ....	35
Figure 3-4: Representation of development of an ordered polysaccharide network showing junction that occur through physical interactions and disordered connecting chains (adapted from Posocco et al., 2015). ....	37
Figure 3-5: Diagram highlighting sol-gel transitions for <i>in situ</i> gelling systems that can occur on exposure to changes in environmental conditions. ....	38
Figure 3-6: the monomers of alginate structure (a) M: $\beta$ -D-mannuronate; G: $\alpha$ -L-guluronate. (b) The alginate chain, chair conformation, (c) alginate chain sequences. M: $\beta$ -D-mannuronate; G: $\alpha$ -L-guluronate (adapted from Draget and Taylor, 2011). ....	40
Figure 3-7: Mechanism of calcium ions binding to G-blocks, proposed by (Morris et al., 1978). ....	41
Figure 3-8: Mechanism of external gelation (adapted from Smith and Miri 2010). ....	42
Figure 3-9: Mechanism of internal gelation (adapted from Smith and Miri, 2010). ....	43
Figure 3-10: Schematic structure of pectin illustrates different domains regions of pectin, (Leclere et al., 2013). ....	45
Figure 3-11: Structure of pectin (a) A repeating segment of pectin chains (b) carboxyl group (c) ester group (d) amide group (Sundar Raj et al., 2012). ....	46
Figure 3-12: Shows Schematic representation of calcium binding to polygalacturonate sequences of LM Pectin, (a) Pectin $\text{Ca}^{2+}$ complex (b) "Egg-box" dimer (c) aggregation of dimers. ....	48
Figure 3-13: The structure of gellan gum (a) is a native form and (b) is a low-acyl form (Osmalek, 2014). ....	50



Figure 3-14: Mechanism of gellan gum gelation. ....	51
Figure 3-15: Gel raft formation of alginate in the stomach, adapted from (Kim, 2014). ....	57
Figure 3-16: Shows using gellan gum fluid gel in a nasal drug delivery systems , adapted from (Mahdi, 2016). ....	59
Figure 4-1: Crosslinking model of calcium alginate (egg box) and EDTA calcium chelating. ....	66
Figure 4-2: <i>In situ</i> gelling experiments using a commercial rheometer. ....	70
Figure 4-3: Rheological measurements for alginate 4% showing variation of G' (filled symbols), G'' (open symbols) vs. time on exposure to A) 50 mM B) 100 mM and C) 200 mM; D) shows comparative values of G' of 4% alginate after 20 min exposure to (50, 100 and 200 mM) of CaCl <sub>2</sub> . ....	71
Figure 4-4: Rheological measurements of 4% alginate shows variation of G' moduli ; A) 4% alginate crosslinked with 200 mM CaCl <sub>2</sub> <i>in situ</i> , B) Gel dissolution using 500 mM EDTA , C) Gel dissolution with 500 mM Na citrate and D) comparative values of G' of 4% alginate after exposure to (500 mM) EDTA and Na citrate .....	73
Figure 4-5: Rheological measurements for pectin 4% showing variation of G' (filled symbols), G'' (open symbols) vs time on exposure to A) 50 mM B) 100 mM and C) 200 mM; D) shows comparative values of G' after 20 min exposure to (50, 100 and 200 mM) of CaCl <sub>2</sub> . ....	74
Figure 4-6: Rheological measurements of 4% pectin shows variation of G'; A) 4% alginate crosslinked with 200 mM CaCl <sub>2</sub> <i>in situ</i> , B) Gel dissolution using 500 mM EDTA , C) Gel dissolution with 500 mM Na citrate and D) comparative values of G' of 4% pectin after exposure to (500 mM) EDTA and Na citrate .....	76
Figure 4-7: Values of G' of <i>in situ</i> gelation time results for 4% alginate and pectin exposed to three different concentrations of CaCl <sub>2</sub> at 20 minutes. ....	77

Figure 4-8: Mechanical spectra of alginate 4% exposure to A) 50 mM B) 100 mM and C) 200 mM of $\text{CaCl}_2$ D) Comparing exposure alginate 4% to (50 , 100 and 200 mM) of $\text{CaCl}_2$ . G' (filled symbols), G'' (open symbols). ....	79
Figure 4-9: Mechanical spectra of pectin 4% exposed to A) 50 mM B) 100 mM and C) 200 mM of $\text{CaCl}_2$ ; D) Comparing exposed pectin 4% to (50 , 100 and 200 mM) of $\text{CaCl}_2$ . G' (filled symbols), G'' (open symbols). ....	80
Figure 5-1: Salivary gland types adapted from (Graney et al., 2009). ....	88
Figure 5-2: Eye anatomy diagram shows lacrimal gland and lacrimal sac adapted from (Sultana et al., 2006). ....	89
Figure 5-3: Anatomy of the stomach mucosa and the cells that produce the gastric fluid (Silbernagl, 2009). ....	90
Figure 5-4: Diagram of <i>in situ</i> gelling experiment using a commercial rheometer. ....	95
Figure 5-5: Rheological measurements of gellan gum (0.25, 0.5, 0.75 and 1%) <i>in situ</i> gelation with artificial saliva showing variation of G' (filled symbols) vs time on exposure to cations present in AS. ....	99
Figure 5-6: Rheological measurements of gellan gum (0.25, 0.5, 0.75 and 1%) <i>in situ</i> gelation with simulated wound fluid showing variation of G' (filled symbols) vs time on exposure to cations. ....	100
Figure 5-7: Rheological measurements of gellan gum (0.25, 0.5, 0.75 and 1%) <i>in situ</i> gelation with LF showing variation of G' (filled symbols) vs time on exposure to cations present in LF. ....	101
Figure 5-8: Rheological measurements of gellan gum (0.25, 0.5, 0.75 and 1%) <i>in situ</i> gelation with GF showing variation of G' (filled symbols) vs time. ....	102
Figure 5-9: Mechanical spectra measurements of gellan gum exposure to ions crosslinked present in AS. G' (filled symbols) & G'' (open symbols), frequency sweep test in a range of frequency between (0.1 -100) $\text{rad/s}^{-1}$ .....	103

Figure 5-10: Mechanical spectra measurements of gellan gum exposure to ions crosslinked present in SWF. G' (filled symbols) & G'' (open symbols), frequency sweep test in a range of frequency between (0.1 -100) rad/s <sup>-1</sup> .....	104
Figure 5-11: Mechanical spectra measurements of gellan gum exposure to ions crosslinked present in LF. G' (filled symbols) & G'' (open symbols), frequency sweep test in a range of frequency between (0.1 -100) rad/s <sup>-1</sup> .....	105
Figure 5-12: Mechanical spectra measurements of gellan gum exposure to ions crosslinked present in GF. G' (filled symbols) & G'' (open symbols), frequency sweep test in a range of frequency between (0.1 -100) rad/s <sup>-1</sup> .....	106
Figure 5-13: Rheological measurements of elastic modulus values (G') of <i>in situ</i> gelation time for different concentrations of gellan exposure to four types of physiological fluids. ....	107
Figure 5-14: Rheological measurements of elastic modulus values (G') at 20 minutes of <i>in situ</i> gelation time for different concentrations of gellan exposure to four types of physiological fluids. ....	108
Figure 5-15: Gelation kinetics for different concentrations of gellan exposure to 4 types of physiological fluids fitted to the Gompertz model showing A) rate constant vs concentration and B) maximum growth rate vs concentration.....	109
Figure 5-16: Comparison of G' during <i>in situ</i> gelation at time zero and at 25 min in samples that has the same final modulus.....	110
Figure 5-17: Profilometry images of the freeze dried samples of 0.25% gellan in GF, 0.75% gellan in LF and in SWF, 1% gellan in AS (a-d) and processed images after binarisation process (e-h).....	112
Figure 5-18: Numerical values of overall porosity of freeze dried gels. ....	113

Figure 5-19: 3D isometric surface images of the freeze dried samples of 0.25% gellan in GF, 0.75% gellan in LF and in SWF, 1% gellan in AS showing valleys and peaks on the surface with the deepest pores represented in blue.....	114
Figure 5-20: 3D surface texture parameters determined using Surfstand® software (a) arithmetical average of surface roughness, (b) highest peak of the surface, (c) lowest valley of the surface and (d) skewness of the surface. ....	115
Figure 5-21: Micro CT images of 0.25% Gellan gelled in gastric fluid, 0.75% gellan gelled in lacrimal fluid, 0.75% gellan gelled in wound fluid and 1% gellan gelled in saliva. ...	116
Figure 5-22: Schematic diagram of a proposed mechanism for achieving similar modulus values in different gellan concentrations. ....	121
Figure 6-1: Schematic diagram of a Rheo-Dissolution cell. ....	126
Figure 6-2: A) Rheo-dissolution cell B) Stainless steel mesh. ....	127
Figure 6-3: Represents experiment set-up of Rheo-dissolution device attached to a Rheometer. ....	130
Figure 6-4: Rheological measurements for 1% alginate methylene blue solution showing a variation of G' (black symbols), G'' (red symbols) vs. time upon exposure to 200 mM CaCl <sub>2</sub> for <i>in situ</i> gelation. A) Mesh opening area 61%. B) Mesh opening area 42%. C) Mesh opening area 39%. D) G' values of <i>in-situ</i> gelation test using three different mesh sizes. ....	132
Figure 6-5: Rheological measurements for 1% alginate methylene blue solution showing a variation of G' (black symbols), G'' (red and blue symbols) vs. time upon exposure to 200 mM CaCl <sub>2</sub> for <i>in situ</i> gelation and for EDTA and sodium dihydrogen citrate gel degradation for mesh opening area 61%. A) <i>In situ</i> gelation. B) <i>In situ</i> gelation and gel degradation by EDTA. C) <i>In situ</i> and gel degradation by sodium dihydrogen citrate. D) Comparison of <i>in situ</i> gel degradation between EDTA and sodium dihydrogen citrate. ....	134

Figure 6-6: Rheological measurements for 1% alginate methylene blue solution showing a variation of G' (Black symbols), G'' (Red and blue symbols) vs. time on exposure to 200 mM of CaCl <sub>2</sub> for <i>in situ</i> gelation and for EDTA and sodium dihydrogen citrate gel degradation for mesh opening area 61%. A) <i>In situ</i> gelation. B) <i>In situ</i> gelation and gel degradation by EDTA. C) <i>In situ</i> and gel degrade by sodium dihydrogen citrate. D) Comparison of <i>in situ</i> gel degradation between EDTA and sodium dihydrogen citrate.	136
--	-----

Figure 6-7: Rheological measurements for 1% alginate methylene blue solution showing a variation of G' (Black symbols), G'' (Red and blue symbols) vs. time on exposure to 200 mM CaCl <sub>2</sub> for <i>in situ</i> gelation and for EDTA and sodium dihydrogen citrate gel degradation for mesh opening area 61%. A) <i>In situ</i> gelation. B) <i>In situ</i> gelation and gel degradation by EDTA. C) <i>In situ</i> and gel degradation by sodium dihydrogen citrate. D) Comparison of <i>in situ</i> gel degradation between EDTA and sodium dihydrogen citrate.	138
---	-----

Figure 6-8: Rheological measurements for 1% alginate methylene blue solution showing a variation of G' (black, red and blue symbols) vs. time on exposure to 200 mM CaCl <sub>2</sub> for <i>in situ</i> gelation and EDTA and Na citrate for gel dissolution.	139
--	-----

Figure 6-9: Calibration curve of absorbance against concentration of methylene blue (MB).	140
---	-----

Figure 6-10: Impact of ion crosslinking (CaCl <sub>2</sub> ) and chelating agents (EDTA and sodium dihydrogen citrate) on methylene blue release from alginate gel.	142
---	-----

Figure 6-11. Rheological measurements of 1% alginate and release time of methylene blue from alginate gel, showing variation of G' (filled black symbols), concentration of MB (filled blue symbols) for A) mesh count 10, B) mesh 40, and C) mesh 60. D) Comparison of release time of methylene blue in EDTA using three different count numbers of mesh.	144
---	-----

Figure 6-12. Rheological measurements of 1% alginate and release time of methylene blue from alginate gel, showing variation of $G'$ (filled black symbols), concentration of MB (filled blue symbols) for A) mesh count 10, B) mesh 40, and C) mesh 60. D) Comparison of release time of methylene blue in Na Citrate using three different count numbers of mesh.....	146
---	-----

## List of Tables

Table 4-1: Alginate and pectin gels (gelled with 200mM CaCl <sub>2</sub> ) dissolution time results using EDTA and Na citrate, (mean=3) .	78
Table 5-1: Concentrations of mono and divalent cations in different types of physiological fluids saliva, lacrimal and wound fluids (Whelton, 1996; Levin et al., 2011; Cutting, 2003).	91
Table 5-2: Preparation of artificial saliva adapted from (Parker et al., 1999).	93
Table 5-3: Comparison of G' at time zero and at 25 min in samples that has the same final modulus (p<0.05). Showing mean values $\pm$ sd (n=3).	111
Table 6-1: Shows size and count number of three different types of mesh.	129
Table 6-2: Dissolution time and release percentage of methylene blue from alginate gel into CaCl <sub>2</sub> (T30 ), EDTA (Tend) and Na citrate (Tend) using three different mesh types .	147

## List of Abbreviations

<b>ABS</b>	Acrylonitrile butadiene styrene
<b>AS</b>	Artificial saliva
<b>CaCl<sub>2</sub></b>	Calcium chloride
<b>CaCO<sub>3</sub></b>	Calcium carbonate
<b>CMC</b>	Carboxy methyl cellulose
<b>DM</b>	Degree of methoxylation
<b>EDTA</b>	Ethylene diamine tetra acetic acid
<b>G</b>	Guluronic acid
<b>G'</b>	Elastic modulus
<b>G''</b>	Viscous modulus
<b>GalpA</b>	Galacturonic acid
<b>GF</b>	Gastric fluid
<b>H.M</b>	High methoxyl
<b>HG</b>	High acyl gellan
<b>HG</b>	Homogalacturonan
<b>L.M</b>	Low methoxyl
<b>LF</b>	Artificial lacrimal fluid
<b>LG</b>	Low acyl gellan
<b>LVR</b>	Linear viscoelastic region
<b>M</b>	Mannuronic acid
<b>NaCl</b>	Sodium chloride
<b>RG-I</b>	Rhamnogalacturonan-I
<b>RGII</b>	Rhamnogalacturonan II
<b>SWF</b>	Simulated wound fluid
<b>XGA</b>	Xylogalacturonan



# **Chapter 1 General Introduction**

# **CHAPTER ONE**

## **GENERAL INTRODUCTION**

### **1.1 Gelling materials**

The intermediate state of matter between solids and liquids is often referred to as gels and these materials are composed of a three dimensional polymer or colloidal network immersed in a fluid (Bakliwal and Pawar, 2010). When the liquid phase of a gel is water, gels can be referred to as hydrogels, or sometimes, described as aqueous gels as the hydrogel name indicates a material swollen in water (Gehrke and Lee, 1990). Polysaccharides are a class of natural materials of which a large number can form hydrogels in specific environmental conditions. The gels can be classified based on the nature of the bonds involved in the development of the three-dimensional solid network which is either by chemical bonds or physical association. Chemical crosslinking forms strong covalent bonds that connect the network together usually by a crosslinker or a functionalized group on the polymer chain. These are sometimes termed chemical gels. Physical gels on the other hand are formed by physical association through hydrogen bonding, electrostatic interactions, hydrophobic interactions and van der Waals forces which maintain and stabilise the gel network (Bakliwal and Pawar, 2010). It is the behaviour of these physical gels prepared from polysaccharides which is the major focus of this thesis.

Polysaccharide materials have traditionally been one of the major focuses of food research, and more recently in pharmaceutical and biomedical materials research, due to their multi functionality as gelling agents, thickeners, suspending agents and stabilisers (Sutherland, 2007). It is however, the gelling ability of polysaccharides which is arguably the most interesting feature of polysaccharides with regard to academic and industrial applications (Smith and Miri, 2011).

### 1.1.1 *In situ* gelling agents

The ability of polysaccharides to form gels in various physiological environments in response to changes in temperature, pH and ionic strength has been of particular interest for pharmaceuticals and biomedical applications. This is in addition to other various advantageous features that include low toxicity, natural source and the relatively low cost of these materials. The concept of *in situ* gelling systems is that the formulations are developed and administered in a pre-gelled liquid state, which then rapidly convert to the solid gelled state on contact with the physiological target site. Thus, increasing the retention time of the formulation at the desired site of action (or uptake) improving the bioavailability of active ingredients (Chitkara et al., 2006; Hatefi and Amsden, 2002). This process is described in Figure 1.1.

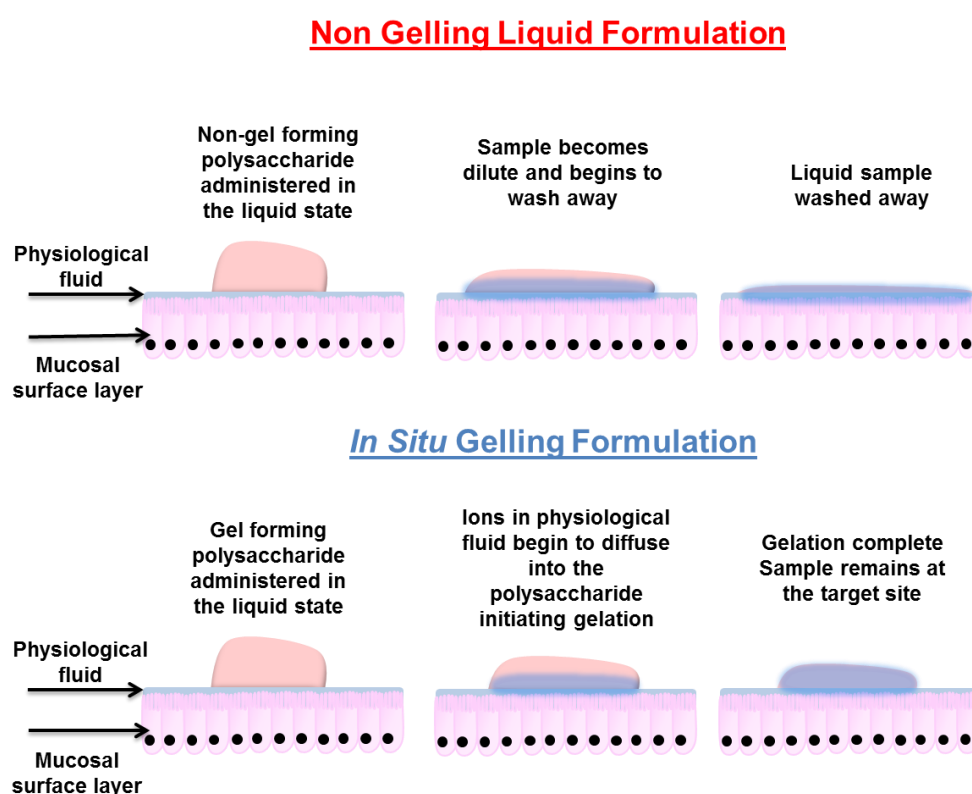
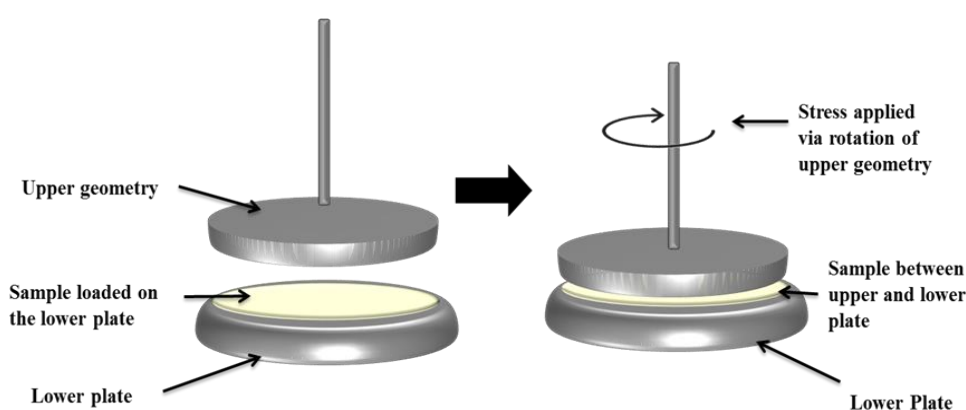


Figure 1-1: Schematic diagram of highlighting the concept of *in situ* gelling formulations in comparison with non-gelling systems.

Accurately measuring the rate of gelation and final gel strength of *in situ* gelling systems can be challenging due to the rapid sol-gel transitions on physiological contact. Measuring the gelation of polysaccharides that gel thermally is relatively straightforward using commercially available rheometers fitted with a Peltier plate that can accurately control the sample temperature. Rapid gelation reactions that occur on contact with ions or by changes in pH however, are much more difficult to measure in real time using conventional rheological equipment.

### 1.1.2 Current techniques for measuring rapid gelation *in situ*

The simplest method to demonstrate gelation is to turn a test tube or vial containing the sample upside-down and then to note whether the sample flows under its own weight. It is assumed that a gelled sample will not flow whereas a viscous sample will show visible flow (Macosko and Larson, 1994). This does not however, provide any meaningful quantitative data. The most useful technique to monitor the gelation is by using a rheometer whereby the sample is placed between a stationary lower plate and an upper plate that applies a shear force to the sample (Figure 1.2.) and depending on the nature of the force applied (either steadily in one direction or oscillation) can be used to measure viscosity and viscoelasticity of materials.



**Figure 1-2: Diagram highlighting the concept of a simple rheological test whereby the sample is placed between a stationary lower plate and a rotating upper plate.**

Controlling environmental conditions however, can be challenging. The bottom plate is usually controlled by a Peltier system allowing for thermal control, but to analyse effects of changes in pH or ionic strength requires environmental conditioning of the polysaccharide prior to loading onto the rheometer. This can be particularly difficult in some gelling polysaccharides such as alginate, pectin and gellan gum as gelation is almost instantaneous. Previous methods used to measure ionic *in situ* gelling polysaccharides have included the controlled release of crosslinking ions from an insoluble source (Draget et al., 1990; Draget, 2000; Draget et al., 2006a), the use of sequestering agent such as ethylene diamine tetra acetic acid (EDTA) to slow down gelation (Toft, 1982) and using the slowly hydrolysing n-glucono delta-lactone (GDL) to gradually lower the pH and release the complexed ions into the polysaccharide solution.

All of these methods allow the mixing of crosslinking ions with the biopolymer without immediate gelation which is not what occurs when applied to physiological systems. Moreover, the gels produced using these methods tend to be considerably more homogeneous than those produced by direct mixing of polysaccharides and free crosslinking ions. Therefore, to replicate physiological exposure and produce gels that are alike to those *in situ* gelling systems, the usual method is to load the polysaccharide of interest into dialysis tubing and then immerse it into a solution containing the required crosslinking ions for various periods of time before removing and cutting the gel to an appropriate size for rheological testing (Kubo et al., 2003; Miyazaki et al., 2000). Another similar method that has been used is to add polysaccharide solutions into tissue culture plates containing filter paper that is soaked with soluble crosslinking ions whereby one is placed beneath the polysaccharide and one placed on top.

The polysaccharide would then be allowed to gel for selected time periods before the rheological properties are measured (Hunt et al., 2010; Jahromi et al., 2011). Unfortunately, neither of these approaches provides a realistic insight into the real time gelation of rapidly gelling systems. Despite the obvious industrial usefulness of such materials in foods, pharmaceuticals and biomedical applications there is an obvious gap in techniques that can suitably quantify rheological behaviour in these rapidly gelling materials. To try to address this problem this thesis describes modifications made to a commercially available rheometer that facilitates rheological measurements of rapidly gelling *in situ* gelling materials in contact with external source of crosslinking ions.

## **1.2 Aims and objectives**

### **1.2.1 Thesis aims**

The overall aims of this work was to develop rheological techniques that are suitable to measure the gelation behaviour of rapid setting ionically gelling polysaccharides *in situ*, by modifying a commercial rheometer.

### **1.2.2 Objectives**

The objectives to achieve the aims of this work were to design two modifications to the lower plate of a rheometer and evaluate the suitability for measuring polysaccharide gelation of a variety of industrially relevant polysaccharides using various crosslinking fluids. Working towards these objectives included the investigation of two different adaptations of the lower plate of a commercially available rheometer.

#### **1.2.2.1 Petri-dish adaptation**

A petri-dish containing a filter paper soaked in crosslinking fluid was covered with a dialysis membrane, which acted as the lower plate of the rheometer, which was then applied to investigate the following tests:

- Gelation and dissolution time of alginate and pectin gels crosslinked with calcium chloride *in situ*.
- Apply the *in situ* gelation method as a model to investigate the impact of simulated physiological fluids on the rheological behaviour of gellan gum.

#### **1.2.2.2 Rheo-dissolution cell adaptation**

The second adaptation used a 3D printed lower plate that was designed to containing a reservoir into which a solution of crosslinking ions could be added to investigate the following tests:

- External gelation of alginate that loaded with methylene blue as a model of drug on exposure to calcium chloride (cross linker ions) *in situ*.
- To investigate dissolution time of alginate gel that formed on exposure to  $\text{CaCl}_2$  using calcium chelating agents (EDTA and sodium citrate).
- The effect of various mesh sizes was investigated in relation to drug accumulation in the reservoir, and on the rheological behaviour, as these are key to validating the method as a potential rheo-dissolution device.

Overall, these objectives were designed to inform on the feasibility of employing various modifications to the lower plate of a rheometer to enable measuring rapid gelation kinetics in a more biorelevant environment than what is currently available.

### 1.3 Thesis structure

This thesis covers the design, development and production of apparatus that can be applied as a lower plate of commercially available rheometers to facilitate the measuring of rapidly gelling polysaccharides on contact with ionic crosslinkers. The development of this apparatus was investigated to create more realistic environment for measuring *in situ* gelling systems which are becoming popular drug delivery systems, retaining drugs at the site of action/uptake for longer subsequently increasing bioavailability.

- Chapter 2 provides background theory to rheological techniques and the functional capacity of commercially available rheometers. This provides the background information on which all the results chapters (Chapter 4-6) are based. Specific methodologies, which apply to the individual developed apparatus that were investigated, are given separately in the appropriate chapters.
- Chapter 3 provides an in depth background of the gel forming polysaccharides used throughout this thesis (alginate, pectin and gellan gum). This presents an insight into their chemical structure and conformational properties, gelation mechanisms and applications as *in situ* drug delivery systems
- The development of apparatus and initial results begin in Chapter 4, which discusses the results obtained developing a technique for measuring the external gelation of alginate (published as “*in situ* rheological measurements of the external gelation of alginate” (Mahdi, Diryak, Kontogiorgos, Morris and Smith, 2016)). This begins with a description of current techniques used to measure external alginate gelation and the difficulties involved in making such measurements. Then information on the development of a modified lower plate for a rheometer is provided highlighting the specifications, components, and dimensions. The final part of Chapter 4 discusses the



potential use of the developed rheometer modification to measure the rapid gelation of alginate on exposure to a source of  $\text{Ca}^{2+}$  ions. Moreover, it is demonstrated that the method is suitable for measuring rapid external gelation but also can be modified to measure dissolution of  $\text{Ca}^{2+}$  crosslinked alginate gels on exposure to  $\text{Ca}^{2+}$  chelating solutions.

- Chapter 5 presents results using the system developed in Chapter 4 and focuses on using the platform to recreate a more realistic physiological environment for *in situ* gelation (submitted for publication as “Experimental simulation of the gelation behaviour of *in situ* cross-linked hydrogels on contact with physiological fluids” (Diryak, Ghorri, Kontogiorgos, Morris and Smith, 2017)). This chapter begins with an introduction to the challenges associated with developing biorelevant models for *in situ* gelling systems and describes various physiological target sites (oral cavity, eye, stomach and skin wounds) and in particular the ionic environment of these sites. Simulated physiological fluid was then used to as a source of crosslinking ions for the *in situ* gelation of gellan gum, to investigate the gelation strength and gelation kinetics at various physiological target sites. Moreover, the microstructures of the gels formed were explored to evaluate how this influences gel strength in the different simulated physiological conditions.
- The final results chapter (Chapter 6) describes the development of a 3D printed lower plate that contains a reservoir in to which different crosslinking solutions could be added. The developed lower plate not only facilitates the delivery of crosslinking solutions to materials during rheological testing but provides the mechanism for sampling from the reservoir which allows quantitative analysis of the release of model active ingredients. The chapter provides details of the lower plate design and demonstrates a proof of concept for “rheo-dissolution” which is defined as simultaneous measurement of rheology and drug release *in situ*.

- The final, chapter (Chapter 7) provides a summary of the conclusions from this thesis along with recommendations for future work.

## 1.4 Publications and presentations

Publications from this thesis are as follows

### Journal Publications:

- Mahdi, M.H., Diryak R., Kontogiorgos V., Morris G.A and Smith, A.M. (2016) *In situ* rheological measurements of the external gelation of alginate Food Hydrocolloids 55, 77-80
- R. Diryak, V. Kontogiorgos, M. U. Ghori, P. Bills, A. Tawfik, G. A. Morris, A. M. Smith, (2018) Behavior of in situ cross- linked hydrogels with rapid gelation kinetics on contact with physiological fluids, Macromolecular Chemistry and Physics 1700584.

### Conference presentations:

- Diryak R., Mahdi, M.H., Murphy, S., Hill, A., Morris G. and Smith, A.M. (2015) *In situ* rheological measurements of the external gelation of alginate. 2nd UK Hydrocolloids Symposium, Birmingham UK
- Diryak R., Morris G.A and Smith, A.M. (2016) Evaluation of *in situ* Gelation of Gellan Gum in Various Simulated Physiological Fluids. AAPS Annual Meeting and Exposition, Denver, USA

## Chapter 2 **Rheology**

## **CHAPTER TWO**

### **RHEOLOGY**

#### **2.1 Introduction to rheology**

The majority of the experimental work undertaken in this thesis is rheological measurements of polysaccharides during gelation and dissolution, therefore the main concepts and fundamental principles of rheology will be discussed. This is then followed by a review of rheometer types with a particular focus on modifications and add-ons that can be applied to commercial rheological equipment to facilitate specific measurements in application specific environments.

The word rheology originates from two Greek words, “rheo” and “logos”; “Rheo” meaning flow and “Logos” meaning “reasoning”. Rheology therefore is the study of deformation and flow of materials. The term rheology was first used by Professor E.C. Bingham and was accepted in 1929 with the formation of the Society of Rheology. Fundamentally, rheology is the analysis of material behaviour under the application of stress and is generally expressed through the relationship between stress and strain in a material as a function of temperature, time, frequency etc. When a force (stress) is applied to a material the resulting deformation (strain) is the response to this action (Martin et al., 2011) therefore how a material behaves under stress provides an insight into the type of material being tested as materials are classified according to their observed physical behaviour. Generally, under stress materials behave in an elastic (solid like) manner or viscous (liquid like) manner with the two extremes being a perfect (Hookean) elastic solid or a perfect Newtonian Liquid. Most materials however, which includes the gel forming polysaccharides investigated in this thesis, have properties that are both elastic and viscous, and therefore are termed viscoelastic (Marriott, 2007)

## 2.2 Stress and strain

Stress is defined as the force (**F**) applied per unit area (**A**) acting upon a material and is expressed in units of pressure (Pa) as expressed in equation 2.1.

$$\tau \text{ (Pa)} = F/A \quad \text{Eq. 2.1}$$

In all rheological measurements, the procedure is to either apply a force to the test material and measure the resulting deformation (strain) or apply a deformation and measure the resistance to the deformation (stress). Force can be applied in various directions which will result in differing deformation. These are compression (or tension) when the force is in the longitudinal direction, shear when the force is applied laterally and bulk stress when the force is isotropic i.e. from all directions (Figure 2.1). The application of stress to a material results in a strain (deformation) which is a dimensionless ratio and therefore has no units as given in equation 2.2.

$$\varepsilon = \Delta l / l \quad \text{Eq. 2.2}$$

Where  $\Delta l$  is the change in length and  $l$  is the original length of the material before the applied stress. The relationship between stress and strain can be used to determine the modulus, however, as stress can be applied in a range of directions the way modulus is calculated also varies.

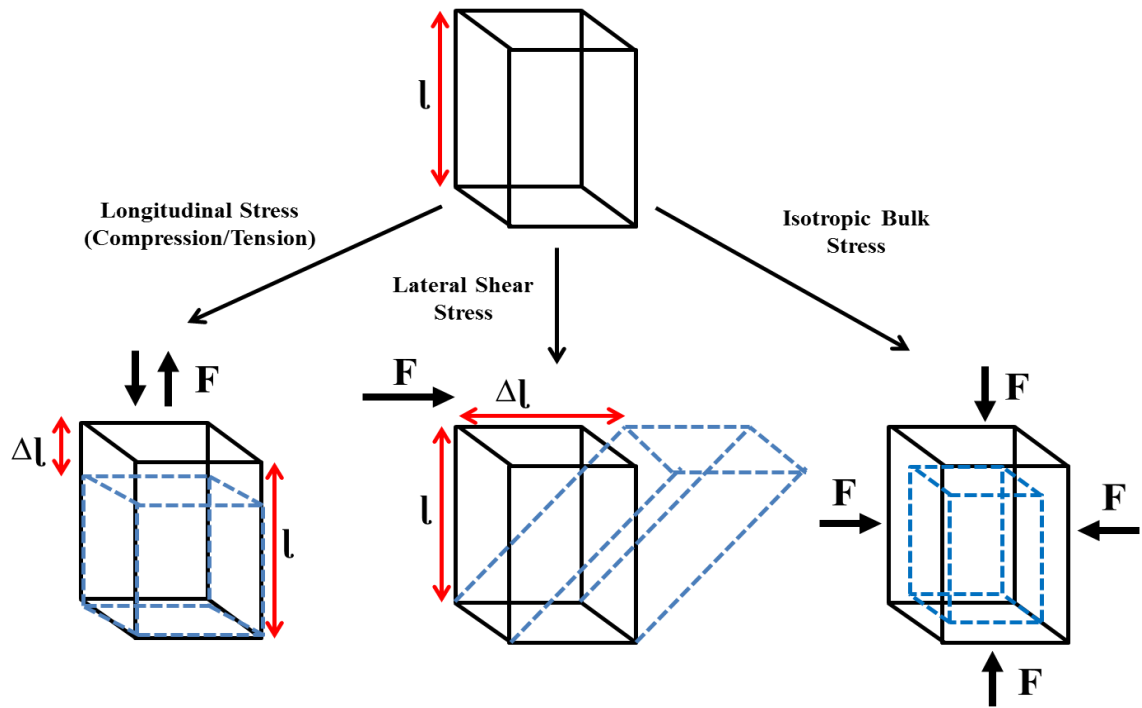


**Figure 2-1: A schematic diagram demonstrating various types of deformation when force is applied in a longitudinal, lateral and isotropic direction (adapted from Mahdi, 2016). See the text for more details**

### 2.2.1 Longitudinal (Young's) modulus

Young's modulus tends only to be determined for materials that have a defined shape and size by the application of longitudinal stress either in compression or in tension. Following an applied force, the energy is stored in the material and once the force is removed the energy is recovered returning the material to its original dimensions. A good example of this behaviour is a spring which remains compressed (or extended under tension) until the stress is removed whereby it recovers to its original position. This mechanical behaviour can be described by Hooke's law which states that stress is proportional to strain but independent of the rate of strain. Therefore, Young's modulus ( $E$ ) is calculated by longitudinal stress  $\tau$  divided by the strain ( $\epsilon$ ) (equation 2.3).

$$E \text{ (Pa)} = \text{stress} / \text{strain} = \tau / \varepsilon \quad \text{Eq. 2.3}$$

### 2.2.2 Shear modulus

Shear modulus ( $G$ ) is more readily used for soft viscoelastic materials that often cannot support their own weight and therefore unsuitable for characterisation using compression or tension. Biopolymers such as the *in situ* gelling polysaccharides investigated in the work described in this thesis are usually characterised in this manner. When determining  $G$  a lateral stress is applied tangentially through an angle  $\theta$  to the test material causing a deformation. The shear stress ( $\sigma$ ) is given by equation 2.4, where  $F$  is the lateral force applied to deform the sample through the angle  $\theta$  and  $A$  is the tangential area.

$$\sigma \text{ (Pa)} = F/A \quad \text{Eq. 2.4}$$

The shear strain ( $\gamma$ ) that occurs as a result of the applied stress is determined using equation 2.5

$$\gamma = \Delta l / l = \tan (\theta) \quad \text{Eq. 2.5}$$

Where  $\Delta l$  is the tangential displacement and  $l$  represents the sample thickness. From the relationship between the shear stress and the shear strain the shear modulus can be calculated accordingly using equation 2.6.

$$G \text{ (Pa)} = \text{shear stress} / \text{shear strain} = \sigma / \gamma \quad \text{Eq. 2.6}$$

### 2.2.3 Bulk modulus

Bulk modulus (**K**) is rarely used to characterise the mechanical properties of soft materials such as polysaccharide gels. The principle of bulk modulus however, is that almost all matter can undergo some level of compression and therefore all have bulk modulus. It is defined as the modulus of volume expansion. If isotropic stress is applied to solid materials, a relative change in volume occurs. The ratio of the isotropic stress to the change in volume is defined as the bulk compression modulus and can be determined using equation 2.7 (Mahdi, 2016).

$$K \text{ (Pa)} = \sigma_v / \epsilon_v \quad \text{Eq. 2.7}$$

Where bulk stress is  $\sigma_v$  and volumetric strain is  $\epsilon_v$ .

## 2.3 Rheological measurements of biopolymer gels

For biopolymer gels which exist as viscoelastic liquids or viscoelastic solids and often change between both of these states during application, rheological measurements are made using oscillatory shear rheometry. This technique allows for simultaneous analysis of both elastic (solid) response and viscous (liquid) response to an applied stress (Picout and Ross-Murphy, 2003). Rheological characterisation using oscillation involves the application of sinusoidal stress (or strain) to a sample immobilised between an upper disc and a lower plate. Usually, the upper disc applies the oscillatory stress while the bottom plate remains stationary. For the vast majority of measurements involving polysaccharide gels, the top, stress loading geometry (upper disk) is either a flattened ‘parallel plate’ or cone that has been truncated (Figure 2.2).



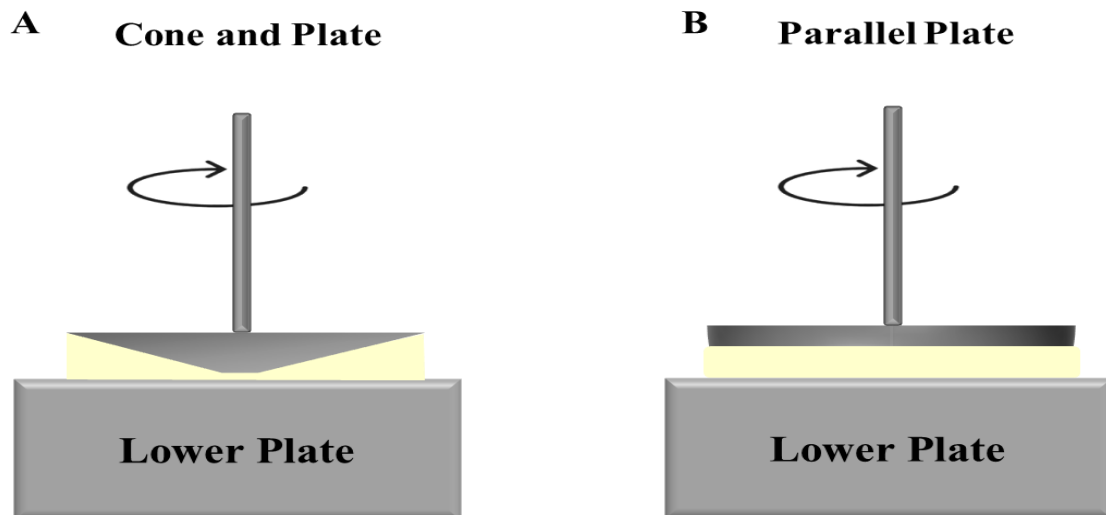


**Figure 2-2: A schematic diagram of basic geometries used for measuring biopolymer gels (A) cone and plate and (B) parallel plate.**

The geometry chosen for the measurements can directly impact results obtained. This is because there are differences in how the stress is transmitted through the sample when using parallel or coned geometries. When using a parallel plate, the applied stress at the outer radius of the parallel plate is much greater than those applied at the inner radius however the software that run most modern rheometers usually take an average value of the applied stress. Cone and plate geometries reduce this problem as the stress is applied uniformly across the geometry diameter and is therefore homogeneously applied to the sample. Moreover, these measuring systems can also show variance dependent upon geometry diameter (Ewoldt et al., 2015) with smaller diameter geometries better suited to stiffer materials and larger geometries more suitable for weak materials due to having a larger surface contact with the sample.

During shear oscillation measurements the sample materials constrained between the geometry and the lower plate is subjected to sinusoidally oscillating stress (or strain), and the viscoelastic material characterisation is revealed by the manner in which the stress is transmitted through the sample. In elastic materials the stress is transferred and stored by the sample whereas in viscous materials the stress is dissipated as heat.

This results in different relationships between oscillation phases of stress and strain between viscous and elastic materials. In perfectly elastic materials stress and strain are completely in phase whereas in perfectly liquid materials are out of phase with one another. Therefore, in viscoelastic materials the phase lag ( $\delta$ ) is somewhere between completely in phase and completely out of phase. This method of measurement can therefore characterise a materials elastic response and viscous response which in turn, provides a useful insight into polymer-polymer interactions and their relative contribution to viscoelasticity.

For instance, if a sinusoidal strain wave at a fixed low amplitude ( $\gamma_0$ ) and angular frequency ( $\omega$ ) as a function of time ( $t$ ) is applied to a sample the strain input will be:

$$\gamma = \gamma_0 \sin \omega t \quad \text{Eq. 2.8}$$

The resulting shear stress will also be a sine wave but with a different stress amplitude ( $\sigma_0$ ) and phase as shown in equation 2.9

$$\sigma = \sigma_0 \sin (\omega t + \delta) \quad \text{Eq. 2.9}$$

Where  $\delta$  is the phase angle between the strain and stress waves.

Purely elastic materials display no phase lag ( $\delta = 0$ ). Perfect liquid materials exhibit a  $\delta$  value of  $90^\circ$  due to viscous losses resulting in out of phase stress and strain. Therefore, viscoelastic materials have a phase lag that falls between  $0^\circ$  and  $90^\circ$  whereby more solid like materials have a phase lag closer to  $0^\circ$  and more liquid like materials closer to  $90^\circ$  (Figure. 2.3). (Osada and Khokhlov, 2001).

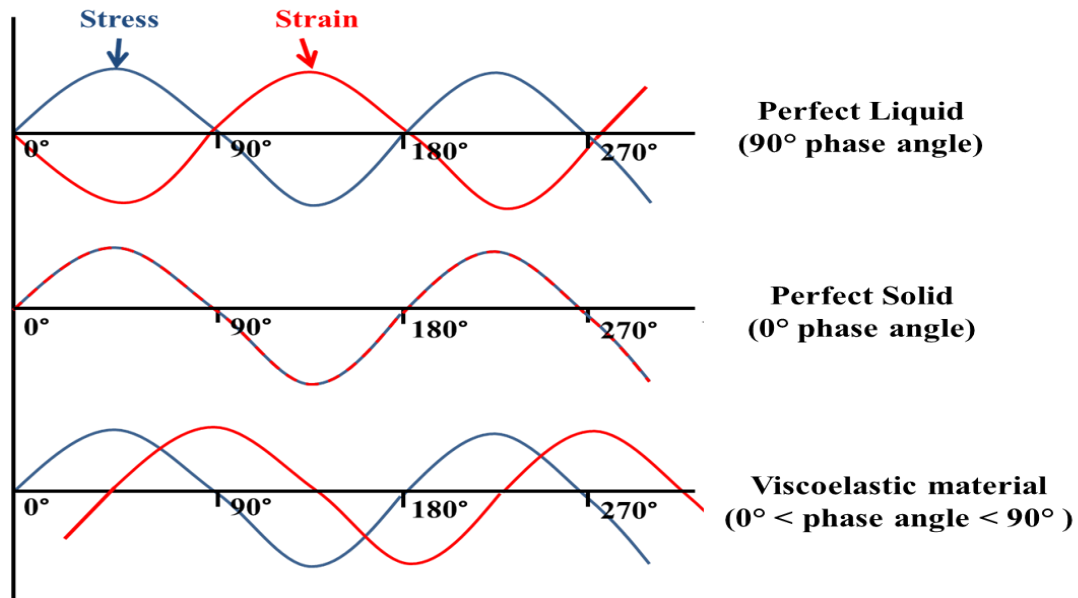


**Figure 2-3: Differences in stress response for elastic, viscous and viscoelastic materials, adapted from (Moxon, 2017).**

Polysaccharide gels are excellent examples of viscoelastic materials and by studying in-phase and out-of-phase behaviour several key parameters can be derived that demonstrate mechanical properties. In practice this is achieved by resolving the in phase and out of phase components. The elastic component of a viscoelastic material is represented by the ratio of in phase stress to strain and is termed the elastic or storage modulus ( $G'$ ). This is representative of the amount of energy stored in a material and how much is recovered per stress/strain cycle and can be calculated using equation 2.10.

$$G' = (\sigma_0 / \gamma_0) \cos \delta \quad \text{Eq. 2.10}$$

In a perfect solid  $G'$  is completely independent of oscillatory frequency or shear stress. Viscoelastic materials on the other hand, show dynamic changes in  $G'$  as a response to changes in frequency or stress.

The viscous component a viscoelastic material is represented the amount of energy dissipated per cycle and can be calculated by the ratio of out-of-phase stress divided by strain (equation 2.11) and is termed the viscous or loss modulus ( $G''$ ).

$$G'' = (\sigma_0 / \gamma_0) \sin \delta \quad \text{Eq. 2.11}$$

The overall stress response is defined by the complex modulus ( $G^*$ ) which is reflective of the ratios of stress and strain amplitudes regardless of storage or loss responses.

$$G^* = \sqrt{(G')^2 + (G'')^2} \quad \text{Eq. 2.12}$$

The complex modulus is frequently used to determine the complex dynamic viscosity ( $\eta^*$ ) which another important indicator of viscoelastic behaviour that can often be interpreted as analogous to the sample viscosity when measured using steady shear rather than oscillation. This is calculated from the ratio between  $G^*$  and the frequency of oscillation (equation 2.13).

$$\eta^* = G^* / \omega \quad \text{Eq. 2.13}$$

From a simpler perspective, in viscoelastic materials such as polysaccharide gels,  $G'$  is a representation of how ‘solid-like’ the sample material is and  $G''$ , how ‘liquid-like’. Therefore, a solid self-supporting gel would generally exhibit a  $G'$  that is higher than  $G''$  as the material is more solid like, with the difference between the two indicative of the material strength. In contrast, if  $G''$  is much larger than  $G'$  the material behaviour would be more liquid like where the energy has dissipated greater than it was stored (Rao, 2013).

### 2.3.1 Common oscillatory tests

Applying small deformation oscillatory methods can be used to elucidate many different properties of polysaccharide gels which include gel strength, elasticity, stress at fail, gelation and melting points and also gelation kinetics. In determining these different mechanical properties using small deformation oscillations it is often necessary to perform such measurements within the linear viscoelastic region (LVR).

### 2.3.2 Determining the linear viscoelastic region

The LVR is the range of stress in which the test material exhibits a proportional strain response figure 2.4 (Coleman and Noll, 1961) Therefore, within the LVR, a viscoelastic material will not be ruptured allowing these dynamic measurements to probe the material's microstructure (Mezger, 2006).

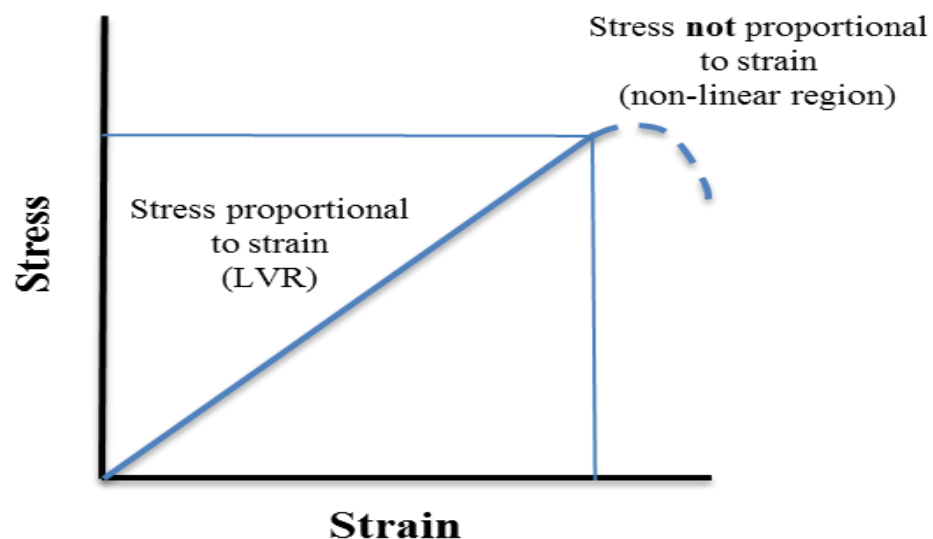


**Figure 2-4: The relationships between stress in strain both within and beyond the LVR of viscoelastic materials.**

The LVR can be determined experimentally by subjecting the test material to a gradually increasing shear stress until the deformation of the sample is sufficiently large and elasticity is lost. This is usually performed on a rheometer by using an amplitude sweep whereby the sample is maintained at a constant temperature and increasing oscillatory stresses are applied at a constant frequency. The strain response is then measured and used to plot  $G'$ . The stress is increased until the modulus begins to decrease due to failure of the sample (Figure 2.5). This indicates the onset of non-linear elasticity and the end of the LVR. Once the LVR has been determined for a particular sample, a stress (or strain) value that is well within the LVR is selected and used in all other small deformation oscillatory analysis that are performed on the sample.

Amplitude sweep measurements are a simple and convenient method of determination of the LVR and in addition provide information on the critical stress (or strain) at failure of the sample which can be useful when designing formulations for industrial application.

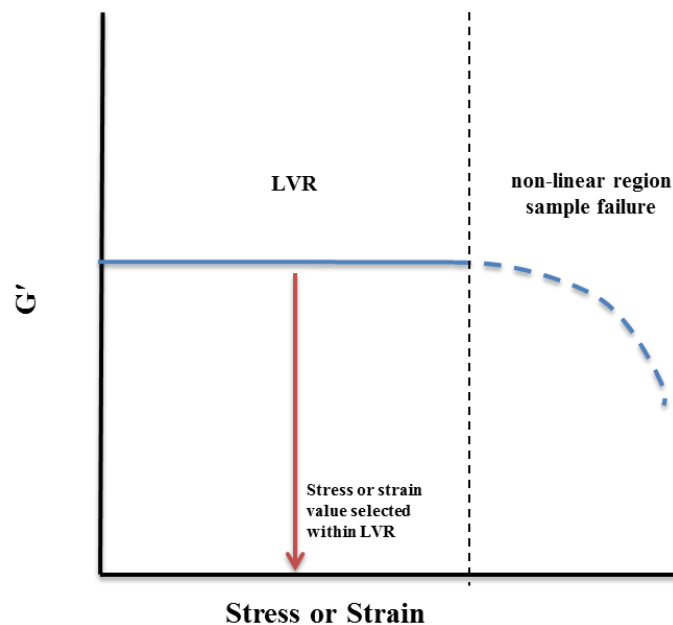


**Figure 2-5: Experimental determination of the LVR to enable the selection of an appropriate stress or strain for use in further small deformation oscillatory testing.**

### 2.3.3 Mechanical spectra (Frequency sweeps)

Once the LVR has been determined mechanical spectra profiles can be obtained by measuring the frequency dependence of  $G'$ ,  $G''$  and  $\eta^*$ . This can provide useful information on characteristic structural properties of polysaccharide samples. Figure 2.6 illustrates the characteristic mechanical spectra for typical polysaccharide systems that include dilute solutions, concentrated biopolymer solutions, and structured biopolymer liquids (weak gels). strong biopolymer gels (true gels).

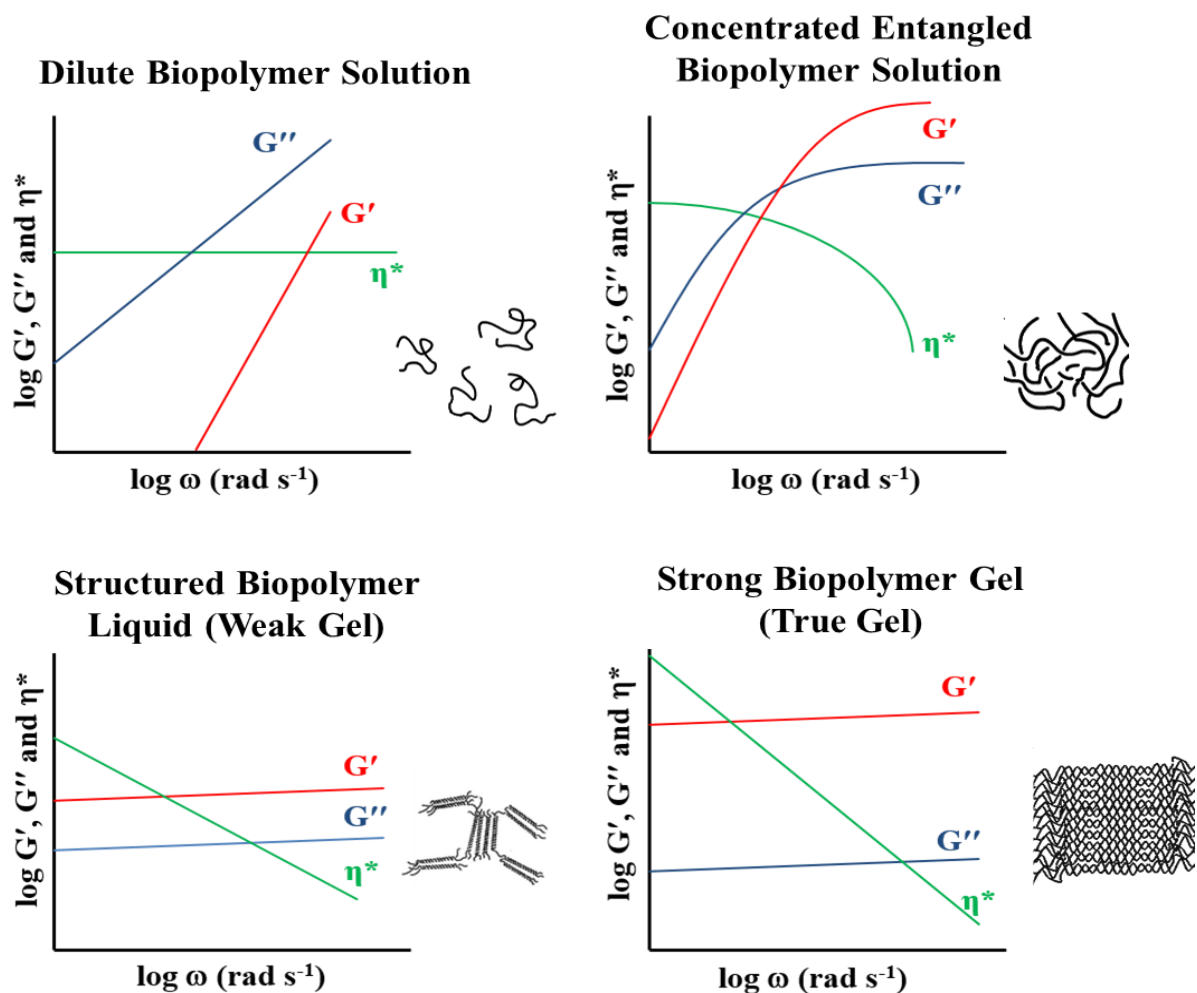


Figure 2-6: Characteristic mechanical spectra of dilute biopolymer solutions, concentrated entangled biopolymer solutions, structured liquids (weak gels) and strong gels , adapted from (Moxon, 2017).

In dilute biopolymer solutions the concentration of polymer molecules is low enough so that they do not interact with one another and are considered to be in isolation and free to move independently. This behaviour is characterised by a dominance of  $G''$  over  $G'$  with both moduli increasing with increasing angular frequency while complex dynamic viscosity is independent of angular frequency. Concentrated entangled biopolymer solutions are also characterised by a dominance of  $G''$  over  $G'$  at low frequencies behaving like a dilute solution. This is because at low frequencies of oscillation the entangled polymer chains have enough time to rearrange within the time period of the oscillation (Morris, 1981; Clark, 1992).

As the frequency of oscillation increases however,  $G'$  becomes greater than  $G''$  displaying solid like behaviour. This is due to the reduced time for entangled polymer to detach from each other between each oscillation manifesting in a solid like response. More simply, molecular chains at higher frequencies behave like a cross-linked gel, as within one oscillation period there is no time for interchain entanglements to come apart. But at lower frequencies, molecular chains have a behaviour similar to dilute polymer solutions, as the long periods of oscillation allow chains to disentangle and rearrange (Miyoshi et al., 1996). Complex dynamic viscosity also transitions from being independent of frequency to inversely proportional to frequency.

Structured biopolymer liquids (sometimes referred to as weak gels) are classified between concentrated entangled biopolymer solutions and strong gels. In concentrated entangled biopolymer solutions, the polymer molecules are entangled whereas in structured biopolymer liquids there are a network of ordered structures associated at junction zones. The mechanical spectrum of structured biopolymer liquids is characterised by a  $G'$  that is higher than  $G''$  with a slight frequency dependence. Complex dynamic viscosity decreases with increasing angular frequency and although an elastic response to small deformations is observed, on exposure to large deformations beyond the LVR structured biopolymer liquids flow and can be poured rather than fracturing which would be the response to high stresses in a 'true' gel (Clark and



Ross-Murphy, 2009). Strong gels (sometimes referred to as firm gels or true gels) have a similar characteristic mechanical spectrum to structured biopolymer liquids, exhibiting a  $G'$  that is greater than  $G''$ , however differences between the two values is much greater at all frequencies (often in the order of 5-50 times greater), (Clark and Ross Murphy, 1987; te Nijenhuis, 1997; Kavanagh and Ross-Murphy, 1998). Complex dynamic viscosity also reduces with increased frequency however true gels cannot be poured responding to excessive stress by fracturing.

### **2.3.4 Determination of the gelation/melting point**

Small deformation oscillatory measurements of  $G'$  and  $G''$  (within the LVR) are often used to detect mechanical changes in viscoelastic properties of polysaccharides when changing from sol to gel and vice versa as both moduli can change significantly. Gelation events can occur as a response to environmental changes such as temperature. Many polysaccharides form thermoreversible gels and this approach is used to evaluate their melting characteristics and gelation behaviour. Thermal gelation (or melting) can be initiated *in situ* on a rheometer fitted with a temperature controlled lower plate. To analyse gelation (or melting), the strain input and angular frequency are kept constant while  $G'$  and  $G''$  monitored as a function of temperature. In thermally gelling systems, prior to gelation values of  $G''$  are greater than the value of  $G'$  however, as the temperature progresses through the samples sol-gel transition temperature a dramatic increase  $G'$  occurs rising to values that are significantly higher than  $G''$ . The point at which  $G'$  and  $G''$  cross is often taken as the gel point (Figure 2.7). Polysaccharides can also undergo changes in rheological behaviour as a function of time under isothermal conditions which can also be analysed in this manner and over time, the pseudo-equilibrium values of the elastic  $G'$  and viscous  $G''$  moduli are reached which are characterised by a pseudo-plateau of the moduli.

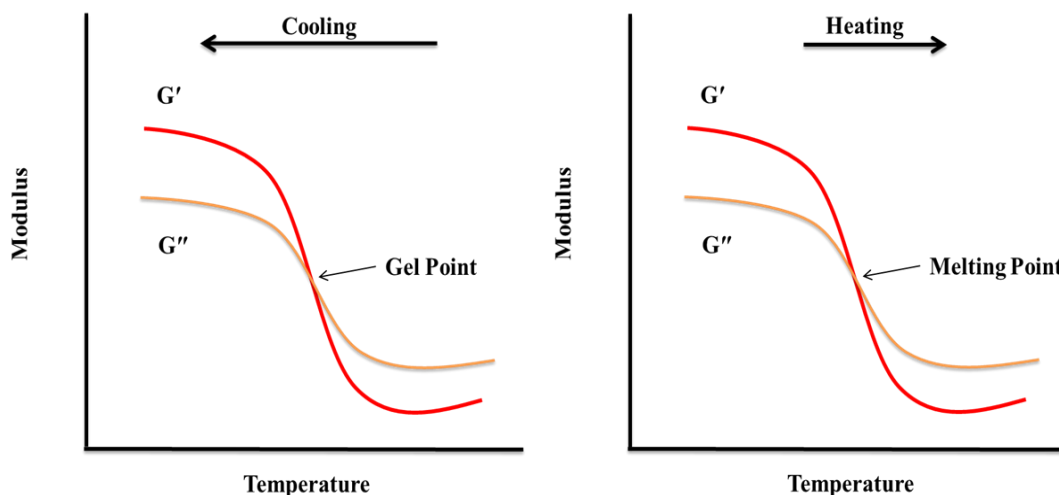


**Figure 2-7: Characteristic temperature sweep showing changes in  $G'$  and  $G''$  as a function of temperature on cooling and heating highlighting the gel point and melting point for a thermoreversible gel.**

## 2.4 Adaptations and limitations

Over the past few decades' rheology has proved a powerful technique in developing the fundamental understanding of polysaccharide behaviour and microstructure in the hydrated state by using precisely controlled stresses and strains at controlled temperatures. These methods are also often developed using parameters that mimic specific industrial processes. This has led to some innovative and high value applications of these materials. The physical behaviour of polysaccharides has traditionally been one of the major focuses of food research, they have also found use in pharmaceutical and biomedical applications. Gel forming polysaccharides used in encapsulation and controlled release technologies are of particular interest and are now widely investigated for such applications.

These systems however, often function by changing state either melting or gelling in various physiological environments. Many of the polysaccharides used for such applications have very rapid gelation kinetics on contact with the physiological environment which may be due to changes in temperature, pH or the presence of salts in physiological fluid (Olhero, 2000).

Imitating temperature dependant changes can easily be measured using commercially available rheometers. Monitoring rapid gelation due to changes in pH or ionic strength, however, is much more challenging. This is because introducing solutions to trigger the gelation of the polysaccharide when loaded between the upper and lower plate of the rheometer cannot be achieved easily. Moreover, if the crosslinking solutions are added prior to loading on the rheometer the gelation reaction often occurs almost instantaneously, therefore the sample will have gelled before the operator can load it on to the rheometer for testing. Methods that have been used to try to overcome this limit are discussed in Chapter 3.

### **2.4.1 Specialised modifications to commercial rheometers**

Despite the lack of equipment that enables samples on a rheometer to have controlled exposure to soluble crosslinkers or chelating agents there are many other modifications that have been developed for similar problems either from a fundamental characterisation perspective or to simulate an application/industrial process.

#### **2.4.1.1 Molecular characterisation rheometer (add-ons)**

Understanding molecular changes during phase transitions is of interest to researchers as it can provide useful information on formation or dissociation of covalent bonds and therefore information on the progress of polymerisation reactions and sol-gel transitions.

This has been achieved by coupling spectroscopic techniques to rheological equipment such as NMR (Callaghan et al., 2000; Nakatani et al., 1990) rheo-SAXS (Somani et al., 2002) Rheo-FTIR (Boulet-Audet et al., 2014) Rheo-Raman (Chevrel et al., 2012) and recently a 3- in- one rheometer, Raman spectrometer and optical microscope (Kotula et al., 2016). These combined techniques have helped shed new light on molecular orientation and viscoelastic behaviour in a variety of polymers and highlights the potential of modified rheological equipment in furthering the understanding of polymer behaviour during physical changes in state.

#### **2.4.1.2 Application specific rheometer accessories**

In addition to coupling analytical equipment the major rheometer manufacturing companies have developed a range of add-ons to their rheology platforms that are designed for specific applications which otherwise cannot be replicated with the standard geometries.

##### **2.4.1.2.1 Light curing lower plate**

The light curing system has a lower glass plate fitted with a light source that can be applied during the rheological measurements. This system is designed to work with a Peltier system to control temperature and facilitates the investigation of UV and visible light initiated curing reactions which are often applied in coatings (Lee et al., 2000) biomedical applications (Higham et al., 2014) and 3D Printing hydrogels (Mironi-Harpaz et al., 2015)

##### **2.4.1.2.2 Electro-rheology accessory**

Some colloidal materials change material behaviour rapidly when subjected to electric fields. The interesting physical behaviour of electrorheological fluids has led to applications in shock absorbers (Stanway et al., 1996).

This has prompted rheometer manufacturers to develop the electrorheology accessory which can apply an external electric stimulus to a sample *in situ* whilst simultaneously measuring rheological changes.

##### **2.4.1.2.3 Relative humidity accessory**

An accessory to control relative humidity is commercially available for measuring materials in controlled environmental conditions and preventing condensation. This system is often required where drying processes are strongly affected by humidity and temperature which ultimately impact on application such as in paints and coatings.

##### **2.4.1.2.4 Immobilization cell**

Another accessory for controlling environmental conditions is the immobilisation cell which allows the characterisation of drying kinetics of paints coatings and slurries. This works by

loading the sample onto a piece of paper which sits upon a perforated lower plate through which a vacuum is applied. The vacuum generated by a pump, forces the solvent of the sample to penetrate into the paper, extracting the moisture from the sample. During this procedure, the rheometer can measure changes in viscosity and viscoelasticity. Changes in viscosity over time are used to characterize the sample on drying which is determined by the solvent retention properties of the sample.

#### **2.4.2 Limitations**

The modifications to standard rheological equipment has provided a greater insight to both fundamental and applied research on gelling materials clearly highlighting the desire for systems that can realistically control the physical environments for testing specific applications. Controlling changes in the chemical environment of samples while undergoing rheological testing however, is much more challenging and there are no commercially available add-ons that suitably address this problem. In bioresponsive materials such as *in situ* gelling drug delivery systems the changes in physical behaviour is often due to changes in the chemical and physical environment. Moreover, the changes in mechanical behaviour often correspond with the controlled release of an active ingredient which also requires analysis. This thesis explores possible modifications to address such issues using *in situ* gelling polysaccharides as test materials.

## **Chapter 3 Polysaccharide Gels**

## **CHAPTER THREE**

### **POLYSACCHARIDE GELS**

#### **3.1 Introduction to polysaccharides**

Polysaccharides are biological polymers composed from monosaccharides, which are linked to each other by glycosidic bonds. They occur throughout nature in plants, microorganisms and animals and play an important role in many biological functions. These include providing structural support, physical protection from the environment and predators, maintaining suitable hydration levels in tissues, as lubricants and as energy sources. There is also a wide range of industrial use of polysaccharides, some of which have taken inspiration from the biological functions. These include uses as a nutritional component of foods, controlling texture in foods, encapsulation of for protection of drugs, scaffolds that provide support for tissue engineering constructs, environmental protection as wound healing dressings, lubrication properties in cosmetics and personal care products.

The ability of polysaccharides to perform so many functions is a result of the diverse chemical and structural compositions of polysaccharides that have their own unique physicochemical properties and therefore can have a versatile functionality. Furthermore, polysaccharides are sourced from renewable resources which are relatively cheap compared with synthetic polymers, which make them particularly desirable for use in many industrial applications (Malafaya et al., 2007). This has led to many different types of polysaccharides being utilised in pharmaceutical and biomedical applications. As polysaccharides are of biological origin, there is a susceptibility to biological variation. However, controlled cultivating and processing techniques minimise variations in batch-to-batch consistency.

Controlled processing and commercialisation of these materials has allowed polysaccharides to become attractive products for use as pharmaceutical and biomedical materials as they are generally biocompatible and naturally degrade or are excreted from the body.

There are also potential for positive physiological interactions that can provide additional functionality. This behaviour is discussed in more detail in the section 3.10.

### 3.2 Polysaccharide structure

There are many different monosaccharide units that can link together to form polysaccharides. The glycosidic bonding between the monosaccharide units is a condensation reaction between the hemiacetal OH group at C1 of one monosaccharide and another OH (at any position usually C4, C3 C6 or C2) group of the adjacent monosaccharide, with the release of water (Figure 3.1).

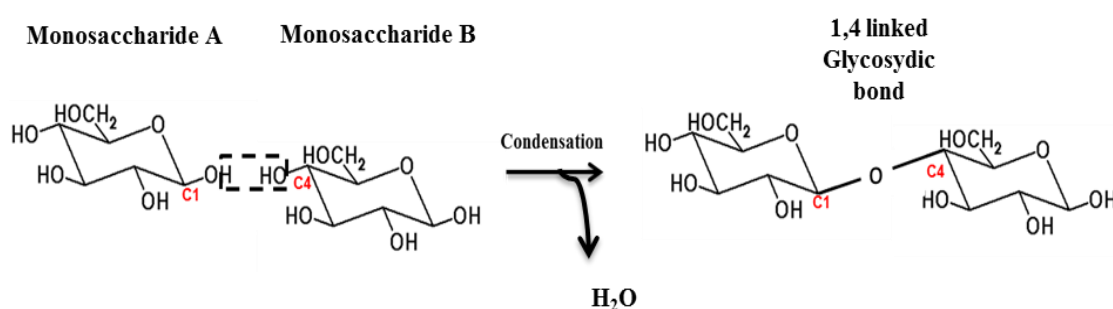


**Figure 3-1: Example of the condensation reaction that occurs during the formation of a glycosidic bond between monosaccharides.**

How polysaccharides behave and therefore their subsequent functionality is dictated by the chemistry of the monosaccharides that form the polysaccharide chains, the linkages between the monosaccharide units the degree of polymerisation and chain conformation. This leads to polysaccharides having a large number of reactive groups, a potential for a wide range of molecular weights and a chemical composition that varies, all of which contribute to their diversity in both property and structure.

Polysaccharides do however, have only two major classifications. Homopolysaccharides are polysaccharides which contain the same type monosaccharide in their polymeric structure, (examples include starch, cellulose glycogen and dextran which are all polysaccharides built up from glucose monosaccharides) and heteropolysaccharides are polysaccharides that have more than one type of monosaccharide present in their structure (Arrigo et al., 2013).



Both polysaccharide types can exist as linear polymers or branched structures that have a backbone adjoining side chains (which can also be branched).

Further classifications of polysaccharides are made according to the monosaccharides present in the polymer chain. For example, homopolysaccharides consisting of the monosaccharide glucose are termed glucans whereas fructose based homopolysaccharides are termed fructans and those consisting of only mannose would be termed mannans. Heteropolysaccharides are more complex as they are composed of two or more different monosaccharide units and can often (but not always) have repeating sequences (Maio et al., 2014). This type of repeating sequence structure is found several polysaccharides sourced from seaweed. These include carrageenan and agarose, (both linear heteropolysaccharides consisting of a repeating disaccharide sequence) and alginate, which is a linear heteropolysaccharide (but it has both homopolymeric regions and heteropolymeric regions within a single polymer chain). In pectin, found in the cell walls of fruits and plants, there is a linear homopolymeric sequence which is occasionally and somewhat randomly interrupted by a different monosaccharide. This structural irregularity can have a distinct impact on physical behaviour. Some bacterial polysaccharides have more complicated repeating structures for example gellan gum, which contains a repeating tetrasaccharide unit and xanthan gum, which has a five sugar residue repeating sequence. There are also polysaccharides with more random structures, with no obvious repeating units (Sutherland, 2001).

These can also be densely branched creating complex structures like those found in plant exudate gums such as gum Arabic. Some polysaccharides contain sugar acids (uronic acids) in their composition which can, depending on the pH of the solution, exist in the protonated acid form ( $\text{COOH}$ ) at pH below the  $\text{pK}_a$  or the deprotonated ( $\text{COO}^-$ ) form at pH above the  $\text{pK}_a$ . Under most biological conditions (with exception of the gastric fluid) the pH is approximately neutral and therefore the ionized form is predominant and hence the polymer will have a

negative charge. This also can occur with amino sugars and can impart a positive charge at pH below the  $pK_a$  of the amino group. This has led to further classifications of polysaccharides into polyelectrolytes and non-polyelectrolytes, with polyelectrolytes being further classified into positively charged polysaccharides such as chitosan and negatively charged polysaccharides such as heparin, hyaluronic acid, alginate, pectin and gellan gum (Arrigo et al., 2013).

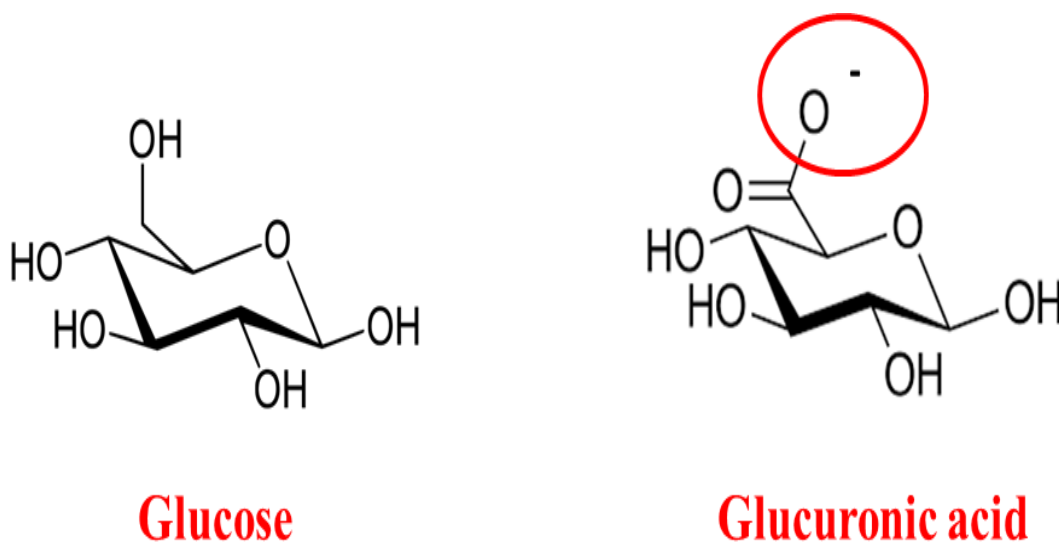


**Figure 3-2: Structural differences between a neutral sugar and an uronic acid showing the presence of a negative charge using glucose and glucuronic acid as an example.**

The presence of charged moieties on a polysaccharide chain can cause individual chains of like charges to repel one another through electrostatic repulsion. Controlling this intermolecular repulsion can be easily achieved by the addition of salt to suppress the charge and in certain charged polysaccharides lead to gelation. Indeed, the presence of salts in physiological fluids is auxiliary for gelation in several *in situ* gelling pharmaceutical systems, which will be discussed later in the thesis.

### **3.3 Polysaccharide gelation**

Arguably, the most interesting feature of polysaccharides with regards to industrial and research interest is their ability to form gels. A gel as defined in chapter one is an intermediate state of

matter containing both solid and liquid components. The solid component comprises a three dimensional network of inter-connected molecules or aggregates which immobilise the liquid continuous phase. Gels have liquid aspect but due to three dimensional network crosslinking behave like a solid (Nerkar et al., 2013). Hydrophilic polymers such as polysaccharides that have capability to absorb and hold large amount of liquid such as water to form three dimensional network are often termed hydrogels (Peppas et al., 2000). Because of their ability to hold a significant amount of water, polysaccharide hydrogels are quite similar to natural living tissues, making them appropriate candidates for use in a wide variety of pharmaceutical and biomedical applications (Coviello et al., 2007). It should be highlighted that the use of the word ‘gel’ can often be interpreted differently in different industries. Indeed, Dorothy Jordon Lloyd (1926) defined ‘the colloidal condition of the gel is one that is easier to recognise than define’. The rheological definition of a gel is “a swollen polymeric system showing no steady-state flow” however within the cosmetics industry products such as shower gel and in the pharmaceutical industry topical gels are used to describe gel based products.

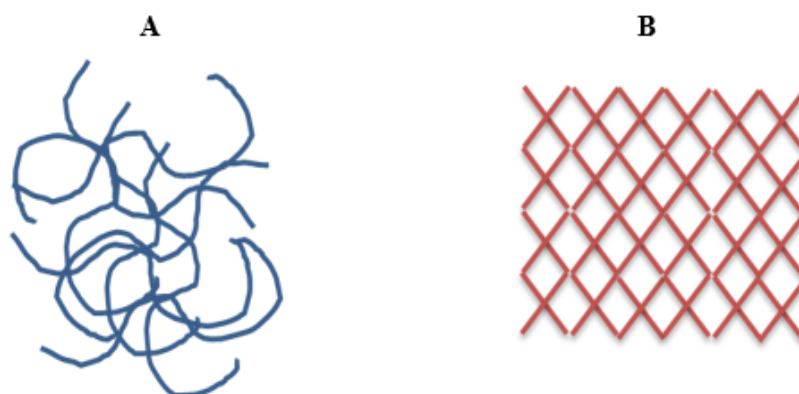


**Figure 3-3: Representation of A) an entangled polymer solution and B) an ordered crosslinked gel.**

These systems, which do not conform to the rheological definition as they both can flow, are in fact highly viscous solutions formed by entanglement of polymer chains rather than a true gel network following the rheological definition.

True gel networks can be classified into two main categories according to the cross-linking among the macromolecules, whether it is chemically or physically based (Yu and Ding, 2008). In synthetic polymers gel networks are often held together by strong covalent chemical crosslinks and are termed chemical gels. Physical gels on the other hand, such as the majority of polysaccharide gels form associations between the polymer chains held together by physical interactions that are weaker than covalent bonds. These physical interactions occur along specific regions of the polysaccharide chains with the formation of ordered junction zones. Depending on the polysaccharide the physical forces that participate in junction zone formation include electrostatic interactions, hydrogen bonding, hydrophobic interactions and van der Waals forces (Clark and Ross-Murphy, 1987). In addition to the junction zones there are also connecting disordered regions of the polymer network which are soluble preventing precipitation. Gels that can be formed by physical crosslinking have great industrial importance, particularly because the gel formation can often be applied under mild conditions without organic solvents (Nishinari et al., 2000). These hydrogels have wide applications in different areas like encapsulation of living cells, biologically friendly scaffolds in tissue engineering and sustained release delivery systems (Rowley et al., 1999; Peppas et al., 2006). Environmentally sensitive hydrogels have the ability to sense changes in pH, temperature, or the concentration of metabolite and release their load as a result of such a change. Thus, hydrogels that undergo physicochemical changes in response to applied stimuli, such as biomolecular binding, are promising materials for drug delivery and tissue engineering (Yang et al., 2008). Moreover, the extent of intermolecular association affects the mechanical behaviour of gel networks.

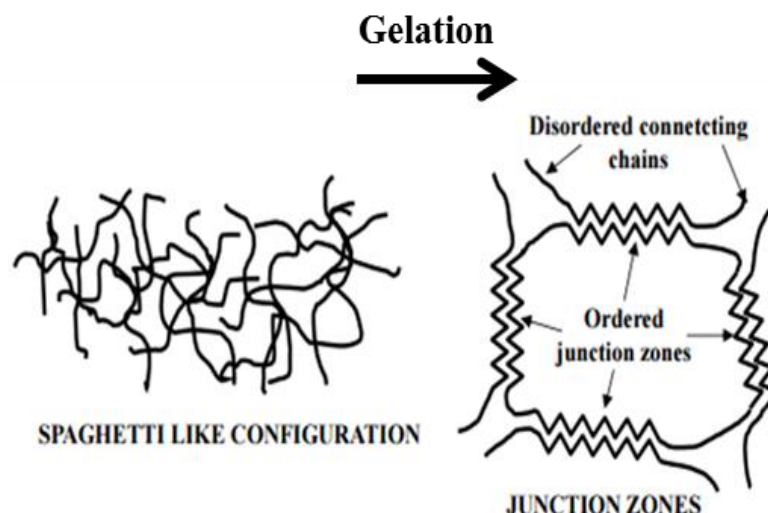


**Figure 3-4: Representation of development of an ordered polysaccharide network showing junction that occur through physical interactions and disordered connecting chains (adapted from Posocco et al., 2015).**

This is manifested in strong and brittle gels when the majority of the polymer chains participate in junction zones formation and weaker gels that are more elastic and occur when the networks are dominated by solubilising disordered regions. It is the variable nature of the physical interactions that allow polysaccharide solutions to form gels as a result of variations in local environmental conditions such as pH, temperature, or ionic strength. Furthermore, weak physical interactions that occur in polysaccharide gels also facilitate dissolution in response environmental changes. This creates opportunities to design gelled systems with behaviour that is physiologically responsive.

The wide range of polysaccharide materials from different origins, composed of different monosaccharides in their molecular chains delivers diverse functional and physicochemical properties and subsequently many potential uses.

### 3.4 *In situ* sol-gel transitions

An *in situ* gel refers to polymer solution which is administered as liquid and undergoes a sol-gel phase transition to firm gel upon exposure to a physiological environment. This transition may be triggered by environmental conditions that include temperature, pH, chemical crosslinks or changes in the ionic environment (Figure 3.5) (Nerkar et al., 2013).

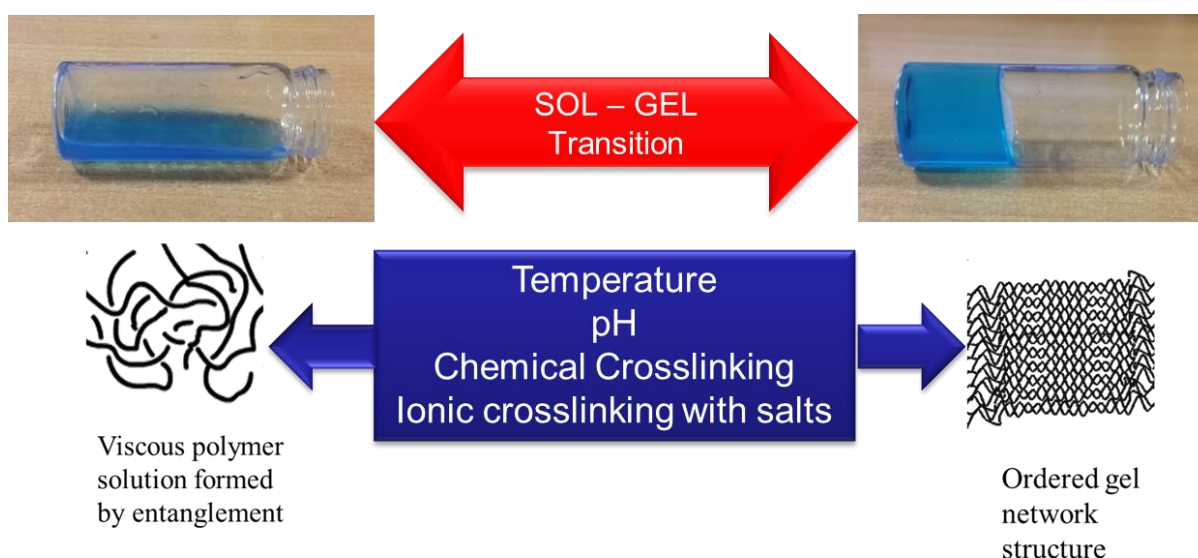


**Figure 3-5: Diagram highlighting sol-gel transitions for *in situ* gelling systems that can occur on exposure to changes in environmental conditions.**

Some polysaccharides have the ability to form firm gels at relatively low polymer concentrations due to being held together by long ordered junction zones, creating an expansive three-dimensional network. In some anionic polysaccharides, the polymer chains can be held together by addition of mono or divalent cations such as  $K^+$ ,  $Na^+$ ,  $Ca^{2+}$  and  $Mg^{2+}$  or  $H^+$ , which suppress the repulsive charge on the polysaccharide resulting in an ordered structure (Phillips and Williams, 2009).

Indeed, several successful pharmaceutical products utilise this mechanism. Examples include the heartburn medication Gaviscon® which contains sodium alginate and relies on  $H^+$  ions in the stomach for its functionality. Another example is the eye drop formulation for treating glaucoma Timoptol-LA®. This formulation uses gellan gum and utilises the salts present in lacrimal fluid. Both examples will be discussed in more detail in the section 3.10.3. It is these anionic polysaccharides that are of particular interest in this thesis, therefore, a deeper understanding of their individual structure and gelation behaviour is required to explain their functional role in formulations and in designing apparatus that is suitable to measure *in situ* sol-gel transitions of these materials.

### 3.5 Alginate

Alginate is polysaccharide extracted from brown algae, and consists of (1→4) linked  $\beta$ -D-mannuronic acid (M) and  $\alpha$ -L-guluronic acid (G) residues varying in proportions (Figure 3.6 a, b). Alginates can be separated into three fractions of the widely differing composition by partial acidic hydrolysis and fractionation, two of these consist of almost homo-polymeric molecules of guluronic and mannuronic acid, respectively, whereas a third fraction contains nearly equal proportions of both monomers. On this basis of the structure, the physical properties are determined by the quantity of M-block, G-blocks and MG-blocks, (Donati and Paoletti, 2009) (Figure 3.6 c).

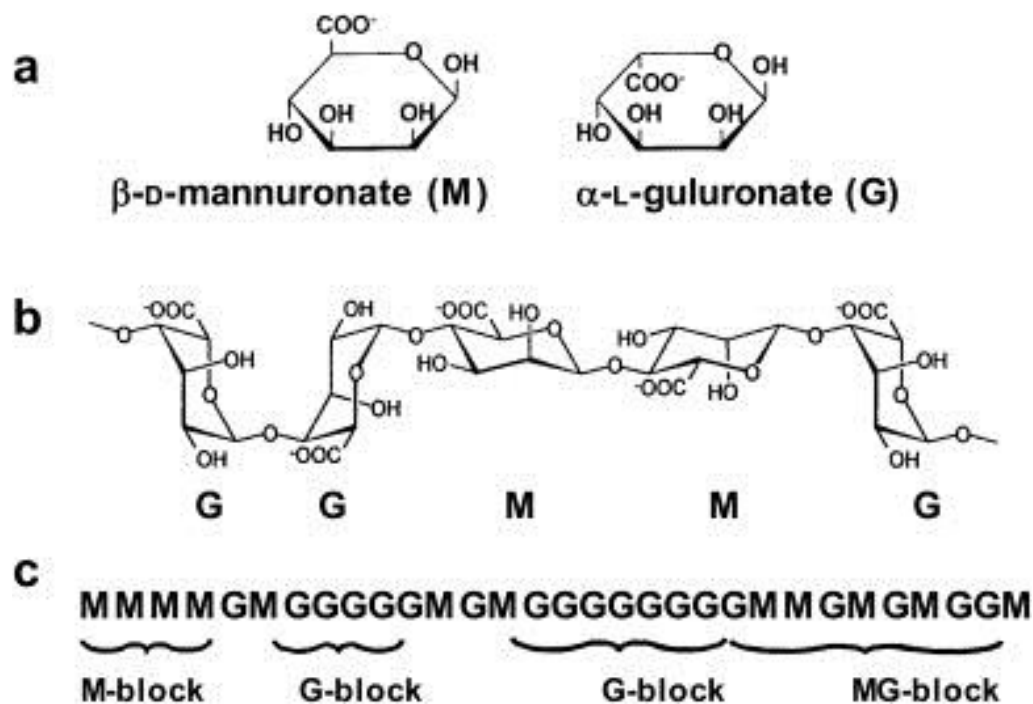


**Figure 3-6: the monomers of alginate structure (a) M:  $\beta$ -D-mannuronate; G:  $\alpha$ -L-guluronate. (b) The alginate chain, chair conformation, (c) alginate chain sequences. M:  $\beta$ -D-mannuronate; G:  $\alpha$ -L-guluronate (adapted from Draget and Taylor, 2011).**

Alginate has many unique properties that facilitate multiple uses, however, low chemical stability is a major problem often encountered in alginate use. Moreover, it has been shown that the physical properties of these polymers in an aqueous medium depend on the M/G ratio and the distribution of G and M units along the chains. The GG blocks that involve axial–axial linkages are more rigid than the di-equatorially links found in MM blocks; consequently, the composition (M/G ratio) and distribution of M and G units in the chains strongly affects the stiffness of the alginate chains and gel formation (Rinaudo, 2008).

### 3.5.1 Alginate gelation

Gel formation of alginate depends on selective binding which occurs with the G block. Thus there is an association between content of L-guluronate residues in the chains and gel strength structural features in the G-blocks cause chelation of multivalent cations as described by the



“egg-box” model (Figure 3.7). Furthermore, the strength selectivity of divalent cations varies from one to another, which takes this order:  $\text{Pb}^{2+} > \text{Cu}^{2+} > \text{Ba}^{2+} > \text{Sr}^{2+} > \text{Ca}^{2+} > \text{Mn}^{2+} > \text{Mg}^{2+}$  (Haug and Smidsrød, 1970).

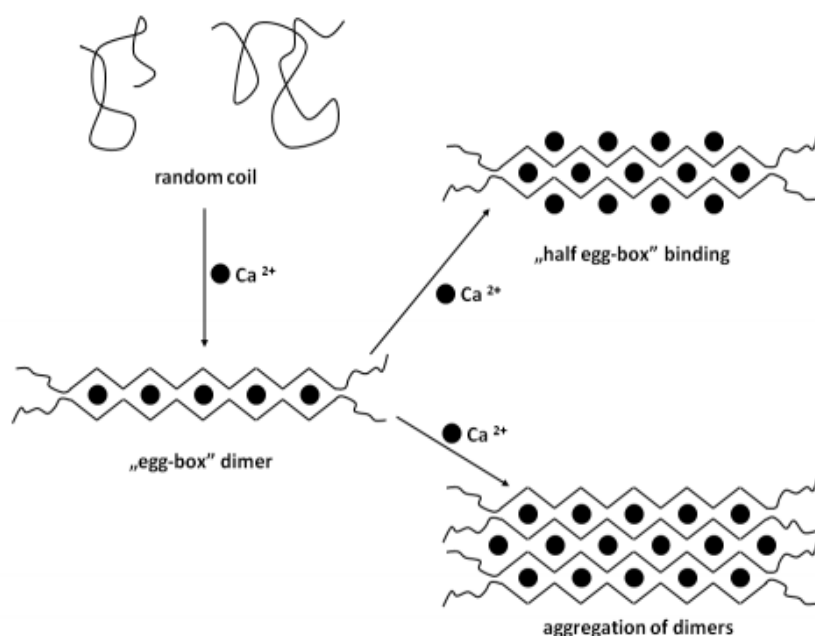


**Figure 3-7: Mechanism of calcium ions binding to G-blocks, proposed by (Morris et al., 1978).**

The gelation of alginate can be achieved under relatively mild conditions with an ionic cross-linking agent such as divalent cations (e.g.,  $\text{Ca}^{2+}$ ). The cross-linking of alginate is mainly achieved by exchange of sodium ions from the guluronic residues with divalent cations, resulting in the formation of an egg-box structure (Figure 3.7). The divalent cations bind to the  $\alpha$ -L-guluronate blocks in a highly cooperative manner (Smidsrød and Skjåk-Bræk, 1990) and each alginate chain forms junctions with other chains to generate cross-linked network structures (Dupuy et al., 1994). There are several methods to produce alginate gels most of them with calcium the favoured crosslinking ion due to its relative safety in pharmaceuticals and foods.

### 3.5.1.1 Mechanism of internal and external gelation

Calcium ions can be delivered to alginate to induce gelation in a variety of ways which can result in different types of gel produced. The most common technique in pharmaceutical use is external gelation whereby  $\text{Ca}^{2+}$  ions are supplied externally to the polymer from a solution of calcium chloride initiating localised gelation instantaneously as the  $\text{Ca}^{2+}$  ions diffuse into the alginate, ultimately resulting in a gel network that is heterogeneous with varying crosslinking density (Skjåk-Bræk et al., 1989).

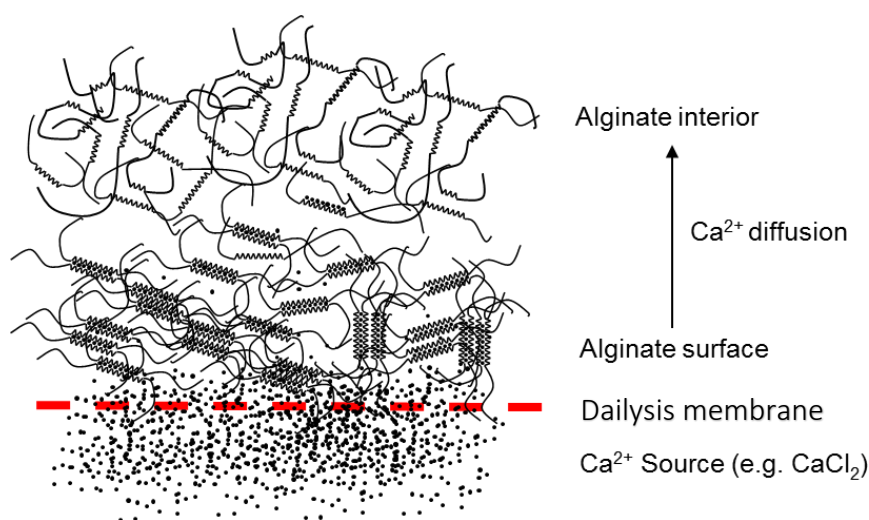


**Figure 3-8: Mechanism of external gelation (adapted from Smith and Miri 2010).**

To produce gels that are homogeneous there are several methods have been developed to enable  $\text{Ca}^{2+}$  ions to be delivered internally. In general, this method uses an inactive form of the cross-linking ion, either bound by a chelating agent such as phosphate, citrate, or EDTA (Skjåk-Bræk et al., 1986) or is distributed throughout the alginate solution as an insoluble salt, for example, calcium sulphate or calcium carbonate (Skjåk-Bræk et al., 1989; Draget et al., 1990; Smidsrod and Draget, 1996). In this technique, usually a solution of a slowly hydrolysing lactone, generally glucono  $\delta$  lactone (GDL) is added to the alginate solution containing the insoluble calcium source.

The addition of GDL slowly lowers the pH over a period of about 1 h, which then liberates the calcium ions within the alginate as the calcium carbonate dissociates at low pH (Figure 3.9).

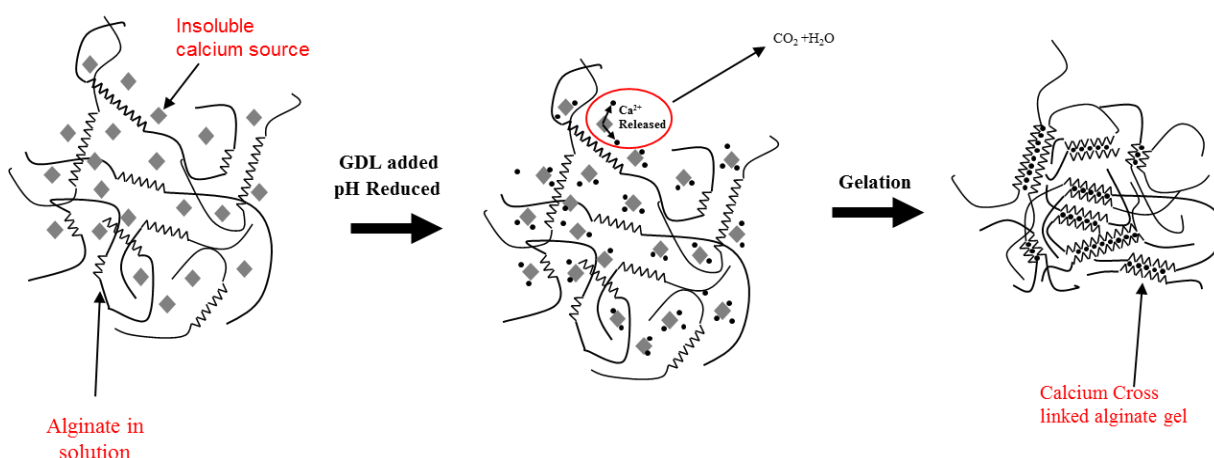


**Figure 3-9: Mechanism of internal gelation (adapted from Smith and Miri, 2010).**

This process is governed by the acidic properties of the sequestering agent; in the case of the Ca–EDTA–GDL system, the final pH of the gels is around 4. When calcium carbonate is used instead of complexed calcium ions, the pH may be set to almost any predetermined value simply by adjusting the relative proportions of calcium salt and GDL (Draget et al., 1990). The solubility of a calcium salt used determines the amount of Ca<sup>2+</sup> ions available to react with the alginate and thus can influence the physical nature of an alginate gel. Calcium salts are either highly water soluble (e. g. CaCl<sub>2</sub>), moderately water soluble (e. g. calcium sulphate) or insoluble at neutral pH but fully soluble in acidic conditions (e. g. anhydrous dicalcium phosphate and calcium carbonate). In the case of highly soluble salts, such as CaCl<sub>2</sub>, Ca<sup>2+</sup> ions are readily available to react with sodium alginate, resulting in instant gel formation and the formation of an inwardly moving gelling zone as highlighted in Figure 3.8. This type of gel formation is described as diffusion or dialysis setting. Gels formed in this way are characteristically strong but heterogeneous (Smidsrød and Draget, 1996). It is also particularly difficult to measure real time gelation kinetics when gelled in this manner.

This is not the case when poorly soluble salts such as calcium carbonate is used, as only a small amount of  $\text{Ca}^{2+}$  ions are readily available to react with the alginate. Consequently, the calcium salt may be mixed with a sodium alginate solution to produce a non-gelling homogenous suspension. The alginate gel forms when the solution is exposed to a trigger calcium salt to dissolve. Therefore, measurements of gelation kinetics can easily be monitored using a rheometer.

Calcium crosslinked alginate gels are thermally stable and therefore cannot be made to melt at physiologically relevant temperatures. However, as alginate gels are, most of the time, crosslinked with calcium ions, substances with a high affinity for calcium (such as EDTA, phosphates or citrates) can sequester the  $\text{Ca}^{2+}$  ions, thus destabilising the gel. Calcium alginate gels can also be destabilised by high concentrations of non-gelling cations, such as  $\text{Na}^+$  due to an ion exchange reaction (Smidsrød and Skjåk-Bræk, 1990). Therefore, once a calcium alginate gel is formed reverting it back to the solution state is easily achieved by addition of a calcium chelating agent or by ion exchange. Using alginates with a higher G content can help to enhance the stability. Indeed, recently it was demonstrated that gel strength could be tuned by addition of oligoguluronates. In alginate gels where  $\text{Ca}^{2+}$  ions are limited in concentration addition of oligoguluronates sequesters the calcium causing reduced gel strength, however, when  $\text{Ca}^{2+}$  ions are abundant within the gel addition of oligoguluronates increases the gel strength (Jørgensen et al., 2007; Sletmoen et al., 2010).

#### **3.5.1.2 Acid gelation**

Alginate will also form gels at low pH where the alginate becomes protonated and forms alginic acid (Draget et al., 1994). Guluronic acid and mannuronic acid are known to have a  $\text{pK}_a$  of 3.65 and 3.38 (Haug, 1961) therefore gradually reducing the pH of alginate to below the  $\text{pK}_a$  of the alginate monomers results in alginic acid gel formation (Draget et al., 1994, 1996, 2003). The

rheological behaviour of alginic acid gels are similar to calcium alginate gels varying in strength with molecular weight and guluronic acid to mannuronic acid ratio. This is an important and useful property of alginates that has been exploited in the pharmaceutical and food industries.

### 3.6 Pectin

Pectins are a complex group of structural heteropolysaccharides containing mostly galacturonic acid units. It is one of the negatively charged, hydrophilic polymers, which are extracted from middle lamella and primary cell walls of plant tissues (Rinaudo, 2008). The backbone of pectin is composed of (1→4) linked  $\alpha$ -D-galacturonic acid units (GalpA) which comprises approximately 70% of pectin (“smooth region”), interrupted by single (1→2) linked  $\alpha$ -L-rhamnose residues (“hairy region”). Pectin segments are classified based on their molecular structure into four main types that include Homogalacturonan (HG), rhamnogalacturonan I (RG-I), rhamnogalacturonan II (RG-II) and xylogalacturonan (XGA). These may be present in pectic polysaccharides that can be isolated from primary cell walls (Figure 3.9). The most abundant type of pectin is Homogalacturonan (HG) that comprises about 65% of pectin (Jackson et al., 2007).

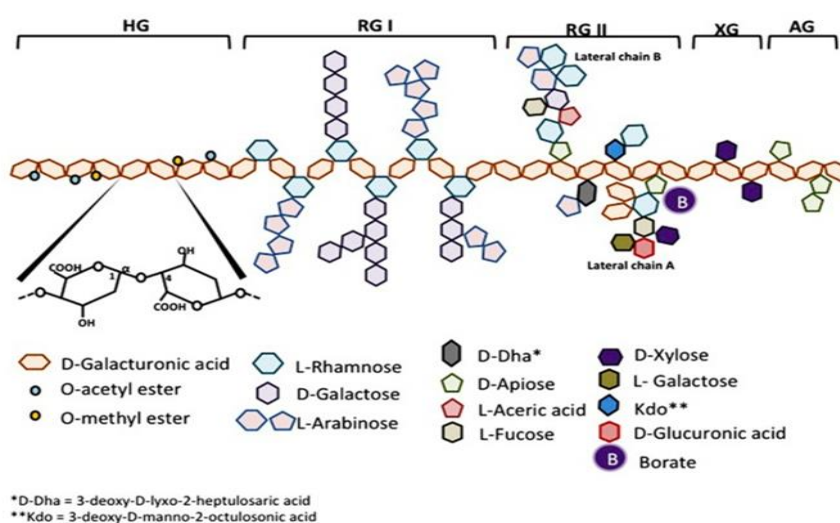


**Figure 3-10: Schematic structure of pectin illustrates different domains regions of pectin, (Leclere et al., 2013).**

The carboxyl groups of the galacturonic acid units are partly esterified by methanol, to an extent dependent on the pectin source and the extraction mode (Figure 3.10, c). The DE is defined by the ratio of methyl-esterified galacturonic acid residues to the total galacturonic acid units present in the pectin sample. (Nelson et al., 1977; Axelos et al., 1991). Additionally, pectin can be amidated by treating pectin with ammonia during processing to convert some of the C-6 methyl ester groups to amide groups (Figure 3.10, d).

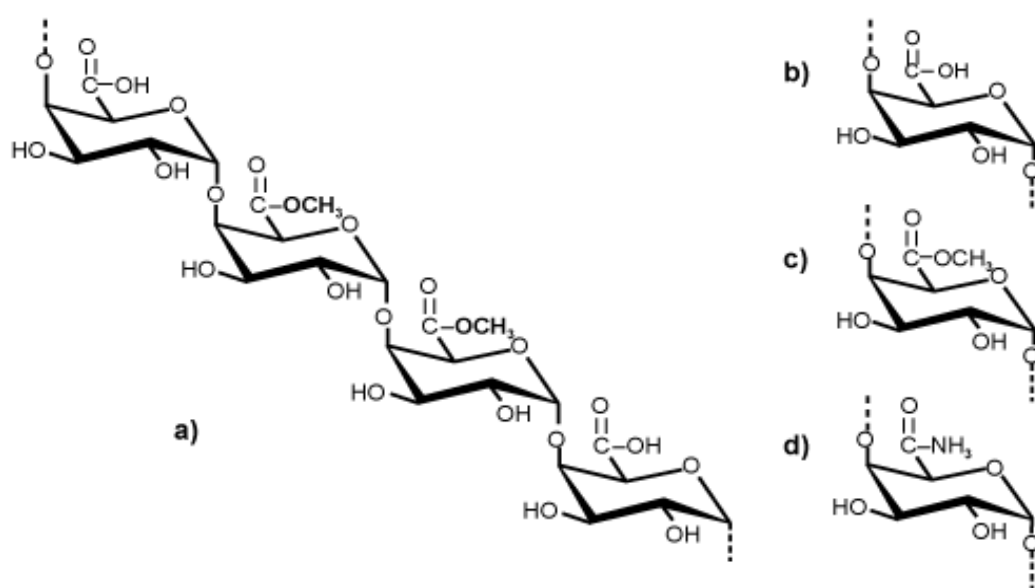


**Figure 3-11: Structure of pectin (a) A repeating segment of pectin chains (b) carboxyl group (c) ester group (d) amide group (Sundar Raj et al., 2012).**

HG is a linear chain of (1→4) linked α-D-galactopyranosyluronic acid (GalpA) residues that are methyl esterified at C6 and can be acetylated on C2 or C3 of GalA residues, (Willats et al., 2001). The esterification of galacturonic acid residues with methanol or acetic acid is a very important structural characteristic of pectic substances. Pectin is classified into two types based on the degree of methyl esterification (DM): high methoxyl (HM) pectin, and low methoxyl (LM) pectin, the degree esterification for HM-pectins (DM > 50%) and LM-pectins (DM < 50%) usually range from 60-75% and 20-40% respectively.

The number and distribution of the methyl-ester groups along the molecule play an important role in the solubility, thickening properties, gelation ability, and conditions required for gelation. Each of these pectins has a different gelation mechanism. The main type of binding between calcium ions and low methoxy pectin is similar to that of alginate with  $\text{Ca}^{2+}$  (egg box model) (see section 3.5.1).

### **3.6.1 Gelation of pectin**

The gelation mechanism of pectins mainly governed by their degree of esterification (DE). HM pectin requires a minimum amount of soluble solids (>55%) and a pH within a narrow range (~3.0) to form a gel which is thermally reversible (Oakenfull and Scott, 1984). The presence and the availability of a controlled quantity of calcium or other divalent cations for gelation are necessary for LM-pectins. LMPs can form gels in the presence of divalent cations (usually  $\text{Ca}^{2+}$ ), through associations between sequences of charged groups belonging to two different chains (Gilsenan et al., 2000) and non-ionic association under acidic condition (at pH below 3) in the absence of cations (Grant et al., 1973).

LM pectins with divalent metal cations  $\text{Ca}^{2+}$  in particular, form electrostatically stabilised gel networks, which is called the “egg-box” model. The gelation results from specific non-covalent ionic interactions between blocks of galacturonic acid residues of the pectin backbone on the distribution of negative carboxylate groups and with calcium divalent ions (Morris et al., 1982; Oakenfull and Scott, 1998; Axelos and Thibault, 1991). The affinity of pectin chains towards calcium increased as the degree of esterification or ionic strength decreased and with increasing of polymer concentration. Calcium-induced gelation is a predominance of low methoxyl pectin gels, when intermolecular junction zones are formed between the smooth HG regions of separate polymer chains which results in gelation, the distribution of the unesterified GalA moiety in the pectin macromolecule have a critical role in the calcium associations since it

affects the reactivity of pectin with cations. The mechanism of LM pectin gelation depends on the chemical structure of the macromolecule (degree of esterification, molecular weight, distribution of rhamnose causing kinks in the chain of pectin) and the environment conditions (pH, ionic strength, concentration of cations, temperature) (Axelos and Thibault, 1991). The block wise distribution of free carboxylic groups supported the calcium binding much more than a random distribution (Ralet et al., 2001). The egg-box model which describes alginate gelation is also used to describe the gelation mechanism of LM pectin, in both biopolymers the “egg-box” is formed in a two-step process – dimerisation followed by aggregation (Figure 3.11), so that on neighbouring polymer chains, a three dimensional network is formed by ionic bonding through calcium bridges (Thibault and Rinaudo, 1986).

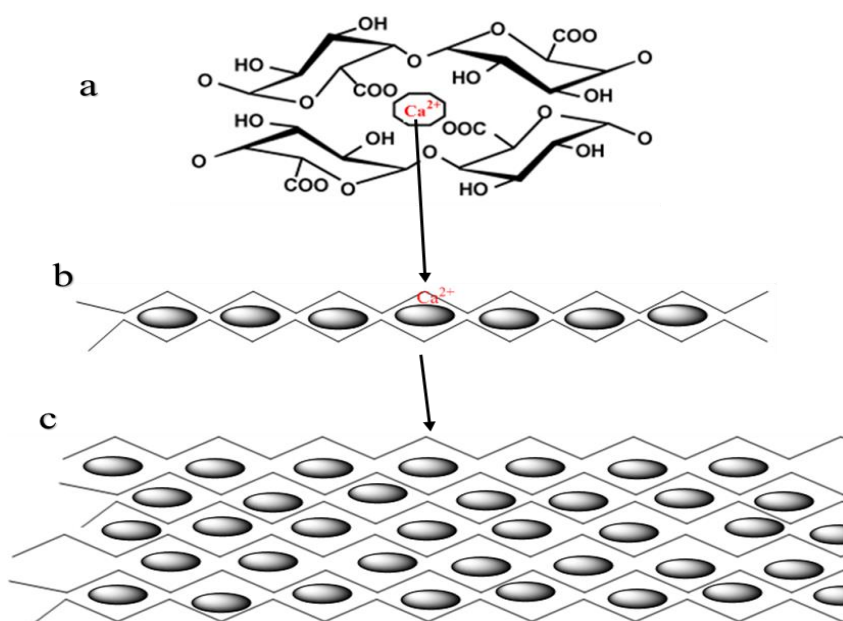


**Figure 3-12: Shows Schematic representation of calcium binding to polygalacturonate sequences of LM Pectin, (a) Pectin  $\text{Ca}^{2+}$  complex (b) "Egg-box" dimer (c) aggregation of dimers.**



### 3.7 Gellan gum

Gellan gum (gellan) is an anionic, high molecular weight extracellular deacetylated polysaccharide produced by bacteria called *Pseudomonas elodea* (*Sphingomonas elodea*) at the completion of the fermentation process. Kaneko and Kang discovered gellan in 1978 and the chemical structure consists of a tetrasaccharide repeating unit of  $\beta$ -D-glucose,  $\beta$ -D-glucuronic acid,  $\beta$ -D-glucose, and  $\alpha$ -L-rhamnose in 2:1:1 ratio joined in a linear chain; there are one glycerate and half acetate per each repeat unit (Jay et al., 1998).

Kelcogel, Gelrite, Phytigel and Gel-Gro are four different trade names of gellan manufactured currently by C. P. Kelco in Japan and USA. Many food industries use Kelcogel as a thickener and gelling agent, whereas the other three types used widely in microbiology and cell culture (Bajaj et al., 2007). Gellan is commercially available in two forms native and deacetylated. In its native form, acetyl groups and glyceryl groups are present as indicated in Figure 3.12a and are often referred to as high acyl gellan (HA gellan).

These acyl groups can be removed by treatment with hot alkali to give deacetylated gellan also termed low acyl gellan (LA gellan) as shown in Figure 3.12b. Both HA and LA form of gellan are commercially available and have different properties. One of the most useful properties of gellan is the ability to form hydrogels at low concentrations (Oliveira et al., 2010). The physical characteristics of the gel are greatly affected by the acyl content. Gels that have a high content of acyl are very soft, elastic and not brittle, while gels with a low acyl content level are firm, brittle and inelastic. Gellan gum has a wide range of applications in the food, pharmaceutical and biotechnology industries because of its biocompatibility, versatile physical properties and the ability to form transparent hydrogels in physiological environments that are thermally stable at body temperature and in acidic media (Matricardi, 2009)

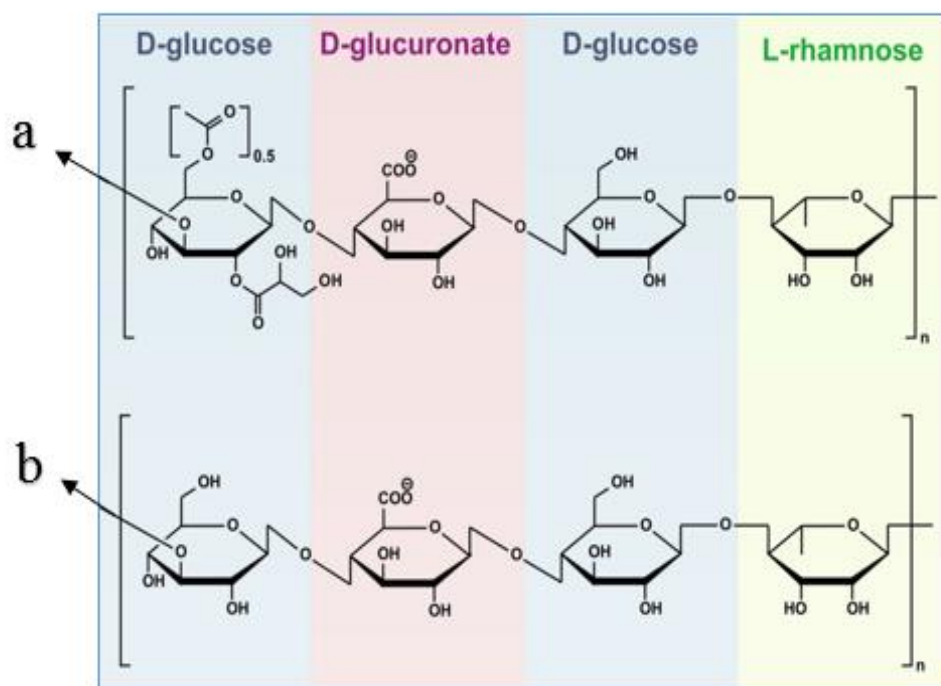


**Figure 3-13: The structure of gellan gum (a) is a native form and (b) is a low-acyl form (Osmalek, 2014).**

### 3.7.1 Gelling characteristics of gellan gum

The anionic nature of gellan gum is caused by the free carboxylate groups present on the glucuronic acid residue in the structure, which gives gellan gum negative charge that is crucial to the gelation mechanism (Sworn, 2009). Gelation occurs as a result of an ordering process that occurs at the molecular level where the polymer chains form a double helical conformation which then aggregate to form the gel network. This involves two stages in the aqueous environment, where the first stage is known as a coil-helix transition that occurs when cooling from  $\sim 85^{\circ}\text{C}$  forming double helices from random coil chains. Following this coil helix transition on further cooling a hydrogel can be formed as a result of aggregation of pairs of double helices (Nitta and Nishinari, 2005). This mechanism of gelation is described by the domain model (Robinson et al., 1991) whereby ordered helices aggregate in junction zones and are connected by disordered soluble chains (Figure 3.13). Aggregation of gellan double helices

under normal circumstances however, is inhibited by electrostatic repulsion due to the presence of the carboxylate groups.

This strength of the repulsive negative charge can be reduced by addition of metal cations or reducing the pH of the aqueous media which then promotes aggregation (Morris et al., 2012). Although there have been some reports for applications of HA gellan in pharmaceutical systems LA gellan is much more widely investigated due to its rapid gelation kinetics on contact with ionic crosslinking species. LA gellan (from now on will be referred to as gellan) following aggregation of the double helices by gel promoting cations, form gels that are thermoreversible, optically transparent, hard and relatively brittle.

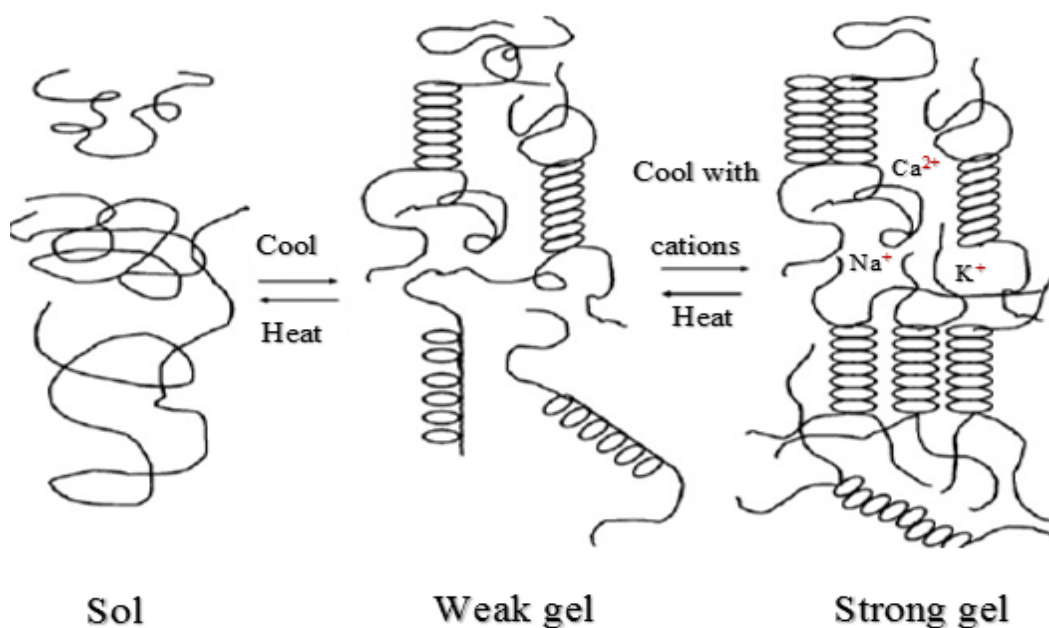


**Figure 3-14: Mechanism of gellan gum gelation.**

### **3.7.2 Acid gelation of gellan**

Reduction in pH also promotes gelation by decreasing the amount of negative charge on the polymer and therefore reducing electrostatic repulsion. This is due to the carboxyl group included within the gellan chain being a weak acid, and therefore, the degree of dissociation of the carboxyl groups is governed by the dissociation constant. Thus, the lower the pH value, the smaller the fraction of dissociated carboxyl groups, resulting in the gellan being less anionic. It is to be expected therefore, that the less charged chains are more likely to aggregate with one another due to lower electrostatic repulsion.

Change in pH does not alter the setting point of the gel but affects melting temperature in some cases. For example, gels prepared with very low levels of monovalent ions melt at around 70°C, at neutral pH but at acidic pH, the melting temperature is increased (Sanderson and Clark, 1984). Yamamoto and Cunha (2007) investigated using GDL to decrease the pH of gellan and they found that decreasing the pH supported easy aggregation, which explains the observed rapid gelation kinetics and the densely linked structure at equilibrium when compared with ionically gelled gellan.

On direct addition of acid to gellan, ordering and aggregation between individual hydrocolloid chains occurs almost immediately upon acidification (Moritaka, et al 1995). This process of direct addition of HCl to gellan gum has been investigated for the production of self-structuring formulations that take advantage of natural digestive processes for applications in the food industry to increase satiety (Bradbeer et al 2014) and in the design of delayed release of pharmaceutical oral liquids (Miyazaki et al 1999; Mahdi et al 2014).

### **3.8 Mechanism of *in situ* gelling in drug delivery system**

Rheological measurements allow for the understanding of the different gelation mechanisms, which can be used in the optimisation of the properties of the hydrogels for tissue reconstruction and drug delivery applications. *In situ* gelation is a process of gel formation at the site of application after the composition or formulation has been applied to the site. As a drug delivery agent, the *in situ* gel has an advantage related to the gel or polymer network being formed *in situ* providing sustained release of the drug and permits the drug to be delivered in a liquid form. At the same time, such gels are convenient to be dropped into the site of action where the physiological environment causes gelation allowing any loaded drug to remain (Edsman et al., 1998). This changing of physical structure leading to the production of a hydrogel in response to externally stimulating media in the surroundings can therefore, be used as a controlled release drug delivery system. Since the early 1950s, stimuli responsive hydrogels have been studied for drug release, and polymers that react to different stimuli have been developed. These stimuli can be chemicals that change pH (Suedee et al., 2010; Du et al., 2005) or ionic strength (Tan et al., 2004). The presence of metabolic chemicals (e.g., enzymes or antigens) (Meyers et al., 2008) or/and physical stimuli for instance temperature, electric fields, solvent composition, light, pressure, sound and magnetic fields (Bae, 1997; Hoffman, 1995; Park et al., 2011).

### **3.9 Application of *in situ* gelling techniques**

There are many applications of using *in situ* gelation in drug delivery systems which can result in advantages such as reduced frequency of administration and improved patient compliance by delivery of more accurate doses and prolonging residence time of the drug at the site of uptake. The mechanisms that may be involved in the *in situ* gel formation are classified based on the environmental stimuli which can include ionic crosslinking and environmental stimuli. (Bakliwal and Pawar, 2010).

### **3.9.1 *In situ* gelation based on ionic crosslinking**

In such a situation where there are elevated concentrations of electrolytes, there is a possibility that the polymers can experience phase transition upon exposure. Monovalent and divalent cations found in physiological fluids, such as sodium and calcium, increase the ionic strength of the gel. The electrostatic repulsive forces between the molecules are subsequently reduced or neutralised, and gelation can occur (Banerjee and Bhattacharya, 2012).

Various polysaccharides are included in the class of ion-sensitive gelling systems. For example, ionic-induced gelation occurs in, alginate, pectin, gellan gum and carrageenan. Gellan gum is perhaps the most sensitive of these materials to ionic gelation, experiencing *in situ* gelling behaviour on contact with both mono and divalent cations that include  $\text{Ca}^{2+}$ ,  $\text{Mg}^{2+}$ ,  $\text{K}^{+}$  and  $\text{Na}^{+}$ . The most common example of a drug delivery system that uses gellan and this ion crosslinking technique to control drug release is timolol maleate ophthalmic solution. In this product gellan forms a clear gel when comes in contact with the monovalent or divalent cations present in the lacrimal fluid. This example will be discussed in more detail in section 3.10.3. In pectin and alginate divalent cations such as  $\text{Ca}^{2+}$ , for gels via the egg box mechanism (discussed in section 3.5.1 and 3.6.1), owing to the interaction with galacturonic acid and a guluronic acid blocks in pectin and alginate respectively (Kubo et al., 2004).

### **3.9.2 *In situ* gelation based on pH triggered systems**

The development of a gel that is induced by pH changes is another method to achieve *in situ* gelation by physiological stimuli. Pendant acidic or basic groups are included in most pH-sensitive polymers, and they accept or release protons as a reaction to the alteration in the environmental pH. Polyelectrolytes therefore, have a huge amount of ionisable groups (Balamuralidhara et al., 2011). Kubo et al have investigated gelation via this method using gellan gum (1.0% w/v) and 1.5% w/v sodium alginate on the subsequent release of para amino

phenol in the stomach of rabbits and rats after oral administration.  $\text{Ca}^{2+}$  was incorporated into the formulation in the complexed form using calcium carbonate ( $\text{CaCO}_3$ ). The results indicated that calcium ions were gradually released in the acidic environment *in situ* due to dissociation of  $\text{CaCO}_3$  causing gelation, which subsequently prolonged the release of para amino phenol to period up to 6 hours (Kubo et al., 2003).

### **3.9.3 Thermally triggered systems**

Thermosensitive polymers can change from solution to a gel by changing the environmental temperature. Polymers that response to this type of stimuli are liquid at ambient temperature and undergo gelation upon contacts with body fluids due to an increase or decrease in temperature (Ruel-Gariepy and Leroux, 2004). Gellan, amylopectin, amylose and agarose are some biopolymers that exhibit temperature sensitivity. These polymers are sols at high temperatures and become gels at lower temperatures by formation and aggregation of double helices (Gutowska et al., 2001). Using these polymers in drug delivery can sustain the drug release for prolonged duration of time. Thermoresponsive sol-gel polymeric systems function through three fundamental methods, negatively thermosensitive, positively thermosensitive and thermally reversible gels (Peppas et al., 2000).

### **3.10 Applicability of *in situ* polymeric drug delivery systems**

The *in situ* gelling systems have been under research several decades. It has been found that levels of pH, temperature or ion activation stimulate these systems. This system described as low viscosity solution that undergoes a phase transition in response to the physiological environment. The gel can prolong the drug contact at the site of administration due to its rheological and mucoadhesive properties as compared to an aqueous solution. The gels also possess a broad application spectrum and can be applied in almost every route of administration. Oral, ophthalmic, rectal, transdermal, subcutaneous and vaginal gels are available for different

pharmaceutical applications (He et al., 2008). In the discovery phase, the gel formulations can be used to enhance the local and systemic exposure of potential lead compounds, which is ideal to establish animal models for various conditions quickly and cost efficiently (Gupta et al., 2002). It remains difficult however to suitably model rapid changes in rheology that occur in physiological conditions especially in ionic and pH driven gelation.

### 3.10.1 Oral delivery

The most famous example of aqueous polysaccharide solution that undergoes gelation following oral ingestion is sodium alginate used in Gaviscon®. Gaviscon® is a reflux suppressant, which is different from usual antacids regarding its functioning (Grover and Smith, 2009). On contact with the gastric fluid the alginate in Gaviscon® rapidly gels forming a raft that floats on the surface of the gastric fluid preventing acid reflux. This is due to the low pH of the gastric fluid causing the formation of an acid gel which is further strengthened by release of  $\text{Ca}^{2+}$  from insoluble  $\text{CaCO}_3$  (which is also in the formulation) that dissociates. This also facilitates the floating gel raft as  $\text{CO}_2$  is released and becomes entrapped in the gel. Alginate raft formation was imaged *in situ* recently by Kim (2016) who showed the development of the gel over a period of 130 s highlighting the rapid gelation (Figure 3.15).

Several previous studies reported that gellan has the potential to be used for oral liquid *in situ* gelling systems containing complexed calcium ions. Once the formulation is administered, the calcium ions are released due to low pH of the stomach, resulting in crosslinking of the gellan *in situ* (Miyazaki et al., 1999; Miyazaki et al., 2001; Kubo et al., 2003) in a similar mechanism to what occurs with alginate in Gaviscon®.



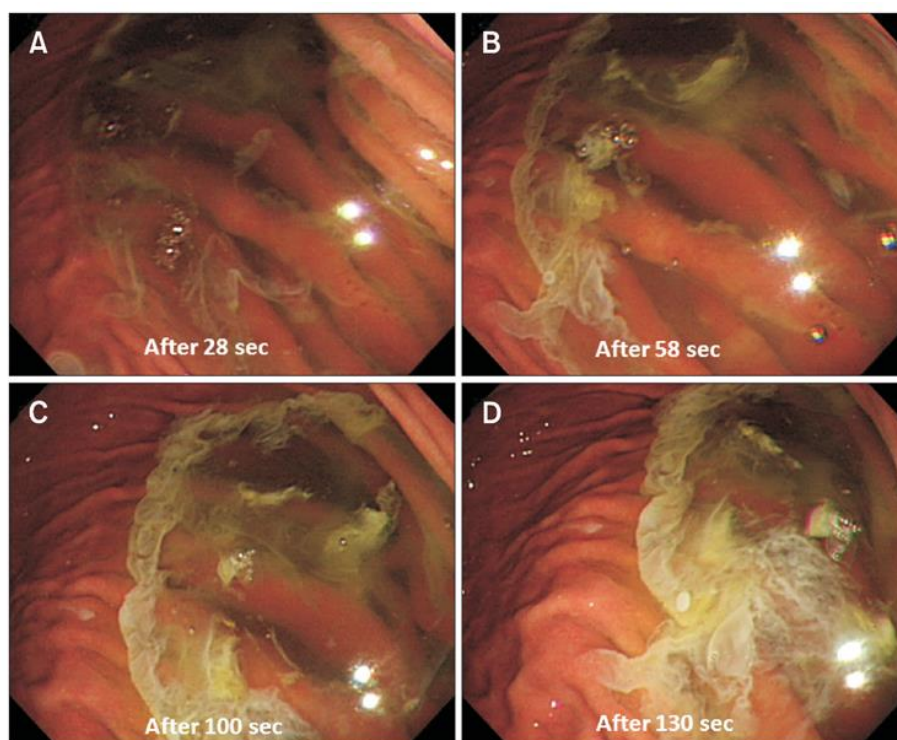


**Figure 3-15: Gel raft formation of alginate in the stomach, adapted from (Kim, 2014).**

Miyazaki et al. (1999) reported formulation of *in situ* gelling gellan as a vehicle for oral delivery of theophylline by addition of calcium chloride mixed with sodium citrate which acted as a  $\text{Ca}^{2+}$  sequestering agent to prevent gelation prior to administration. When the drug loaded gellan mixture was administered orally, calcium ions were slowly released in the acidic media of stomach leading to gelation of gellan *in situ*. This resulted in increased bioavailability with prolonged theophylline drug release in rats and rabbits compared with the commercially available theophylline liquid dosage form (Miyazaki et al., 1999).

Low methoxy pectin solutions (1 and 2 % w/v) have also been used as an oral *in situ* gelling system. Kubo et al used these formulations for oral delivery of paracetamol by adding low methoxy pectin solutions (1 and 2 % w/v) with complexed calcium ions to examine the potential of sustained drug release. The calcium ions were released in the acidic environment of the stomach which caused gelation of the low methoxy pectin *in situ* leading to prolong paracetamol drug release over a period of 6 h (Kubo et al., 2004).

### 3.10.2 Nasal delivery

Due to the excellent ability to form a gels *in situ* on exposure to physiological concentrations of cations, gellan gum is a good candidate to use in nasal formulations. LA gellan gum has generated interest as a promising polymer for use in nasal formulations because of its ability to form strong, clear gels *in situ*. Researchers have experimented to use micro-particle and liquid nasal delivery systems, but there are issues such as erosion and quick clearance either by post nasal drip where by the formulation is rapidly moved to the nasopharynx and is ultimately swallowed. This is facilitated by the microvilli on the nasal mucosa. However, by using particulate gel formulations, these issues can be resolved (Mahajan and Gattani, 2009a). Mahdi et al examined mixtures of low and high acyl gellan sheared gels to improve mucoadhesive properties in nasal drug delivery systems. The sheared gel systems contain gelled micro-particles suspended in a dilute solution of un-crosslinked polymer Figure 3.16. Rheological behaviour and mucoadhesion of fluid gels were investigated for two types of gellan and their blends. The results revealed that the mucoadhesive properties were improved when using high acyl gellan compared with LA gellan, however, the rheological properties prevented suitable administration from the spray device when the HA gellan was in the solution form. By creating microparticles of high acyl gellan and also when blended with LA gellan reduced the viscosity of the formulation sufficient to spray through a standard nasal spray device while maintaining the improved adhesion time on mucosal membrane (Mahdi et al., 2015).

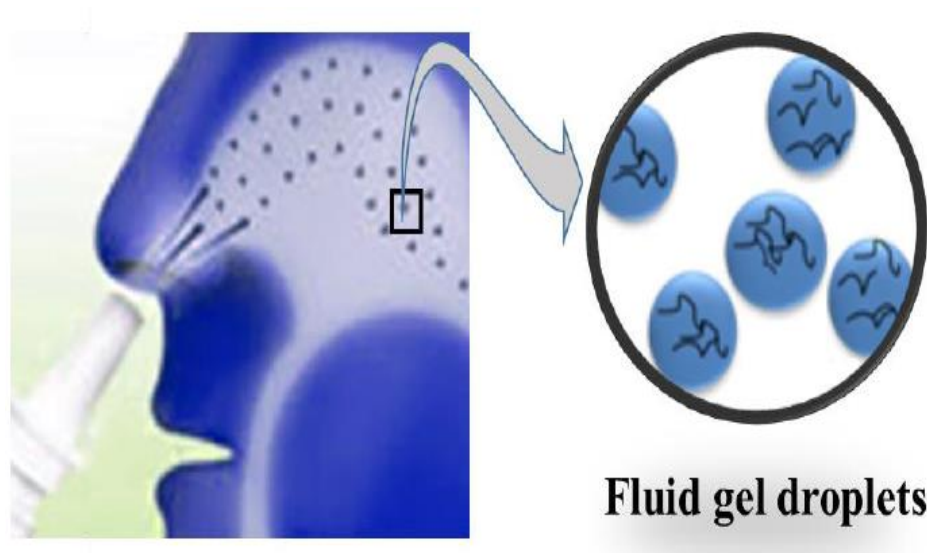


**Figure 3-16: Shows using gellan gum fluid gel in a nasal drug delivery systems , adapted from (Mahdi, 2016).**

### **3.10.3 Ocular delivery**

There are challenges to deliver drugs to the eye such as restricted precorneal permeability and rapid clearance of the dose by the action of both the lacrimal fluid and blinking, which results in a short precorneal contact time. Therefore, only a small amount of the medication is delivered and maintained in the place of action, (Gurtler et al., 1995). Subsequently, this leads to poor bioavailability (Osmelak et al., 2014). Due to these limitations, *in situ* gelling systems with the prolonged drug release are particularly useful as the elastic properties of gels can resist ocular drainage. The idea of naturally producing a gel on site (e.g. in the cul-de-sac of the eye) was first described in the early 1980s. It is known that owing to the lesser rates of drainage from the cornea, as a result of an increase the viscosity of a drug formulation in the precorneal region, facilitates bioavailability increase.

The cations in lacrimal fluid in the eye can interact with polymer solutions to form weak gel before convert to strong gel with increase the amount of cations (Lang, 1995). Middleton and Robinson have formulated sol-gel system having mucoadhesive property to deliver the steroid fluorometholone to the eye. The formulation was demonstrated on rabbits and showed sustained

release behaviour of the drug when compared with conventional eye drops (Middleton and Robinson, 1991). Natural polymers such as gellan gum, alginate and xyloglucan have been favoured for *in situ* gel based ocular delivery. These materials have been investigated for the delivery of various compounds to the eye to treat a range of disorders. These include actives release intraocular pressure in glaucoma, such as antimicrobial agents, anti-inflammatory agents and autonomic drugs (Bakliwal and Pawar, 2010). Arguably the gentlest and most patient friendly approach to improve the delivery the drugs to the eye via *in situ* gelling systems is to use LA gellan, which utilises the ionic composition of lacrimal fluid to induce gelation. Indeed, ophthalmic formulations are the most frequently encountered examples of LA gellan in current commercial pharmaceutical use (Grover and Smith, 2009).

Lacrimal fluid consists of a complex mixture of proteins, vitamins, sugars and lipids but importantly also contains a range of electrolytes that include  $\text{Ca}^{2+}$ ,  $\text{Na}^{+}$  and  $\text{K}^{+}$  at concentrations sufficient to crosslink gellan gum. In addition, the gels formed by LA gellan in particular are optically transparent which has obvious benefits for ocular application. It is well tolerated and can be used without the risk of any toxic effects (Rozier et al., 1989) increasing the ocular retention time and ocular availability of the drug to a greater extent (Cohen et al., 1997). Timoptol-LA<sup>®</sup> (timolol maleate) is one such eye drop formulation that is on the market, and uses gellan gum a gel forming excipient that sustains the release of the active ingredient timolol maleate. This ophthalmic formulation is applied as a liquid and upon contact with the lacrimal fluid undergo sol gel transition due to the cross-linking with mono and divalent ions (Shedden et al., 2001). This formulation is easily dispensed in the form of drops due to the relatively low viscosity of gellan gum in solution. On contact with the surface of the eye, the formulation induces lacrimal fluid secretion reflex that effectively deliverers more cross-linking ions to the gellan gum causing the gel to increase in strength. The gel then controls the release by providing a diffusional barrier for the drug, which is subsequently released more gradually than

in immediate release formulations of timolol eye drops (Grover and Smith, 2009). This results in the patient only administering the drug once a day rather than twice a day with conventional drops, which subsequently improves patient compliance and therefore improved therapeutic outcomes.

#### **3.10.4 Wound healing hydrogels**

In 1989, Rosiak et al. used hydrogels as the basic material used for manufacturing of wound dressings. Since then, many modifications have been undertaken to improve their physical and chemical properties. Hydrogels have attracted special attention among wound dressings design as they offer the ability to be used as moist wound dressing materials. In addition to keep the wound moist, hydrogels can also play an important role in stimulating the proliferation of fibroblasts to recover the defected area and they have been shown reduce the pain at the wound site as they are non-adherent and cool the surface of the wound (Choi et al., 2015). Unlike dry hydrocolloid dressings, hydrogels cannot absorb much exudate and are thus not suitable for wounds producing a high amount of exudates. The most extensively used polysaccharides for hydrogel preparation in wound healing are alginate, hyaluronic acid, and carboxymethylcellulose (CMC) (Lin et al., 2009).

Alginate has shown to be particularly useful with a range of dressings that are commercially available in various forms for the treatment of both acute and chronic wounds (Lee and Mooney 2012). It is often applied as calcium alginate fibres that can absorb significant volumes of fluid (up to 15-20 times their own weight (Jones, 1999)). In addition, application of the dressing at the wound site also results in the exchange of ions from the calcium alginate fibres with monovalent ions of the exudate and blood causing swelling and solubilisation of the alginate, thus, forming a protective gel coat of which maintains an optimal healing temperature and moisture content.

The cross-linked alginate hydrogels can also be used in are available for use as sheet hydrogels that can be applied to dry wounds, however, a secondary dressing is usually required to cover the wound such as gauze when they applied as a gel (Debra and Cheri, 1998). The gentle formation of gels via cross-linking calcium ions have also resulted in alginate being investigated as cell scaffolds for tissue engineering (Corkhill et al., 1989; Kokabi et al., 2007) and further advances have resulted in dressings that contain drugs such as anti-microbials (Kim et al., 1999) and even protein based growth factors (Liao et al., 2005). Moreover, this route of drug delivery in wounds has advantages of continent method to administer locally acting drugs while avoiding first pass metabolism effects, gastrointestinal irritation, and metabolic degradation associated with oral administration (Prakash et al., 2010).

What is apparent in all of these systems is that functionality and efficacy relies on changes in rheological behaviour on contact with physiological fluids which can be rapid or more prolonged depending on the *in situ* gelling/degrading polymer used and the composition of the physiological fluids which vary in different regions of the body. The following chapters explore potential ways to monitor this behaviour in real time in a selection of ionotropic *in situ* gelling polysaccharides (alginate pectin and gellan) and propose more realistic models that could be used when formulating novel *in situ* gelling drug delivery systems.

## **Chapter 4 *In situ* rheological measurements of the external gelation of alginate and pectin**

Aspects of the introduction and the results presented in this chapter are published in Food Hydrocolloids.

Mahdi, M.H., Diryak, R., Kontogiorgos, V., Morris, G.A. and Smith, A.M., 2016. *In situ* rheological measurements of the external gelation of alginate. Food Hydrocolloids, 55, pp.77-80.

## CHAPTER FOUR

### ***IN SITU* RHEOLOGICAL MEASUREMENTS OF THE EXTERNAL GELATION OF ALGINATE AND PECTIN**

#### **4.1 Introduction**

Due to their unique physicochemical properties, alginates and pectins have many applications in the pharmaceutical and biomedical industries. Of particular interest to these industries is the ability for solutions of anionic polysaccharides such as alginate to undergo a temperature independent sol-gel transition in the presence of multivalent cations (e.g.  $\text{Ca}^{2+}$ ) (Smidsrød and Draget, 1996) and on exposure to acidic pH (generally  $< \text{pH } 3$ ) (Draget et al., 1994, 1996, 2003, 2006b). This behaviour makes alginate particularly suitable for 3D cell culture and bioresponsive drug delivery systems as these environmental conditions can be found in various physiological fluids and therefore have the potential to undergo a sol-gel transition *in situ*. In addition to alginate, the gelling properties of pectin have led to intensive use in the food industry.

High methoxy pectin (HM) gels which formed at low pH ( $\approx 3$ ) in the presence of high concentrations of sucrose and low methoxy pectin (LM) gels that are obtained from interacting pectin with calcium ions are the most common ways to produce pectin gels (May, 1990). The factors that influence the properties of pectin gels are classified to intrinsic and extrinsic factors. Intrinsic factors include the degree of esterification (DE), molecular weight and distribution of the charged groups along the pectin chain which have great importance in the gelation properties, while the extrinsic variables are temperature, pH, ionic strength, and co-solute concentrations. Between these factors, the DE plays the most important role for pectin gelation. (Oakenfull, 1991; Axelos and Thibault, 1991).



The simplest and most widely used method to form gels of alginate and LM pectin is to drop a solution of either polymer via a syringe into a solution of calcium chloride where instantaneous gelation occurs via the external gelation method described in section 3.5.1.1 (Kierstan and Bucke, 1977; Hulst et al., 1985; Matsumoto et al., 1986; Sugiura et al., 2005; Clark et al., 2008). Although there have been lots of work performed that exploits this sol-gel transition the rapid gelation and heterogeneous nature of the gels formed from a direct mixture of crosslinking ions has made the measurement of the rheological behaviour particularly difficult to measure. Several methods have been developed to overcome and provide further understanding to the fundamental structural aspects of alginate gelation. These methods include the controlled release of divalent ions from an insoluble source (Draget et al., 1990; Draget, 2000; Draget et al., 2006a) or by use of a sequestering agent such as ethylene diamine tetraacetic acid (EDTA) (Toft et al., 1982) and using the slowly hydrolysing n-glucono delta lactone (GDL) to lower the pH and release the complexed calcium into the alginate solution.

These methods can also be employed for gelling pectin. The gels produced using these methods tend to be considerably more homogeneous than those produced by direct mixing of alginate or pectin to an external crosslinking source as occurs when making alginate beads for example. Moreover, slowly releasing crosslinking ions that are complexed and suspended within the alginate/pectin solution is a very different mechanism to which occurs when alginate or pectin comes into contact with crosslinking ions in physiological environments. The most frequently used method to replicate physiological exposure is to loading the polymer solutions into a dialysis tubing. The loaded sample is then immersed into a solution of containing the required crosslinking ions for various periods of time before removing and cutting the crosslinked gel to an appropriate size for mechanical testing by either a rheometer (Miyazaki et al., 2000; Kubo et al., 2003) or large deformation mechanical tester.

Another method that has been used is to pour sodium alginate or LM pectin into tissue culture plates containing filter paper impregnated with soluble crosslinking ions (one placed beneath the polymer solution and one on top). The polymer is then allowed to gel for a specific time before the mechanical properties are measured (Hunt et al., 2010, Jahromi et al., 2011). Neither of these external gelation methods, however, offers an insight into the gelation of these polysaccharides polymers in real time. Another area of interest is the dissolution of the gel as dissolution rate of drug delivery vehicles is important factor in releasing entrapped drugs. Alginates and pectins can be dissolved in the presence of calcium chelating agents such as EDTA and sodium citrate (Smeds and Grinstaff, 2001) or monovalent cations and complex anions such as phosphate, citrate, and lactate, which have a high affinity for calcium ions (Smidsrød and Skjåk-Bræk, 1990). The process induced using chelating agents shown in the Figure 4.1. Due to the removal of calcium ions from alginates, the cross-linking unravels which results in destabilisation of the matrix (Sutherland, 1991) and will result in release of any entrapped active ingredients.

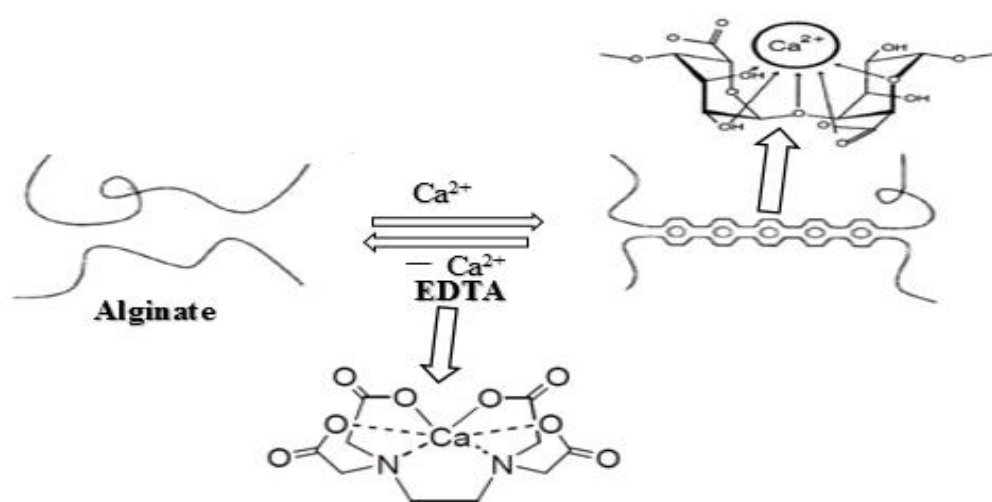


**Figure 4-1: Crosslinking model of calcium alginate (egg box) and EDTA calcium chelating.**

In this study, a novel rheological measurements method designed to investigate *in situ* gelation and gel dissolution of alginate and pectin when exposed to an external source of calcium ions ( $\text{CaCl}_2$ ) and calcium chelating agents (EDTA and Na citrate) were studied. In order to achieve this, a Malvern Gemini rheometer, with a modified lower plate was used to allow the exposure to an external source of crosslinking ions to facilitate the rheological measurement of alginate and pectin gelation and dissolution *in situ*.

## **4.2 Material and methods**

### **4.2.1 Materials**

Dialysis tubing (14000 MWCO) was purchased from (Thermo Scientific Ltd, UK) the filter paper used was Whatman Grade 1 supplied by Fisher Scientific UK. Sodium alginate was purchased Sigma-Aldrich (UK) and was described as medium molecular weight (80,000–120,000) with an M:G ratio of 0.39:0.61. Pectin was obtained from CP Kelco (Leatherhead, UK) and was reported to have an average degree of methyl esterification (DE) of 35.5 %. All the other chemicals were obtained from Sigma-Aldrich (UK) and were of analytical grade and were used without any further purification.

### **4.2.2 Solutions preparation**

#### **4.2.2.1 Preparation of alginate solutions**

Solutions of 4% w/w alginate were made by dispersing weighed amount of alginate in 100 ml distilled water and stirring at 60 °C for 30 min. Any evaporated water was replaced, and the sample was stored in a sealed vial before use.

#### **4.2.2.2 Preparation of pectin solutions**

Solutions of 4% w/v pectin were prepared by dispersing weighed amount of pectin in 100 ml distilled water at 60°C with a magnetic stirrer until completely dissolved any evaporated volumes were replaced.

#### **4.2.2.3 Preparation of calcium chloride solution**

Three different concentrations of CaCl<sub>2</sub> (50,100 and 200 mM) were prepared by dissolving the weighed amount of calcium chloride dihydrate in 100 ml deionized water.

#### **4.2.2.4 Preparation of ethylene diamine tetraacetic acid (EDTA) solution**

The preparing of 500 mM of EDTA was carried out by dissolving the weighed amount of EDTA powder in 100 ml warm deionized water with continuous stirring for 30 min. The pH was then adjusted to pH 7.0 using 1 M NaOH.

#### **4.2.2.5 Preparation of sodium citrate (Na citrate) solution**

Na citrate was prepared at a concentration of 500 mM in the same manner as the EDTA, by dissolving the correct amount Na citrate powder in 100 ml warm deionized water with continuous stirring for 30 min and the pH adjusted to pH to 7.0 using 1 M NaOH.

### **4.2.3 Rheological methods**

In this study, the *in situ* gelation test and the dissolution time of alginate and pectin were measured. The experimental setup used a Malvern Gemini Nano HR rheometer with a modified lower plate as shown in Figure 4.2. There is no standard technique for measuring the *in situ* gelation and gel dissolution on exposure to an external chemical stimulus. Therefore, to understand the *in situ* gelation of the polymers on controlled exposure to cations, minor modifications to the Bohlin Gemini Nano HR rheometer were made.

#### 4.2.3.1 *In situ* gelation

Briefly, a petri dish containing a filter paper soaked with the  $\text{CaCl}_2$  solution was securely attached to the lower plate of the rheometer. The theoretical amount of total calcium added was estimated by weighing the filter paper before and after soaking.

This was calculated as 2.5, 5 and 10 mg of calcium for 50, 100 and 200 mM  $\text{CaCl}_2$  solutions respectively. A dialysis membrane (MWCO 14,000 Da) which had previously been hydrated in deionized water was placed on top of the filter paper to prevent the sample being imbibed by the filter paper. The gap was then zeroed, the samples of alginate were loaded onto the dialysis tubing, and light silicone oil was used around the periphery of the geometry to prevent evaporation. Small deformation oscillatory measurements of storage and loss moduli ( $G'$  and  $G''$ ) were then performed as a function of time at 0.5% strain and a frequency of  $10 \text{ rad s}^{-1}$  using a 55 mm diameter parallel plate geometry with a 1 mm gap. All measurements were performed within the linear viscoelastic region previously determined using amplitude sweeps. Alginate and pectin solutions measured in the same way but using filter paper soaked with deionized water served as the control.

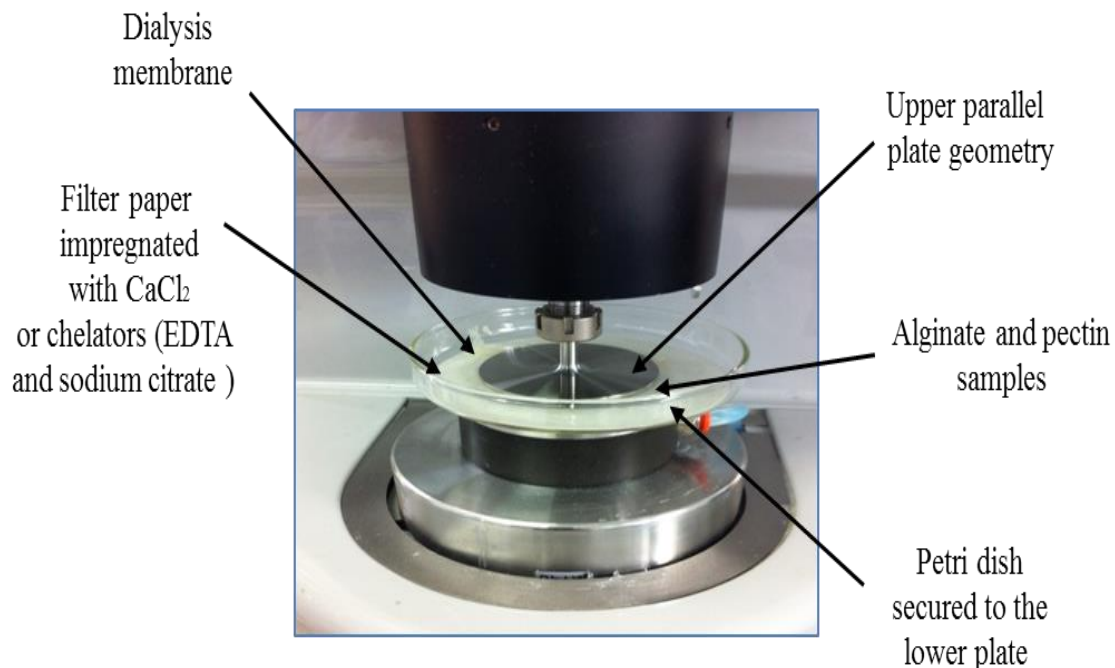


**Figure 4-2: *In situ* gelling experiments using a commercial rheometer.**

#### **4.2.3.2 *In situ* gel dissolution (degradation)**

Following a 20 min exposure to the  $\text{CaCl}_2$  solution, the geometry was raised, and the filter paper was carefully removed from the petri dish and replaced with a filter paper impregnated with a calcium chelator (500 mM either EDTA or Na citrate). The rheological measurements of  $G'$  and  $G''$  as a function of time were then resumed using the same conditions as used in the gelation measurements. During the procedure of changing the filter paper, the crosslinked gels remained adhered to the upper geometry which facilitated the change without significantly disturbing the gel. Moreover, no significant changes in normal force were apparent following the change of filter paper.

### **4.3 Results**

#### **4.3.1 Alginate *in situ* gelation results**

To evaluate the kinetics of the gelation process *in situ*, alginate 4% and three different concentrations of calcium chloride ( $\text{CaCl}_2$ ) were prepared at room temperature.

Variation of storage modulus  $G'$  and loss modulus  $G''$  were examined using the oscillation test described in section 4.2.3.1. Figure 4.3 A-C shows *in situ* gelation of alginate upon exposure to  $\text{CaCl}_2$ . Over the first minute of the test, there is a clear sharp increase in both moduli as the onset of gelation occurs. Increasing the concentration of the  $\text{CaCl}_2$  caused an increase in the final gel strength (measured at 20 min) with  $G'$  increasing from approximately 300 Pa at 50 mM  $\text{CaCl}_2$  to 1500 Pa at 200 mM  $\text{CaCl}_2$  (Figure 4.3D).

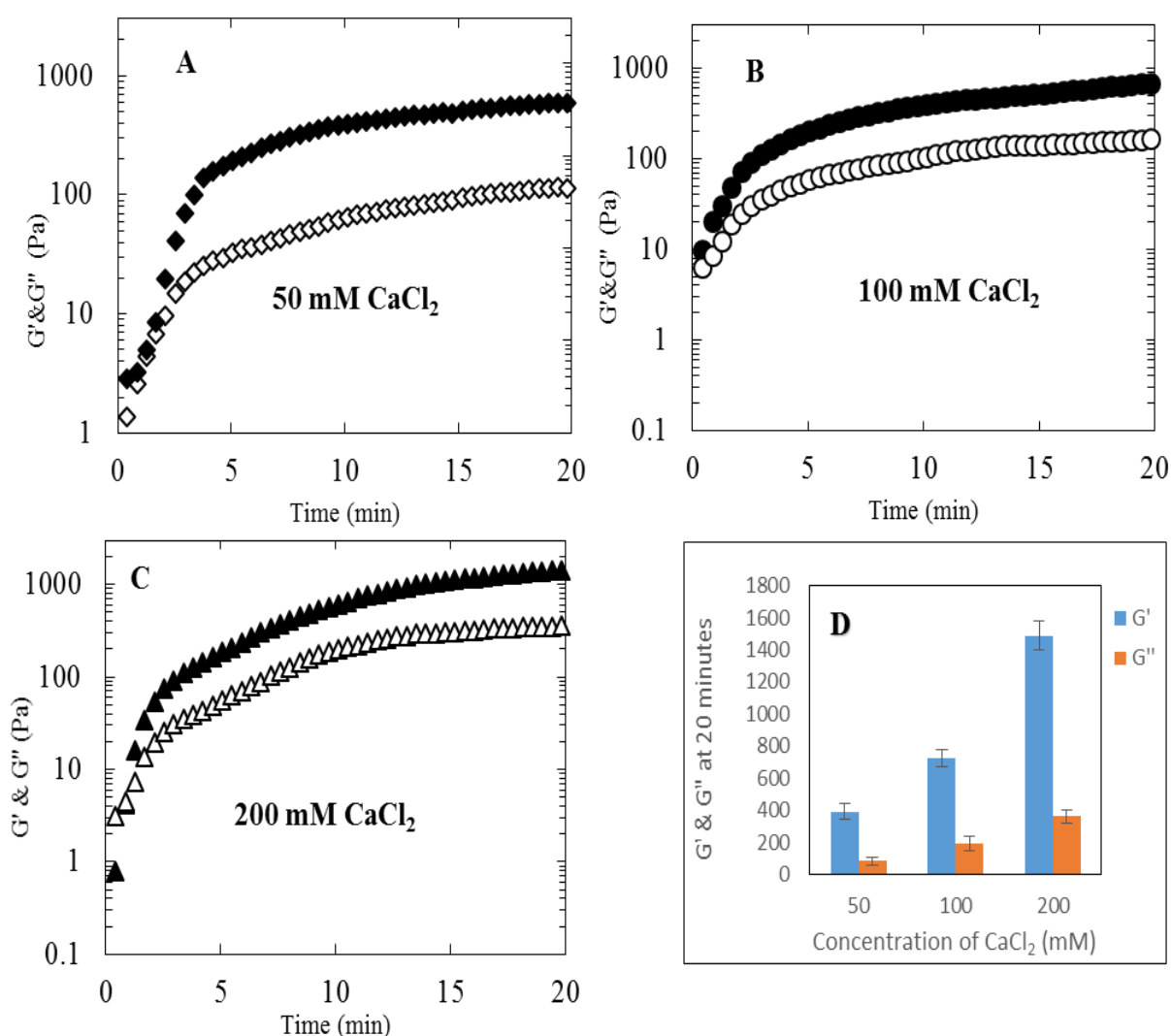


**Figure 4-3: Rheological measurements for alginate 4% showing variation of  $G'$  (filled symbols),  $G''$  (open symbols) vs. time on exposure to A) 50 mM B) 100 mM and C) 200 mM; D) shows comparative values of  $G'$  of 4% alginate after 20 min exposure to (50, 100 and 200 mM) of  $\text{CaCl}_2$ .**

### 4.3.2 Alginate gel *in situ* dissolution results

Alginate gels that are formed on exposure to ion crosslinking externally can be converted back from gel to the sol state using calcium chelating agents such as EDTA and Na citrate. To measure this process a 4 % w/w alginate gels crosslinked *in situ* with 200 mM  $\text{CaCl}_2$  (Figure 4.4A) were exposed independently following 20 min gelation to 500 mM EDTA (Figure 4.4B) and Na citrate (Figure 4.4C).

The results indicate that EDTA was a much stronger calcium chelator than Na citrate causing  $G'$  to return to a similar modulus to that of the original sodium alginate, prior to crosslinking, after only 35 min of exposure. In contrast, sodium citrate only reduced  $G'$  by one order of magnitude in comparison with the two orders of magnitude achieved when using EDTA (Figure 4.4D).



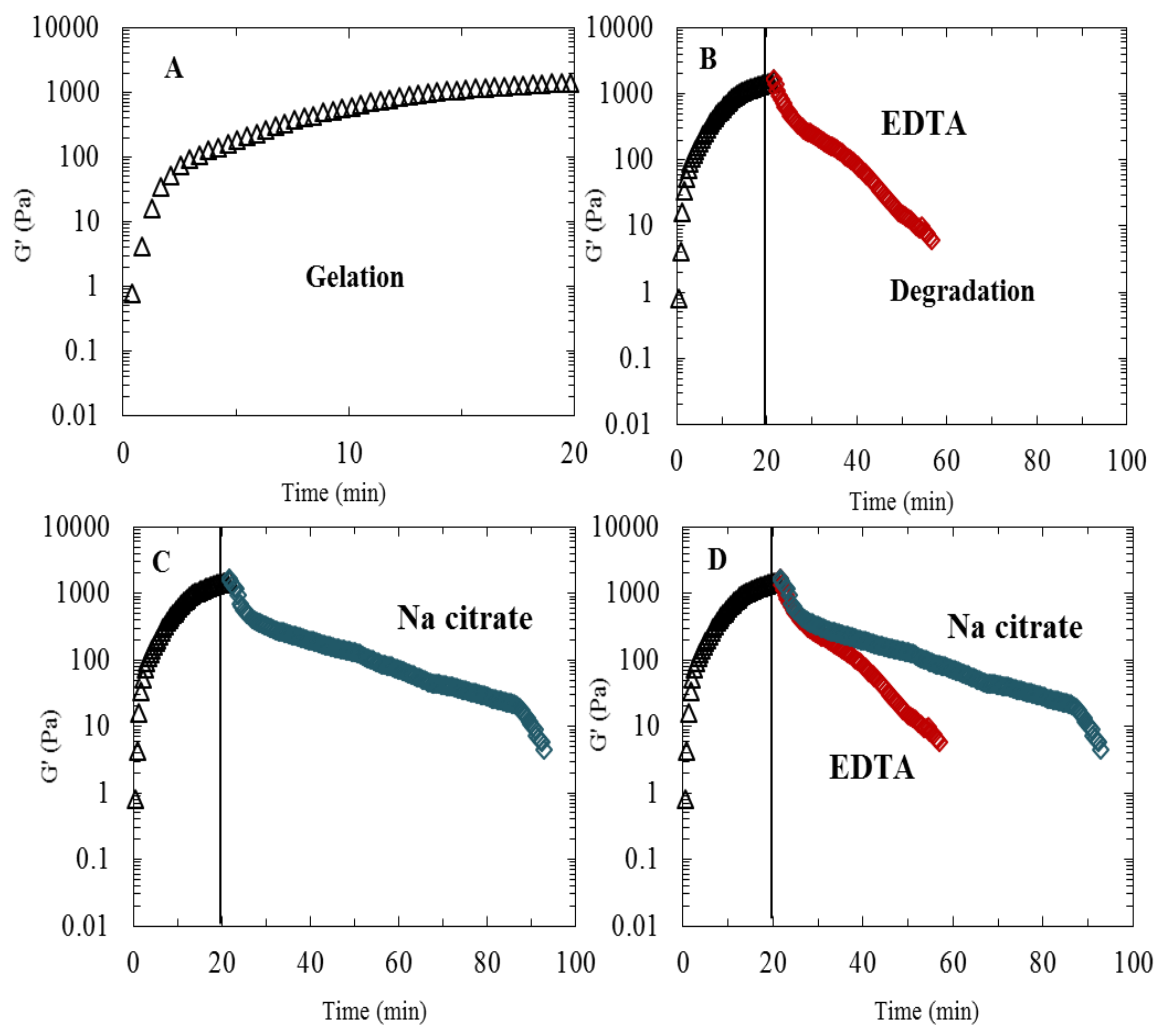


**Figure 4-4: Rheological measurements of 4% alginate shows variation of  $G'$  moduli ; A) 4% alginate crosslinked with 200 mM  $\text{CaCl}_2$  *in situ* , B) Gel dissolution using 500 mM EDTA , C) Gel dissolution with 500 mM Na citrate and D) comparative values of  $G'$  of 4% alginate after exposure to (500 mM) EDTA and Na citrate .**

#### 4.3.3 Pectin *in situ* gelation results

To examine any differences in the rheological behaviour when LM Pectin is gelled *in situ* a 4% LM pectin solution and three different concentrations of calcium chloride (50, 100 and 200 mM) were prepared at room temperature. Variation of storage modulus  $G'$  and loss modulus  $G''$  were examined in order to evaluate external gelation *in situ*.

Figures 4.5 A-C shows gelation of LM pectin upon exposure to  $\text{CaCl}_2$ . Over the first minute of the test there is a clear sharp increase in both moduli as the onset of gelation occurs similar to what was observed with alginate in Figure 4.4 however there was not a clear difference between the  $G'$  and  $G''$  values. Although increasing the concentration of the  $\text{CaCl}_2$  caused an increase in the final moduli values (measured at 20 min) with  $G'$  increasing from approximately ~300 Pa at 50 mM  $\text{CaCl}_2$  to ~900 Pa at 200 mM  $\text{CaCl}_2$  (Figure 4.5D). Values of  $G''$  were similar indicating a more fluid behaviour and a less firm gel when compared with the alginate.

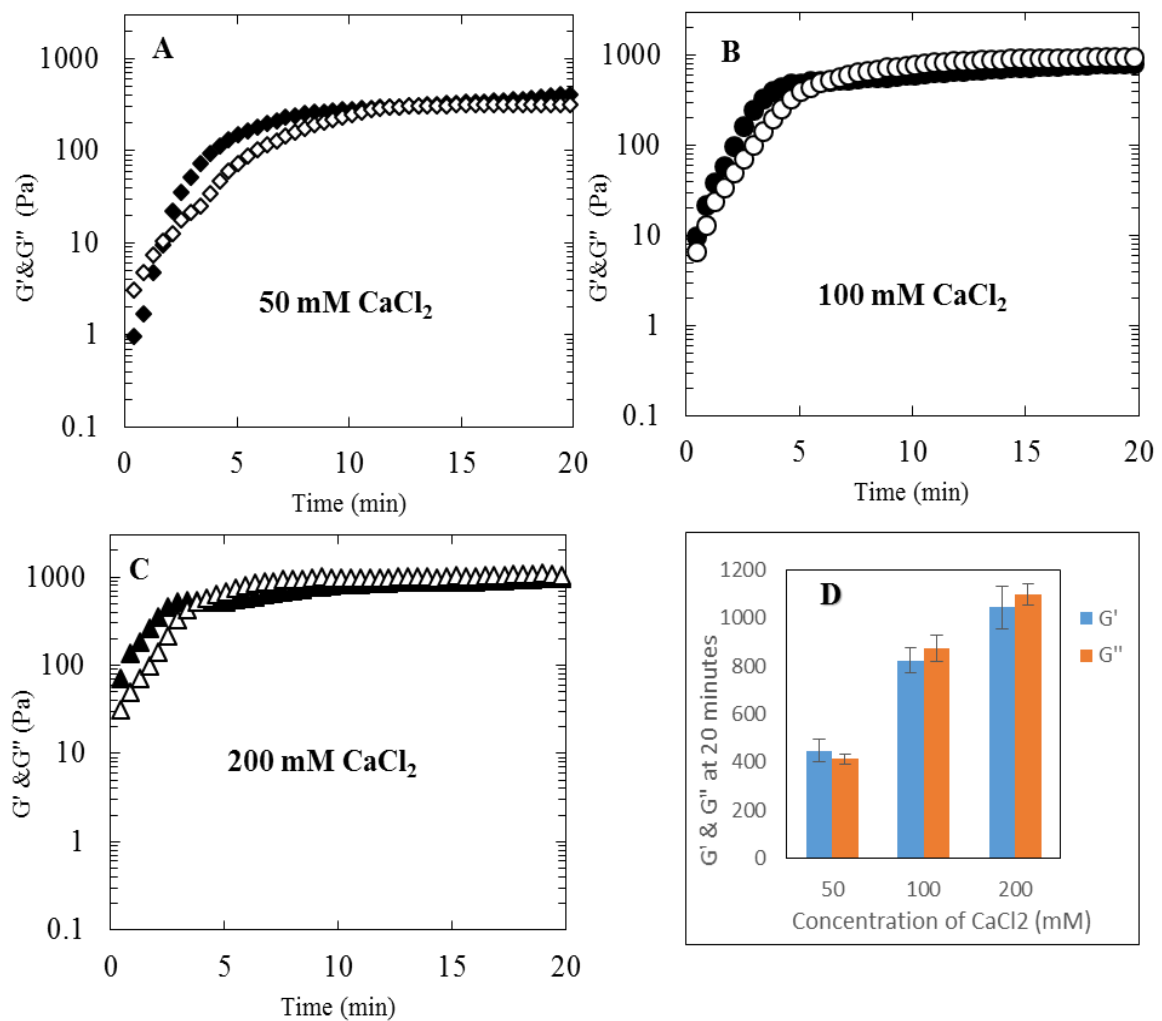


**Figure 4-5: Rheological measurements for pectin 4% showing variation of  $G'$  (filled symbols),  $G''$  (open symbols) vs time on exposure to A) 50 mM B) 100 mM and C) 200 mM; D) shows comparative values of  $G'$  after 20 min exposure to (50, 100 and 200 mM) of  $\text{CaCl}_2$ .**

#### 4.3.4 Pectin *in situ* gel dissolution results

Similar to alginate, LM pectin formed on exposure to crosslinking ions externally, can also be converted back from gel to the sol state using the calcium chelating agents EDTA and Na citrate. To measure how the chelation progressed 4 % w/w LM pectin gels were crosslinked *in situ* with 200 mM  $\text{CaCl}_2$  (Figure 4.6A) and then exposed independently following 20 min gelation to 500 mM EDTA (Figure 4.6B) and Na citrate (Figure 4.6C).

As in the alginate gels the EDTA was found to be a much stronger calcium chelator than Na citrate causing  $G'$  to return to a similar modulus to that of the LM pectin prior to crosslinking, after only 29 min of exposure. In contrast, sodium citrate only reduced  $G'$  by one order of magnitude in comparison with the two orders of magnitude achieved when using EDTA (Figure 4.6D).

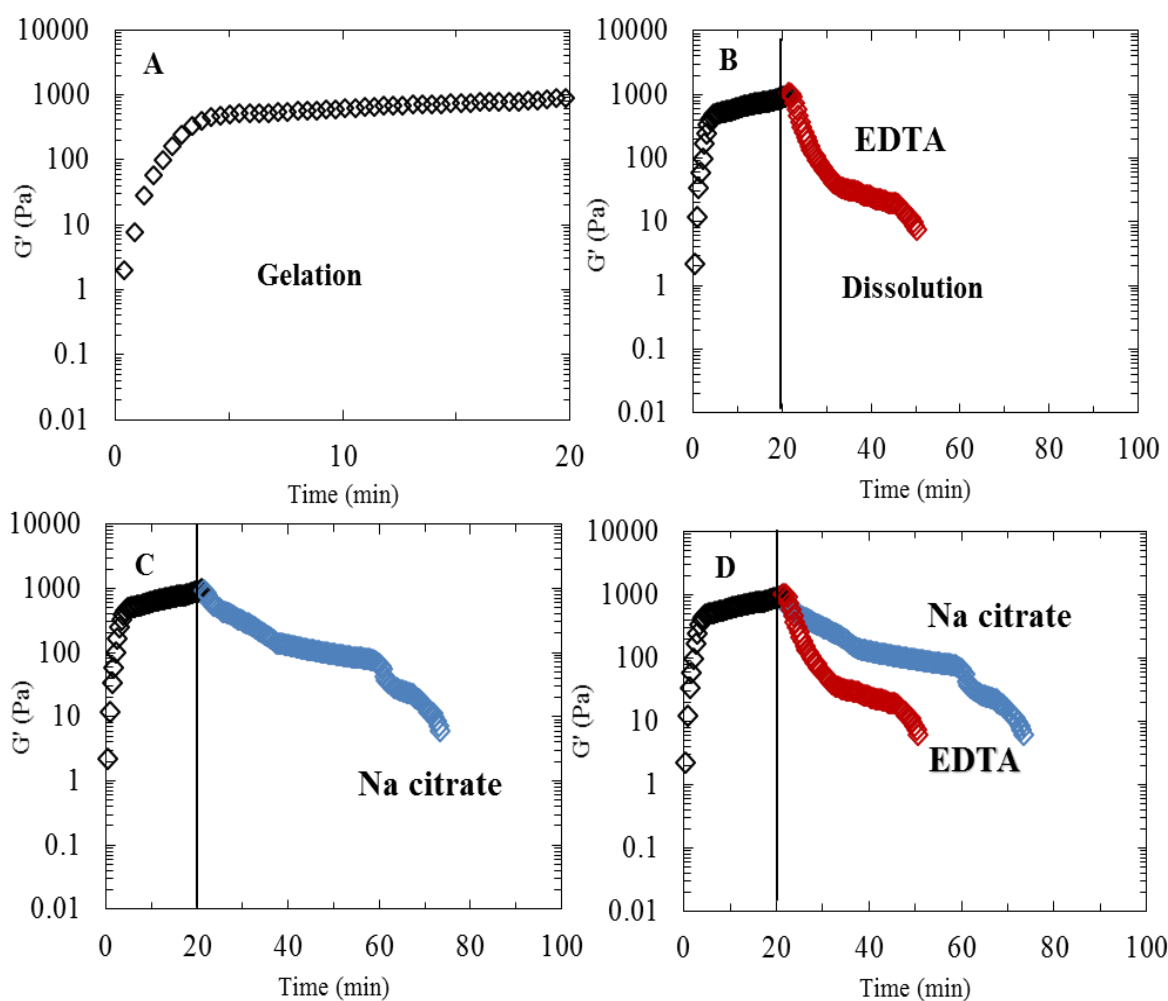


**Figure 4-6: Rheological measurements of 4% pectin shows variation of  $G'$ ; A) 4% alginate crosslinked with 200 mM  $\text{CaCl}_2$  *in situ* , B) Gel dissolution using 500 mM EDTA , C) Gel dissolution with 500 mM Na citrate and D) comparative values of  $G'$  of 4% pectin after exposure to (500 mM) EDTA and Na citrate .**

#### 4.3.5 Comparing the *in situ* gelation ( $G'$ ) values and dissolution time between alginate and pectin.

Values of storage modulus  $G'$  for 4% of alginate and pectin upon exposure to three different concentrations of  $\text{CaCl}_2$  (50, 100 and 200 mM) *in situ* were taken at the end of *in situ* gelation test (20 min) which appears the strength of gelation for both polymers. The results in the Figure 4.7 shows high significant different of  $G'$  values between alginate and pectin with  $G' \sim 1500$  Pa

for alginate and 1000 Pa for pectin when exposed to high concentration of  $\text{CaCl}_2$  (200 mM). At exposure to the low concentrations of  $\text{CaCl}_2$  (50 and 100 mM) the  $G'$  values for pectin were slightly higher than alginate with  $G'$  (412, 392 Pa and 823, 726 Pa) respectively. The strong alginate gels that formed from polymer crosslinking with 200 mM of  $\text{CaCl}_2$  will take more time to degrade the gel by EDTA and Na citrate compared with weak pectin gels that formed with the same condition as shown in the Table 4.1.

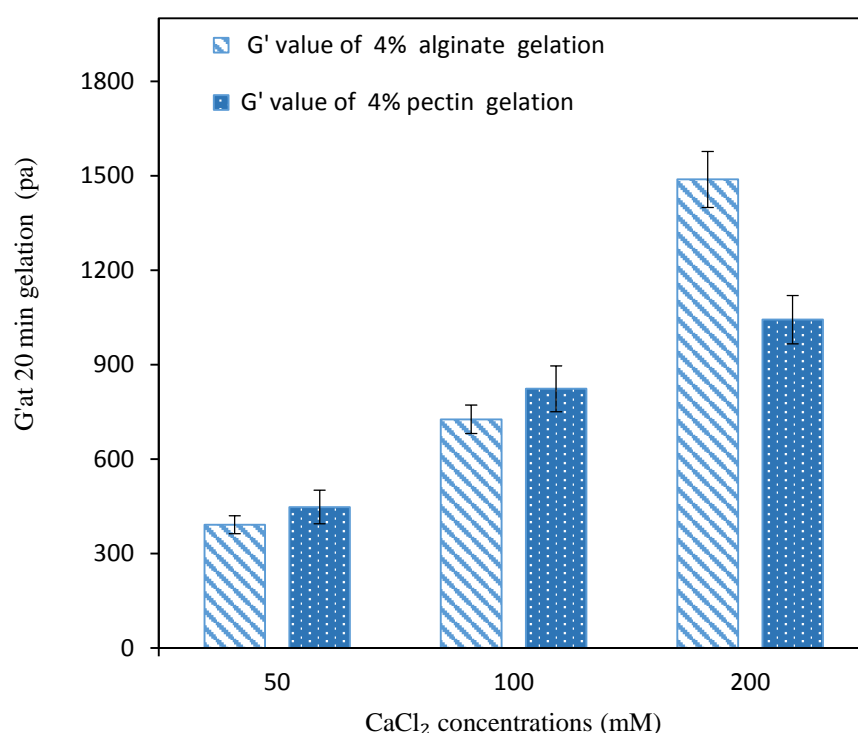


**Figure 4-7: Values of  $G'$  of *in situ* gelation time results for 4% alginate and pectin exposed to three different concentrations of  $\text{CaCl}_2$  at 20 minutes.**

**Table 4-1: Alginate and pectin gels (gelled with 200mM CaCl<sub>2</sub>) dissolution time results using EDTA and Na citrate, (mean n=3 ± SD).**

Types of polymers	Concentrations % (w/v)	Time needed to degrade the gel using EDTA (min)	Time needed to degrade the gel using Na citrate (min)
Alginate	4.0 %	35 (2.5)	73 (3.2)
Pectin	4.0 %	29 (2.1)	53 (1.8)

#### 4.3.6 Mechanical spectra

To determine the impact of *in situ* gelation on the gel strength frequency sweep measurements were taken after each *in situ* gelation test (20 min of exposure to CaCl<sub>2</sub>) for each of the samples to evaluate gels state. The strain was kept constant at 0.5%, whereas the angular frequency  $\omega$  varied from 0.1 to 100 rad s<sup>-1</sup>. The parameters G' and G'' were calculated and plotted as a function of frequency to reveal the mechanical spectra.

The frequency sweep measurements of 4% alginate exposure to 50, 100 and 200 mM of CaCl<sub>2</sub> revealed that a true gel was formed with G' much greater than G'' across the frequency range tested (Figure 4.8). Increasing concentration of CaCl<sub>2</sub> caused the moduli values to increase, which indicated that the strength of the gel increased with soaking the filter paper in greater concentrations of CaCl<sub>2</sub>. The behaviour of alginate was in contrast to the same frequency sweep measurements taken for 4% LM pectin where G' and G'' were approximately the same values across the frequency range. Moduli did increase with increasing CaCl<sub>2</sub> concentration however there was no significant difference between G' and G'' (Figure 4.9).

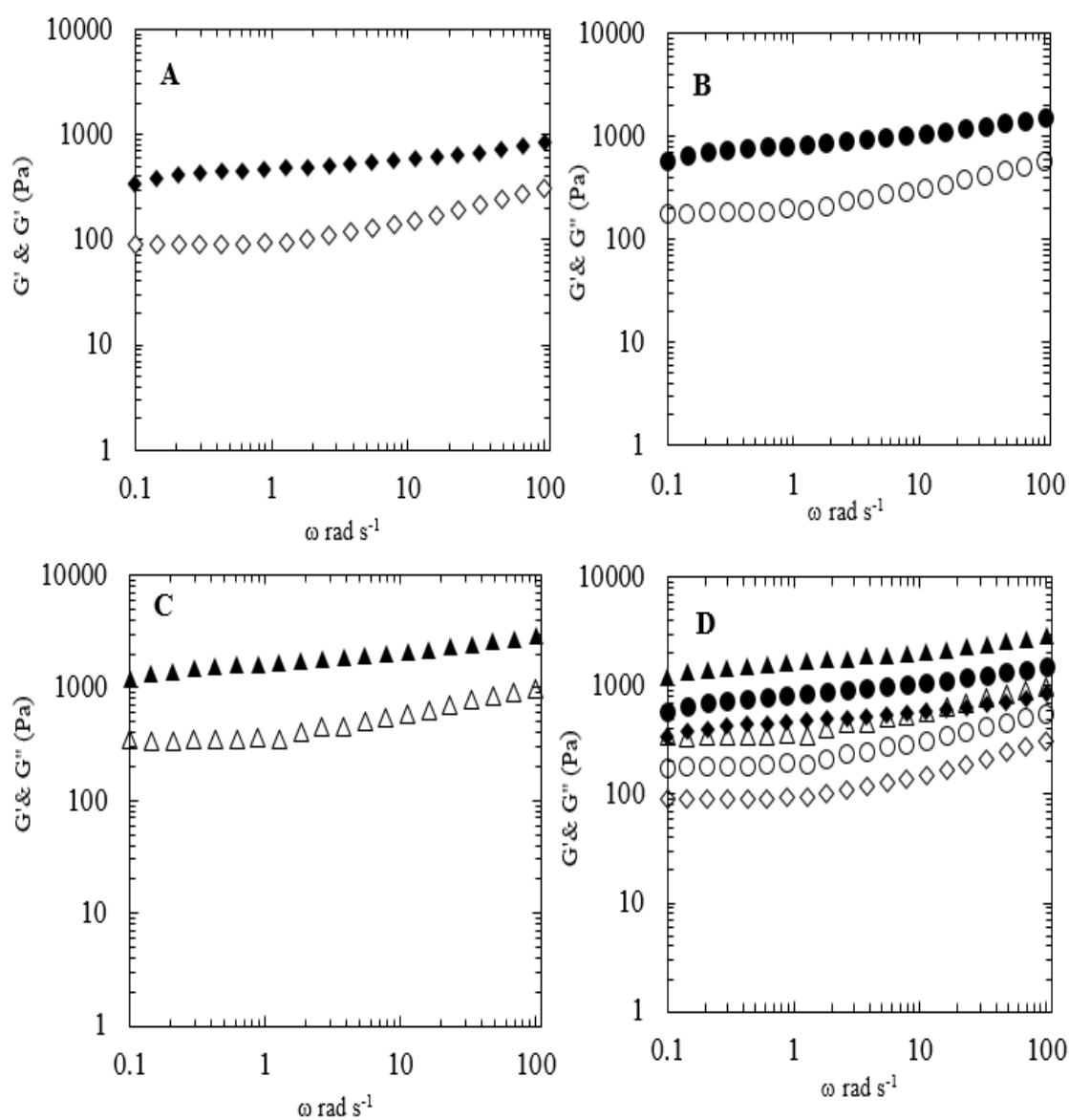


**Figure 4-8: Mechanical spectra of alginate 4% exposure to A) 50 mM B) 100 mM and C) 200 mM of  $\text{CaCl}_2$  D) Comparing exposure alginate 4% to (50 , 100 and 200 mM) of  $\text{CaCl}_2$  .  $G'$  (filled symbols),  $G''$  (open symbols).**

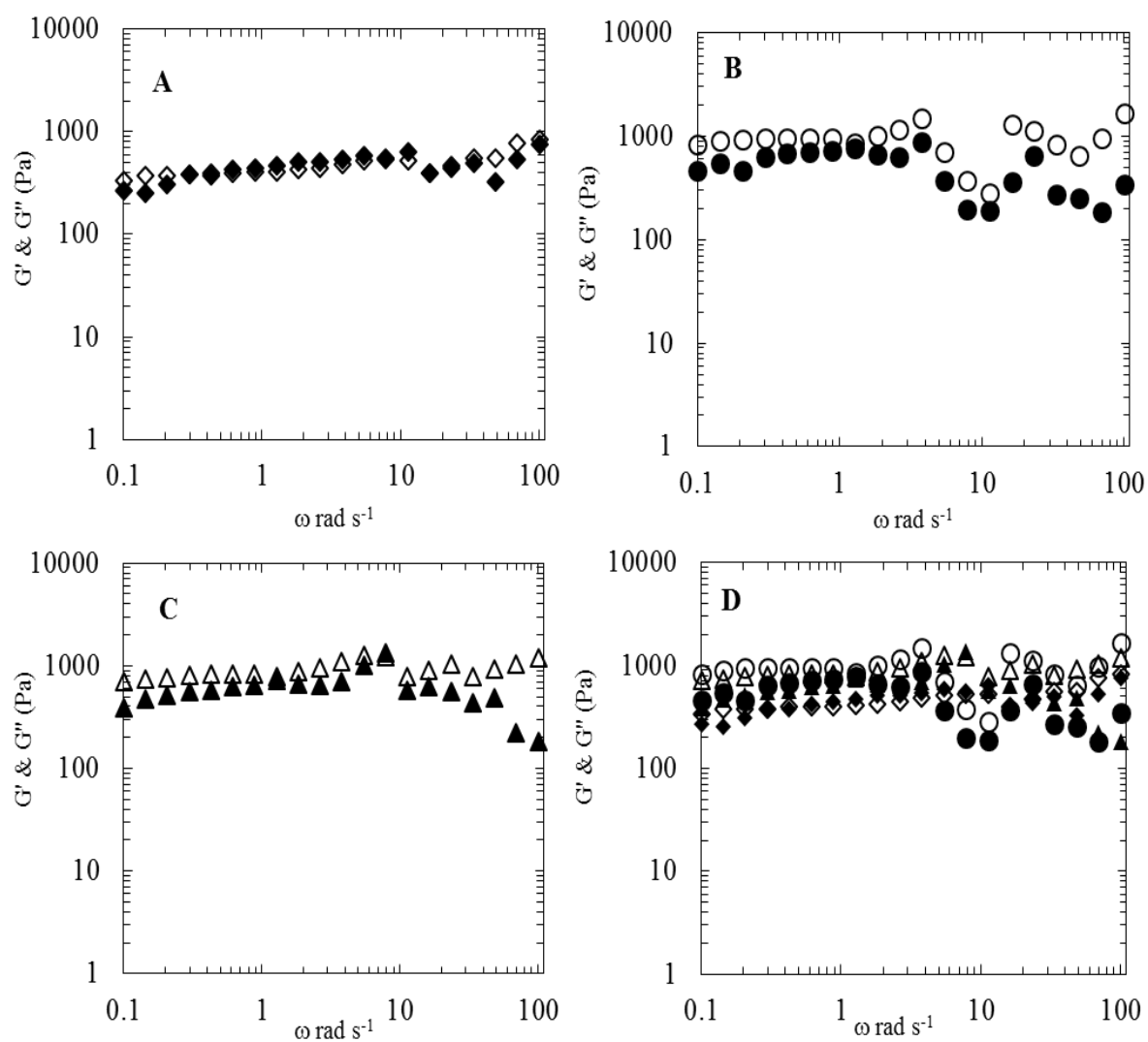


**Figure 4-9: Mechanical spectra of pectin 4% exposed to A) 50 mM B) 100 mM and C) 200 mM of  $\text{CaCl}_2$  ; D) Comparing exposed pectin 4% to (50 , 100 and 200 mM) of  $\text{CaCl}_2$  .  $G'$  (filled symbols),  $G''$  (open symbols).**



#### 4.3.7 Discussion

In order to deeply understand the influence of  $\text{Ca}^{2+}$  concentration on the gelling properties of alginate and pectin, elastic modulus  $G'$  and viscous modulus  $G''$  of both polysaccharide polymers were tested on exposure to three different concentrations of  $\text{CaCl}_2$  (50, 100 and 200 mM) *in situ*. In addition to gelation gel dissolution was also examined when treated with calcium chelators (EDTA and Na citrate). The changes in  $G'$  and  $G''$  showed the gelation behaviour of alginate and pectin when exposed to an external source of calcium chloride. Both moduli were measured by using a modified Malvern Gemini rheometer. The concentration of the alginate and pectin polymers were chosen at 4% to ensure a good signal to noise ratio from the non-crosslinked sample and to facilitate a strong and rapid gelling reaction to emphasise the ability to measure the rapid changes in moduli. Figure. 4.3 A-C shows a rapid increase in  $G'$  and  $G''$  over the first 3 min of exposure with  $G'$  overtaking  $G''$  within 2 min in all the concentrations of  $\text{CaCl}_2$  tested. The gelation reaction was allowed to proceed for 20 min and the values for  $G'$  were recorded and showed an increase that was proportional to the concentration of  $\text{CaCl}_2$  (Figure. 4.3D). This proportional increase in  $G'$  has been shown previously with alginate crosslinked by internal gelation mechanisms (Draget et al., 2006a). Similar increases in moduli were obtained with 4% LM pectin on exposure to 50, 100 and 200 mM of  $\text{CaCl}_2$ , however the values of  $G'$  and  $G''$  were very close to one another (Figure 4.5 A-D) indicating a weaker more fluid network when compared with the alginate. This is likely due to the difference in gelling capacity between the two polymers. Although moduli increased with increasing concentration of  $\text{CaCl}_2$  for both polymers it was interesting that at concentrations of 50 and 100 mM of  $\text{CaCl}_2$  the pectin and the alginate had values of  $G'$  that were not significantly different. However, at 200 mM  $\text{CaCl}_2$  the alginate value of  $G'$  was much greater than that of the LM pectin (Figure 4.7). This can be explained by the pectin reaching a saturated state for calcium binding at high concentration of  $\text{CaCl}_2$ , (Lips et al., 1991; Garnier et al., 1994).

The simplest method for converting calcium crosslinked alginate and pectin gels back to sol state is by immersing the gels in a solution of a calcium chelator such as EDTA or Na citrate. Once the calcium ions are removed from the gel, its structure is lost and it reverts back to the liquid state. This reversal of the gelation process is particularly important in systems where cells or bioactives are immobilised in the gels that require releasing from the gel matrix. To highlight the potential of this method to analyse changes in rheological properties of gels on exposure to external sources of salts, the effect of commonly used calcium chelators on 4% alginate and pectin crosslinked for 20 minutes by an external source of 200 mM  $\text{CaCl}_2$  were studied (Figure. 4.4 and 4.6 respectively). From the results obtained EDTA was shown clearly to be a more potent calcium chelator than Na citrate, causing  $G'$  to return to a similar modulus to that of the original polymer solution, before crosslinking, after only 35 minutes of exposure for 4% alginate and 29 minutes for 4% pectin. In contrast, Na citrate only reduced  $G'$  by one order of magnitude in comparison with the two orders of magnitude achieved when using EDTA. This can be explained by EDTA having a higher calcium ion binding constant than Na citrate as previously demonstrated by Keowmaneechai and McClements (2002). Differences were also observed in the dissolution time of both alginate and pectin (Table 4.2) when treated with EDTA and Na citrate, with EDTA having a more rapid effect. Interestingly the time needed to degrade pectin gels were shorter than alginate gels with both EDTA and Na citrate. When EDTA was used the alginate samples took 35 min to degrade and 29 min in the pectin, whereas there was a much larger disparity when Na citrate was used with the alginate taking 73 min and the pectin only 53 min. This is thought to be a result of the differences in the availability of sites for egg box junctions to be formed. The high guluronate content of the alginate used provides many potential binding sites for the calcium ions which results in a strong gel formation. On the other hand, the binding sites on the LM pectin and subsequent gel strength will be strongly dependent

on the distribution of the rhamnose side chains and the distribution of the methyl groups which for the material used in this study is unknown (Powell et al.,1982).

Further insight into the strength of the gels produced was achieved using frequency sweep tests to reveal the mechanical spectra of alginate and LM pectin after each gelation test. The mechanical spectra of 4% alginate after exposure to 50, 100 and 200 mM of  $\text{CaCl}_2$  showed  $G' > G''$  (Figure 4.8 A-C) across the frequency range tested with only slight frequency dependence of the moduli. This indicates that the alginate had formed strong gels in all three concentrations of  $\text{CaCl}_2$  used, with an increase in gel strength as the concentration of  $\text{CaCl}_2$  increased (Figure 4.8D). Indeed, all of the gels tested were strong enough to resist failure even at high a frequency of oscillation ( $100 \text{ rad s}^{-1}$ ) The mechanical spectra of the 4% LM pectin however, when treated with the same concentrations of  $\text{CaCl}_2$ , revealed a material with much weaker gel behaviour with  $G' \approx G''$  (Figure 4.9A-C). In addition, the at higher frequencies there was evidence of failure in the high frequency range especially in the 100mM and 200mM  $\text{CaCl}_2$  samples further supporting the hypothesis that the higher concentrations of calcium saturated the potential binding sites of the LM pectin. Therefore, when LM pectin gels where exposed to the calcium chelators less calcium is needed to be sequestered from the pectin to cause dissolution and consequently resulted in a more rapid dissolution time when compared with the alginate (Table 4.1). Overall this method has shown enough sensitivity to discriminate the gelling characteristics of similar gel forming materials alginate and LM pectin and the effects of changes in concentrations of external crosslinkers and chelating agents.

## 4.4 Conclusion

This study has demonstrated a novel method to measure the rapid changes in rheological properties of alginate and pectin during external gelation on exposure to  $\text{CaCl}_2$ . Differences in gel strength could also be measured when changing the source concentrations of  $\text{CaCl}_2$ .

Moreover, the dissolution of calcium crosslinked alginate and pectin gels can also be monitored in real time by replacing a crosslinking ion source for a calcium chelator. Indeed, results obtained using this method showed that EDTA was a more effective chelator than Na citrate. This method is not only suitable for measuring rapid gelation kinetics on exposure to cross-linkers but has potential applications in modelling the *in situ* gelation behaviour in simulated physiological environments.

#### **4.5 Limitations and future perspectives**

The limitations of using this Petri dish gelation method are identified as follows: Firstly, it is crucial to begin the measurements at a consistent time following loading of the sample as this is particularly important with rapid gelling systems such as alginate. Secondly, the quantification of ion concentrations diffused into the sample is unknown and could result in the possibility of an inhomogeneous gel with the sample being more crosslinked close to the filter paper. This effect would have greater significance, however, on thicker gels, i.e., those measured with a larger gap size. It is proposed that this technique could be applied to other biopolymers such as gellan, carrageenans and other materials that gel in the presence of metal ions, small molecule crosslinkers or by changes in pH. The wider implication of this is an ability to choose isolated biopolymers for many different industry applications where there may be a need for rapid or slow gelation. For example, this system could be used as a model for understanding changes in rheological behaviour when biopolymers are exposed to various physiological fluids.

This could, therefore, have particular applications in designing bioresponsive delivery systems in the food, pharmaceutical and biomedical industries. This aspect of potential application is investigated in Chapter 5.

## **Chapter 5 Experimental simulation of the gelation behaviour of *in situ* cross-linked gels on contact with physiological fluids**

Aspects of this chapter have been published in Macromolecular Chemistry and Physics.

Diryak, R., Kontogiorgos, V., Ghorri, M.U., Bills, P., Tawfik, A., Morris, G.A. and Smith, A.M., 2018. Behavior of *in situ* cross-linked hydrogels with rapid gelation kinetics on contact with physiological fluids. Macromolecular Chemistry and Physics. 1700584.

## CHAPTER FIVE

### EXPERIMENTAL SIMULATION OF THE GELATION BEHAVIOUR OF *IN SITU* CROSS-LINKED GELS ON CONTACT WITH PHYSIOLOGICAL FLUIDS

#### 5.1 Introduction

Among many polymeric drug delivery/cell delivery systems *in situ* gelling polymers have shown particular promise. *In situ* gelling systems are polymeric formulations that are in the liquid state prior to administration and then undergo rapid gelation under physiological conditions with the gel strength and rate of gelation often critical to their function. The sol-gel transition of *in situ* gelling polymers depends on one or a combination of different environmental triggers such as pH changes, temperature modulation, solvent exchange, and the presence of ions (Madan et al., 2009). The development of *in situ* gel systems has received considerable attention over the past 25 years (Peppas and Langer, 1994), sparked by the numerous advantages of such delivery systems. These include, ease of administration and reduced frequency of administration, and improved patient compliance (Bakliwal and Pawar, 2010). There are many polymers natural and synthetic (gellan gum, alginate acid, xyloglucan, pectin, chitosan, poly (DL-lactic acid), poly (DL-lactide-co-glycolide) and poly-caprolactone) that can undergo physiological *in situ* gelation and therefore could potentially be used for drug delivery or cell delivery via multiple administration routes (Madan et al., 2009). Xyloglucan for example, forms thermally reversible gels on warming to body temperature (Miyazaki et al., 2001). Some other polysaccharides are pH depended such as carbopol (polyacrylic acid based) which undergo sol-gel transition at alkaline pH (~pH 7) while other polymers such as gellan gum, alginate and pectin undergo sol-gel transitions at acidic pH (~pH 3.5) (Madan et al., 2009). Gellan gum can also undergo sol-gel transition in presence of physiological concentrations of cations (Sworn, et al., 1995; Morris et al., 2012).

### **5.1.1 Physiological fluids**

#### **5.1.1.1 Wound fluid (Exudate)**

Wound fluid is mostly made up from a heterogeneous mix of endogenous and exogenous sources, comprising a provisional matrix of exudates or transudates originating from the blood (Loffler, 2011). Exudate is derived from fluid leaking out of blood vessels, closely resembling blood plasma. The fluid leaks into body tissues determined by the permeability of the capillaries and the hydrostatic and osmotic pressure across the capillary walls. Most of the leaked fluid is usually reabsorbed into capillaries, and the small amount that is not reabsorbed returns to the central circulation through the lymphatic system. Wound exudate contains a variety of substances including water, nutrients, electrolytes, inflammatory mediators, white blood cells, protein-digesting enzymes and growth factors. Electrolytes species that are present include sodium, potassium, calcium and magnesium. The values of these electrolytes in wound exudate are similar to the values found in plasma, (Table 5.1) (Cutting, 2003).

#### **5.1.1.2 Saliva**

The human saliva is a complex mixture of different fluids; secreted by a set of major and minor salivary glands. Salivary fluid is an exocrine secretion consisting of approximately 99% water, containing a variety of electrolytes (sodium, potassium, calcium, chloride, magnesium, bicarbonate, phosphate) and proteins, represented by enzymes, immunoglobulins and other antimicrobial factors, mucosal glycoproteins, traces of albumin and some polypeptides and oligopeptides of importance to oral health (Denny et al.,2008). There are three major salivary glands, which are parotid, sublingual and submandibular glands (Figure 5.1). All these glands are under the control of autonomic nervous system. A human has salivary secretion of 1.5 liters per day. It has slightly alkaline pH which is 7.4.

It contains mucins along with some enzymatic proteins like lipase and salivary amylase. Some other compounds like lactoferrins, cystatin, histatins and some thiocyanate ions are also present (Silbernagl, 2009).

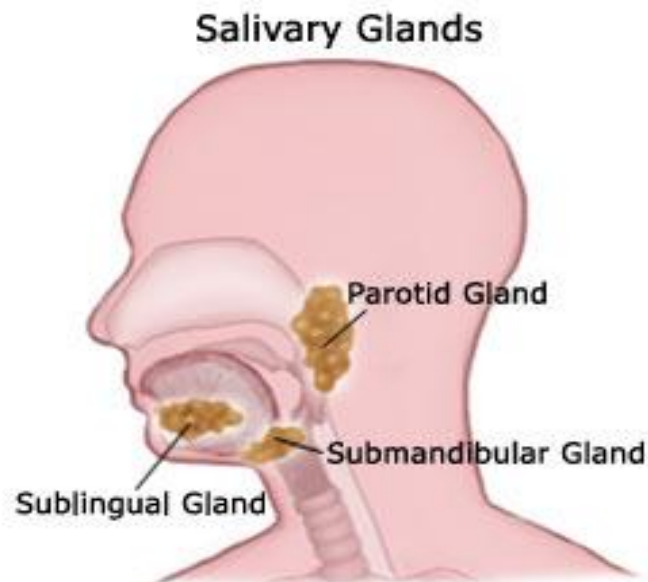


**Figure 5-1: Salivary gland types adapted from (Graney et al., 2009).**

#### **5.1.1.3 Lacrimal fluid**

A smooth ocular surface is responsible for good visual activity. This property is provided to eye by lacrimal fluid (LF) which covers the whole ocular surface. It serves as a barrier, lubricant, nutrient, and as anti-microbial protectant. It improves the optical properties of eye and the maintenance of a normal lacrimal fluid is thus important for a smooth ocular surface. Three different types of responses cause the LF production: basal response, emotional and reflex response (Figure 5.2). The lacrimal gland produces 2-3 ml of LF daily due to the basal response of the eye. It is calculated from dye dilution tests from corneal epithelial cells desquamation (Ehlers et al., 1972). The thickness of lacrimal fluid reported by investigative methods was 3-45 $\mu$ m but results from the newer measurement methods like interferometry and optical coherence tomography showed that values around 3-4  $\mu$ m are more accurate (Bron et al., 2004).



LF lipids and proteins provide a high surface pressure and thus help stabilise the fluid.  $\text{Na}^+$ ,  $\text{K}^+$ ,  $\text{Cl}^-$ ,  $\text{HCO}_3^-$  and low levels of  $\text{Mg}^{2+}$  and  $\text{Ca}^{2+}$  are the principal electrolytes in the basal lacrimal fluid. The LF is usually isotonic with serum but it has a higher concentration of  $\text{K}^+$  ions compared to serum (Gilbard, 1994). These electrolytes in the LF can promote the phase transition of *in situ* gelling systems. Consequently, using polymers in ophthalmic formulations that gel in the presence of certain electrolytes promotes the increased ocular bioavailability of ophthalmic drugs by prolonging the contact time in the corneal and conjunctival epithelium (Nanjawade et al., 2007; Rajoria and Gupta, 2012).

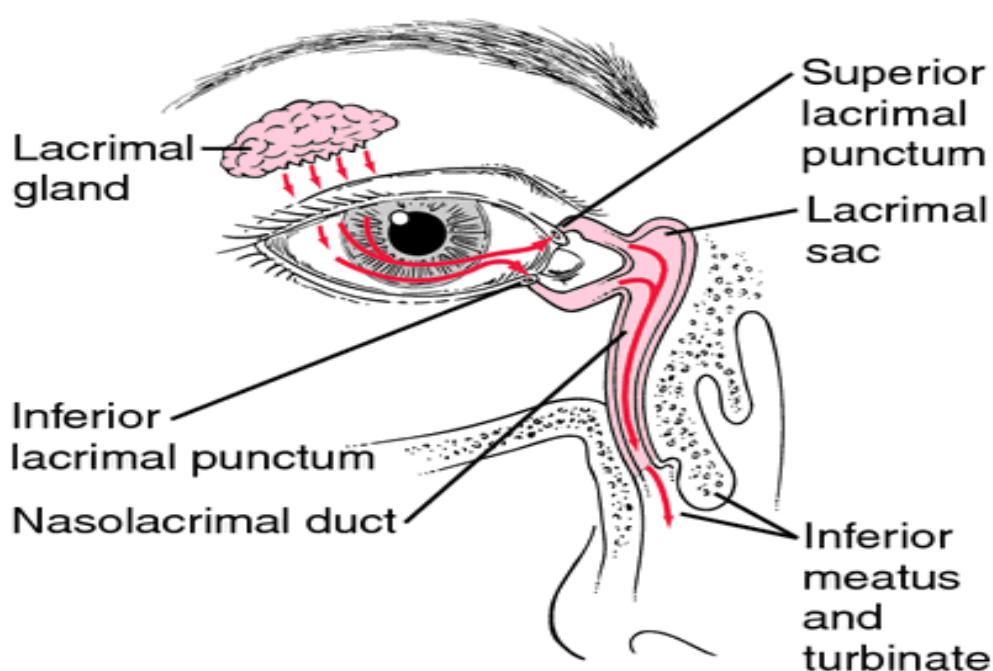


**Figure 5-2: Eye anatomy diagram shows lacrimal gland and lacrimal sac adapted from (Sultana et al., 2006).**

#### 5.1.1.4 Gastric fluid

Gastric fluid is produced in the stomach from the mucosal membrane cells (Figure 5.3) which comprises of:

- Mucus component
- Enzyme component
- Acidic and Ionic components

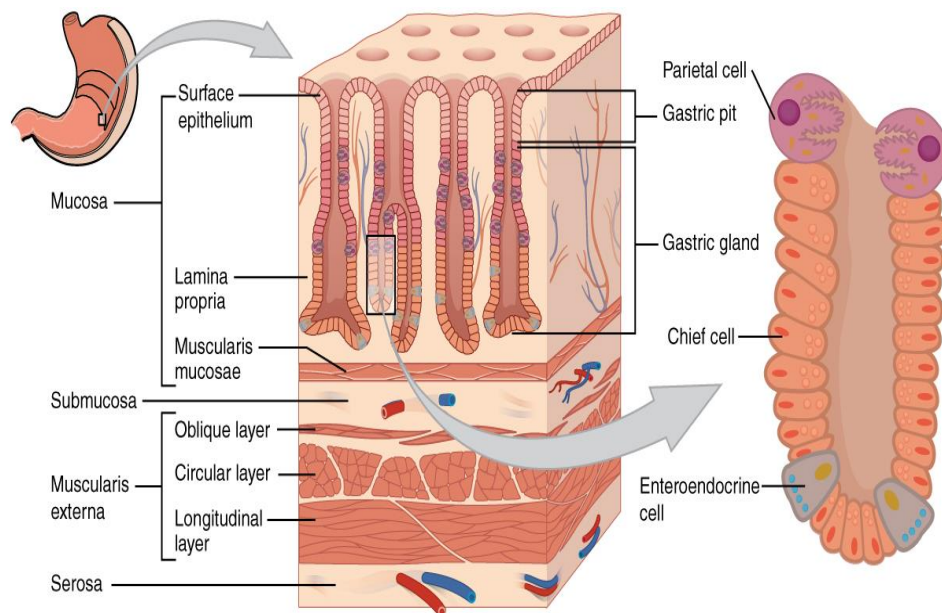


**Figure 5-3: Anatomy of the stomach mucosa and the cells that produce the gastric fluid (Silbernagl, 2009).**

Normally, 2-3 L of gastric juice are produced in the stomach of an adult human per day. The secretions have variable acidic and ionic compositions which depend upon the rate of volume flow or rate of secretion of the gastric juice  $H^+$  and  $Na^+$  concentrations significantly depend upon the rate of secretion. Correspondingly, the concentrations of  $Cl^-$  and  $K^+$  increase with the increase in rate of volume flow of gastric juice (Quigley and Turnberg, 1987).

The pH of stomach is 0.8 when HCl concentration is at its maximum. When ingested food enters the stomach it balances the pH level and raises it to between 1.8 and 4, which is when the enzymatic action of pepsin and gastric lipase initiates. Whereas lower pH provides a bactericidal effect (Silbernagl, 2009).

#### 5.1.1.5 Gelation in physiological fluids

In the present study the impact of different physiological fluids on the rheological properties of gellan gum were investigated using the same method that was used to measure the external gelation of alginate and pectin in chapter four. Changes in rheological behaviour of gellan were measured *in situ* at different simulated application sites (oral, ocular and topical). Four different types of physiological fluids which have different ion concentrations were prepared as shown in the Table 5.1 (simulated wound fluid, artificial saliva, artificial lacrimal fluid and simulated gastric fluid) and used in the study. Following the measurements of gelation, the gelation kinetics were modelled and the gelled samples were recovered and the resulting microstructure was analysed. These experiments were designed to provide an insight into predicting the material behaviour of gellan when it comes into contact with commonly encountered delivery sites.

**Table 5-1: Concentrations of mono and divalent cations in different types of physiological fluids saliva, lacrimal and wound fluids (Whelton, 1996; Levin et al., 2011; Cutting, 2003).**

Types of cations	Concentration in saliva (mM)	Concentration in lacrimal fluid (mM)	Concentration in wound fluid (mM)
Na <sup>+</sup>	5.8	145	135-145
K <sup>+</sup>	19.5	20	3.5-5.0
Ca <sup>2+</sup>	0.88	0.6	2.2-2.6

## **5.2 Materials and methods**

### **5.2.1 Materials**

Low acyl gellan gum (kelcogel) was from cp Kelco (Leatherhead, UK). Fetal Bovine Serum (FBS), Maximum Diluent Recovery (MDR), Dialysis tubing (14000 MWCO) and all chemicals were from Sigma Aldrich (UK). The filter paper used was Whatman Grade 1 purchased from Fisher Scientific (UK).

### **5.2.2 Methods**

#### **5.2.2.1 Preparation of gellan solution**

Gellan solutions were prepared by dissolving low acyl gellan gum in deionised water at 85 °C (to produce solutions 0.25%, 0.5%, 0.75% and 1% w/w final polymer concentration). The samples were then allowed to quiescently cool to room temperature prior to use.

#### **5.2.2.2 Preparation of physiological fluids**

Artificial physiological fluids were prepared according to formulations outlined in published literature. All physiological fluids were prepared without addition of enzymes.

##### **5.2.2.2.1 Preparation of stimulated gastric fluid**

Artificial gastric fluid was prepared by prepared from a 1M HCl stock solution (Sigma Aldrich) which was diluted 10 fold with deionised water and then the pH of the resulting 0.1M HCl solution was adjusted to pH 2 by dropwise addition of 0.1 M NaOH.

#### 5.2.2.2.2 Preparation of stimulated saliva fluid

Artificial saliva was prepared following the formulation reported by Parker et al (1999) using the chemical components given in Table 5.2. All of the salts were dissolved in 1 L of deionised water and then the pH of solution was adjusted accordingly to pH 6.7 by dropwise addition of 0.1 M NaOH or 0.1M HCl.

**Table 5-2: Preparation of artificial saliva adapted from (Parker et al., 1999).**

Component	Quantity (g/ L)
$\text{KH}_2\text{PO}_4$	0.34
$\text{Na}_2\text{HPO}_4$	0.43
$\text{KHCO}_3$	1.5
$\text{NaCl}$	0.58
$\text{MgCl}_2$	0.14
$\text{CaCl}_2$	0.22
Citric acid	0.03

#### 5.2.2.2.3 Preparation of stimulated lacrimal fluid

The composition of simulated lacrimal fluid was adopted from a lacrimal fluid analysis (Stjernschantz and Astin, 1993). This was prepared using 6.8 g NaCl, 2.2 g  $\text{NaHCO}_3$ , 0.084 g  $\text{CaCl}_2$  and 1.4 g KCl dissolved in 1 L deionized water and the pH adjusted to pH 7.4.

#### 5.2.2.2.4 Preparation of stimulated wound fluid

Simulated wound fluid was prepared according to the formulation described by Bowler et al., 2012. Briefly, foetal bovine serum (FBS) was mixed in a 50:50 v/v ratio with maximum diluent recovery media (peptone saline diluent) that contained 8.5 g/L NaCl. The pH of the formulated simulated wound fluid was adjusted accordingly to pH 7.4.

#### 5.2.2.3 Experimental of *in situ* gelation

The experimental setup used a Malvern Gemini Nano HR rheometer with a modified lower plate (Figure 5.4) similar to apparatus described in Chapter 4. Briefly, a petri dish containing a filter paper was securely attached to the lower plate of the rheometer. A semi permeable membrane (MWCO 14,000 Da) which had previously been hydrated in deionised water was placed on top of the filter paper to prevent the sample being imbibed by the filter paper. The gap was zeroed and gellan the samples were then loaded onto the semi permeable membrane. Once loaded a light silicone oil was carefully applied around the periphery of the geometry to prevent evaporation. Small deformation oscillatory measurements of storage modulus ( $G'$ ) were then performed as a function of time at 0.5% strain and a frequency of  $10 \text{ rad s}^{-1}$  using a 55 mm diameter parallel plate geometry with a 1 mm gap.

Measurements were performed at  $32^\circ\text{C}$  for gellan with SWF to represent skin temperature and  $37^\circ\text{C}$  for the other types of physiological fluids. Following 5 minutes of measurements being taken 10 mL of physiological fluid was added to the filter paper on the lower plate to trigger gelation. Control samples of gellan were measured in the same way with deionized water added to the filter paper in place of the physiological fluids. All measurements were performed within the linear viscoelastic region previously determined from amplitude sweeps. Frequency sweeps were performed after each gelation test at 0.5 % strain and frequency range ( $\omega$ )  $0.1\text{--}100 \text{ rad s}^{-1}$ . All measurements were performed in triplicate and average data plotted  $\pm$  standard deviation.

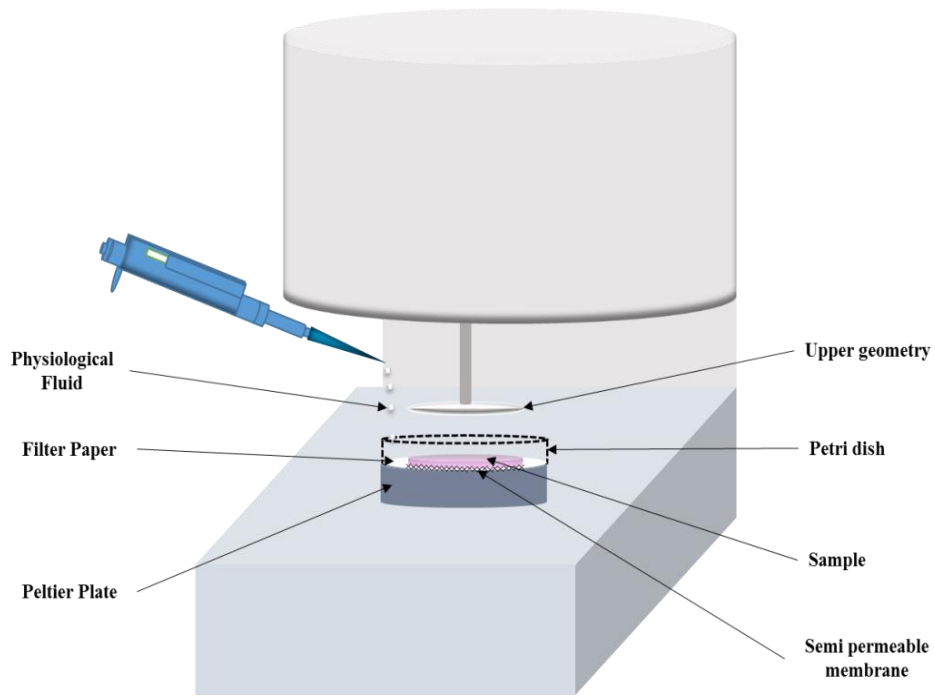


**Figure 5-4: Diagram of *in situ* gelling experiment using a commercial rheometer.**

#### 5.2.2.4 Kinetic modelling

The evolution of storage modulus with time can be described by the Gompertz double exponential growth model:

$$\log G'(t) = \log G'_{\infty} e^{-e^{(b-ct)}} \quad \text{Eq. 5.1}$$

Where  $\log G'(t)$  is storage modulus as a function of time and  $\log G'_{\infty}$  is the value of  $\log G'$  at the plateau region of the curve. In this model the maximum growth rate is given by  $\frac{c \log G'_{\infty}}{e}$  and constant  $c$  represents the scaling of storage modulus along the y-axis (rate constant).

The growth rate values were estimated and plotted vs concentration for all samples. Non-linear regression fitting was performed using GraphPad Prism v.6 (GraphPad software, San Diego, USA).

#### **5.2.2.5 Microstructure analysis**

To assess how the different fluids impacted on the microstructure of the gels, samples were removed from the rheometer following gelation, lyophilized and the microstructure analysed using surface texture analysis and micro computed x ray tomography.

##### **5.2.2.5.1 Freeze drying protocol**

Freeze-drying, also known as lyophilisation, a drying process often used to eliminate the water from materials. Freeze-drying techniques are suitable for a wide range of hydrogel materials, including natural and synthetic hydrophilic polymers to produce solid porous structures. This method uses rapid cooling to produce thermodynamic instability within a system and cause phase separation. The solvent is then removed by sublimation under the vacuum. This technique was applied to produce porous gellan gum hydrogels that formed upon crosslinked to the physiological fluids *in situ*. At the end of each *in situ* gelation test gellan gum hydrogel samples removed carefully and each sample was stored in a separate petri dish. The samples were kept in a fridge at 4°C for 24 hours' prior the freeze-drying. Freeze-drying of the samples were carried out by quenching in liquid nitrogen, followed by sublimation of the solvent. The samples were freeze dried overnight in Christ Alpha 2-4 plus at the temperature - 80°C and the vacuum was at - 60 °C. In order to avoid any influence of moisture, the samples were kept in a vacuum desiccator in presence of silica gel for a few days before the tests (microstructure analysis).

##### **5.2.2.5.2 Polymer network and surface texture analysis**

Polymer network and surface texture of freeze dried gels were examined using Talysurf CCI 3000 optical 3D surface profiler which have the capability of measuring over one million data points in less than 10 seconds with a resolution of 0.01nm. Briefly, a sample of freeze dried gel (1 × 1 cm) was fixed on a stainless steel wafer (3 × 3 cm) using the double sided transparent



tape (Scotch™ Brand, UK). The uniform gel fixation process was confirmed using an optical microscope equipped with 5.0MP camera (Supereyes®, UK).

The sample was then carefully placed under the microscopic arm of the profiler in a cleanroom environment and  $800 \times 800 \mu\text{m}$  regions were scanned to obtain reliable statistics. The height variation in the resulting topography maps is represented by a colour scheme and the topographical information can be reliably inferred from the given colour scheme. Various 3D surface texture parameters were determined using Surfstand® Software (University of Huddersfield) (Blunt and Jiang, 2003; Ghori et al., 2017). Moreover, using ImageJ version 1.47i the images were binaries using Sauvola method (Sauvola and Pietikäinen, 2000) and porosity of freeze dried gels was determined using BoneJ particle analyser plug-in (Doubé et al., 2010).

#### **5.2.2.5.3 Micro computed tomography (Micro CT)**

Prior to imaging the samples were fixed in pipette tubes and allowed to stabilise at room temperature for a period of 24 hours. Samples were imaged using a Nikon XTH 225 micro-computed tomography system (Nikon Metrology, Tring, UK) with a tungsten reflection X-ray target. Datasets were acquired at 80 kV, 3.5W with a resulting voxel size of 9 microns. Each dataset consisted of 1583 individual X-ray projections which were then reconstructed using CT Pro (Nikon Metrology, Tring, UK), standard algorithms were used for noise reduction and beam hardening compensation. Compensation was carried out using two horizontal slices at opposite extremities of each dataset to take into account any shading gradient across the image. Image exposure was set at 500 ms and a 0.5 mm Cu filter was used to remove low energy X-rays from reaching the sample. The acquired data processing, surface determination process and defect analysis was carried out using the VGStudio Max (Volume Graphics GmbH, Heidelberg, Germany) software package.

Data relating to the plastic pipette and surrounding air was removed from the analysis by demarcation of the dataset shading histogram repeatably between datasets. Cross-sections were then taken at pre-determined points through each sample such that qualitative comparison could be performed.

## **5.3 Results**

### **5.3.1 *In situ* gelation of gellan gum using artificial saliva (AS)**

Artificial saliva was prepared and used as cross-linker media for gellan to measure the *in vitro in situ* gelation of four different gellan concentrations (0.25 %, 0.5 %, 0.75 % and 1 % w/w). Gelation of the gellan occurred as soon as the was added saliva indicated by an increase in  $G'$  which continued to develop over the following 20 min of the test however the modulus did not reach a true plateau in this time frame. Increasing the concentration of gellan gave an increase in modulus, as would be expected gel with a relatively low gel stiffness  $\sim 10$  Pa at 0.25 % w/w compared to  $\sim 100$  Pa at 1 % w/w gellan. (Figure 5.5).

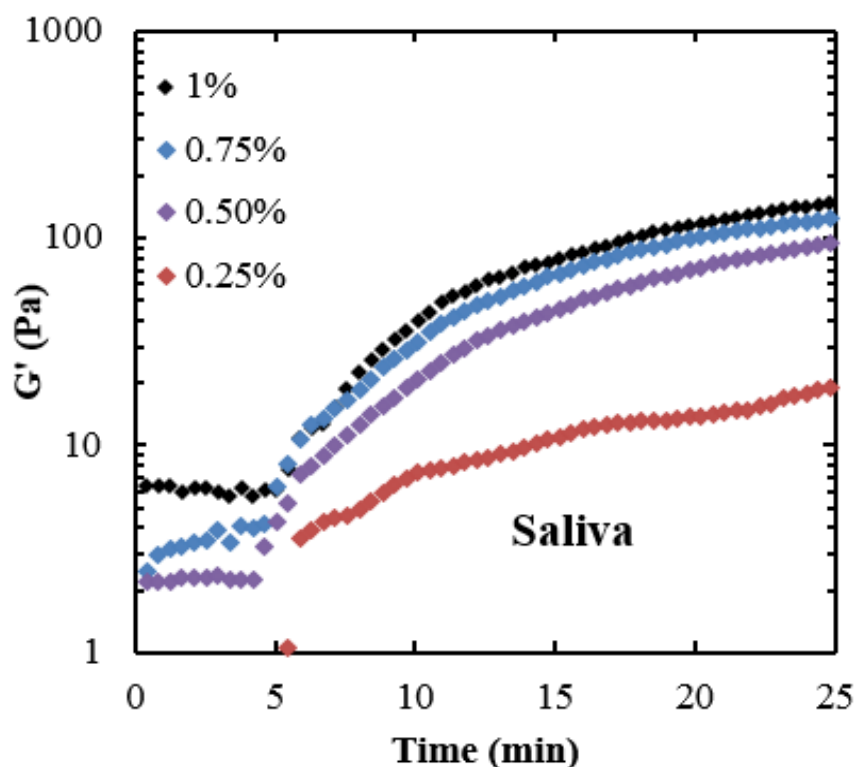


**Figure 5-5: Rheological measurements of gellan gum (0.25, 0.5, 0.75 and 1%) *in situ* gelation with artificial saliva showing variation of  $G'$  (filled symbols) vs time on exposure to cations present in AS.**

### 5.3.2 *In situ* gelation of gellan gum with simulated wound fluid (SWF)

To mimic topical wound conditions, simulated wound fluid (SWF) was prepared and used as crosslinking media. The *in situ* gelation of four different concentrations of gellan (0.25 %, 0.5 %, 0.75 % and 1 % w/w) were measured as shown in (Figure 5.6). The gelation of gellan in SWF appears more rapid than in AS and  $G'$  reaches a plateau region with 5 min of exposure to the SWF for 0.25 % and 0.5% w/w gellan concentrations indicating the maximum gelation strength was achieved in this short time frame. At 0.5% and 1 % w/w gellan the plateau region took significantly longer to reach taking ~15 min. Increasing the concentration also increased the final modulus values (although 0.5% and 0.75% were similar the rate at which each sample achieved their maximum value was quicker in 0.5% compared with 0.75%).

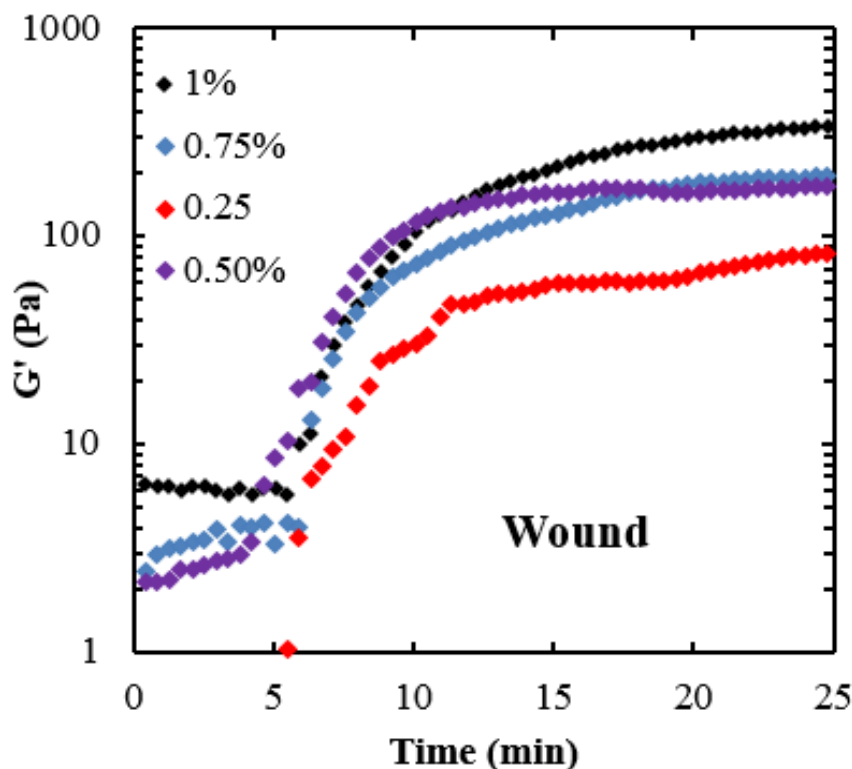


**Figure 5-6: Rheological measurements of gellan gum (0.25, 0.5, 0.75 and 1%) *in situ* gelation with simulated wound fluid showing variation of  $G'$  (filled symbols) vs time on exposure to cations.**

### **5.3.3 *In situ* gelation test of gellan with simulated lacrimal fluid (LF)**

To study the gelation behaviour of gellan *in situ*, artificial lacrimal fluid (LF) was prepared and used as crosslinking media for four different gellan concentration (0.25 %, 0.5 %, 0.75 % and 1 % w/w). The gelation behaviour on exposure to crosslinking cations in the LF gave similar profiles (Figure 5.7) to that of the SWF (Figure 5.6). This is due to the similar electrolyte composition of the lacrimal fluid and wound fluid with wound fluid having slightly more calcium ions than lacrimal fluid but much less potassium content as shown in Table 5.1. Interestingly the onset and development of structure indicated by the increase in modulus is much smoother reaching plateau sooner in the LF as compared with the SWF. This is likely due

to the SWF having a high protein content, which may slow down and interfere with the development of the gellan network.

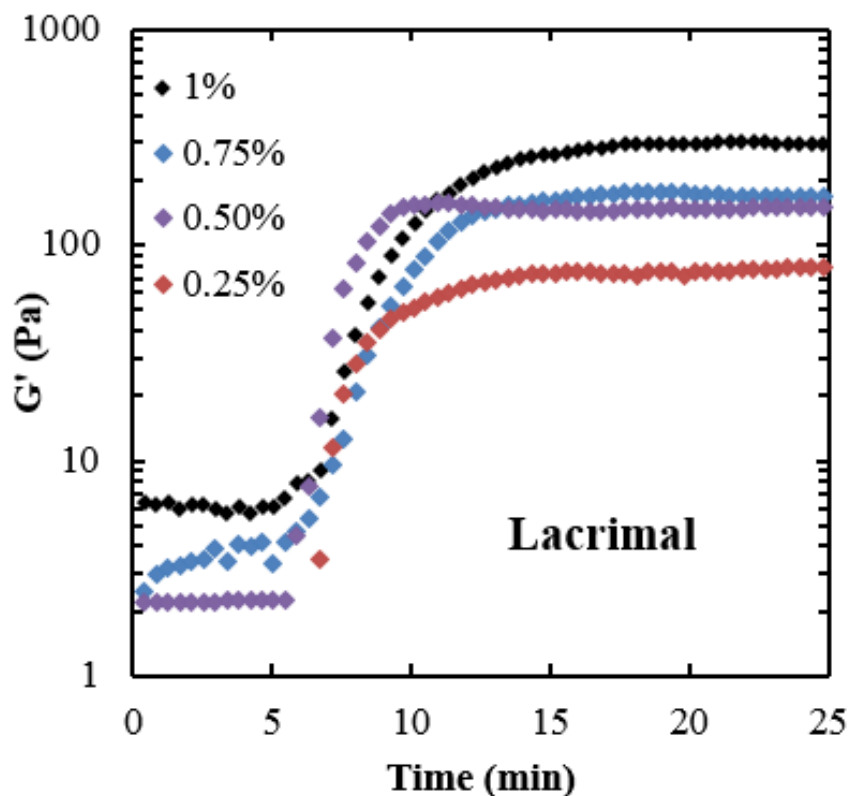


**Figure 5-7: Rheological measurements of gellan gum (0.25, 0.5, 0.75 and 1%) *in situ* gelation with LF showing variation of  $G'$  (filled symbols) vs time on exposure to cations present in LF.**

#### **5.3.4 *In situ* gelation of gellan gum using gastric fluid (GF)**

Simulated gastric fluid was prepared and used as crosslinking media for gellan to measure the *in situ* gelation of four different gellan concentrations (0.25 %, 0.5 %, 0.75 % and 1 % w/w). The onset of gelation on exposure to GF was extremely rapid reaching the plateau region within a couple of minutes for all concentrations (Figure 5.8). The final modulus values were also very high when compared with the other types of simulated physiological fluids tested (Figure 5.9).

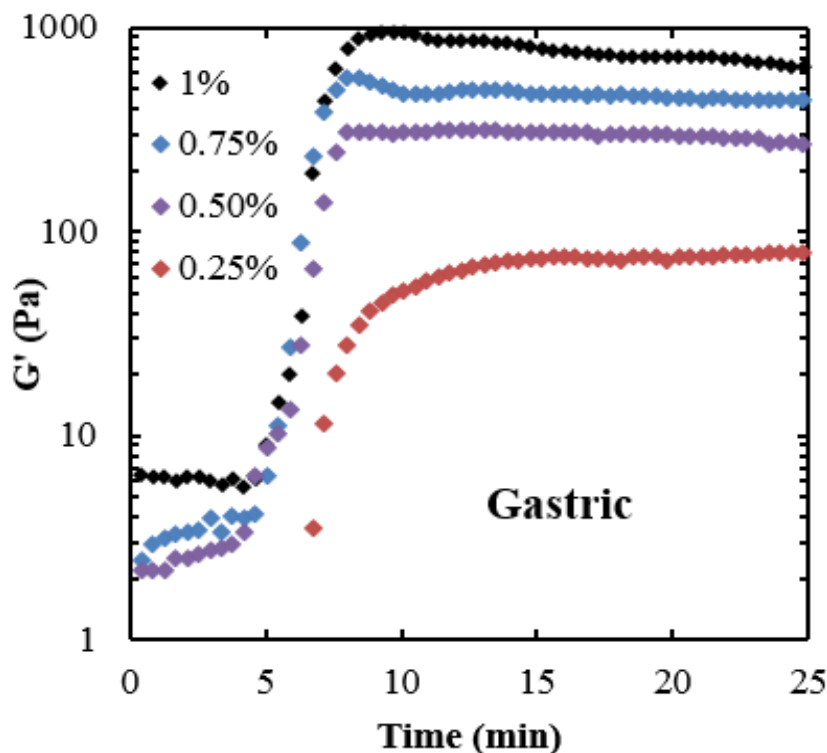


**Figure 5-8: Rheological measurements of gellan gum (0.25, 0.5, 0.75 and 1%) *in situ* gelation with GF showing variation of  $G'$  (filled symbols) vs time.**

### 5.3.5 Frequency dependence

Frequency sweep tests were applied after each *in situ* gelation experiment to examine the gel state created by exposure gellan solution to crosslinking media; the shear stress was kept constant, whereas the angular frequency  $\omega$  varied from 0.1 to 100  $\text{rad s}^{-1}$ . Figure 5.9 shows mechanical spectra for gellan (0.25, 0.5, 0.75 and 1%) after gelation by cations that present in AS and the results shows increasing  $G'$  and  $G''$  proportional to the increase in the gellan concentration across the frequency range. There is some frequency dependence of shown at high frequencies indicating some flexibility on the network. This can be explained by the low concentrations of ions in the AS fluid leading to a shorter and fewer junction zones and therefore a more fluid network.

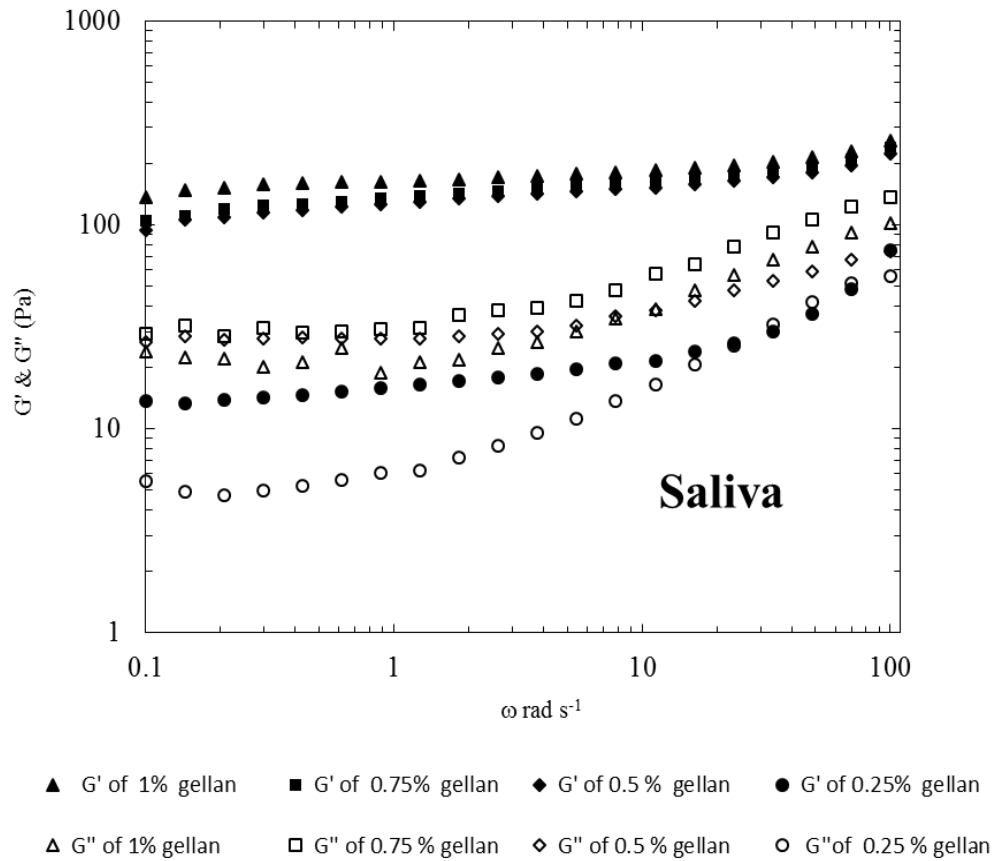


**Figure 5-9: Mechanical spectra measurements of gellan gum exposure to ions crosslinked present in AS. G' (filled symbols) & G'' (open symbols), frequency sweep test in a range of frequency between (0.1 -100) rad/s<sup>-1</sup>.**

Figure 5.10 shows G' and G'' as a function of frequency for different types of gellan gels formed after 20 minutes' exposure to cations that present in SWF and the results reveal increasing the G' and G'' values as concentration increased with only slight frequency dependence as the frequency approached 100 rad s<sup>-1</sup>.

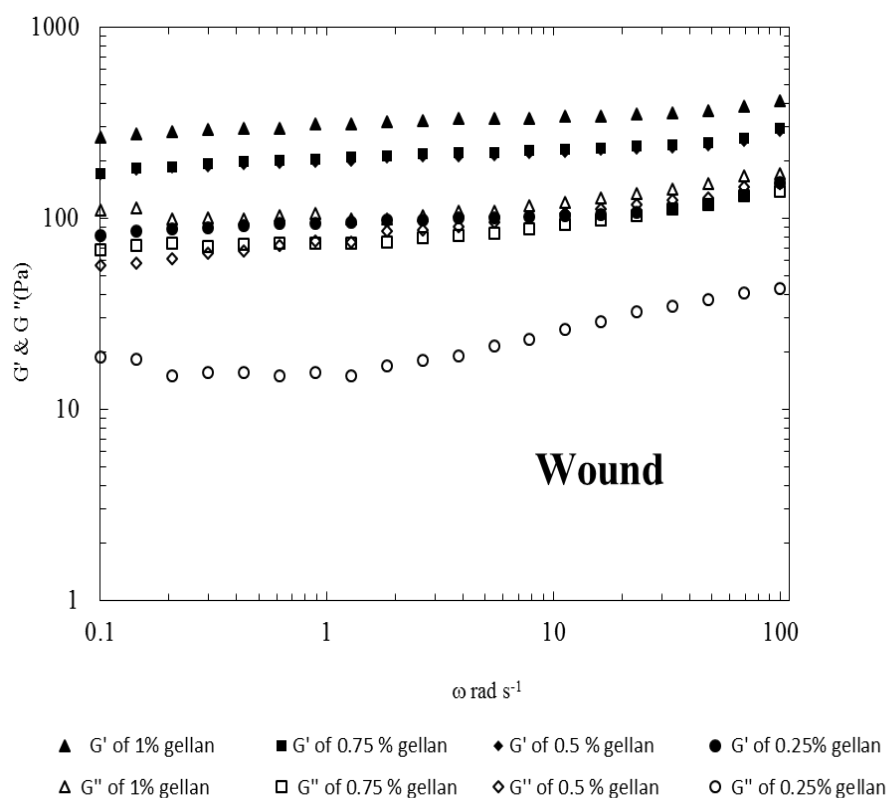


**Figure 5-10: Mechanical spectra measurements of gellan gum exposure to ions crosslinked present in SWF. G' (filled symbols) & G'' (open symbols), frequency sweep test in a range of frequency between (0.1 -100) rad/s<sup>-1</sup>.**

Figure 5.11 shows mechanical spectra for of gellan gels that formed after 20 minutes' exposure to cations that present in LF and the results similar to results that obtained with SWF, which might be expected due to the similar electrolyte content in the two fluids.



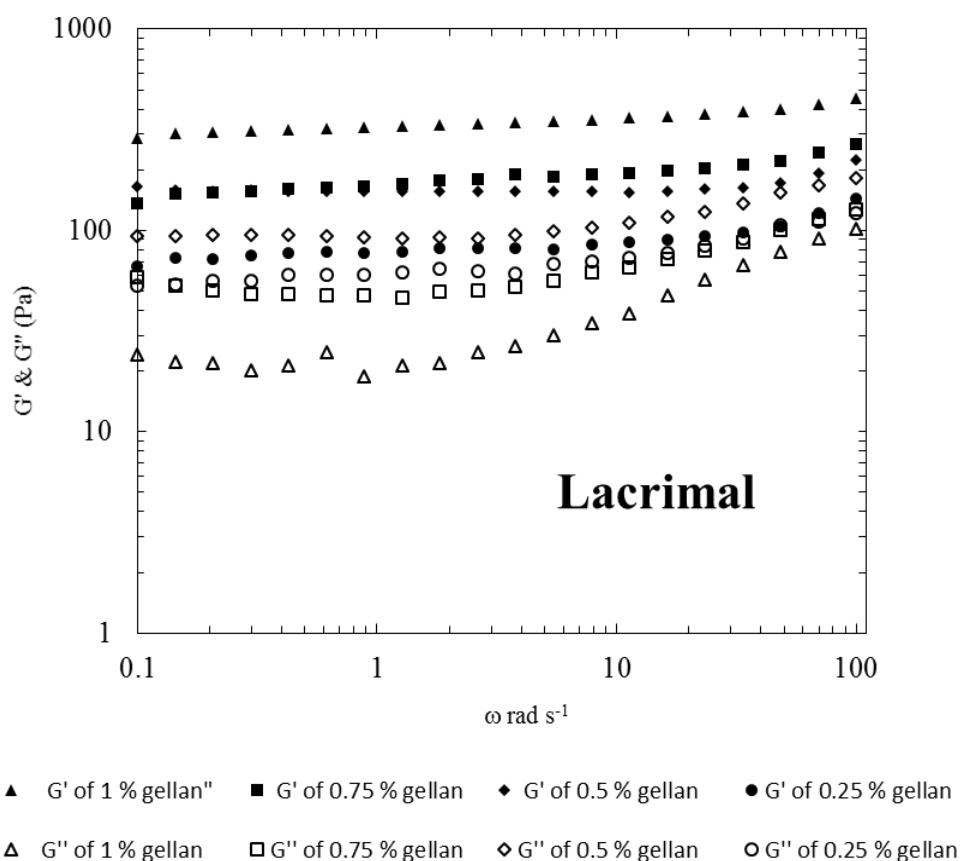


**Figure 5-11: Mechanical spectra measurements of gellan gum exposure to ions crosslinked present in LF. G' (filled symbols) & G'' (open symbols), frequency sweep test in a range of frequency between (0.1 -100) rad/s<sup>-1</sup>.**

Figure 5.12 shows mechanical spectra for different types of gellan gels that formed after 20 minutes' exposure to acidic media (GF) and the results shows strong gels formation compared with the other types of fluids. The gels were also showed evidence of failure at high frequencies indicating a strong but brittle network.

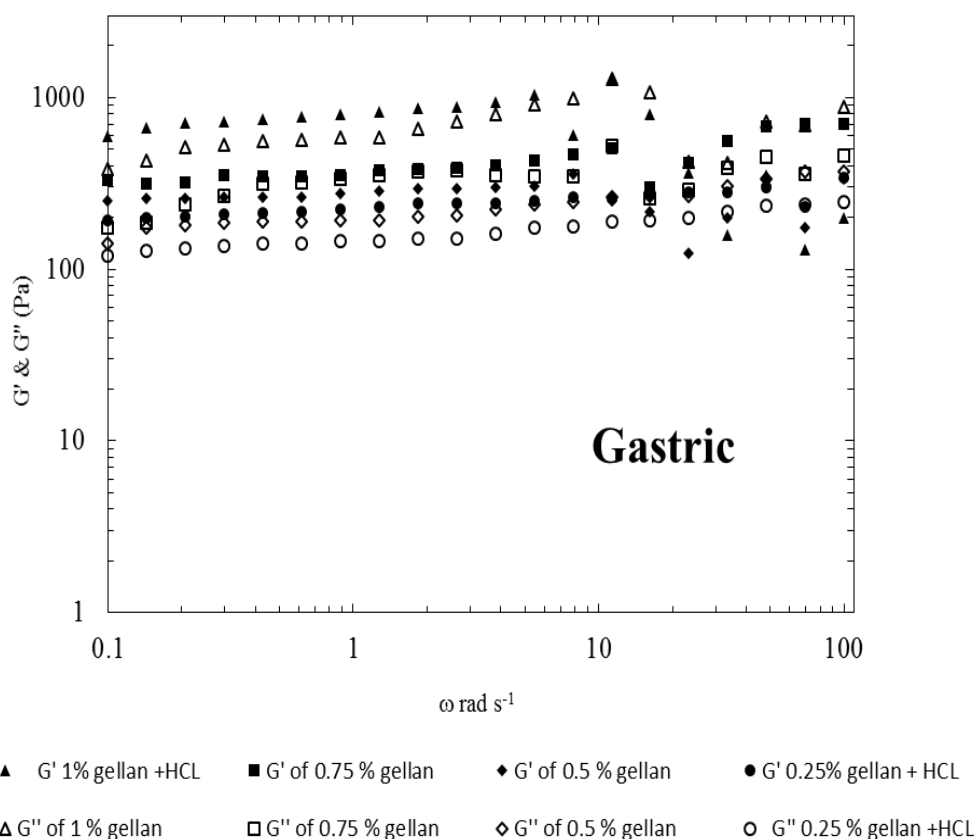


**Figure 5-12: Mechanical spectra measurements of gellan gum exposure to ions crosslinked present in GF. G' (filled symbols) & G'' (open symbols), frequency sweep test in a range of frequency between (0.1 -100) rad/s<sup>-1</sup>.**

### 5.3.6 Comparison of *in situ* gelation of gellan gum (0.25, 0.5, 0.75 and 1%) with four different types of physiological fluids

When comparing the *in situ* gelation of gellan (0.25, 0.5, 0.75 and 1%) upon exposure to different types of artificial physiological fluids it was evident that gelation occurs with all four different types of physiological fluids even when the concentration of gellan was as low as 0.25% w/w (Figure 5.13). Addition of artificial saliva gave the lowest gel strength with the gastric fluid producing the strongest gels which was evident across all the concentrations tested. Furthermore, stiffness of the gels formed following 20 min exposure were shown to be concentration dependent for all the fluids tested with the gastric fluid forming the stiffest gels and the saliva the least stiff with the lacrimal and wound fluid producing gels that were not significantly different from each other ( $P < 0.05$ ) (Figure 5.14)

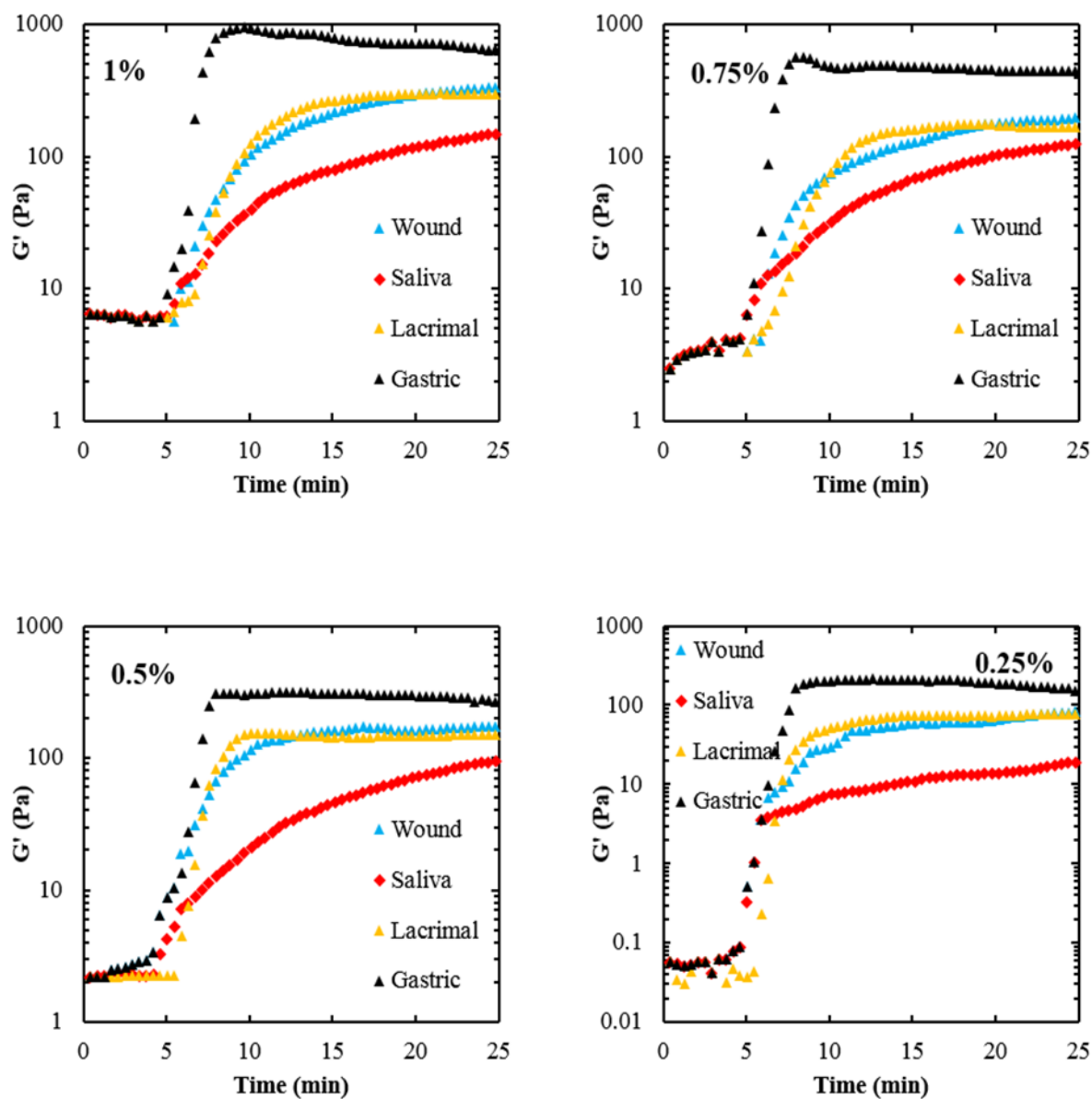
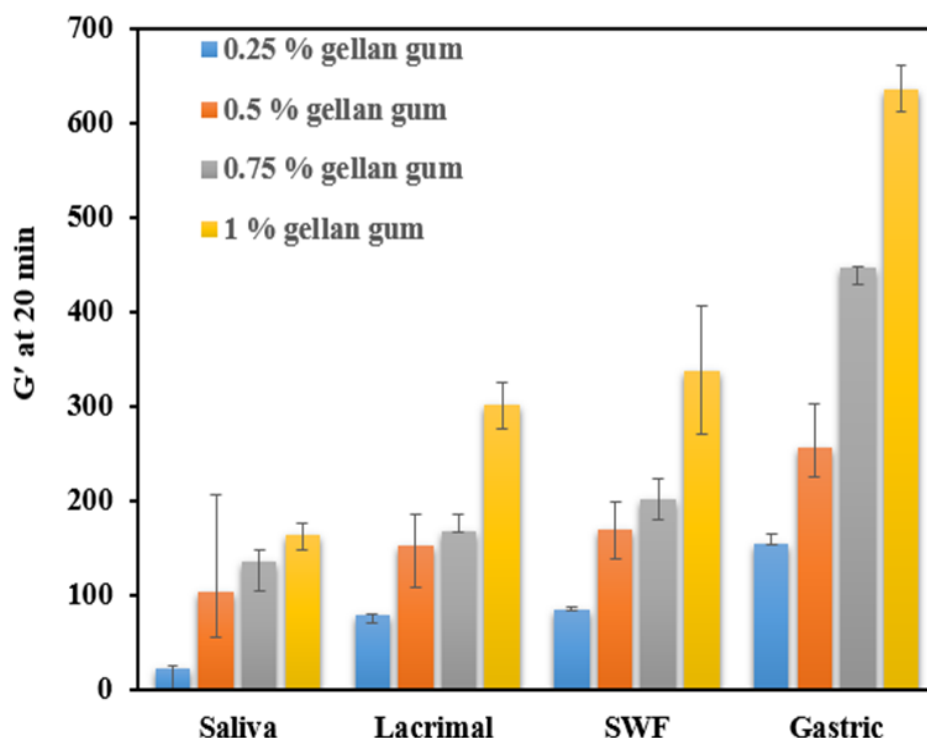


Figure 5-13: Rheological measurements of elastic modulus values ( $G'$ ) of *in situ* gelation time for different concentrations of gellan exposure to four types of physiological fluids.



**Figure 5-14: Rheological measurements of elastic modulus values ( $G'$ ) at 20 minutes of *in situ* gelation time for different concentrations of gellan exposure to four types of physiological fluids.**

### 5.3.7 Gelation kinetics

To investigate the kinetics of the *in situ* sol-gel transitions of gellan in the different physiological fluids the gelation curves were fitted to the Gompertz model (Eq. 5.1) (Winsor 1933 PNAS) and the rate constant and maximum growth rate were calculated. Rate constants were found to follow zero order kinetics (Figure 5.15A) in each of the physiological fluids revealing concentration independent gelling behaviour. This means that storage modulus reaches its pseudo-plateau value at the same time, irrespectively of concentration. Therefore, to achieve maximum rigidity requires appreciably different maximum growth rates as final gel strength varies with concentration. The maximum growth rate gives insights into addressing this complication. For that reason, growth kinetics, at the inflection point of the gelation curves, were plotted confirming concentration dependent maximum growth rates (Figure 5.15B).

This is important as rate of gel network growth can provide an insight into microstructure development.

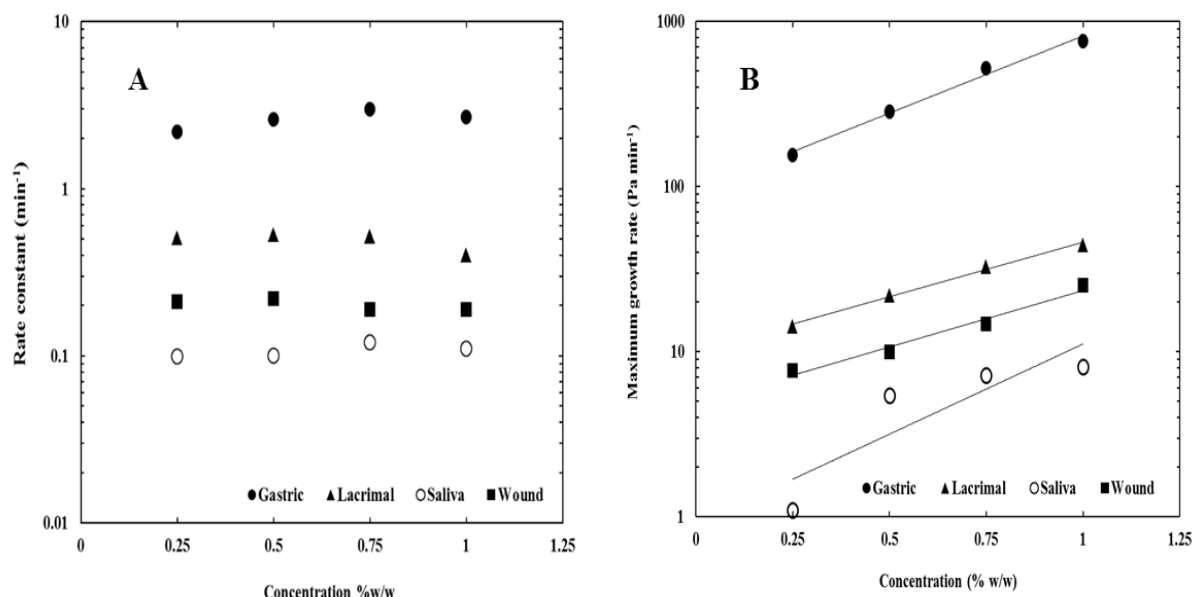


**Figure 5-15: Gelation kinetics for different concentrations of gellan exposure to 4 types of physiological fluids fitted to the Gompertz model showing A) rate constant vs concentration and B) maximum growth rate vs concentration.**

### 5.3.7.1 Microstructure growth

It was observed that the stiffness of the 1 % w/w gellan in AS and the 0.75 % w/w gellan in LF or SWF produced gels that had the same stiffness as a 0.25 % w/w gel exposed to GF (Figure 5.16). Although the stiffness of these gels (1% in saliva, 0.75% lacrimal and wound and 0.25% gastric) are essentially the same following 20 min exposure, the microstructure of these gels are likely to be different as microstructure development is dependent on polymer concentration and gelation kinetics (Hoare and Kohane, 2008; de Luna, et al 2017). Indeed, the modulus at time zero are vastly different (orders of magnitude) between the samples due to the differences in concentration (table 5.4). In addition, the gelation kinetics for each of these samples are also different with the rate constants ranging from 2.2 min<sup>-1</sup> in the GF compared to 0.1 min<sup>-1</sup> in the AS (Table 5.4), therefore the structuring that occurs during the gelation is likely to produce

significantly different microstructure in terms of overall porosity, pore size and size of junction zones between the polymer chains. To investigate this further the samples were freeze dried and then analysed using surface profilometry and micro CT.

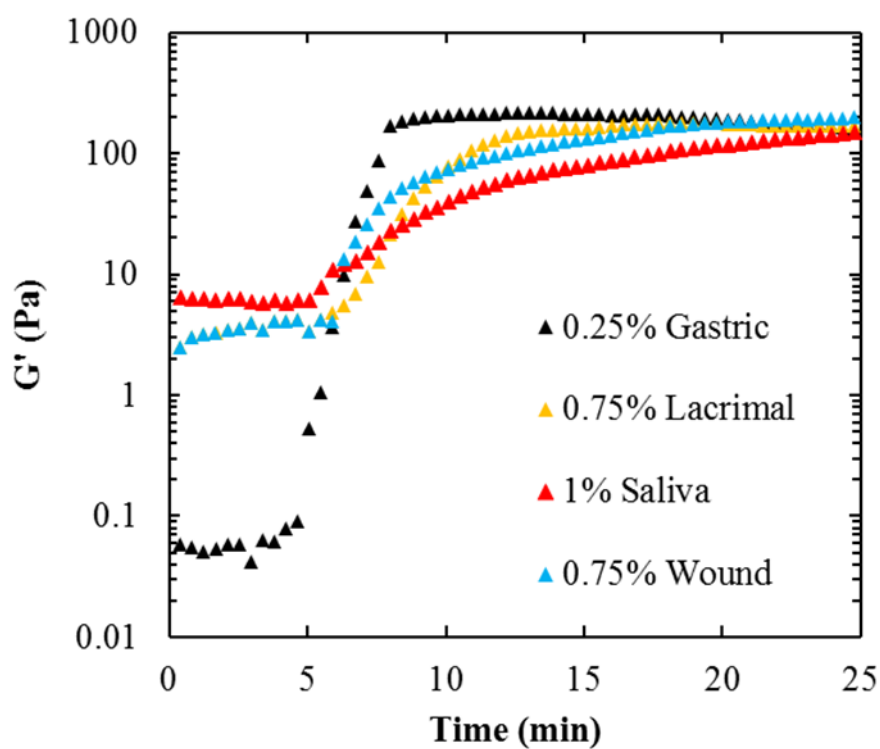


**Figure 5-16: Comparison of  $G'$  during *in situ* gelation at time zero and at 25 min in samples that has the same final modulus.**

**Table 5-3: Comparison of  $G'$  at time zero and at 25 min in samples that has the same final modulus ( $p < 0.05$ ). Showing mean values  $\pm$  sd ( $n=3$ ).**

SPF and Concentration of gellan (% w/w)	$G'$ (Pa) at $t = 0$ min	$G'$ (Pa) at $t = 25$ min	rate constant ( $\text{min}^{-1}$ )
Gastric 0.25%	$0.05 \pm 0.006$	$154.5 \pm 24.7$	2.2
Lacrima 0.75%	$2.54 \pm 0.15$	$167.7 \pm 17.5$	0.5
Wound 0.75%	$2.59 \pm 0.24$	$178.6 \pm 30.0$	0.2
Saliva 1.0%	$6.21 \pm 1.2$	$163.0 \pm 13.1$	0.1

### 5.3.8 Polymer network and surface texture analysis results

The 3D surface profiler was employed to study the polymer network and surface texture of freeze dried gels. Noteworthy, all freeze dried network structures of the samples that had the same stiffness at the end of the *in situ* gelation tests revealed noticeable differences in microstructure. It is evident from the results that all the gels have successfully established polymeric skeleton. Qualitatively it was inferred from the results that the fibres of polymeric skeleton were most uniform in 1% w/w gelled in saliva and more heterogeneous in the 0.25% w/w gelled in gastric fluid. The 0.75% w/w gelled in lacrimal and simulated wound fluid showed the fibres that were similar to one another and intermediate between the saliva and the gastric fluid gels (Fig. 5.17. a-d). In order to quantitatively understand the gelled microstructure, the acquired images were subjected to binarisation process. The Sauvola method, which is a variation of Niblack's method (Sauvola and Pietikäinen, 2000), was successfully used for local binarisation and it was implemented with tiling, which was used to enhance the efficiency. Additionally, the binarisation constants  $k$  and  $r$  values were 0.5 and 23128, respectively. It was noticed that the Sauvola has given a flexible binarisation option as if there the local contrast of

noticeable magnitude, the threshold can be selected close to mean value. Where, if there is negligible contrast the threshold can be selected below the overall mean value, by an amount proportional to the normalised local standard deviation. In our case, all the images have shown noticeable contrast magnitude, hence, threshold was selected close to the overall mean values and the processed images are depicted in Fig. 5.17 e-h. Moreover, the overall porosity ( $\epsilon$ ) was quantitatively determined using BoneJ particle analyser plug-in and depicted in Fig. 5.18. The 1% w/w gelled in saliva had the densest structure ( $\epsilon = 18.07 \pm 3.02$  %) with small void regions this was in contrast to the 0.25% w/w gelled in gastric fluid ( $\epsilon = 64.44 \pm 5.37$  %) which had a highly porous network. The 0.75% gelled in lacrimal fluid ( $\epsilon = 39.48 \pm 2.68$  %) and in SWF ( $\epsilon = 38.34 \pm 7.36$  %) had similar levels of voids that were intermediate to the gastric fluid and saliva.

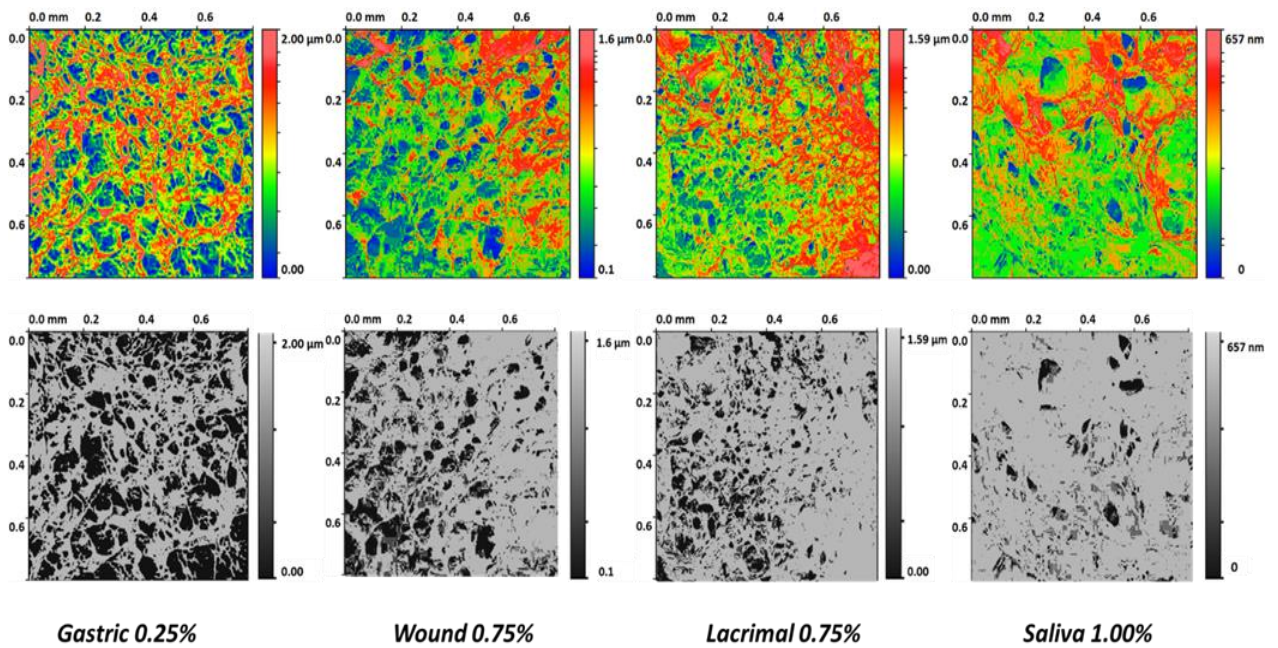


**Figure 5-17: Profilometry images of the freeze dried samples of 0.25% gellan in GF, 0.75% gellan in LF and in SWF, 1% gellan in AS (a-d) and processed images after binarisation process (e-h).**



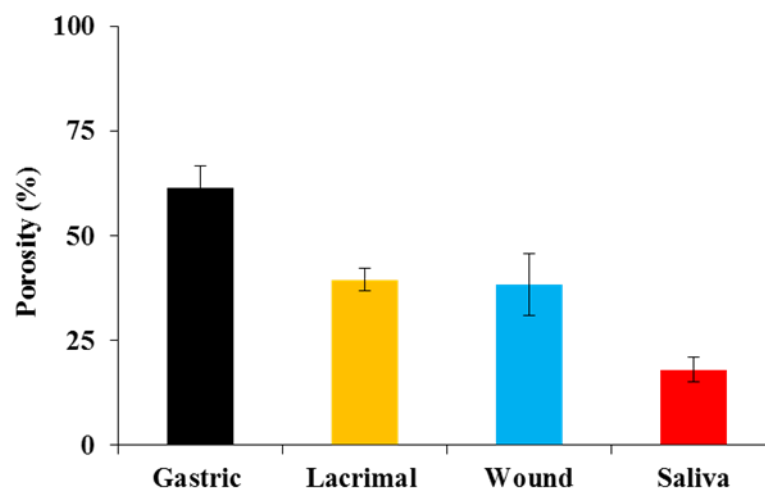


**Figure 5-18: Numerical values of overall porosity of freeze dried gels.**

To better understand the morphology and impact of various artificial biological liquids on morphology and microstructure of freeze dried gels, various 3D surface texture parameters were used. To illustrate this 2D images were converted into 3D isometric images (Fig 5.19) and various surface texture parameters, listed in Table 5.4, were quantitatively determined using Surfstand® software (Blunt and Jiang, 2003). The peak heights and depths of valleys can be qualitatively understood following the colour scheme where red and dark blue shows the highest and lowest point in the region of interest, respectively. It is evident from the images that the 0.25% w/w gelled in gastric fluid had shown noticeable blue areas whereas just few in the case of 1% w/w gelled in saliva. Moreover, the overall *z-axis* values also provide a qualitative view of the texture of the sample being extremely rough (0.25% w/w gelled in gastric fluid) to relatively smooth (1% w/w gelled in saliva). Whereas 0.75% gelled in lacrimal fluid and in SWF were of intermediate to GF and AS. Detailed measurements of quantitatively evaluated 3D surface texture parameters are presented in Fig. 5.20 a-d. It is evident that the  $S_a$  of 0.25 % w/w in GF was three folds higher in magnitude ( $167.8 \pm 4.0$  nm) in comparison to 1% AS ( $58.6 \pm 1.2$  nm) whereas 0.75% in LF ( $89.0 \pm 4.2$  nm) and SWF ( $72.0 \pm 1.8$  nm) were in transitional range in comparison to two extremes. Interestingly the same trend was followed in  $S_p$ ,  $S_v$  and

$S_{sk}$ . Prominently, the  $S_{sk}$  value was greater than zero so the roughness asperities were not symmetrical, hence, below the mean plane of the height distribution.

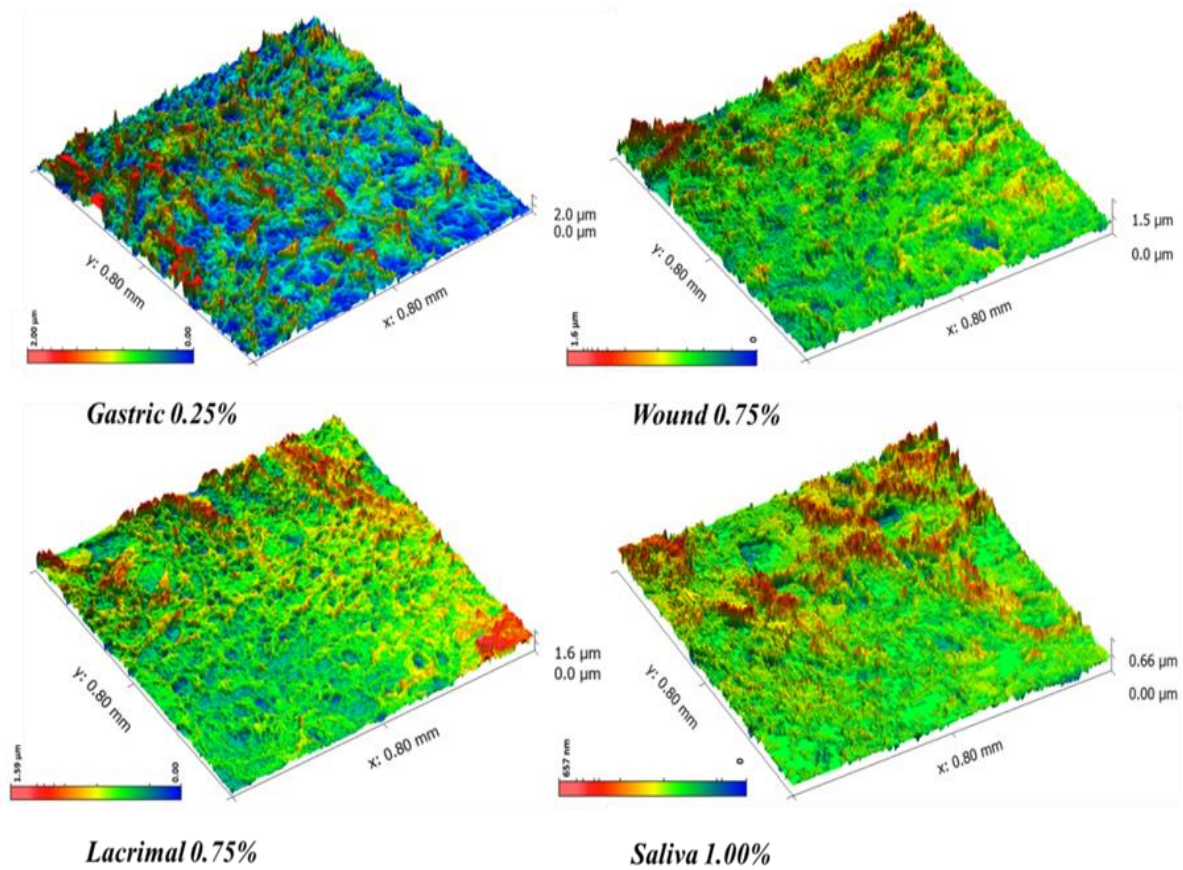


**Figure 5-19: 3D isometric surface images of the freeze dried samples of 0.25% gellan in GF, 0.75% gellan in LF and in SWF, 1% gellan in AS showing valleys and peaks on the surface with the deepest pores represented in blue.**

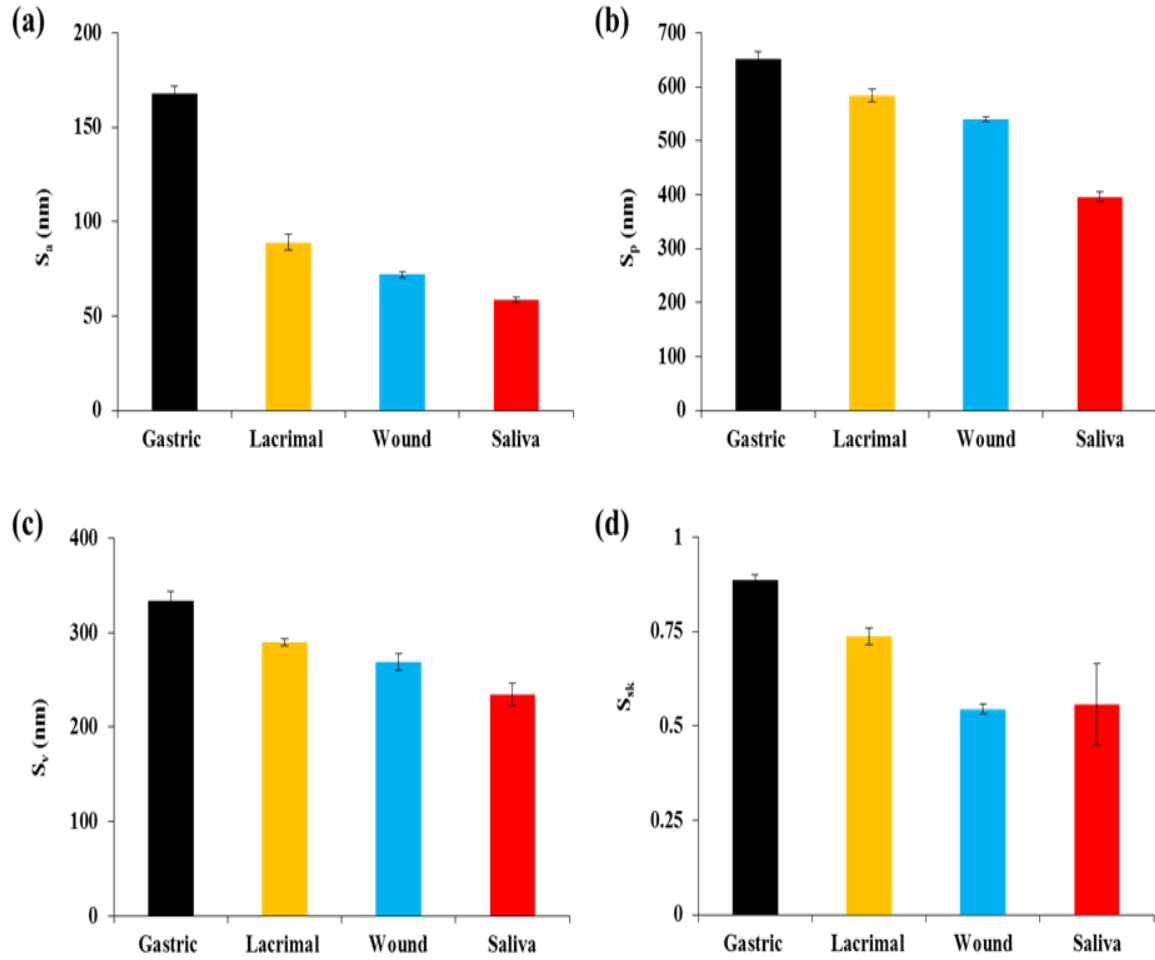


**Figure 5-20: 3D surface texture parameters determined using Surfstand® software (a) arithmetical average of surface roughness, (b) highest peak of the surface, (c) lowest valley of the surface and (d) skewness of the surface.**

### 5.3.9 Micro CT imaging

To gain an insight into the internal structure micro CT was used as a non-destructive imaging technique. Images shown in Figure 5.21 show the internal network structure of the freeze dried gels as slices for 0.25% gellan gelled in gastric fluid, 0.75% gellan gelled in lacrimal fluid, 0.75% gellan gelled in wound fluid and 1% gellan gelled in saliva. The images reveal that the packing of the gellan appears to be denser when gelled in the gastric fluid when compared to the other samples. The lacrimal fluid and wound fluid gels having a structure similar to one another with the gellan in saliva showing the least dense.

This was an unexpected finding as the gellan gelled in the artificial saliva was the most concentrated (1 %) and the gellan gelled with the gastric fluid contained the lowest polymer concentration (0.25 %).

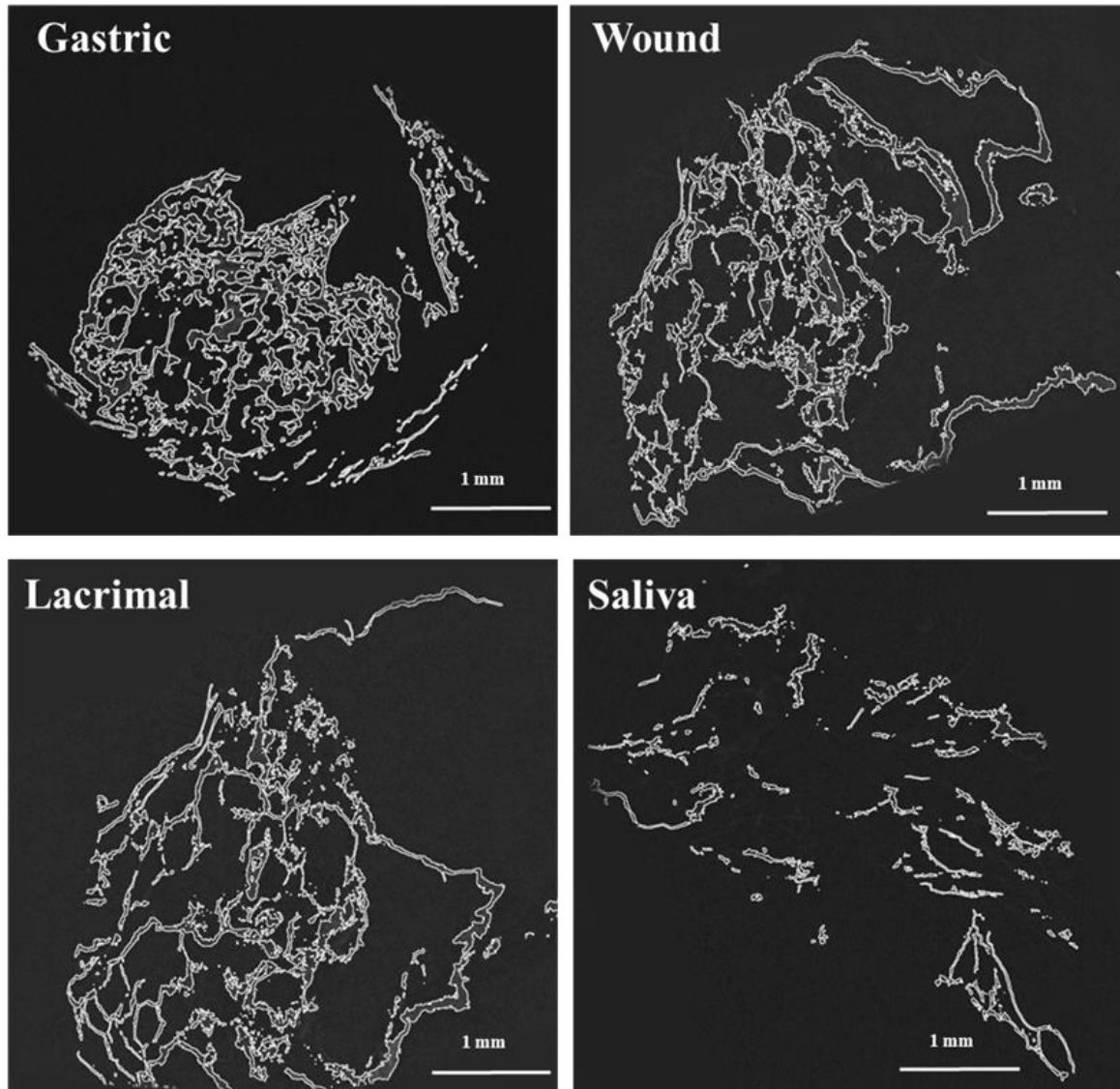


**Figure 5-21: Micro CT images of 0.25% Gellan gelled in gastric fluid, 0.75% gellan gelled in lacrimal fluid, 0.75% gellan gelled in wound fluid and 1% gellan gelled in saliva.**

## 5.4 Discussion

*In situ* gelation of gellan was measured upon exposure to different types of artificial physiological fluids using dynamic oscillation measurements as a function of time. The concentration of gellan was varied (0.25, 0.5, 0.75 and 1%), while the proportions of the different cations in four types of artificial physiological fluids were kept constant. Gellan gum solutions without cations served as a control. When blank samples (control) were measured the  $G'$  value remained unchanged throughout the duration of the test. At this stage, the only cations present in the resulting solution are those present as counter ions to the charged groups of the polymer chains. These low concentrations of cations are not sufficient to facilitate aggregation and subsequent gel formation as they become diluted in bulk of the solution. Therefore, gellan gum can undergo coil - helix transition but not sol-gel transition (Morris et al., 2012). When ions concentrations exposed to the gellan samples are increased by addition of extraneous salt such as that is present in physiological fluid, the gellan can undergo sol-gel transition, therefore causing  $G'$  to sharply increase. Increasing gellan concentration means more  $\text{COO}^-$  available to bind with ions (as long as the ions are present in sufficient concentration), and then stronger gel will form (Morris et al., 2012).

In the present study, samples of gellan gum were prepared at concentrations of 0.25%, 0.5% 0.75% and 1% w/w then loaded onto a modified rheometer and small deformation oscillatory measurements of storage modulus ( $G'$ ) were taken as a function of time. After 5 minutes the samples were exposed to a range of simulated physiological fluids *in situ* and measurements were continued for a further 20 minutes. A rapid growth in  $G'$  occurred almost instantaneously as the physiological fluids were added corresponding to the onset of gelation due to the ions present in the physiological fluids (Figures 5.5, 5.6, 5.7 and 5.8). Addition of artificial saliva gave the lowest gel strength (Figure 5.5) with the gastric fluid producing the strongest gels (Figure 5.8).

This can be attributed to  $H^+$  having a much greater affinity to the uronic acid on the gellan than that of the group 1 and group 2 metal ions in the other fluids. Indeed, when studying of the effect of monovalent and divalent cations Grasdalen and Smidsrød (1987) described HCl as the most potent gel-former for gellan. This was evident across all the concentrations tested (Figure 5.13). Furthermore, stiffness of the gels formed following 20 min exposure were shown to be concentration dependent for all the fluids tested with the gastric fluid forming the stiffest gels and the saliva the least stiff with the lacrimal and wound fluid producing gels that were not significantly different from each other ( $P < 0.05$ ) (Figure 5.14). This was further supported by the mechanical spectra of the gels formed in the different fluids (Figures 5.9, 5.10, 5.11, and 5.12) with the modulus values and difference between  $G'$  and  $G''$  greatest in the gastric gels and lowest in the saliva gels. This indicated that a stronger more brittle gel was formed in the presence of the gastric fluid and a softer more elastic gels were formed with the other fluids.

It was noticed the gelation process appeared to proceed very differently when gelled in the different fluids (Figure 5.13). To investigate this observation further, the kinetics of the *in situ* gelation curves of gellan in the different physiological fluids the were fitted to the Gompertz model (Eq. 5.1) and the rate constant and maximum growth rate were calculated. Gelation in each of the physiological fluids revealed concentration independent gelling behaviour however the calculated gelation rate constants where dramatically different when gelation occurred in the different fluids  $\sim 2.2, 0.5, 0.2, 0.1 \text{ s}^{-1}$  in gastric, lacrimal wound and saliva respectively (Figure 5.15A). It was anticipated, that as a result of the large variation in gelation rate constants between the gels formed in the different fluids (Figure 5.15A) and maximum growth rate being concentration dependant (Figure 5.15B), that microstructure development of these gels may also vary. Indeed, the modulus values of the 1% gellan in saliva and the 0.75% gellan in lacrimal fluid or wound fluid produced gels that had very similar moduli as a 0.25% gel exposed to gastric fluid.

Despite this apparent similarity the microstructure of these gels are likely to be very different as microstructure development is dependent on polymer concentration and gelation kinetics.

To investigate in more detail if this was the case the gels were recovered from the rheometer and freeze dried prior to investigation of the polymer network by surface texture analysis and micro CT. The surface texture profiles revealed a more porous network with larger surface peaks and valleys in the gastric fluid gels (Figure 5.17, 5.18) which also had a significantly rougher surface (Figure 5.19, 5.20) when compared with the other freeze dried gels. This is thought to be a result of the concentration difference between the samples (0.25 % GF, 0.75 % LF, 0.75 % SWF and 1 % AS). When the same samples were imaged using micro CT it was observed that the internal microstructure of the freeze dried gel was the most densely packed (Figure 5.21) and in particular contrast with the gel that was formed in the saliva which appeared much more loosely packed. This seemed to contradict what was found in the surface texture analysis where the gastric fluid gels were highly porous and the saliva gel relatively homogeneous. This contradiction however, can be explained. Firstly, the densely packed structure observed in the gastric gel was formed at the greatest gelation rate (rate constant =  $2.2 \text{ s}^{-1}$ ) this is due to the mechanism of gelation of gellan when exposed to low pH whereby the negative charges on the gellan chain are rapidly removed leading to formation of strong aggregated bundles of the polymer. Indeed, Yamamoto and Cunha reported that local aggregation of the molecules in acid gelled gellan also resulted in a structure with larger pores (Yamamoto and Cunha 2007). Moreover, Bradbeer et al (2014) suggests that the rate of aggregation using direct HCl addition is expected to be much higher than the rate achieved by slower more controlled gelation process resulting in altered elasticity and strength of the overall gellan structure. This can be observed in the mechanical spectra of the different gels Figure 5.9 – 5.12 where the gastric gels appear stronger (higher modulus values) but more brittle (failure at high frequencies) than the gels formed in the other fluids.

It is likely that the more densely aggregated bundles of the gastric gels would lead to a more heterogeneous bulk structure with more surface undulations as observed in the surface profiles (Figure 5.19, 5.20) with the saliva gels having a smoother surface texture due to a higher polymer concentration and network relatively heterogeneous structure that is slowly developed (rate constant =  $0.1 \text{ s}^{-1}$ ). The lower porosity measured in the saliva gels however, are not evident in the micro CT images with relatively few areas of densely packed polymer chains and large areas that appear as voids. It is believed that this is down to the resolution of the micro CT imaging unable to detect the fine mesh of the gel network and only showing areas of densely packed polymer (Figure 5.21). The relative low concentration of crosslinking ions in the saliva would lead to a less aggregated system. This has been shown previously by Milas and Rinaudo (1996) who reported a threshold in concentrations required for the association of gellan helices into aggregates as 20 mM for  $\text{K}^+$  and 45 mM for  $\text{Na}^+$ , which is consistent with the order of effectiveness reported by Grasdalen and Smidsrød (1987) for gelation of gellan with Group I cations. Taking this into account, the concentration of these species in the AS used to make the gels were 19 mM and 5.8 mM for  $\text{K}^+$  and  $\text{Na}^+$  respectively. Therefore, any strong bundles of aggregates would be minimal as was observed in the micro CT images of the saliva gel. The microstructure of the gels formed in the wound fluid and the lacrimal fluid appeared to be similar with some areas of dense aggregation of the gellan chains. This is a result of the content of ions in both fluids being similar and in concentrations (145mM  $\text{Na}^+$  and 20 mM  $\text{K}^+$ ) above the thresholds for aggregation of gellan helices. It should be mentioned that freeze dried gel structures can be affected by the ice crystal nucleation and growth during the freezing step. Therefore, the freezing of the gels was performed in liquid nitrogen to minimise ice crystal growth.



It is however a possibility that the microstructure could have been effected by ice crystals as softer gels may be more likely to accommodate the ice crystals as the gel network is able to support more stretch, resulting in larger pores after freeze-drying (Scherer, 1990). However, as the gels produced from 1% gellan in saliva, the 0.75% gellan in lacrimal fluid or wound fluid and 0.25% gel exposed to gastric fluid produced gels that had very similar moduli. It is proposed that this is due to the strength of the junctions being greater (but in fewer number) in the large dense bundles of gellan chains formed in the gastric fluid in contrast to more numerous, loosely associated junctions in the saliva which ultimately result in similar modulus values.

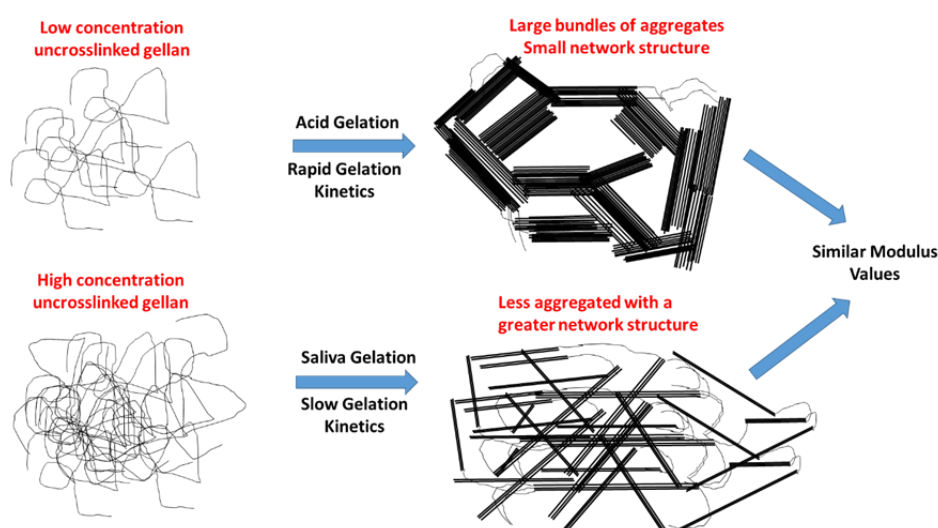


**Figure 5-22: Schematic diagram of a proposed mechanism for achieving similar modulus values in different gellan concentrations.**

What is apparent however is that there is a complex interplay between polymer concentration gel forming ion species and subsequent gelation kinetics that result in very different microstructures which will ultimately impact on functionality. Understanding these processes can lead to having a more informed approach when designing *in situ* gelling delivery systems for different target sites in the body.

## 5.5 Conclusion

This study highlights the potential applicability of the modified rheometer to measure *in situ* gel forming polymers on exposure to an external source of cross-linkers. Gellan gum formed gels with several different compositions of physiological fluid (AS, SWF, LF and GF). The method showed sensitivity for small variations in ions content and polymer concentration which resulted in different microstructures. Optimum gelation strength and kinetics on external contact with physiological fluid can be easily detected by using this method. This may be an effective method in the design of *in situ* gelling drug delivery systems with tuned gel strength, gelation kinetics and microstructure all of which will subsequently influence functionality and industrial application.

## **Chapter 6 Novel model for simultaneous measurement of rheology and drug release**

## CHAPTER SIX

### NOVEL MODEL FOR SIMULTANEOUS MEASUREMENT OF RHEOLOGY AND DRUG RELEASE

#### 6.1 Introduction

The mechanism of *in situ* gelation of different types of biopolymers namely alginate, pectin and gellan that induced by using external source of ion crosslinker and physiological fluid has been discussed in chapters 4 and 5 respectively. The method was adapted by introducing a modification to the lower plate of the rheometer to enable the investigation of the aforementioned polymers rheological behaviour as well as gel dissolution characteristics. The results have shown rapid gelation upon the exposure to crosslinking cations and acidic media *in-situ*. Polymers in the presence of mono and divalent cations and acid media undergo sol-gel transition, which allows using these types of polymers in the drug delivery system as drug carriers (Lin and Ayres, 1992; Azarmi et al., 2003). The release of drug into the external medium can be achieved by using different mechanisms including diffusion, matrix swelling, and chemical degradation in response to external stimuli (Huang et al., 2007). Ion crosslinking is one the main methods of inducing polymers to produce hydrogels for prolonging drug release. This chapter provides development to the previous method that was used in chapters 4 and 5 by the addition of a new modification to the lower plate of a rheometer, which allows investigation of the rheological behaviour with the potential for analysing release of a drug simultaneously. Several modifications have been applied to rheometers recently that have been developed for similar problems either from a fundamental characterisation perspective or to simulate an application/industrial process. Section 2.4 in the chapter two of this thesis provide a detailed explanation regarding the adaptations of specialised modifications to commercial rheometers, these adaptations includes using spectroscopic techniques to rheological

equipment such as NMR (Callaghan et al., 2000; Nakatani et al., 1990) rheo-SAXS (Somani et al., 2002) Rheo-FTIR (Boulet-Audet et al., 2014) Rheo-Raman (Chevrel et al., 2012).

These methods also include a light curing lower plate (Lee et al., 2000), electro-rheology accessory (Stanway et al., 1996), relative humidity accessory and immobilization cell. However, none of these methods allows the study of the gelation/dissolution of polymer gels while simultaneously measuring the release of molecules loaded into the polymer gels as what occurs when using *in situ* gelling drug delivery systems. To overcome these problems, a new rheometer add-on was designed which was named the Rheo-dissolution cell that can be attached to a rheometer and enables the examination of the rheological behaviour with the potential for analysing dissolution of a drug simultaneously. This was designed with a mesh that performs the function of the lower plate of the rheometer beneath which is a reservoir which can hold crosslinking solutions or release media such as simulated body fluids. Figure 6.1 shows an illustration of the Rheo-dissolution cell and represents the first prototype which was used throughout the study.

The aim of the work in this chapter therefore, was to validate the potential of the rheo-dissolution cell. This was investigated with the following objectives:

- Measure the changes in rheological behaviour of alginate by measuring *in situ* gelation and gel dissolution using ion crosslinking and chelating agents respectively.
- Investigate the impact of mesh opening size on gelation and dissolution.
- Analyse the release of a model drug loaded into an alginate solution during gelation and dissolution of the gel

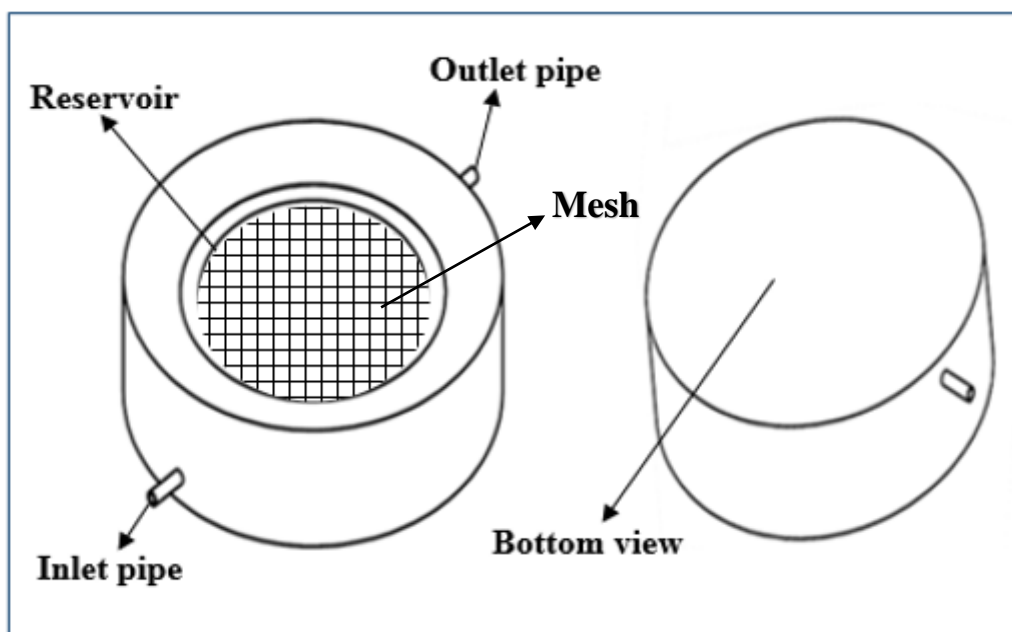


**Figure 6-1: Schematic diagram of a Rheo-Dissolution cell.**

## **6.2 Rheo-dissolution cell device**

The rheo-dissolution cell was 3D printed using acrylonitrile butadiene styrene polymers (ABS). The cell was designed as a circle reservoir with an opening on the top that is covered with stainless steel mesh during the experiments. The cell was designed with two places for sampling using an inlet pipe and outlet pipe. The inlet is used to load solutions or buffers such as the ionic solution contained within the reservoir whereas the outlet allows withdrawal of the sample for analysis. The cell can be attached to the lower plate of a commercial rheometer that allows examination the rheological behaviour with the potential for analysing dissolution of a drug simultaneously, as shown in Figure 6.3. The reservoir of the rheo-dissolution cell is capable of holding a volume of 55 ml. The mesh which is placed on the top of the reservoir (where samples are loaded) is removable, therefore can be interchanged with different mesh sizes.

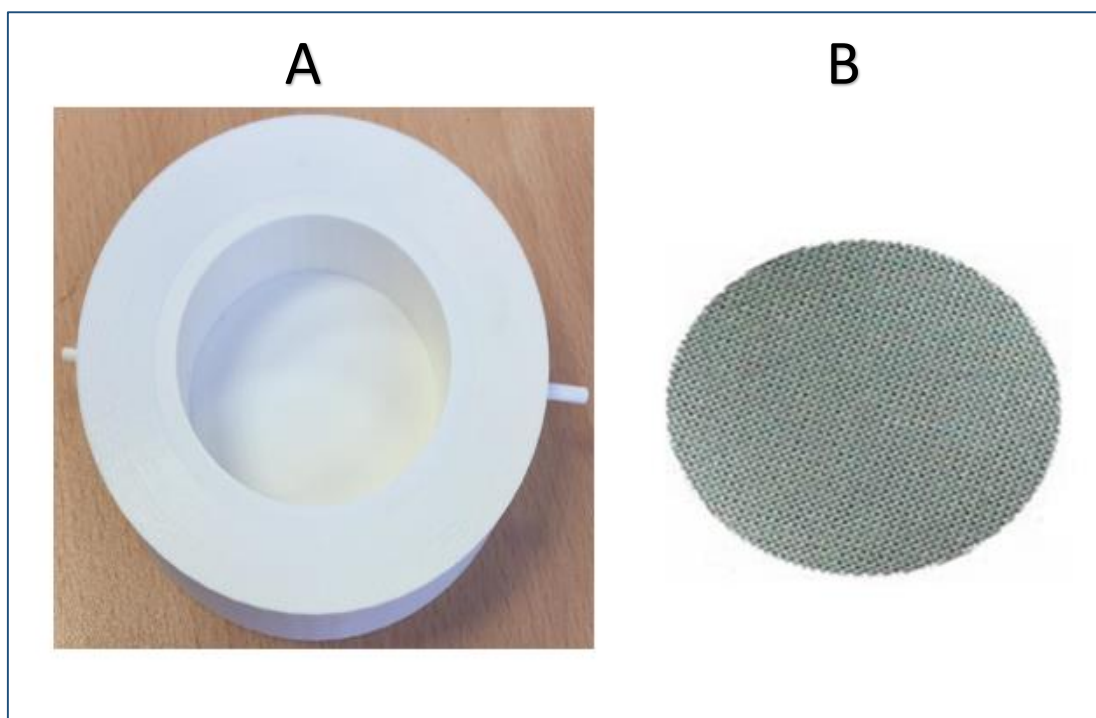


**Figure 6-2: A) Rheo-dissolution cell B) Stainless steel mesh.**

## **6.3 Material and methods**

### **6.3.1 Material**

All chemicals used in the experiment were purchased from (Sigma-Aldrich Ltd, UK), (Thermo Scientific Ltd, UK) and (Fisher Scientific Ltd, UK): Ethylene diamine tetraacetic acid disodium salt dihydrate (EDTA) [Sigma Aldrich Ltd, UK]. Sodium dihydrogen citrate and Sodium alginate, medium molecular weight (80,000–120,000) with an M:G ratio of 0.39:0.61 [Sigma Aldrich Ltd, UK] Dialysis tubing (14000 MWCO) [Thermo Scientific Ltd, UK] Whatman Grade 1 filter paper [Fisher Scientific Ltd, UK].

### **6.3.2 Samples and reagents preparation**

#### **6.3.2.1 Preparation of 1% alginate labelled solution for rheology measurements**

The model drug loaded alginate solution was prepared by dissolving 1 g of alginate powder and 50 mg of methylene blue in 100 ml of warm deionized water (60°C). The mixture was stirred using a magnetic stir bar until completely dissolved. Any evaporated solution was replaced with warm deionized water.

#### **6.3.2.2 Preparation calcium chloride solution (200 mM)**

The solution of  $\text{CaCl}_2$  was prepared by dissolving the correct weight of calcium chloride dihydrate powder in 100 ml deionized water.

#### **6.3.2.3 Preparation of EDTA solution and sodium dihydrogen citrate**

500 mM of EDTA and Na citrate were prepared as described in Chapter Four, section 4.2.2.4 and 4.2.2.5 respectively).

### **6.3.3 Rheological measurements**

The rheological measurements were conducted by using Kinexus rotational rheometer (Malvern, UK) with the rheo-dissolution cell replacing the lower plate rheometer. The temperature of the rheo-dissolution fluid in the reservoir was maintained at 25°C throughout the tests. The cells cylindrical reservoir, contained 55 ml of the test solutions, which included 200 mM  $\text{CaCl}_2$  for the *in situ* gelation test and 500 mM EDTA or Na citrate for gel degradation test. The stainless steel mesh was then placed onto the surface of the cell and a dialysis membrane (MWCO 14000 Da) was placed on top of mesh (to prevent the sample gelling within the mesh) before the rheometer geometry gap was zeroed. The fluid was then topped up to ensure the mesh and the dialysis membrane was fully wetted before the sample of alginate was



loaded onto the surface of the dialysis membrane. Small deformation oscillatory measurements of storage and loss moduli ( $G'$  and  $G''$ ) were then performed as a function of time at 0.5% strain and a frequency of  $10 \text{ rad s}^{-1}$  using 50 mm diameter parallel plate geometry with a 0.7 mm gap. Rheological evaluations of 1% alginate loaded with 50 mg methylene blue were performed with 200 mM  $\text{CaCl}_2$  in the reservoir. Following a 30 min exposure to  $\text{CaCl}_2$  solution, the solution was carefully removed from the cell and replaced with 500mM EDTA or Na citrate buffer. The rheological measurements of  $G'$  and  $G''$  as a function of time was resumed using the same conditions as used in the *in situ* gelation measurements. The study performed in this chapter used three different mesh sizes, as shown in Table 6.1. This was to investigate how the size of the mesh might affect release of the drug into the surrounding medium; therefore, three mesh sizes 10, 40, and 60 mesh counts where used.

**Table 6-1: Shows size and count number of three different types of mesh.**

Mesh count	Nominal Aperture	Wire Diameter	Opening Area
10	1980 $\mu\text{m}$	560 $\mu\text{m}$	61%
40	411 $\mu\text{m}$	280 $\mu\text{m}$	42%
60	263 $\mu\text{m}$	160 $\mu\text{m}$	39%

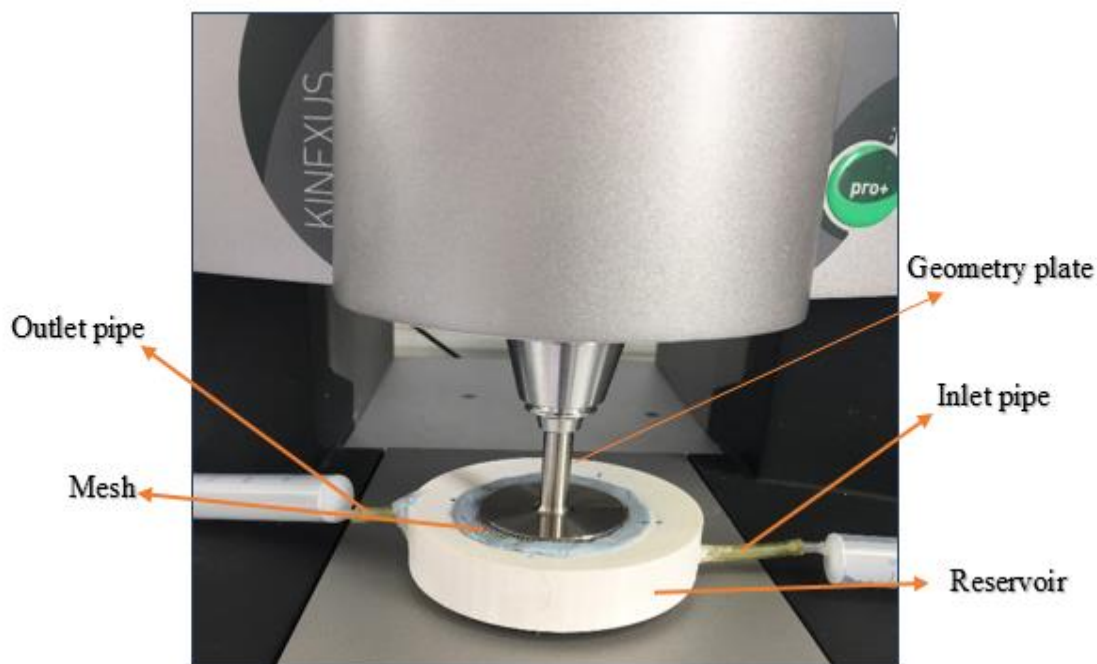


**Figure 6-3: Experimental set-up of Rheo-dissolution device attached to a Rheometer.**

#### **6.3.4 Release study**

*In vitro* release of methylene blue from alginate gelled *in situ* using 200 mM  $\text{CaCl}_2$  was evaluated by UV spectrophotometry. Methylene blue stock solution was prepared by dissolving  $10.0 \pm 0.1$  mg of methylene blue crystal in deionised water, and then the filling the volumetric flask volume to 100 ml using the same solvent. A sample of the stock was scanned using a UV-Vis spectrophotometer to identify the maximum absorbance band of methylene blue ( $\lambda_{\text{max}}$ ), which was determined to be 665 nm. The release studies were divided into two parts. The first part of the study-evaluated release during the *in situ* gelation process and the second part investigated the effect of gel degradation by chelating agents (EDTA and sodium dihydrogen citrate) on the release behaviour. At suitable time intervals, samples of the fluids in the reservoir were collected and the absorbance was measured using UV-Vis spectrophotometer at 665 nm.

### **6.3.5 Statistical Analysis**

Statistical significance ( $p < 0.05$ ) between test groups was determined by one-way analysis of variance (ANOVA) in order to determinate any statistically significant differences between the test groups.

## **6.4 Results**

### **6.4.1 Rheology results**

#### **6.4.1.1 *In situ* gelation results for alginate 1% using three different types of mesh**

*In situ* gelation occurred in all the different mesh sizes used. However, the final gel strength was affected by mesh size. The largest % mesh opening area (61%) gave the greatest modulus values after 30 min gelation with  $G' \sim 7000$  Pa and  $G'' \sim 2000$  Pa (Figure 6.4A). The smaller mesh opening areas 42% (Figure 6.4B) and 39% (Figure 6.4C) gave final moduli values of  $G' \sim 4000$  Pa  $G'' \sim 1000$  Pa and  $G' \sim 2000$  Pa  $G'' \sim 900$  Pa respectively. Comparisons of the values of  $G'$  for all mesh sizes are shown in Figure 6.4D.

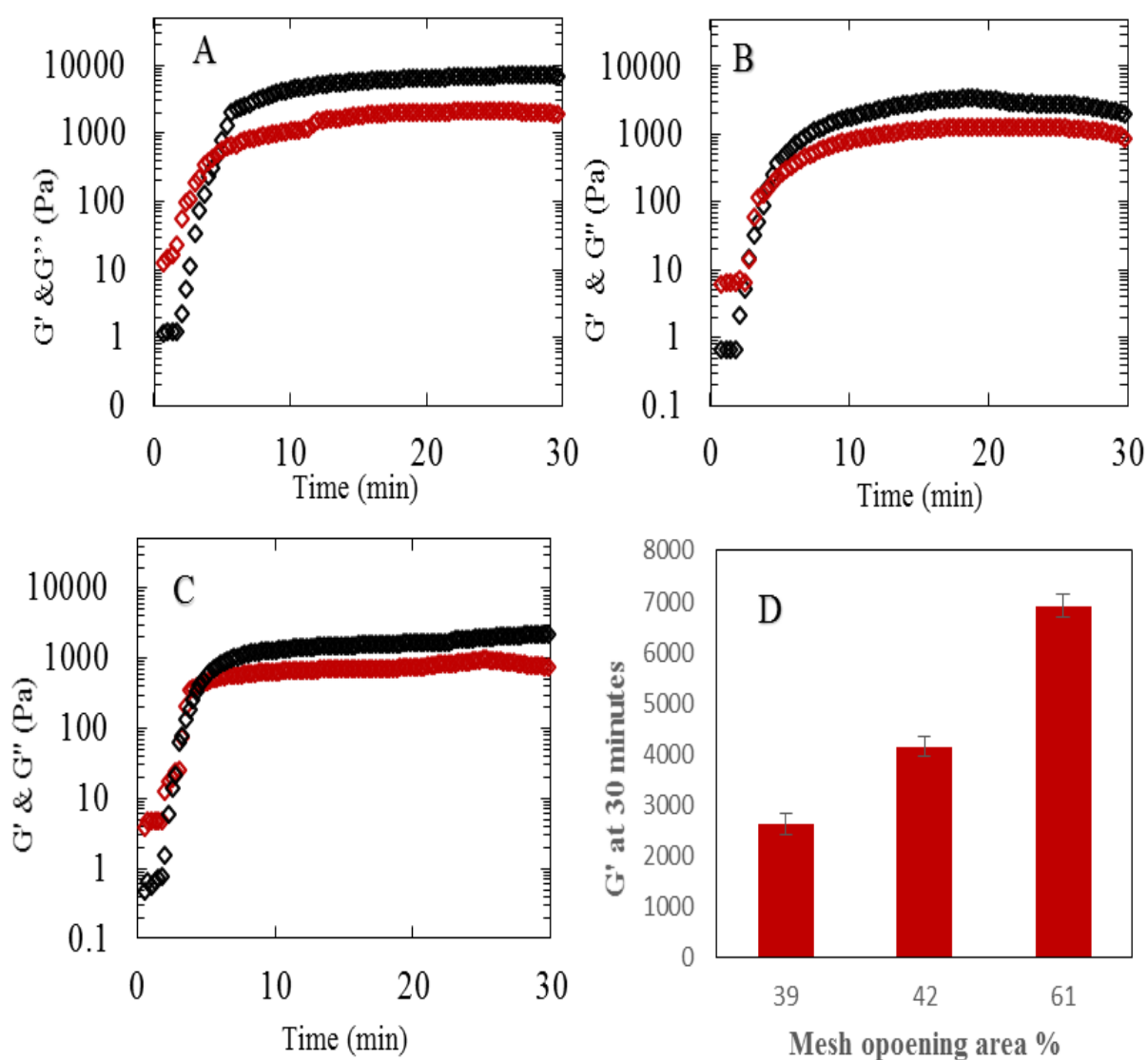


**Figure 6-4: Rheological measurements for 1% alginate methylene blue solution showing a variation of  $G'$  (black symbols),  $G''$  (red symbols) vs. time upon exposure to 200 mM CaCl<sub>2</sub> for *in situ* gelation. A) Mesh opening area 61%. B) Mesh opening area 42%. C) Mesh opening area 39%. D)  $G'$  values of *in-situ* gelation test using three different mesh sizes.**

#### **6.4.1.2 *In situ* gel dissolution results for alginate 1% using mesh size 10 (opening area 61%)**

Alginate gels that are formed on exposure to ion crosslinking externally can be degraded using calcium chelating agents such as EDTA and Na citrate. To measure this process a 1 % w/w alginate labelled with 50 mg of methylene blue crosslinked *in situ* with 200 mM CaCl<sub>2</sub> that filled in the Rheo-dissolution cell (Figure 6.5A) where exposed independently following 30 min gelation to 500 mM EDTA (Figure 6.5B) and Na citrate (Figure 6.5C). The results indicate that EDTA was a much stronger calcium chelator than Na citrate causing G' to return to a similar modulus to that of the original sodium alginate, prior to crosslinking, after only 35 min of exposure when using mesh with large opening area (61%). Na citrate took longer time than EDTA to degrade the gels 45 min (Figure 6.4D). The opening area of the mesh plays a critical role in the dissolution time of gels.

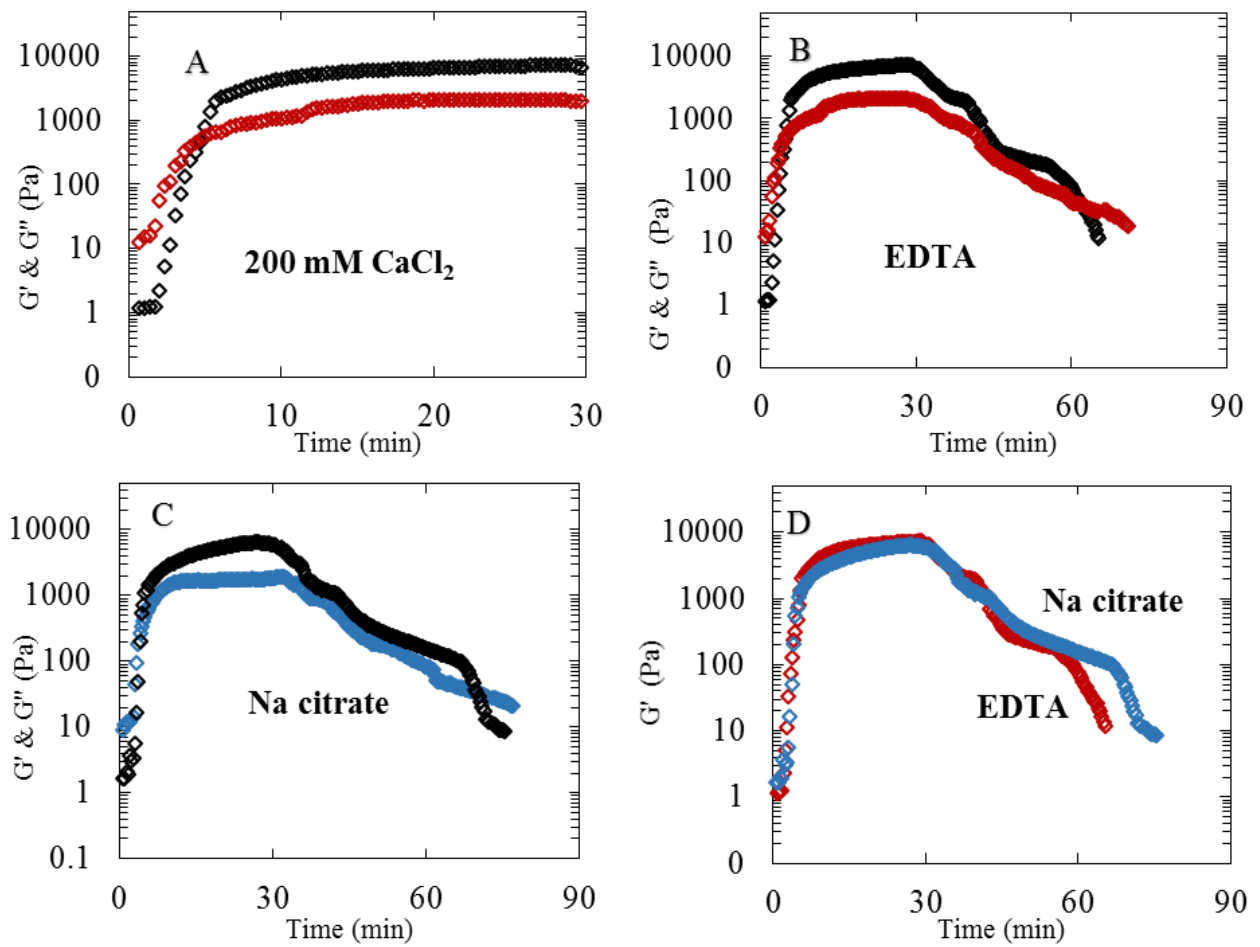


**Figure 6-5: Rheological measurements for 1% alginate methylene blue solution showing a variation of  $G'$  (black symbols),  $G''$  (red and blue symbols) vs. time upon exposure to 200 mM  $\text{CaCl}_2$  for *in situ* gelation and for EDTA and sodium dihydrogen citrate gel degradation for mesh opening area 61%. A) *In situ* gelation. B) *In situ* gelation and gel degradation by EDTA. C) *In situ* and gel degradation by sodium dihydrogen citrate. D) Comparison of *in situ* gel degradation between EDTA and sodium dihydrogen citrate.**

#### **6.4.1.3 *In situ* gel dissolution results for alginate 1% using mesh size 40 (opening area 42%)**

To measure the *in situ* gel dissolution process of 1% alginate methylene blue gels crosslinking cations replaced by EDTA and Na citrate after *in situ* gelation test. The strength of alginate gel that formed using small opening area mesh (42%) at the same condition used with large opening area mesh has been decreased as results to reach less amount of  $\text{Ca}^{2+}$  compared to large mesh (Figure 6.6A). The opening area of mesh effect on the dissolution time also because with small opening area limited amount of EDTA can be interact with gel sample to remove the  $\text{Ca}^{2+}$  from the gel leading gel degradation and the time was 49 min compared with large area mesh which take only 35 min (Figure 6.6B) while using Na citrate needed 64 min to degrade gels (Figure 6.6C). The EDTA was shown to have more potential to degrade the gel than Na citrate (Figure 6.6D).

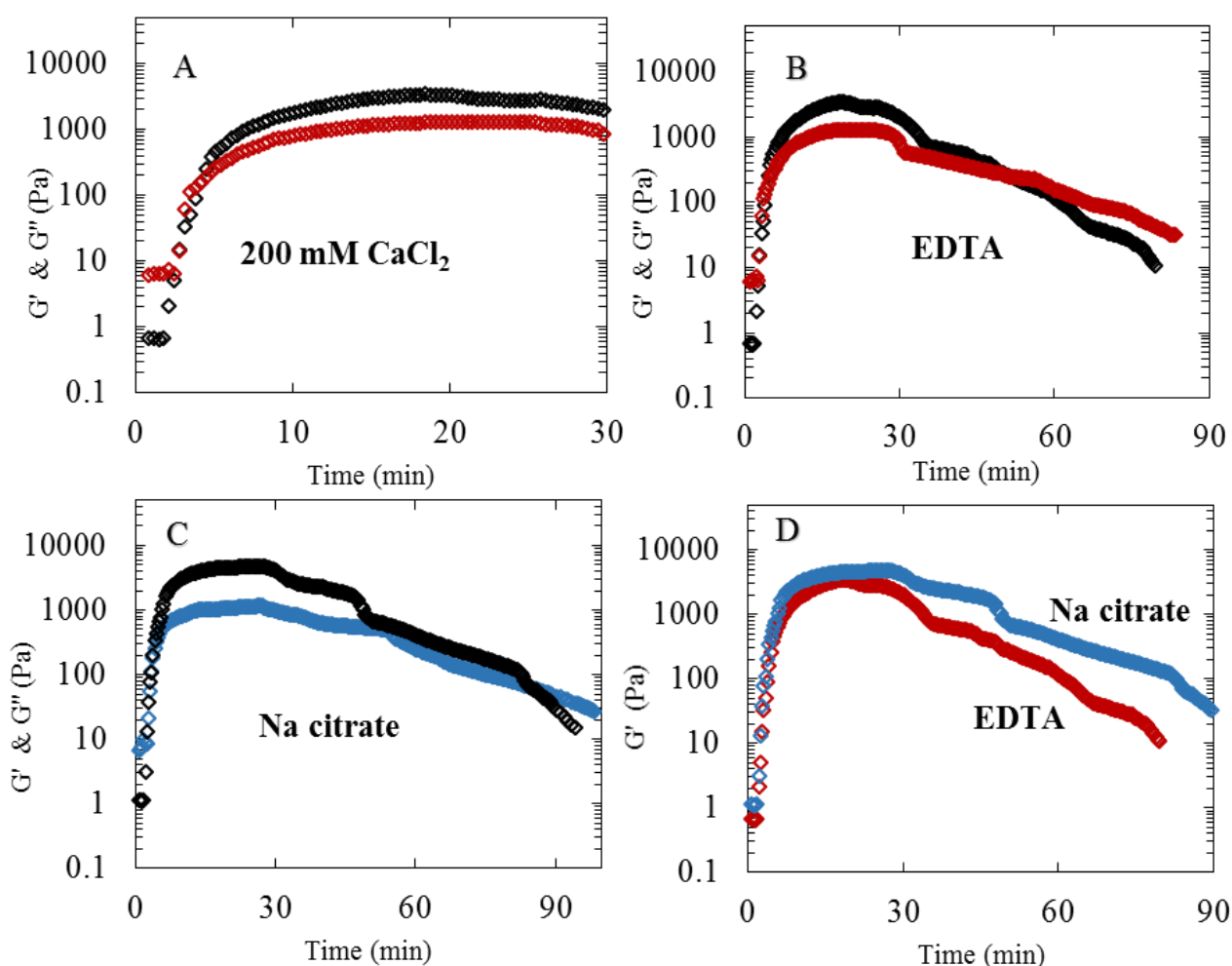


**Figure 6-6: Rheological measurements for 1% alginate methylene blue solution showing a variation of  $G'$  (Black symbols),  $G''$  (Red and blue symbols) vs. time on exposure to 200 mM of  $\text{CaCl}_2$  for *in situ* gelation and for EDTA and sodium dihydrogen citrate gel degradation for mesh opening area 61%. A) *In situ* gelation. B) *In situ* gelation and gel degradation by EDTA. C) *In situ* and gel degrade by sodium dihydrogen citrate. D) Comparison of *in situ* gel degradation between EDTA and sodium dihydrogen citrate.**



#### **6.4.1.4 *In situ* gel dissolution results for alginate 1% using mesh size 60 (opening area 39%)**

To measure the *in situ* gel dissolution of alginate using smallest opening area mesh the same set up of measuring *in situ* gelation and gel dissolution with large and medium area mesh was applied. The smallest mesh opening area (39%) made the weakest gels compared with the other two types of area mesh large and medium (Figure 6.7A). Dissolution time using EDTA was 60 min, which was longer than medium and large area meshes (Figure 6.7B) while with Na citrate dissolution the dissolution time was 77 min (Figure 6.7C). Figure 6.7 D shows comparison of dissolution time between EDTA and Na citrate and the results shows rapid dissolution by EDTA than Na citrate.

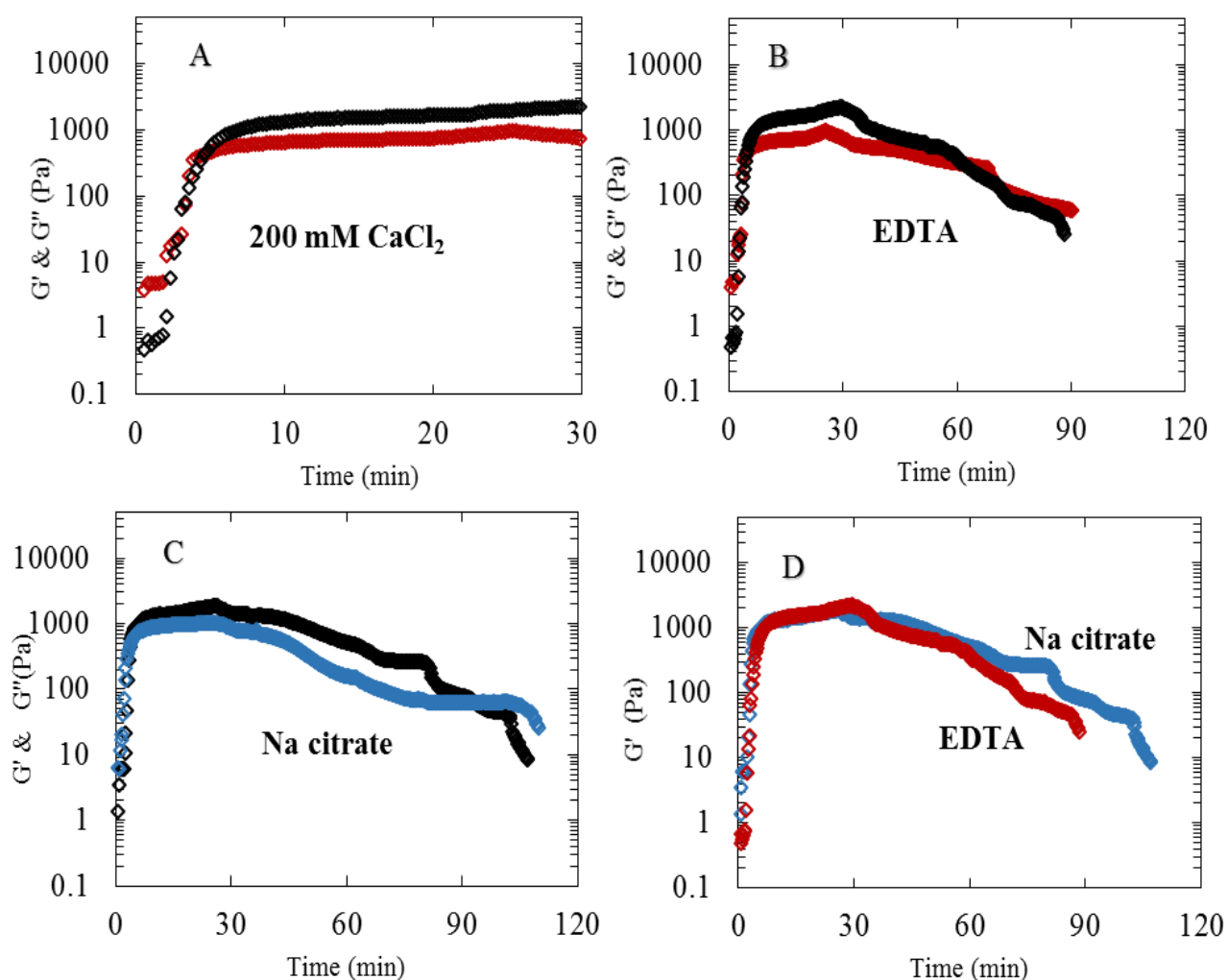


**Figure 6-7: Rheological measurements for 1% alginate methylene blue solution showing a variation of  $G'$  (Black symbols),  $G''$  (Red and blue symbols) vs. time on exposure to 200 mM  $\text{CaCl}_2$  for *in situ* gelation and for EDTA and sodium dihydrogen citrate gel degradation for mesh opening area 61%. A) *In situ* gelation. B) *In situ* gelation and gel degradation by EDTA. C) *In situ* and gel degradation by sodium dihydrogen citrate. D) Comparison of *in situ* gel degradation between EDTA and sodium dihydrogen citrate.**

#### 6.4.1.5 *In situ* gel dissolution results for alginate 1% using three different types of mesh

The alginate methylene blue gels that formed on exposure to 200 mM of  $\text{CaCl}_2$  through three types of mesh (10,40 and 60) that have opening area (61,42 and 39%) respectively, can be degraded by removing  $\text{Ca}^{2+}$  ions using calcium chelating agents EDTA and Na citrate as shown in the figure 6.8. The results indicate that the EDTA have more power to chelate calcium faster than Na citrate in all cases with three different types of mesh.

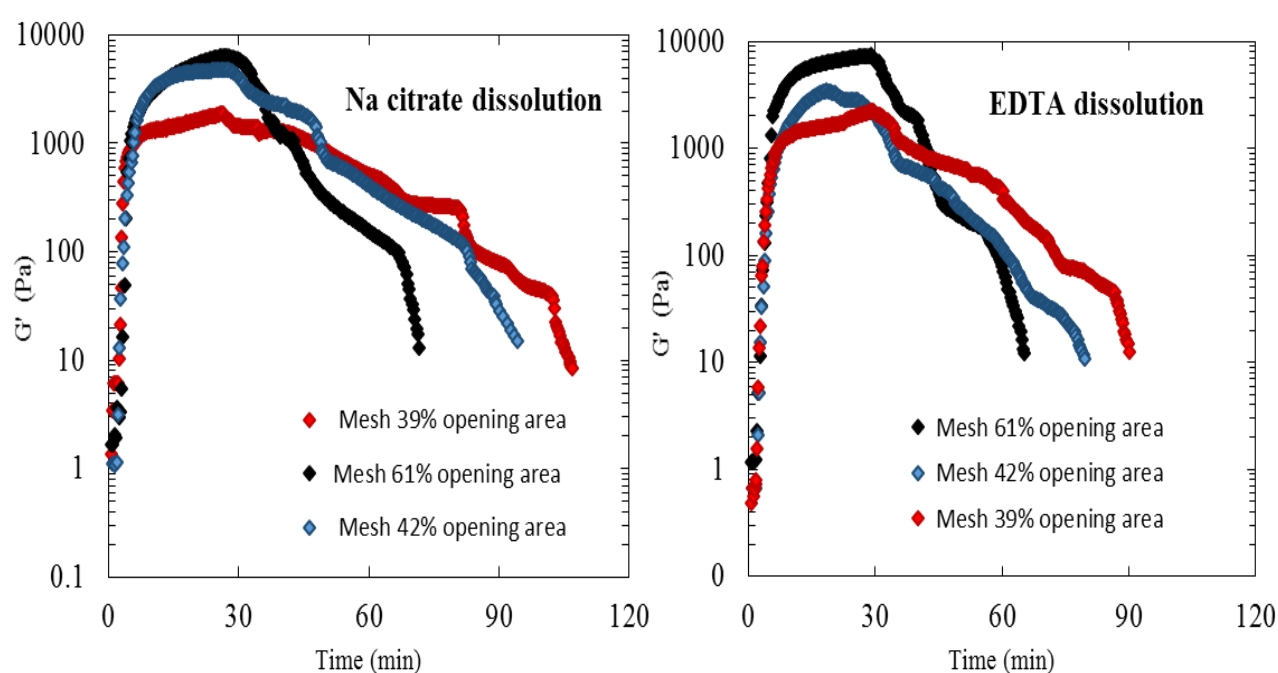


**Figure 6-8: Rheological measurements for 1% alginate methylene blue solution showing a variation of  $G'$  (black, red and blue symbols) vs. time on exposure to 200 mM  $\text{CaCl}_2$  for *in situ* gelation and EDTA and Na citrate for gel dissolution.**

## 6.4.2 Release time results

### 6.4.2.1 Calibration curve of methylene blue

The calibration curve of methylene blue was prepared over the range (2.5, 5, 10, 20, 30, 40, 50 or 100 ml). Serial dilution was performed using the stock solution of methylene blue to prepare the corresponding calibration points as shown in Figure 6.9.

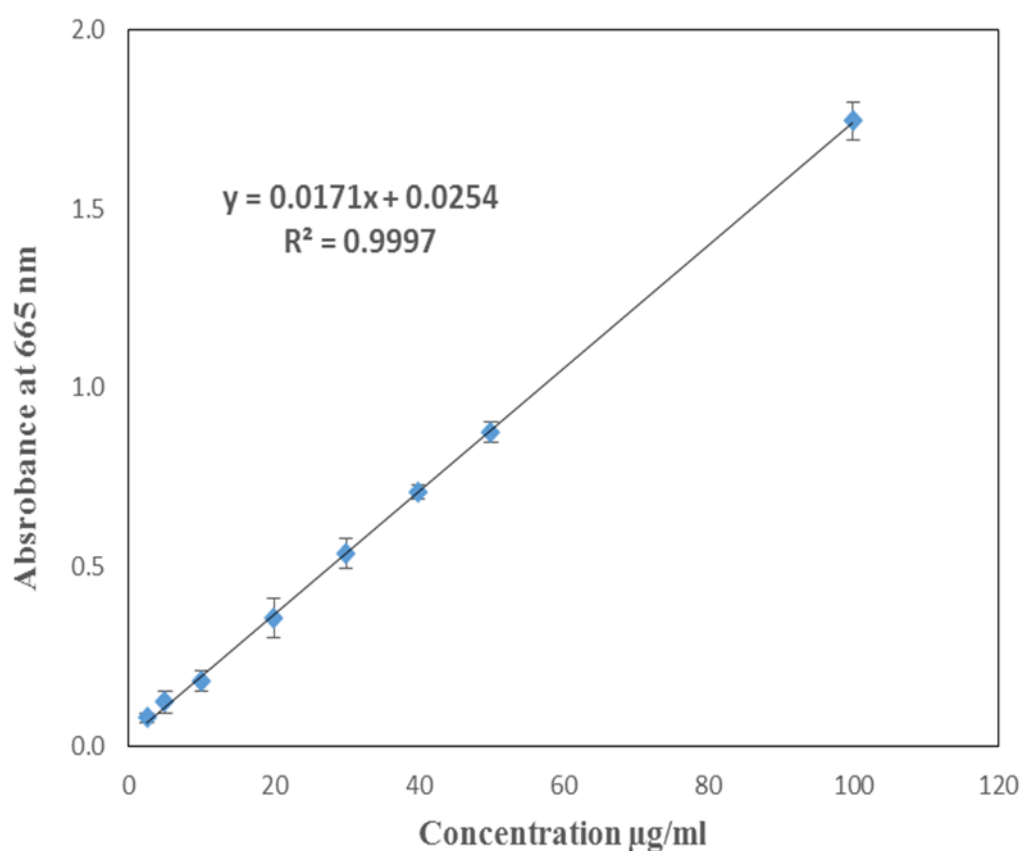


**Figure 6-9: Calibration curve of absorbance against concentration of methylene blue (MB).**

The calibration curve was linear over the range used with correlation coefficient ( $r^2 = 0.999$ ). Limit of detection (LOD) and limit of quantification (LOQ) are important parameters that are used to describe the smallest concentrations of a sample that can be reliably measured by an analytical procedure.

LOD is defined as minimal concentration of analyte that can be detected with a certain degree of confidence and LOQ is defined as the minimal concentration that can be measured with acceptable accuracy. LOD and LOQ are quantified by using equations 6.1 and 6.2 respectively.

$$\text{LOD} = 3.3 \sigma/S \quad \text{Eq. 6.1}$$

$$\text{LOQ} = 10 \sigma/S \quad \text{Eq. 6.2}$$

Where  $\sigma$  is the standard deviation of Y-intercept and S is the slope of the calibration curve. The LOD and LOQ were 1.2 and 3.6  $\mu\text{g/mL}$  respectively. The concentration of methylene blue released from the sample was determined from the corresponding calibration curves. All experiments were carried out in triplicate.

#### **6.4.2.2 Release time**

To measure the concentration of methylene blue that was released from the gel during gelation and gel degradation the absorbance of the  $\text{CaCl}_2$  solution and EDTA and sodium dihydrogen citrate solutions were measured at 665 nm and the concentrations calculated using the following methylene calibration curve equation:  $y = 0.0171x + 0.0254$

To calculate % release, a total of 2 ml of alginate which contained 1 mg of methylene blue (taken as 100%) was loaded onto the rheometer. The samples of fluid in the reservoir were measured for absorbance at 665 nm and the concentration values calculated from the calibration curve were multiplied by the dilution factor of 55 corresponding to the volume of the reservoir (55ml) then converted to percentage. The concentration of methylene blue that released in the  $\text{CaCl}_2$  during the gelation time (30 min) using three different size of mesh was increased as the opening area of mesh decreased and the results were 6.8, 9.2 and 14.1  $\mu\text{g/mL}$  with mesh opening area 61%, 42% and 39% respectively.

The rate of methylene blue released shown an increase during the dissolution time with EDTA and Na citrate as results of gels degradation with three different size of mesh. The amounts that released in EDTA with three size of mesh 61%, 42% and 39% were 9.5, 15.6 and 18.2  $\mu\text{g/mL}$  and in Na citrate 11, 17.1 and 19  $\mu\text{g/mL}$  respectively (Figure 6.10).

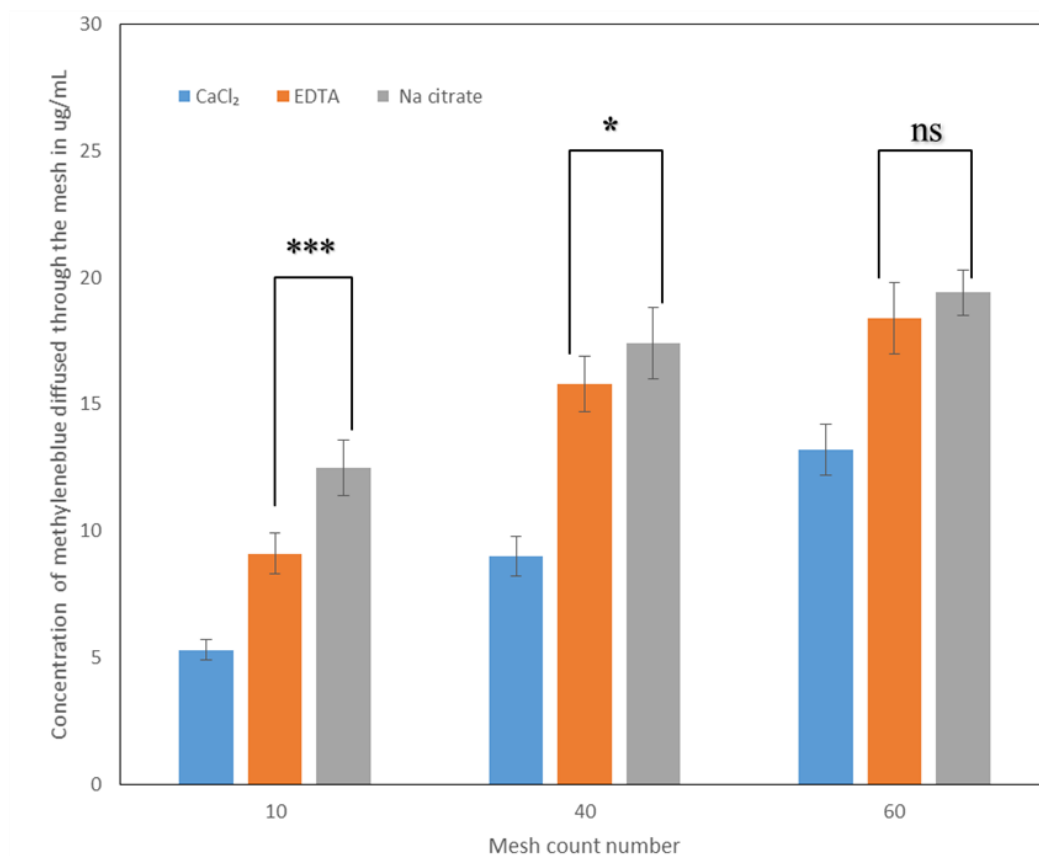


**Figure 6-10: Impact of ion crosslinking (CaCl<sub>2</sub>) and chelating agents (EDTA and sodium dihydrogen citrate) on methylene blue release from alginate gel. Single factor Anova test used in order to determinate statistically significant differences between EDTA and Na citrate and the results were as the following : (\*\* P< 0.01 , \* P< 0.05 and NS = non-significant).**

#### **6.4.2.3 Simultaneous measurements of gelation, gel dissolution using EDTA and release of methylene blue**

To study the effect of gelation and gel dissolution on the release of a model drug loaded in the alginate using the rheo-dissolution cell, rheological data and the absorbance of methylene blue that was released during the gelation and gel dissolution time were recorded. The rheology test applied by measured  $G'$  of loaded alginate during the gelation and gel dissolution with three different mesh sizes (61, 42 and 39 %). The results show an increase in the  $G'$  with the large opening area mesh, 61 % (Figure 6.11A) and the values decreased as the area of mesh decreased with medium opening area mesh 42 % (Figure 6.11B) and small area mesh 39 % as shown in the Figure 6.11C. The values of  $G'$  return to the original values prior the gelation using chelating agents EDTA and Na citrate in the gel dissolution test. Methylene blue release was measured by absorbance at 665 nm using UV-Vis spectrophotometer and calculating the concentration of methylene blue that had diffused through the mesh into the reservoir fluids during the gelation and gel dissolution process. The results showed an increase the concentration of methylene blue release as the opening area of mesh decreased and as the strength of gels decreased (Figure 6.11 A, B and C). Figure 6.11 D shows comparison of the percentage of methylene blue between gelation by  $\text{CaCl}_2$  and gel dissolution by EDTA and the results shows that the (%) of methylene blue that released in  $\text{CaCl}_2$  during the gelation process made up the largest percentage of the total release recorded following dissolution in EDTA in the three different sizes of mesh. The results of total methylene blue released % using three sizes of mesh opening area (61 %, 42 % and 39 %) in EDTA were 52.2 %, 85.8 % and 100.1 % whereby 37.3%, 50.7 % and 77.3 % of which was released in the  $\text{CaCl}_2$  during gelation.

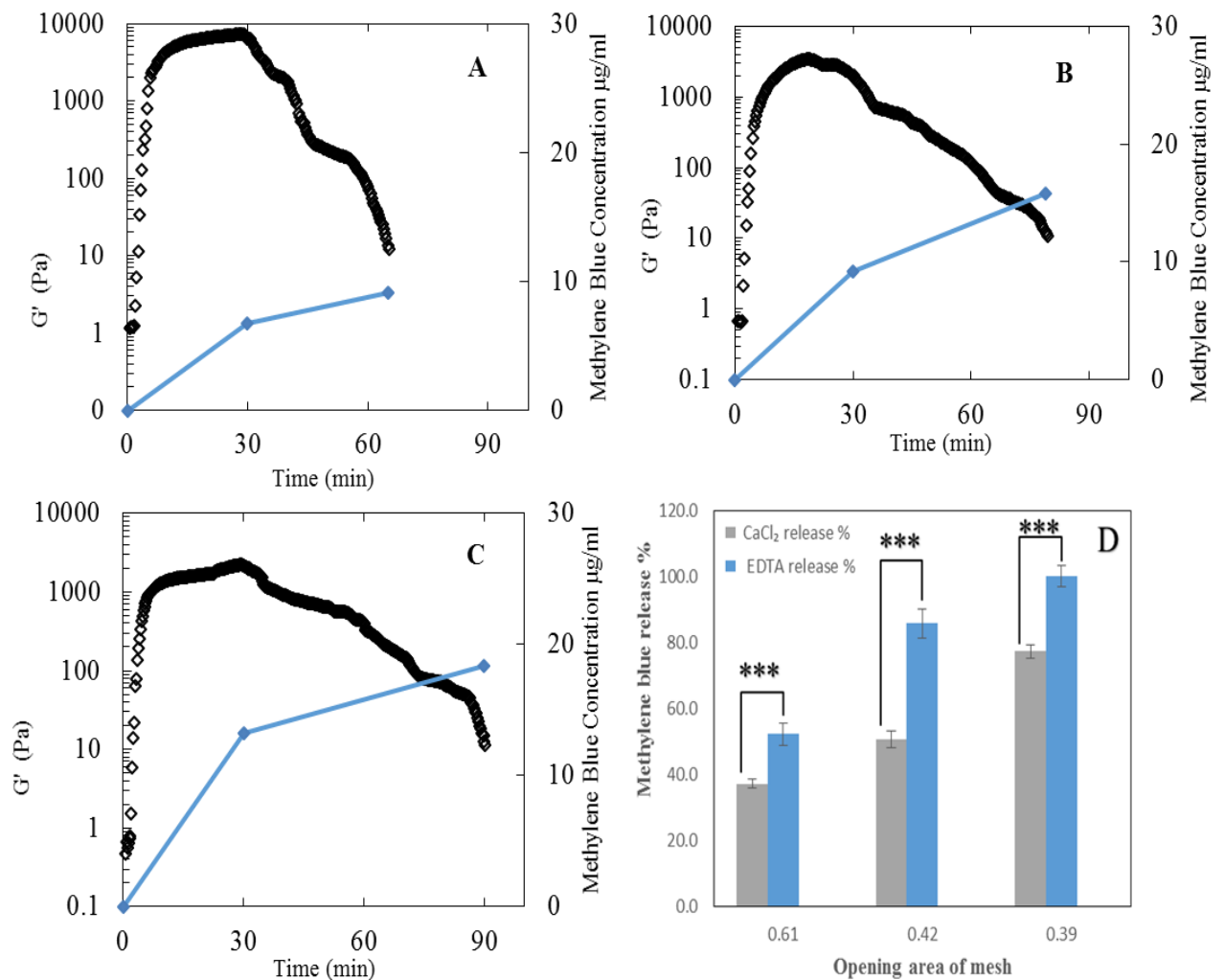


**Figure 6-11. Rheological measurements of 1% alginate and release time of methylene blue from alginate gel, showing variation of  $G'$  (filled black symbols), concentration of MB (filled blue symbols) for A) mesh count 10, B) mesh 40, and C) mesh 60. D) Comparison of release time of methylene blue in EDTA using three different count numbers of mesh. Single factor Anova test used in order to determinate statistically significant differences between EDTA and  $\text{CaCl}_2$  and the results were as the following: (\*\*\*)  $P < 0.001$ , (\*\*)  $P < 0.01$ , (\*)  $P < 0.05$  and NS = non-significant).**



#### **6.4.2.4 Simultaneous measurements of gelation, gel dissolution using Na citrate and release of methylene blue**

To measure the gelation and gel dissolution using Na citrate and release of methylene blue simultaneously the same set up that used with EDTA were applied. The results showed increase in the  $G'$  with large opening area mesh, 61 % (Figure 6.12A), which then decreased when opening area of mesh reduced to 42 % (Figure 6.12B) and 39 % mesh opening area as shown in the Figure 6.12C. The values of  $G'$  return to the original values prior the gelation using the chelating agent Na citrate in the gel dissolution test. Methylene blue release results showed an increase the concentration of methylene blue release as the opening area of mesh decreased and as the strength of gels decreased (Figure 6.12 A, B and C). Figure 6.12 D shows comparison of the percentage of methylene blue between gelation by  $\text{CaCl}_2$  and gel dissolution by Na citrate and the results shows that the (%) of methylene blue that released in  $\text{CaCl}_2$  during the gelation process made up the largest percentage of the total release recorded following dissolution in Na citrate in the three different sizes of mesh in a similar manner to what occurred when treated with EDTA. The results of total methylene blue released % using three sizes of mesh opening area (61 %, 42 % and 39 %) in Na citrate were 60.5 %, 94.1 % and 104.5 % whereby 37.3%, 50.7 % and 77.3 % of which was released in the  $\text{CaCl}_2$  during gelation. The time that needed to dissolve the gel using EDTA was shorter than Na citrate. In contrast, the percentage of methylene blue released in Na citrate was more than the percentage that released in EDTA for all the three size area mesh as shown in Table 6.2.

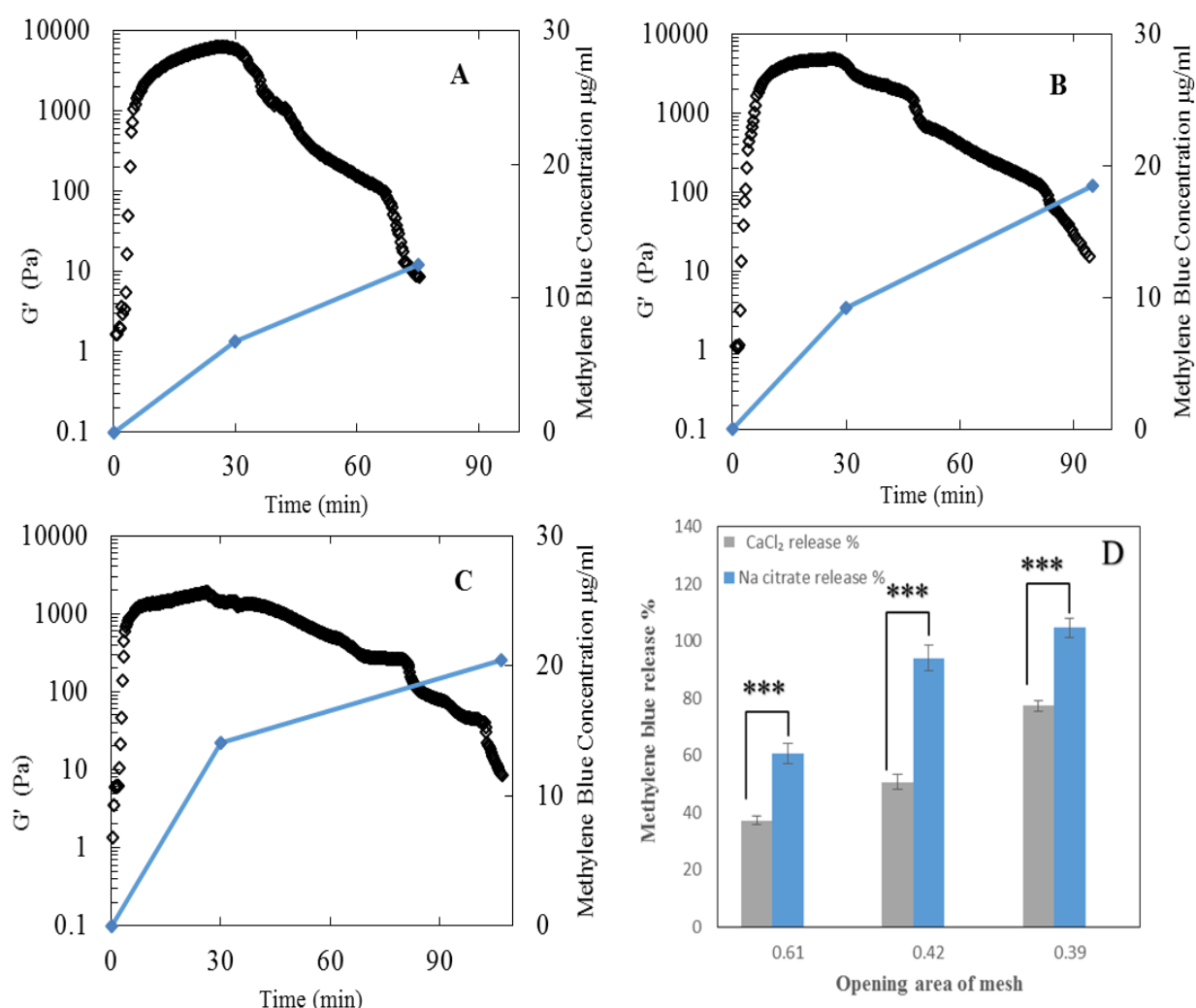


**Figure 6-12. Rheological measurements of 1% alginate and release time of methylene blue from alginate gel, showing variation of  $G'$  (filled black symbols), concentration of MB (filled blue symbols) for A) mesh count 10, B) mesh 40, and C) mesh 60. D) Comparison of release time of methylene blue in Na citrate using three different count numbers of mesh. Single factor Anova test used in order to determinate statistically significant differences between Na citrate and  $\text{CaCl}_2$  and the results were as the following: (\*\*\*)  $P < 0.001$ , \*\*  $P < 0.01$ , \*  $P < 0.05$  and NS = non-significant).**

#### 6.4.2.5 Comparison of dissolution time and % release of methylene blue from 1% alginate using three different mesh sizes

The release of methylene blue into all the fluids the alginate was exposed to during gelation and dissolution on the rheo-dissolution cell, are given for each of the mesh sizes in Table 6.2. Release in the  $\text{CaCl}_2$  during gelation ( $t_{30}$ ) increased with a reduction in the mesh size from 37.3% in the largest mesh size up to 77.3% in the smallest mesh. The release of methylene blue at  $t_{\text{end}}$  (time taken for complete dissolution of the gel) also increased with increasing mesh size in both EDTA and Na citrate. The difference between  $t_{30}$  and  $t_{\text{end}}$ , which is effectively the total release into the chelation media during gel dissolution, was greater in Na citrate than EDTA in all mesh sizes; however, it is important to point out that the time at  $t_{\text{end}}$  was also greater in the Na citrate which may account for the increased release. These data have clearly shown that the majority of the release of methylene blue occurred during the gelation period in all samples however it appeared that increased gel strength produced when using a larger mesh opening, reduced the release.

**Table 6-2: Dissolution time and release percentage of methylene blue from alginate gel into  $\text{CaCl}_2$  ( $t_{30}$ ), EDTA ( $t_{\text{end}}$ ) and Na citrate ( $t_{\text{end}}$ ) using three different mesh types .**

	EDTA				Na citrate		Difference
Mesh (% opening)	% released in $\text{CaCl}_2$ at 30 min ( $t_{30}$ )	$t_{\text{end}}$ (min)	% release at $t_{\text{end}}$	% difference between $t_{30}$ and $t_{\text{end}}$	$T_{\text{end}}$ (min)	% release at $t_{\text{end}}$	% difference between $t_{30}$ and $t_{\text{end}}$
10 (61%)	37.3 ( $\pm 0.3$ )	35	52.3( $\pm 0.6$ )	15.0	45	60.5( $\pm 0.7$ )	23.2
40 (42%)	50.6 ( $\pm 0.5$ )	49	85.8( $\pm 0.8$ )	35.2	64	94.1( $\pm 0.9$ )	43.5
60 (39%)	77.3 ( $\pm 0.4$ )	60	100.1( $\pm 0.6$ )	22.8	77	104.5( $\pm 0.8$ )	27.2

## 6.5 Discussion

Changes in elastic modulus  $G'$  and viscous modulus  $G''$  were measured for a 1% alginate methylene blue solution upon exposure to 200 mM  $\text{CaCl}_2$  for *in situ* gelation test and 500 mM calcium chelator (EDTA or Na citrate) to measure *in situ* gel dissolution time using the rheo-dissolution cell attached to the lower plate of a Malvern Kinexus rheometer as described in section 6.2. This technique allowed for the simultaneous measurement of gelation of the alginate and gel dissolution and release of methylene blue. The concentration of the alginate was chosen at 1% to ensure gelation that was suitable to facilitate diffusion of methylene blue from the gel. In Figure 6.4 (A-C), a rapid increase in  $G'$  and  $G''$ , was observed over the first few minutes of exposure, with  $G'$  overtaking  $G''$  within 5 minutes upon contact with 200 mM  $\text{CaCl}_2$ . The tests were performed using three different mesh sizes as the lower plate. It was found that the opening area of mesh played an important role in the gelation process and release time. Onset of gelation (indicated by rapid increases in  $G'$  and  $G''$ ) occurred over the first few minutes of contact with the  $\text{CaCl}_2$ , with  $G'$  overtaking  $G''$  within 5 minutes for all of the mesh sizes used (Figure 6.4). The resultant gel stiffness however, following 30 min exposure to  $\text{CaCl}_2$ , was dependent on % mesh opening with gels on the largest mesh (61% opening) having a significantly greater  $G'$  value than that of the medium (42% opening) and smallest mesh (39% opening)  $G' = (7046 \pm 95)$ ,  $(4217 \pm 123)$ , and  $(2151 \pm 87)$  Pa, respectively (Figure 6.4D). This is likely due to the increased availability of calcium ions that can come into contact with the gel for the duration the gelation test in the larger mesh opening.

At 30 min the 200 mM  $\text{CaCl}_2$  in the reservoir was replaced by a solution of calcium chelator (500 mM EDTA or 500 mM Na citrate) which resulted in the alginate returning to the original liquid state indicated by a rapid drop in moduli values (Figures 6.5, 6.6 and 6.7). The obtained results, generally followed a similar pattern to the results that were reported in Chapter 4 using

the petri dish method, showing that EDTA was a more potent calcium chelator than Na citrate (Figure 6.8). This was the case in all mesh sizes used (Figures 6.5, 6.6 and 6.7). The opening area of mesh however, did have an impact on the gel dissolution time for each chelator. When the opening area of mesh was large, it allowed the calcium crosslinked alginate polymers greater surface contact with the chelating agent, and subsequently, a shorter time for the breakdown of the gel structure than when the mesh with small opening areas were used (Figure 6.8).

As proof of concept and to highlight the potential of this method to analyse release of molecules from the polymer sample during the gelation and gel dissolution, the alginate samples were prepared containing methylene blue. Samples of the fluids housed in the reservoir of the rheo-dissolution cell were taken and analysed for methylene blue release during the process at selected time points ( $t_0$  as soon as the sample was loaded,  $t_{30}$  following 30 min exposure to  $\text{CaCl}_2$  and  $t_{\text{end}}$  following complete degradation of the gel). The release end point time was adjusted according to the point at which the gels had degraded determined when both  $G'$  and  $G''$  returned to a similar modulus to that of the original alginate samples prior to crosslinking, which was within 120 min for all samples. This experiment proved a success with methyl blue being detected in both the  $\text{CaCl}_2$  during gelation and in the calcium chelating fluids. Mesh opening size however, appeared to influence the quantities released.

Between  $t_0$  and  $t_{30}$  (during the gelation period) 37.3 %, 50.6 %, 77.3 % of the total methylene blue was detected when using the large mesh, medium mesh, and small mesh respectively. Initially, this appears counter intuitive as one might expect the larger opening to facilitate diffusion of the methylene blue. However, as the larger mesh size gives a much stiffer gel ( $G' \sim 7000$ ) in comparison with the small mesh size ( $G' \sim 2000$ ) (Figure 6.4). This increased level of crosslinking in the alginate matrix may have reduced the extent of methylene blue release

keeping it entrapped in the gel more efficiently. This has been reported by other researchers when entrapping drugs in alginate beads where by entrapment efficiency is improved by increasing the  $\text{CaCl}_2$  concentration during gelation (Mandel et al., 2010; Manjanna et al., 2013). Indeed, Manjanna et al (2013) reported a 20% increase in the retention of aceclofenac sodium in alginate beads when the concentration of  $\text{CaCl}_2$  was increased from 1% to 5% resulting a much stronger gel. At high concentrations of  $\text{CaCl}_2$ , a strong and rigid gel is formed, and this gel does not allow the rapid release time at high speed. Similar results were reported by Azarmi et al. (2003) using sodium alginate to sustain drug release of acetazolamide tablets and Nokhodchi and Tailor (2004) studying sustained release of theophylline from polymeric matrices using *in situ* crosslinking of sodium alginate with calcium and aluminium ions. Both of these studies observed slower drug release at high calcium salt concentrations and rapid release at low calcium salt concentrations that was attributed to insufficient crosslinking required to produce an insoluble barrier (Azarmi et al., 2003; Nokhodchi and Tailor, 2004). This behaviour has also been reported in gellan gum (Mahdi et al. 2014), where the stiffness of gels reduced the rate of ibuprofen release.

During gel dissolution the methylene blue continued to be released as the gel was returned to the solution state using chelating agents EDTA and Na citrate but in lower quantities than that what was released into the  $\text{CaCl}_2$ . The experiment was stopped when both  $G'$  and  $G''$  returned to a similar modulus to that of the original alginate samples prior to crosslinking. Table 6.2 shows the release time of methylene blue from alginate gels during both gelation in  $\text{CaCl}_2$  and dissolution of the gel in solutions of EDTA and Na citrate using the three different mesh sizes. The results revealed that the quantity of methylene blue released appeared to be influenced by gel strength and the dissolution time as the quantity of release decreased in the stiffer gels, but as the dissolution time ( $t_{\text{end}}$ ) was also shorter as result of greater extent of chelation in the large mesh size. Therefore, the quantity released at  $t_{\text{end}}$  was also reduced. A likely explanation of

this behaviour is, as the gel is degrading the release is governed by diffusion of the soluble methylene blue through the polymer chains as which was more rapid in the EDTA as the viscoelasticity is reduced more quickly than in the Na citrate. However as release through hydrated polymer networks tends to be via first order release kinetics the drug release rate depends on its concentration. The results indicate that this is also the case here in the small mesh/ weakest gels 77% of the methylene blue has already been released from the alginate so therefore has a lower concentration.

In the case of the strongest gel, containing the highest concentration of methylene blue (at the point when the  $\text{CaCl}_2$  was transferred to the chelating fluid) release is retarded. Previous work by Mahdi et al reported that release of ibuprofen from gellan gum gels required  $G'$  values below  $\sim 4000$  Pa before a rapid onset of release was observed. This could be the case here with the strongest gels which have values of  $G'$  in excess of 7000 Pa whereas the medium mesh and the small mesh gels were  $\sim 4000$  and 2000Pa respectively. Interestingly the release from the weakest gel (small mesh) appeared lower than the medium gel however the starting concentration was much less as 77% had already been lost in the  $\text{CaCl}_2$  leaving only 23% to be released compared with 50% in the medium gel, and as release through entangled polymeric networks usually. These results highlight the complex interplay between viscoelasticity of the substrate and molecular diffusion of the solute in polymeric drug delivery systems. Ideally, the release studies would have had more sampling time points that continued until all of the methylene blue was released, as this would have provided a greater understanding of the release kinetics in each sample for a better comparison. However, as these studies were performed on a bespoke system the sampling method in place was relatively crude and caused vibrations impacting on the sensitive oscillatory measurements performed by the rheometer. Therefore sampling of the fluid was kept to a minimum. In addition, as the overall aim of the study was to design and evaluate the potential of the system. Whereby rheological measurements of

rapidly gelling or dissolving hydrogels on contact with external crosslinkers or chelators could be performed while simultaneously measuring release of an entrapped substance. Proving this was possible has since led to an improved design of the rheo-dissolution cell that incorporates a pump to allow flow through the reservoir and a sampling port that minimises vibrations during sampling and is currently being explored using *in situ* gelling ophthalmic eye drops containing pharmaceutical actives.

## 6.6 Conclusion

The rheological study of alginate solutions demonstrated that *in situ* gelation occurred upon exposure to  $\text{CaCl}_2$  and that these gels were degraded by EDTA and Na citrate using the rheo-dissolution cell technique. The release study using the rheo-dissolution cell investigated release of methylene blue from the gels while simultaneously measuring rheology of alginate during gelation and dissolution. The release behaviour of methylene blue from alginate gels in  $\text{CaCl}_2$ , EDTA, and Na citrate solutions were dependent on the stiffness of the gels. The stiffness, and hence drug release, could be controlled with concentration and exposure time to cross-linked ions which in the rheo-dissolution system could be controlled by the mesh size used as the lower plate. It is believed that this is the first report of such simultaneous measurements and presents a new system whereby the physical response of biopolymers to changing environments can be modelled (for example changes in pH, ionic strength or additional additives i.e. crosslinkers/chelators). Therefore, having the potential to be used as a model for measuring the changes in rheological behaviour and drug release simultaneously when liquid or gel formulations are exposed to various physiological fluids. The wider application of this system is the ability to use any polymer for many different industrial applications where there may be a need for rapid or slow gelation while monitoring molecules that are released from the sample in real time.



## **Chapter 7 General Conclusions and Future Recommendations**

## CHAPTER SEVEN

### GENERAL CONCLUSIONS AND FUTURE RECOMMENDATIONS

The main purpose of this research was to develop a model for rheological measurements of *in situ* gelation of bioresponsive polymers on contact with externally delivered chemical stimulus using a commercially available rheometer. Two new methods were designed to evaluate rheological behaviour in preparations of three types of biopolymers alginate, LM pectin and gellan gum. In particular, the alginate and pectin were investigated for *in situ* gel production on external exposure to three different concentrations of  $\text{CaCl}_2$  (50, 100 and 200 mM). The degradation/dissolution of the gels were also investigated using chelating agents rather than crosslinking agents. Gellan gum *in situ* gelation was evaluated on exposure to a range of physiological fluids that had various ionic compositions. In addition, a new device called a “Rheo-dissolution cell” was developed that contained a fluid reservoir and a stainless steel mesh plate and was used to measure the *in situ* gelation of alginate (containing methylene blue as a model drug) on exposure to  $\text{Ca}^{2+}$  while simultaneously measuring the release of methylene blue.

Therefore, different types of gels were produced through various external gelation mechanisms using two new techniques that involved minor modifications of a rheometer, one by attaching a petri dish to the lower plate of rheometer and the other by replacing the lower plate with a Rheo-dissolution cell. The following sections summarise the main conclusions made for each of the experimental results chapters.

## 7.1 Evaluation of external gelation of alginate and pectin by rheological measurements

Chapter 4 highlighted a potential new application method for monitoring external gelation of alginate and pectin gels. Rheological properties of both biopolymers were measured by using a modification to the lower plate of Malvern Gemini rheometer. This was achieved by attaching a petri dish containing a filter paper and dialysis membrane soaked in  $\text{CaCl}_2$  to the lower plate. Once the samples were loaded changes in rheological behaviour was measured *in situ* for gelation. The following gelation the filter paper was replaced with one that was soaked in a calcium chelator (EDTA or Na citrate) and gel dissolution was then measured. Small deformation oscillatory measurements of storage and loss moduli ( $G'$  and  $G''$ ) were measured for both gelation and dissolution, and plotted as a function of time.

The changes in  $G'$  and  $G''$  revealed that rapid gelation behaviour of alginate and pectin occurred when exposed to an external source of  $\text{CaCl}_2$  with increase in both moduli. Moreover, stronger gels were formed when the concentration of  $\text{CaCl}_2$  increased. The gel degradation results demonstrated that EDTA was clearly a more potent calcium chelator than Na citrate, causing  $G'$  to return to a similar modulus to that of the original alginate and pectin prior to crosslinking more quickly. From a technical perspective, it was identified that the measurements were required to begin at a consistent time following loading of the sample as this is particularly crucial in rapid gelling systems such as alginate. Also, quantity of the samples loaded was also important for accurate comparisons. In addition to measuring alginate and LM pectin, it was proposed that this technique could be applied to studying gelation of gellan, carrageenans and other biopolymers that gel in the presence of metal ions, small molecule crosslinkers or by changes in pH. In particular, using artificial physiological fluids to investigate changes in the rheological behaviour of gellan gum on exposure to mono and divalent ions (or by changing in the pH) that are present in the body fluids.

Gellan is particularly responsive to small changes in pH, ionic strength and ionic species and could therefore, provide useful information in developing *in situ* gelling pharmaceutical delivery systems.

## **7.2 Effect of physiological body fluids on the rheological behaviour of gellan gum**

Chapter 5 highlighted the potential to adapt the system developed in chapter 4 to measure gellan gum gel formation on contact with several different artificial physiological fluids (Saliva, wound fluid, Lacrimal fluid and Gastric fluid) which contain different ionic (and acidic) compositions. The results of *in situ* gelation of tests with different types of physiological fluids revealed that gellan made the stiffest gels with artificial gastric fluid (GF) followed by lacrimal fluid (LF) and simulated wound fluid (SWF) which were similar to each other and the weakest gel formed was with artificial saliva (AS). This was explained by the concentrations of gel forming ions available in the different fluids and the selectivity of the gellan to form gels with  $H^+ < Ca^{2+} < Mg^{2+} < K^+ < Na^+$ . There were also large differences in the gelation kinetics between the gels formed in the different fluids giving vastly different gelation rate constants  $\sim 2.2\ s^{-1}$  for the gastric fluid and  $0.1\ s^{-1}$  for the saliva. It was also found that gelation kinetics and polymer concentration had a dramatic effect on microstructure. Despite similar modulus values of the gels prepared with 0.25% w/w gellan in GF, 0.75% w/w in LF and SWF, and 1% w/w in AS, the microstructure appeared vastly different. The rapidly produced GF crosslinked gels formed dense aggregates with a rougher surface texture when compared with the AS crosslinked gels, that formed at a much slower rate, which had a much smoother less porous structure.

The ion dependency of gellan gum therefore the presence of varying concentrations and species of ions in different physiological fluids resulted in not only gels with different mechanical properties but also impacts on gelation kinetics and the subsequent microstructure. This simple modification to a commercially available rheometer can facilitate in the understanding of the

gelation process of rapidly gelling materials, which could be an important tool when developing such drug delivery systems. The success of these *in situ* gelation experiments and potential application to designing drug delivery systems led to ideas for the development of a modified rheometer plate which can be used to simultaneously measure rheological properties and drug release from *in situ* gelling systems.

### **7.3 Novel model for simultaneous measurement of rheology and drug release (the Rheo-dissolution cell)**

Chapter 6 focussed on designing a new device to overcome the limitations of the petri dish method that was applied in chapter four and five. The device that was developed was called a rheo-dissolution cell that can be attached to a rheometer and allows the examination of the rheological behaviour with the potential for analysing dissolution of a drug simultaneously. The rheo-dissolution cell was a novel device made from acrylonitrile butadiene styrene polymers (ABS) and was 3D printed using additive layer manufacturing. The device was designed as a circle reservoir (capable of holding 55 ml of solution) with an opening on the top that is covered with stainless steel mesh on to which the gel forming samples are loaded during the experiments allowing contact with the fluid in the reservoir. Alginate (1% w/w) was prepared containing methylene blue solution as a model drug and gelation experiments were performed in presence of  $\text{CaCl}_2$  added to the reservoir and the changes in rheological measurements of  $G'$  and  $G''$  were taken as a function of time. Following gelation, the  $\text{CaCl}_2$  was replaced with a calcium chelator (EDTA or Na citrate) and gel dissolution was then measured. At three time points  $t_0$  (prior to gelation)  $t_{30}$  (30min gelation) and  $t_{\text{end}}$  (following gel dissolution) samples of the reservoir fluid were taken and analysed for methylene blue. Three different mesh sizes were used for validation purposes.

Rapid increase in  $G'$  and  $G''$  was demonstrated over the first few minutes of exposure to  $\text{CaCl}_2$ , with  $G'$  overtaking  $G''$  within 5 minutes upon contact time. It was found that the value of  $G'$  at

the end of the gelation period increased as the size of mesh opening area increased from which it was concluded that this occurred because of an increased surface exposure to  $\text{Ca}^{2+}$  producing a stronger gel. The dissolution of the gels on exposure to the calcium chelators were similar to what was observed in chapter 4, indicating that EDTA is a more potent calcium chelator than Na citrate.

The release of methylene blue in the gelation period and in the dissolution period showed that release was dependent on the stiffness of the gels, which in turn, is controlled by the concentration and exposure time of the cross-linking ions used. The results obtained suggest that the rheo-dissolution cell has the potential to be used as rheological add-on for measuring drug release from gel bases formulations. When using the rheo-dissolution cell however, was found that the mesh size used as the lower plate also affected the gel stiffness and gel dissolution, and consequently, release of methylene blue, therefore mesh sizes should be chosen to adequately represent the application environment. This highlights flexibility in the system that could deliver wider applications of the rheo-dissolution cell. These findings are believed to be the first to utilise and successfully to examine rheological properties for *in situ* gelling formulations while at the same time measuring release of an entrapped solute. Overall, highlighting the complex molecular interplay that occurs between the gelling/dissolving polymers and the release of an entrapped drug, opening up potential for further investigation.

The work presented in this thesis has led to further projects using and further developing the rheo-dissolution cell. This has included the addition of a pump system through the inlet and outlet pipes. This allows for a constant flow through which is more representative of the dynamic environment of physiological systems. In addition to this, a sampling port has been since installed into the inlet and outlet pipes of the flow through system, which allows withdrawal and addition of the sample without disturbing the rheometer facilitating a greater number of sampling time points.

Future work it is anticipated that a stainless steel rheo-dissolution cell will be engineered rather than using ABS polymer which will allow for incorporation of more accurate temperature control which can be crucial when measuring thermally sensitive materials.

Ultimately, the work presented in this thesis has introduced new methods to monitor the *in situ* ionotropic gelation and dissolution of polymers by providing a mechanism to deliver solutions of chemical crosslinkers or chelating agents. In addition to gelation and dissolution the work provides a proof of concept of a rheo-dissolution cell for the simultaneous measurement of rheology and drug release in the presence of gelling or dissolution media offering new methods to explore *in situ* gelling systems. It is anticipated that the ease of manufacture and application of these methods, will prompt further research on a variety of polymers that are responsive to external contact with crosslinking solutions or dissolution media, and for the rheo-dissolution cell, release of entrapped solutes. Furthermore, the wide varieties of materials that could be applied to these systems go beyond just pharmaceutical applications and have the potential to be applied in several other industrial disciplines.

## **Chapter 8      References**



## CHAPTER EIGHT

### REFERENCES

- Axelos, M.A.V. and Thibault, J.F., 1991. The chemistry of low-methoxyl pectin gelation. The chemistry and technology of pectin, 1(6), pp.109-118.
- Azarmi, S., Valizadeh, H., Barzegar-Jalali, M. and Löbenberg, R., 2003. *In situ* cross-linking of polyanionic polymers to sustain the drug release of acetazolamide tablets. *Pharmazeutische Industries*, 65(9), pp.877-881.
- Bae, Y.H., 1997. Stimuli-Sensitive Drug Delivery, in: K. Park (Ed.), *Controlled Drug Delivery: Challenge and Strategies*, American Chemical Society, Washington, DC, pp. 147–160.
- Bajaj, I.B., Survase, S.A., Saudagar, P.S. and Singhal, R.S., 2007. Gellan gum: fermentative production, downstream processing and applications. *Food Technology and Biotechnology*, 45(4), p.341-343.
- Bakliwal, S.R. and Pawar, S.P., 2010. In-situ gel: new trends in controlled and sustained drug delivery system. *International Journal of PharmTech Research*, 2 (2), pp. 1398-1408.
- Balamuralidhara, V., Pramodkumar, T.M., Srujana, N., Venkatesh, M.P., Gupta, N.V., Krishna, K.L. and Gangadharappa, H.V., 2011. pH sensitive drug delivery systems: A review. *American Journal of Drug Discovery and Development*, 1(1), pp.24-48.
- Banerjee, S. and Bhattacharya, S., 2012. Food gels: gelling process and new applications. *Critical Reviews in Food Science and Nutrition*, 52(4), pp.334-346.
- Blunt, L. and Jiang, X., 2003. Advanced techniques for assessment surface topography: development of a basis for 3D surface texture standards "surfstand". *Kogan Page Science*.pp.17-40.
- Boulet-Audet, M., Byrne, B. and Kazarian, S.G., 2014. High-throughput thermal stability analysis of a monoclonal antibody by attenuated total reflection FT-IR spectroscopic imaging. *Analytical Chemistry*, 86(19), pp.9786-9793.
- Bowler, P.G., Welsby, S., Towers, V., Booth, R., Hogarth, A., Rowlands, V., Joseph, A. and Jones, S.A., 2012. Multidrug-resistant organisms, wounds and topical antimicrobial protection. *International Wound Journal*, 9(4), pp.387-396.
- Bradbeer, J.F., Hancocks, R., Spyropoulos, F. and Norton, I.T., 2014. Self-structuring foods based on acid-sensitive low and high acyl mixed gellan systems to impact on satiety. *Food Hydrocolloids*, 35, pp.522-530.
- Bron, A.J., Tiffany, J.M., Gouveia, S.M., Yokoi, N. and Voon, L.W., 2004. Functional aspects of the tear film lipid layer. *Experimental Eye Research*, 78(3), pp.347-360.

- Callaghan, P.T. and Gil, A.M., 2000. Rheo-NMR of semidilute polyacrylamide in water. *Macromolecules*, American Chemical Society, 33(11), pp.4116-4124.
- Chevrel, M.C., Hoppe, S., Falk, L., Nadège, B., Chapron, D., Bourson, P. and Durand, A., 2012. Rheo-Raman: A Promising technique for *in situ* monitoring of polymerization reactions in solution. *Industrial & Engineering Chemistry Research*, 51(49), pp.16151-16156.
- Chitkara, D., Shikanov, A., Kumar, N. and Domb, A.J., 2006. Biodegradable injectable *in situ* depot-forming drug delivery systems. *Macromolecular Bioscience*, 6(12), pp.977-990.
- Choi, B., Loh, X.J., Tan, A., Loh, C.K., Ye, E., Joo, M.K. and Jeong, B., 2015. Introduction to *in situ* forming hydrogels for biomedical applications. In *In-Situ Gelling Polymers for Biomedical Applications*, pp. 5-35
- Clark, A.H. and Ross-Murphy, S.B., 1987. Structural and mechanical properties of biopolymer gels. *Advances in Polymer Science*, 83, pp. 57-192.
- Clark, A.H. and Ross-Murphy, S.B., 2009. Biopolymer network assembly: measurement and theory. *Modern Biopolymer Science: Bridging the Divide between Fundamental Treatise and Industrial Application*, 1 (1), pp.7-13.
- Clark, A.H., 1992. Gels and gelling. In: *Physical chemistry of foods*. Henry G. Schwartzberg, Richard W. Hartel, Technology & Engineering, 1(5), pp.263-305.
- Clark, S., Cross, M.L., Smith, A., Court, P., Vipond, J., Nadian, A., Hewinson, R.G., Batchelor, H.K., Perrie, Y., Williams, A. and Aldwell, F.E., 2008. Assessment of different formulations of oral *Mycobacterium bovis* Bacille Calmette-Guérin (BCG) vaccine in rodent models for immunogenicity and protection against aerosol challenge with *M. bovis*. *Vaccine*, 26(46), pp.5791-5797.
- Cohen, S., Lobel, E., Trevgoda, A. and Peled, Y., 1997. A novel *in situ*-forming ophthalmic drug delivery system from alginates undergoing gelation in the eye. *Journal of Controlled Release*, 44(2), pp.201-208.
- Coleman, B.D. and Noll, W., 1961. Foundations of linear viscoelasticity. *Reviews of Modern Physics*, 33(2), p.239.
- Corkhill, P.H., Hamilton, C.J. and Tighe, B.J., 1989. Synthetic hydrogels VI. Hydrogel composites as wound dressings and implant materials. *Biomaterials*, 10(1), pp.3-10.
- Coviello, T., Matricardi, P., Marianecchi, C. and Alhaique, F., 2007. Polysaccharide hydrogels for modified release formulations. *Journal of Controlled Release*, 119(1), pp.5-24.
- Cutting, K.F., 2003. Wound exudate: composition and functions. *British Journal of Community Nursing*, 8(3), pp.4-9.

- D'Arrigo, G.I., Alhaique, F. and Matricardi, P., 2013. Macro and Nano shaped polysaccharide hydrogels as drug delivery systems. *Center for Pharmaceutical Biotechnology & Nanomedicine*, 1(1), pp.2-18.
- Debra, J.B. and Cheri, O., 1998. Wound healing: Technological innovations and market overview. *Technology Catalysts International Corporation*, 2, pp.1-185.
- de Luna, M.S., Altobelli, R., Gioiella, L., Castaldo, R., Scherillo, G. and Filippone G., 2017. Role of polymer network and gelation kinetics on the mechanical properties and adsorption capacity of chitosan hydrogels for dye removal. *Journal of Polymer Science Part B: Polymer Physics*, doi:10.1002/polb.24436
- Denny, P., Hagen, F.K., Hardt, M., Liao, L., Yan, W., Arellanno, M., Bassilian, S., Bedi, G.S., Boontheung, P., Cociorva, D. and Delahunty, C.M., 2008. The proteomes of human parotid and submandibular/sublingual gland salivas collected as the ductal secretions. *Journal of Proteome Research*, 7(5), pp.1994-1996.
- Deshpande, S.S., Deshpande, U.S. and Salunkhe, D.K., 1995. Food acidulants. *Food Additive Toxicology*. University of Manitoba, Canada, 1(2), pp.11-87.
- Donati, I. and Paoletti, S., 2009. Material properties of alginates. In *Alginates: Biology and Applications*, 13(1), pp. 1-53.
- Doube, M., Kłosowski, M.M., Arganda-Carreras, I., Cordelières, F.P., Dougherty, R.P., Jackson, J.S., Schmid, B., Hutchinson, J.R. and Shefelbine, S.J., 2010. BoneJ: free and extensible bone image analysis in ImageJ. *Bone*, 47(6), pp.1076-1079.
- Draget, K. I., Moe, S. T., Skjåk-Bræk, G and Smidsrød, O. (2006a). Alginates. Food polysaccharides and their applications. *Food Science and Technology*, 67(9), pp. 289-334.
- Draget, K.I, 2000. Alginates. In: Philips GO, Williams PA (Eds) *Handbook of Hydrocolloids*. Woodhead Publishing Limited, pp 379–393.
- Draget, K.I. and Taylor, C., 2011. Chemical, physical and biological properties of alginates and their biomedical implications. *Food Hydrocolloids*, 25(2), pp.251-256.
- Draget, K.I., Skjåk-Bræk, G. and Smidsrød, O., 1994. Alginic acid gels: the effect of alginate chemical composition and molecular weight. *Carbohydrate Polymers*, 25(1), pp.31-38.
- Draget, K.I., Østgaard, K. and Smidsrød, O., 1990. Homogeneous alginate gels: a technical approach. *Carbohydrate Polymers*, 14(2), pp.159-178.
- Draget, K.I., Skjåk-Bræk, G. and Stokke, B.T., 2006. Similarities and differences between alginic acid gels and ionically crosslinked alginate gels. *Food Hydrocolloids*, 20(2), pp.170-175.

- Draget, K.I., Skjåk-Bræk, G., Christensen, B.E., Gåserød, O. and Smidsrød, O., 1996. Swelling and partial solubilization of alginic acid gel beads in acidic buffer. *Carbohydrate Polymers*, 29(3), pp.209-215.
- Draget, K.I., Stokke, B.T., Yuguchi, Y., Urakawa, H. and Kajiware, K., 2003. Small-angle X-ray scattering and rheological characterization of alginate gels. 3. Alginic acid gels. *Biomacromolecules*, 4(6), pp.1661-1668.
- Du, J., Tang, Y., Lewis, A.L. and Armes, S.P., 2005. PH-sensitive vesicles based on a biocompatible zwitterionic diblock copolymer. *Journal of the American Chemical Society*, 127(51), pp.17982-17983.
- Dupuy, B., Arien, A. and Minnot, A.P., 1994. FT-IR of membranes made with alginate/polylysine complexes. Variations with the mannuronic or guluronic content of the polysaccharides. *Artificial Cells, Blood Substitutes, and Biotechnology*, 22(1), pp.71-82.
- Edsman, K., Carlfors, J. and Petersson, R., 1998. Rheological evaluation of poloxamer as an *in situ* gel for ophthalmic use. *European Journal of Pharmaceutical Sciences*, 6(2), pp.105-112.
- Ehlers, N., Kessing, S.V. and Norn, M.S., 1972. Quantitative amounts of conjunctival mucous secretion and tears. *Acta Ophthalmologica*, 50(2), pp.210-214.
- Ewoldt, R.H., Johnston, M.T. and Caretta, L.M., 2015. Experimental challenges of shear rheology: how to avoid bad data. In *Complex Fluids in Biological Systems*, pp. 207-241.
- Garnier, C., Axelos, M.A. and Thibault, J.F., 1994. Selectivity and cooperativity in the binding of calcium ions by pectins. *Carbohydrate Research*, 256(1), pp.71-81.
- Gehrke, S.H. and Lee, P.I., 1990. Hydrogels for drug delivery systems. *Drugs and The Pharmaceutical Sciences*, 41, pp.333-392.
- Ghori, M.U., Mohammad, M.A., Rudrangi, S.R.S., Fleming, L.T., Merchant, H.A., Smith, A.M. and Conway, B.R., 2017. Impact of purification on physicochemical, surface and functional properties of okra biopolymer. *Food Hydrocolloids*, 71, pp.311-320.
- Gilbard, J.P., 1994. Human tear film electrolyte concentrations in health and dry-eye disease. *International ophthalmology clinics*, 34(1), pp.27-36.
- Gilsenan, P.M., Richardson, R.K. and Morris, E.R., 2000. Thermally reversible acid-induced gelation of low-methoxy pectin. *Carbohydrate Polymers*, 41(4), pp.339-349.
- Graney, D.O., Jacobs, J.R. and Kern, R., 1993. Anatomy-salivary glands. In *Otolaryngology Head and Neck Surgery*, pp. 977-982.

- Grant, G.T., Morris, E.R., Rees, D.A., Smith, P.J. and Thom, D., 1973. Biological interactions between polysaccharides and divalent cations: the egg-box model. *Federation of European Biochemical Societies Journal*, 32(1), pp.195-198.
- Grasdalen, H. and Smidsrød, O., 1987. Gelation of gellan gum. *Carbohydrate Polymers*, 7(5), pp.371-393.
- Grover, L.M. and Smith, A.M., 2009. Hydrocolloids and medicinal chemistry applications. In: *Modern Biopolymer Science: Bridging the Divide between Fundamental Treatise and Industrial Application*. Elsevier, pp. 595-618.
- Gupta, P., Vermani, K. and Garg, S., 2002. Hydrogels: from controlled release to pH-responsive drug delivery. *Drug Discovery Today*, 7(10), pp.569-579.
- Gurtler, F., Kaltsatos, V., Boisramé, B. and Gurny, R., 1995. Long-acting soluble bioadhesive ophthalmic drug insert (BODI) containing gentamicin for veterinary use: optimization and clinical investigation. *Journal of Controlled Release*, 33(2), pp.231-236.
- Gutowska, A., Jeong, B. and Jasionowski, M., 2001. Injectable gels for tissue engineering. *The Anatomical Record*, 263(4), pp.342-349.
- Hatefi, A. and Amsden, B., 2002. Biodegradable injectable *in situ* forming drug delivery systems. *Journal of Controlled Release*, 80(1), pp.9-28.
- Haug, A. and Smidsrød, O., 1970. Selectivity of some anionic polymers for divalent metal ions. *Acta Chemical Scandinavica Journal*, 24(3), pp.843-854.
- Haug, A., 1961. Dissociation of alginic acid. *Acta Chemical Scandinavica Journal*, 15(4), pp.950-952.
- He, C., Kim, S.W. and Lee, D.S., 2008. *In situ* gelling stimuli-sensitive block copolymer hydrogels for drug delivery. *Journal of Controlled Release*, 127(3), pp.189-207.
- Higham, A.K., Bonino, C.A., Raghavan, S.R. and Khan, S.A., 2014. Photo-activated ionic gelation of alginate hydrogel: real-time rheological monitoring of the two-step crosslinking mechanism. *Soft Matter*, 10(27), pp.4990-5002.
- Hoare, T.R. and Kohane, D.S., 2008. Hydrogels in drug delivery: Progress and challenges. *Polymer*, 49(8), pp. 1993-2007
- Hoffman, A.S., 1995. "Intelligent" polymers in medicine and biotechnology. In *Macromolecular Symposia Journal*, Wiley Online Library, 98(1), pp. 645-664.
- Huang, C.Y., Chen, C.M. and Lee, Y.D., 2007. Synthesis of high loading and encapsulation efficient paclitaxel-loaded poly (n-butyl cyanoacrylate) nanoparticles via miniemulsion. *International Journal of Pharmaceutics*, 338(1), pp.267-275.

- Hulst, A.C., Tramper, J., Van't Riet, K. and Westerbeek, J.M.M., 1985. A new technique for the production of immobilized biocatalyst in large quantities. *Biotechnology and Bioengineering*, 27(6), pp.870-876.
- Hunt N.C., Smith, A.M., Gbureck, U., Shelton, R.M. and Grover, L.M., 2010. Encapsulation of fibroblasts causes accelerated alginate hydrogel degradation. *Acta Biomaterialia Journal*, 6(9), pp.3649-3656.
- Jackson, C.L., Dreaden, T.M., Theobald, L.K., Tran, N.M., Beal, T.L., Eid, M., Gao, M.Y., Shirley, R.B., Stoffel, M.T., Kumar, M.V. and Mohnen, D., 2007. Pectin induces apoptosis in human prostate cancer cells: correlation of apoptotic function with pectin structure. *Glycobiology*, 17(8), pp.805-819.
- Jahromi, S.H., Grover, L.M., Paxton, J.Z. and Smith, A.M., 2011. Degradation of polysaccharide hydrogels seeded with bone marrow stromal cells. *Journal of The Mechanical Behavior of Biomedical Materials*, 4(7), pp.1157-1166.
- Jay, A.J., Colquhoun, I.J., Ridout, M.J., Brownsey, G.J., Morris, V.J., Fialho, A.M., Leitão, J.H. and Sá-Correia, I., 1998. Analysis of structure and function of gellans with different substitution patterns. *Carbohydrate Polymers*, 35(3-4), pp.179-188.
- Jones, V., 1999. Alginate dressings and diabetic foot lesions. *The Diabetic Foot Journal*, 2, pp.8-14
- Jørgensen, T.E., Sletmoen, M., Draget, K.I., and Stokke, B.T., 2007. Influence of oligoguluronates on alginate gelation, kinetics, and polymer organization. *Biomacromolecules*, 8(8), pp.2388-2397.
- Kavanagh, G.M. and Ross-Murphy, S.B., 1998. Rheological characterisation of polymer gels. *Progress in Polymer Science*, 23(3), pp.533-562.
- Keowmaneechai, E. and McClements, D.J., 2002. Influence of EDTA and citrate on physicochemical properties of whey protein-stabilized oil-in-water emulsions containing CaCl<sub>2</sub>. *Journal of Agricultural and Food Chemistry*, 50(24), pp.7145-7153.
- Kierstan, M. and Bucke, C., 1977. The immobilization of microbial cells, subcellular organelles, and enzymes in calcium alginate gels. *Biotechnology and Bioengineering*, 19(3), pp.387-397.
- Kikwai, L., Babu, R.J., Prado, R., Kolot, A., Armstrong, C.A., Ansel, J.C. and Singh, M., 2005. In vitro and in vivo evaluation of topical formulations of spantide II. *American Association of Pharmaceutical Scientists*, 6(4), pp. 565-572.
- Kim, H. J., Lee, H. C., Oh, J. S., Shin, B. A., Oh, C. S., Park, R. D., Yang, K. S., and Cho, C. S., 1999. Polyelectrolyte complex composed of chitosan and sodium alginate for wound dressing application. *Journal of Biomaterials Science Polymer Edition*, 10, pp.543-556

- Kim, H.M., 2016. Raft Formation of Sodium Alginate in the Stomach. *Journal of Neurogastroenterology and Motility*, 22(4) pp. 705-706
- Kokabi, M., Sirousazar, M. and Hassan, Z.M., 2007. PVA–clay nanocomposite hydrogels for wound dressing. *European Polymer Journal*, 43(3), pp.773-781.
- Kotula, A.P., Meyer, M.W., De Vito, F., Plog, J., Hight Walker, A.R. and Migler, K.B., 2016. The rheo-Raman microscope: Simultaneous chemical, conformational, mechanical, and microstructural measures of soft materials. *Review of Scientific Instruments*, 87(10), p.105105.
- Kubo, W., Konno, Y., Miyazaki, S. and Attwood, D., 2004. *In situ* gelling pectin formulations for oral sustained delivery of paracetamol. *Drug Development and Industrial Pharmacy*, 30(6), pp.593-599.
- Kubo, W., Miyazaki, S. and Attwood, D., 2003. Oral sustained delivery of paracetamol from *in situ*-gelling gellan and sodium alginate formulations. *International Journal of Pharmaceutics*, 258(1), pp.55-64.
- Lang, J.C., 1995. Ocular drug delivery conventional ocular formulations. *Advanced Drug Delivery Reviews*, 16(1), pp.39-43.
- Leclere, L., Van Cutsem, P. and Michiels, C., 2013. Anti-cancer activities of pH-or heat-modified pectin. *Frontiers in Pharmacology*, 4, pp.128.
- Lee, J.Y., Cole, T.B., Palmiter, R.D. and Koh, J.Y., 2000. Accumulation of zinc in degenerating hippocampal neurons of ZnT3-null mice after seizures: evidence against synaptic vesicle origin. *Journal of Neuroscience*, 20(11), pp. 79.
- Lee, K.Y. and Mooney D.J., 2012, Alginate: Properties and biomedical applications. *Progress in Polymer Science*, 37(1) pp. 106-126.
- Levin, L.A., Nilsson, S.F., Ver Hoeve, J., Wu, S., Kaufman, P.L. and Alm, A., 2011. *Adler's Physiology of the Eye*. Elsevier Health Sciences, pp.350-362.
- Lin, S.Y. and Ayres, J.W., 1992. Calcium alginate beads as core carriers of 5-aminosalicylic acid. *Pharmaceutical Research*, 9(9), pp.1128-1131.
- Lin, Y.K., Matsumoto, Y., Kuroyanagi, Y. and Kagawa, S., 2009. A bilayer hyaluronic acid wound dressing to promote wound healing in diabetic ulcer. *Journal of Bioactive and Compatible Polymers*, 24(5), pp.424-443.
- Lips, A., Clark, A.H., Cutler, N. and Durand, D., 1991. Measurement of cooperativity of binding of calcium to neutral sodium pectate. *Food Hydrocolloids*, 5(1-2), pp.87-99.
- Lloyd, D.J., 1926. Chemistry of the proteins and its economic applications. *Journal of The American Pharmaceutical Association*, 16(6), p.279.

- Löffler, M., Schmohl, M., Schneiderhan-Marra, N. and Beckert, S., 2011. Wound fluid diagnostics in diabetic foot ulcers. In *Global Perspective on Diabetic Foot Ulcerations*.1 (4), pp.48-49.
- Macosko, C.W and Larson, R G., 1994. Rheology: principles, measurements, and applications. *Advances in Interfacial Engineering*, 2(5), pp.181-188.
- Madan, M., Bajaj, A., Lewis, S., Udupa, N. and Baig, J.A., 2009. *In situ* forming polymeric drug delivery systems. *Indian Journal of Pharmaceutical Sciences*, 71(3), p.242.
- Mahajan, H.S. and Gattani, S.G., 2009a. Gellan gum based microparticles of metoclopramide hydrochloride for intranasal delivery: Development and Evaluation. *Chemical and Pharmaceutical Bulletin*, 57(4), pp.388-392.
- Mahdi, M.H., 2016. Development of gellan gum fluid gel as modified release drug delivery systems (Doctoral dissertation, University of Huddersfield).
- Mahdi, M.H., Conway, B.R. & Smith, A.M., 2014. Evaluation of gellan gum fluid gels as modified release oral liquids. *International Journal of Pharmaceutics*, 475(1), pp.335-343.
- Mahdi, M.H., Conway, B.R. and Smith, A.M., 2015. Development of mucoadhesive sprayable gellan gum fluid gels. *International Journal of Pharmaceutics*, 488(1), pp.12-19.
- Mahdi, M.H., Diryak, R., Kontogiorgos, V., Morris, G.A. and Smith, A.M., 2016. *In situ* rheological measurements of the external gelation of alginate. *Food Hydrocolloids*, 55, pp.77-80.
- Miao, M., Bai, A., Jiang, B., Song, Y., Cui, S.W. and Zhang, T., 2014. Characterisation of a novel water-soluble polysaccharide from *Leuconostoc citreum* SK24. 002. *Food hydrocolloids*, 36, pp.265-272.
- Malafaya, P.B., Silva, G.A. and Reis, R.L., 2007. Natural–origin polymers as carriers and scaffolds for biomolecules and cell delivery in tissue engineering applications. *Advanced Drug Delivery Reviews*, 59(4), pp.207-233.
- Mandal, B., Alexander, K.S. and Riga, A.T., 2010. Evaluation of the drug-polymer interaction in calcium alginate beads containing diflunisal. *Die Pharmazie - An International Journal of Pharmaceutical Sciences*, 65(2), pp.106-109.
- Manjanna, K.M., Rajesh, K.S. and Shivakumar, B., 2013. Formulation and optimization of natural polysaccharide hydrogel microbeads of aceclofenac sodium for oral controlled drug delivery. *American Journal of Medical Sciences and Medicine*, 1(1), pp.5-17.
- Marriott, C., 2007. Rheology. In: *Aulton's Pharmaceutics, The Design and Manufacture of Medicines*. Third Ed, Churchill Livingstone Elsevier, pp.42-59.
- Martin, A.N., Sinko, P.J. and Singh, Y. 2011, Rheology. In D. B. Troy, ed., *Martin's Physical Pharmacy and Pharmaceutical Sciences: Physical Chemical and Biopharmaceutical Principles in the Pharmaceutical Sciences*. Sixth Ed, pp. 469-492.



- Matricardi, P., Cencetti, C., Ria, R., Alhaique, F. and Coviello, T., 2009. Preparation and characterization of novel gellan gum hydrogels suitable for modified drug release. *Molecules*, 14(9), pp.3376-3391.
- Matsumoto, S., Kobayashi, H. and Takashima, Y., 1986. Production of monodispersed capsules. *Journal of Microencapsulation*, 3(1), pp.25-31.
- May, C.D., 1990. Industrial pectins: sources, production and applications. *Carbohydrate Polymers*, 12(1), pp.79-99.
- Meyers, S.R., Kenan, D.J. and Grinstaff, M.W., 2008. Enzymatic Release of a Surface-Adsorbed RGD Therapeutic from a Cleavable Peptide Anchor. *Chemistry Medicinal Journal*, 3(11), pp.1645-1648.
- Mezger, T.G., 2006. Flow behaviour and viscosity. In *The rheology handbook: for users of rotational and oscillatory rheometers*. Second Ed, pp.19-29.
- Middleton, D.L. and Robinson, J.R., 1991. Design and evaluation of an ocular bioadhesive delivery system. *Iranian Journal of Pharmaceutical Research*, 1(14), pp.200-206.
- Milas, M. and Rinaudo, M., 1996. The gellan sol-gel transition. *Carbohydrate Polymers*, 30(2), pp.177-184.
- Mironi-Harpaz, I., Hazanov, L., Engel, G., Yelin, D. and Seliktar, D., 2015. In-Situ architectures designed in 3D cell-Laden hydrogels using microscopic laser photolithography. *Advanced Materials*, 27(11), pp.1933-1938.
- Miyazaki, S., Aoyama, H., Kawasaki, N., Kubo, W. and Attwood, D., 1999. *In situ*-gelling gellan formulations as vehicles for oral drug delivery. *Journal of Controlled Release*, 60(2), pp.287-295.
- Miyazaki, S., Kawasaki, N., Kubo, W., Endo, K. and Attwood, D., 2001. Comparison of *in situ* gelling formulations for the oral delivery of cimetidine. *International Journal of Pharmaceutics*, 220(1), pp.161-168.
- Miyazaki, S., Kubo, W. and Attwood, D., 2000. Oral sustained delivery of theophylline using in-situ gelation of sodium alginate. *Journal of Controlled Release*, 67(2), pp.275-280.
- Miyoshi, E., Takaya, T. and Nishinari, K., 1994. Gel-sol transition in gellan gum solutions. I. Rheological studies on the effects of salts. *Food Hydrocolloids*, 8(6), pp.505-527.
- Miyoshi, E., Takaya, T. and Nishinari, K., 1996. Rheological and thermal studies of gel-sol transition in gellan gum aqueous solutions. *Carbohydrate Polymers*, 30(2-3), pp.109-119.
- Moritaka, H., Nishinari, K., Taki, M. and Fukuba, H., 1995. Effects of pH, potassium chloride, and sodium chloride on the thermal and rheological properties of gellan gum gels. *Journal of Agricultural and Food Chemistry*, 43(6), pp. 1685-1689

- Morris, E.R., Cutler, A.N., Ross-Murphy, S.B., Rees, D.A. and Price, J., 1981. Concentration and shear rate dependence of viscosity in random coil polysaccharide solutions. *Carbohydrate polymers*, 1(1), pp.5-21.
- Morris, E.R., Nishinari, K. and Rinaudo, M., 2012. Gelation of gellan—a review. *Food Hydrocolloids*, 28(2), pp.373-411.
- Morris, E.R., Powell, D.A., Gidley, M.J. and Rees, D.A., 1982. Conformations and interactions of pectins: I. Polymorphism between gel and solid states of calcium polygalacturonate. *Journal of Molecular Biology*, 155(4), pp.507-516.
- Morris, E.R., Rees, D.A., Thom, D. and Boyd, J., 1978. Chiroptical and stoichiometric evidence of a specific, primary dimerisation process in alginate gelation. *Carbohydrate Research*, 66(1), pp.145-154.
- Moxon, S.R., 2016. Development of biopolymer hydrogels as complex tissue engineering scaffolds (Doctoral dissertation, University of Huddersfield).
- Nakatani, A.I., Kim, H., Takahashi, Y., Matsushita, Y., Takano, A., Bauer, B.J. and Han, C.C., 1990. Shear stabilization of critical fluctuations in bulk polymer blends studied by small angle neutron scattering. *The Journal of Chemical Physics*, 93(1), pp.795-810.
- Nanjawade, B.K., Manvi, F.V. and Manjappa, A.S., 2007. Retracted: *In situ*-forming hydrogels for sustained ophthalmic drug delivery. *Journal of Controlled Release*, 122(2), pp.119-134.
- Nelson, D.B., Smit, C.J.B. and Wiles, R.R., 1977. Commercially important pectic substances. *Food Colloids*, pp.418-437.
- Nerkar, T.S., Gujrathi, N.A., Rane, B.R., Bakliwal, S.R. and Pawar, S.P., 2013. In-situ gel: A novel approach in sustained and controlled drug delivery system. *International Journal of Pharmaceutical Sciences and Research*, 4(4), pp.1-18.
- Nishinari, K., Zhang, H. and Ikeda, S., 2000. Hydrocolloid gels of polysaccharides and proteins. *Current Opinion in Colloid & Interface Science*, 5(3), pp.195-201.
- Nitta, Y. and Nishinari, K., 2005. Gelation and gel properties of polysaccharides gellan gum and tamarind xyloglucan. *International Journal of Biological Macromolecules*, 5(3), pp.47-52.
- Nokhodchi, A., Tailor, A., 2004. *In situ* cross-linking of sodium alginate with calcium and aluminium ions to sustain the release of theophylline from polymeric matrices. *II Farmaco Journal*, 59, pp.999–1004.
- Oakenfull, D. and Scott, A., 1984. Hydrophobic interaction in the gelation of high methoxyl pectins. *Journal of Food Science*, 49(4), pp.1093-1098.
- Oakenfull, D. and Scott, A., 1998. Milk gels with low methoxyl pectins. *Special Publication-Royal Society of Chemistry*, 218, pp.212-221.

- Oakenfull, D.G., 1991. The chemistry of high-methoxyl pectin gelation. Walter, RH The chemistry and technology of pectin. Academic Press, pp. 87–108
- Olhero, S.M., Tari, G., Coimbra, M.A. and Ferreira, J.M.F., 2000. Synergy of polysaccharide mixtures in gel casting of alumina. *Journal of The European Ceramic Society*, 20(4), pp.423-429.
- Oliveira, J.T., Martins, L., Picciochi, R., Malafaya, P.B., Sousa, R.A., Neves, N.M., Mano, J.F. and Reis, R.L., 2010. Gellan gum: a new biomaterial for cartilage tissue engineering applications. *Journal of Biomedical Materials Research Part A*, 93(3), pp.852-863.
- Osada, Y. and Khokhlov, A., 2001. Thermoreversible and irreversible physical gels from biopolymers. In: *Polymer Gels and Networks*. Marcel Dekker, 2, pp.27-33.
- Osmalek, T., Froelich, A. and Tasarek, S., 2014 Application of gellan gum in pharmacy and medicine. *International Journal of Pharmaceutics*, 466, pp.328-340.
- Park, H., Park, K. and Shalaby, W.S., 2011. Biodegradable drug delivery systems. In: *Biodegradable hydrogels for drug delivery*. Technomic Publishing Company, 1(8), pp.189-219.
- Parker, S., Martin, D., & Braden, M. 1999. Soft acrylic resin materials containing a polymerisable plasticiser II: Water absorption characteristics. *Biomaterials*, 20(1), pp.55-60.
- Peppas, N.A. and Langer, R., 1994. New challenges in biomaterials. *American Association for The Advancement of Science*, 263(5154), pp.1715-1719.
- Peppas, N.A., Bures, P., Leobandung, W. and Ichikawa, H., 2000. Hydrogels in pharmaceutical formulations. *European Journal of Pharmaceutics and Biopharmaceutics*, 50, pp. 27-46
- Peppas, N.A., Hilt, J.Z., Khademhosseini, A. and Langer, R., 2006. Hydrogels in biology and medicine: from molecular principles to bionanotechnology. *Advanced Materials*, 18(11), pp.1345-1360.
- Phillips, G.O. and Williams, P.A. eds., 2009. Introduction to food hydrocolloids. In: *Handbook of hydrocolloids*. Woodhead Publishing Limited, 2(1), pp.14-22.
- Picout, D.R. and Ross-Murphy, S.B., 2003. Rheology of biopolymer solutions and gels. *The Scientific World Journal*, 3, pp.105-121.
- Posocco, B., Dreussi, E., De Santa, J., Toffoli, G., Abrami, M., Musiani, F., Grassi, M., Farra, R., Tonon, F., Grassi, G. and Dapas, B., 2015. Polysaccharides for the delivery of antitumor drugs. *Materials*, 8(5), pp.2569-2615.
- Powell, D.A. Morris E.R, Gidley M.J and Rees D.A 1982. Conformations and interactions of pectins: II. Influence of residue sequence on chain association in calcium pectate gels. *Journal of Molecular Biology*, 155(4), pp.517-531.

- Prakash, P.R., Rao, N.R. and Chowdary, S., 2010. Formulation, evaluation and anti-inflammatory activity of topical etoricoxib gel. *Asian Journal of Pharmaceutical and Clinical Research*, 3, p.126.
- Quigley, E.M.M. and Turnberg, L.A., 1987. pH of the microclimate lining human gastric and duodenal mucosa in vivo: studies in control subjects and in duodenal ulcer patients. *Gastroenterology*, 92(6), pp.1876-1884.
- Rajoria, G. and Gupta, A., 2012. In-Situ Gelling System: A novel approach for ocular drug delivery. *American Journal of PharmTech Research*, 2(4), pp.24-53.
- Ralet, M.C., Dronnet, V., Buchholt, H.C. and Thibault, J.F., 2001. Enzymatically and chemically de-esterified lime pectins: characterisation, polyelectrolyte behaviour and calcium binding properties. *Carbohydrate Research*, 336(2), pp.117-125.
- Rao, A., 2013. Rheology of fluid, semisolid, and solid foods: principles and applications. Springer Science & Business Media, 3(6), pp.366-380.
- Rinaudo, M., 2008. Main properties and current applications of some polysaccharides as biomaterials. *Polymer International*, 57(3), pp.397-430.
- Robinson, G., Manning, C.E and Morris, E.R .1991. Conformation and physical properties of the bacterial polysaccharides gellan, welan, and rhamsan. *Food Polymers, Gels and Colloids*, 82 (2), p.22-33.
- Rosiak, J., Rucinska-Rybus, A. and Pekala, W., 1989. Method of manufacturing hydrogel dressings. US Patent 4871490 A
- Rowley, J.A., Madlambayan, G. and Mooney, D.J., 1999. Alginate hydrogels as synthetic extracellular matrix materials. *Biomaterials*, 20(1), pp.45-53.
- Rozier, A., Mazuel, C., Grove, J. and Plazonnet, B., 1989. Gelrite®: A novel, ion-activated, in-situ gelling polymer for ophthalmic vehicles. Effect on bioavailability of timolol. *International Journal of Pharmaceutics*, 57(2), pp.163-168.
- Ruel-Gariepy, E. and Leroux, J.C., 2004. *In situ*-forming hydrogels—review of temperature-sensitive systems. *European Journal of Pharmaceutics and Biopharmaceutics*, 58(2), pp.409-426.
- Sanderson, G.R. and Clark, R.C., 1984. Gellan gum, a new gelling polysaccharide. *Gums and Stabilisers for The Food Industry*, 2, pp.201-210.
- Sauvola, J. and Pietikäinen, M., 2000. Adaptive document image binarization. *Pattern Recognition*, 33(2), pp.225-236.
- Scherer, G.W., 1990. Theory of drying. *Journal of the American Ceramic Society*, 73(1), pp.3-14.
- Schneider, C.A., Rasband, W.S. and Eliceiri, K.W., 2012. NIH Image to ImageJ: 25 years of image analysis. *Nature Methods*, 9(7), pp.671-675.

- Shedden, A.H., Laurence, J., Barrish, A. and Olah, T.V., 2001. Plasma timolol concentrations of timolol maleate: timolol gel-forming solution (Timoptic-XE®) once daily versus timolol maleate ophthalmic solution twice daily. *Documenta Ophthalmologica*, 103(1), pp.73-79.
- Silbernagl, S. and Despopoulos, A., 2009. *Colour atlas of physiology*. Thieme Publishing Group, 6(6), pp.138-147.
- Skjåk-Bræk, G., Grasdalen, H. and Smidsrød, O., 1989. Inhomogeneous polysaccharide ionic gels. *Carbohydrate Polymers*, 10(1), pp.31-54.
- Skjåk-Bræk, G., Smidsrød, O. and Larsen, B., 1986. Tailoring of alginates by enzymatic modification *in vitro*. *International Journal of Biological Macromolecules*, 8(6), pp.330-336.
- Sletmoen, M., Draget, K.I., and Stokke, B.T., 2010. Alginate oligoguluronates as a tool for tailoring properties of Ca-alginate gels. *Macromolecular Symposia*, 291-292, pp.345-353
- Smeds, K.A. and Grinstaff, M.W., 2001. Photocrosslinkable polysaccharides for *in situ* hydrogel formation. *Journal of Biomedical Materials Research*, 54(1), pp.115-121.
- Smidsrod, O. and Draget, K.L., 1996. Chemistry and physical properties of alginates. *Carbohydrates in Europe*, 14 (1996), pp. 6-13.
- Smidsrød, O. and Skjåk-Bræk, G 1990. Alginate as immobilization matrix for cells. *Trends in Biochemical Sciences*, 8, pp.71-78.
- Smith, A. M. and Miri, T. 2011. Alginates in Foods. In: *Practical Food Rheology: An Interpretive Approach*. 1(6), pp. 113-128.
- Smith, A.M. and Miri, T., 2010. Alginates in foods. *Practical Food Rheology: An Interpretive Approach*, Norton, I.T., Spyropoulos, F. and Cox, P, pp.113-132.
- Somani, R.H., Yang, L., Hsiao, B.S., Agarwal, P.K., Fruitwala, H.A. and Tsou, A.H., 2002. Shear-induced precursor structures in isotactic polypropylene melt by in-situ rheo-SAXS and rheo-WAXD studies. *Macromolecules*, 35(24), pp.9096-9104.
- Stanway, R., Sproston, J.L. and El-Wahed, A.K., 1996. Applications of electro-rheological fluids in vibration control: a survey. *Smart Materials and Structures*, 5(4), p.464.
- Stjernschantz, J. and Astin, M., 1993. Anatomy and physiology of the eye. Physiological aspects of ocular drug therapy. In *Biopharmaceutics of Ocular Drug Delivery*, pp. 1-25.
- Suedee, R., Jantararat, C., Lindner, W., Viernstein, H., Songkro, S. and Srichana, T., 2010. Development of a pH-responsive drug delivery system for enantioselective-controlled delivery of racemic drugs. *Journal of Controlled Release*, 142(1), pp.122-131.
- Sugiura, S., Oda, T., Izumida, Y., Aoyagi, Y., Satake, M., Ochiai, A., Ohkohchi, N. and Nakajima, M., 2005. Size control of calcium alginate beads containing living cells using micro-nozzle array. *Biomaterials*, 26(16), pp.3327-3331.

- Sultana, Y., Jain, R., Aqil, M. and Ali, A., 2006. Review of ocular drug delivery. *Current Drug Delivery*, 3(2), pp.207-217.
- Sundar Raj, A.A., Rubila, S., Jayabalan, R. and Ranganathan, T.V., 2012. A review on pectin: Chemistry due to general properties of pectin and its pharmaceutical uses. *Scientific Reports*, 1, pp.550-1.
- Sutherland, I.W., 1991. Alginates, In: Byrom D. *Biomaterials: Novel Materials from biological sources*. Institute of Cell and Molecular Biology, 1 (7), pp. 307-331.
- Sutherland, I.W., 2001. Microbial polysaccharides from Gram-negative bacteria. *International Dairy Journal*, 11(9), pp.663-674.
- Sutherland, I.W., 2007. Biotechnology of microbial polysaccharides in food. *Food Science and Technology*, 165, p.583.
- Sworn, G., France, D. and France, S., 2009. Gellan gum. In *Handbook of Hydrocolloids*, Second Edition. Woodhead, Oxford, pp. 204 – 227.
- Sworn, G., Sanderson, G.R. and Gibson, W., 1995. Gellan gum fluid gels. *Food Hydrocolloids*, 9(4), pp.265-271.
- Tan, B.H., Tam, K.C., Lam, Y.C. and Tan, C.B., 2004. Microstructure and rheology of stimuli-responsive nanocolloidal systems effect of ionic strength. *Langmuir*, 20(26), pp.11380-11386.
- Te Nijenhuis, K., 1997. Poly (vinyl methacrylate). *Thermoreversible Networks: Viscoelastic Properties and Structure of Gels*, pp.67-81.
- Thibault, J.F. and Rinaudo, M., 1986. Chain association of pectic molecules during calcium-induced gelation. *Biopolymers*, 25(3), pp.455-468.
- Toft, K., 1982. Interactions between pectins and alginates. *Progress in food and nutrition science*, 6, pp. 89-96.
- Whelton, H. (1996) *Introduction: The anatomy and physiology of salivary glands*. *Saliva and Oral Health*. London: British Dental Association, 1-4
- Willats, W.G., McCartney, L., Mackie, W. and Knox, J.P., 2001. Pectin: cell biology and prospects for functional analysis. In *Plant Cell Walls*, 47, pp.9–27.
- Yamamoto and Cunha., 2007. Acid gelation of gellan: Effect of final pH and heat treatment conditions. *Carbohydrate Polymers*, 68(3), pp. 517-527
- Yang, H., Liu, H., Kang, H. and Tan, W., 2008. Engineering target-responsive hydrogels based on aptamer-target interactions. *Journal of the American Chemical Society*, 130(20), pp.6320-6321.
- Yu, L. and Ding, J., 2008. Injectable hydrogels as unique biomedical materials. *Chemical Society Reviews*, 37(8), pp.1473-1481.